

AD-A075 658

AIR FORCE FLIGHT DYNAMICS LAB WRIGHT-PATTERSON AFB OH

F/O 22/2

INVESTIGATION OF A DEPLOYABLE POLYURETHANE FOAM GROUND IMPACT A--ETC(U)

JUL 79 S R MEHAFFIE

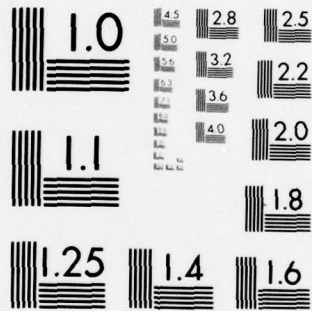
UNCLASSIFIED AFFDL-TR-78-145-VOL-2

NL

1 OF 3

AD  
A075658





MICROCOPY RESOLUTION TEST CHART  
NATIONAL BUREAU OF STANDARDS-1963-A



AFFDL-TR-78-145  
Volume II

LEVEL

A070077

2

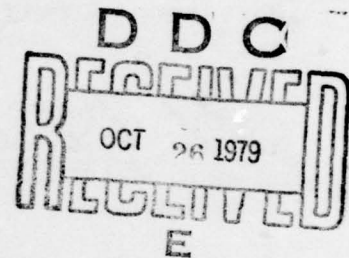
A075658

INVESTIGATION OF A DEPLOYABLE POLYURETHANE FOAM GROUND  
IMPACT ATTENUATION SYSTEM FOR AEROSPACE VEHICLES

Volume II. FIAS Test No, 49-91

Stephen R. Mehaffie

Recovery and Crew Station Branch  
Vehicle Equipment Division



July 1979

TECHNICAL REPORT AFFDL-TR-78-145, VOLUME II

Final Report for Period November 1976 to May 1978

DDC FILE COPY

Approved for public release; distribution unlimited.

AIR FORCE FLIGHT DYNAMICS LABORATORY  
AIR FORCE WRIGHT AERONAUTICAL LABORATORIES  
AIR FORCE SYSTEMS COMMAND  
WRIGHT-PATTERSON AIR FORCE BASE, OHIO 45433

79 10 26 004

NOTICE

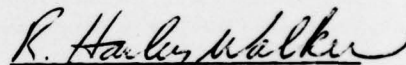
When Government drawings, specifications, or other data are used for any purpose other than in connection with a definitely related Government procurement operation, the United States Government thereby incurs no responsibility nor any obligation whatsoever; and the fact that the government may have formulated, furnished, or in any way supplied the said drawings, specifications, or other data, is not to be regarded by implication or otherwise as in any manner licensing the holder or any other person or corporation, or conveying any rights or permission to manufacture, use, or sell any patented invention that may in any way be related thereto.

Reference to named commercial products in this report are not to be considered in any sense as an endorsement of the product by the United States Air Force or the Government.

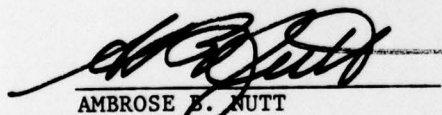
This report has been reviewed by the Information Office (OI) and is releasable to the National Technical Information Service (NTIS). At NTIS, it will be available to the general public, including foreign nations.

This technical report has been reviewed and is approved for publication.

  
STEPHEN R. MEHAFFIE  
Project Engineer

  
R. HARLEY WALKER  
Crew Escape and Subsystems Branch  
Vehicle Equipment Division

FOR THE COMMANDER

  
AMBROSE B. NUTT  
Director  
Vehicle Equipment Division

"If your address has been changed, if you wish to be removed from our mailing list, or if the addressee is no longer employed by your organization please notify AFFDL/FER, WPAFB, Ohio 45433 to help us maintain a current mailing list."

Copies of this report should not be returned unless return is required by security considerations, contractual obligations, or notice on a specific document.

UNCLASSIFIED

SECURITY CLASSIFICATION OF THIS PAGE (When Data Entered)

REPORT DOCUMENTATION PAGE		READ INSTRUCTIONS BEFORE COMPLETING FORM
1. REPORT NUMBER AFFDL-TR-78-145, Vol. 2	2. GOVT ACCESSION NO.	3. RECIPIENT'S CATALOG NUMBER
4. TITLE (and Subtitle) INVESTIGATION OF A DEPLOYABLE POLYURETHANE FOAM GROUND IMPACT ATTENUATION SYSTEM FOR AEROSPACE VEHICLES, VOL. II. FIAS TEST NO. 4991 Volume Numbers	5. TYPE OF REPORT & PERIOD COVERED Final Report Nov 76 - May 78	
7. AUTHOR(s) Stephen R. Mehaffie	6. PERFORMING ORG. REPORT NUMBER	
9. PERFORMING ORGANIZATION NAME AND ADDRESS Recovery and Crew Station Branch Air Force Flight Dynamics Laboratory Wright-Patterson Air Force Base, Ohio	8. CONTRACT OR GRANT NUMBER(s) 16 1964	
11. CONTROLLING OFFICE NAME AND ADDRESS Air Force Flight Dynamics Laboratory Air Force Systems Command Wright-Patterson Air Force Base, Ohio 45433	10. PROGRAM ELEMENT, PROJECT, TASK AREA & WORK UNIT NUMBERS 17 19645003 12 209	
14. MONITORING AGENCY NAME & ADDRESS (if different from Controlling Office)	12. REPORT DATE July 1979	
	13. NUMBER OF PAGES 229	
	15. SECURITY CLASS. (of this report) Unclassified	
	15a. DECLASSIFICATION/DOWNGRADING SCHEDULE	
16. DISTRIBUTION STATEMENT (of this Report) Approved for public release; distribution unlimited.		
17. DISTRIBUTION STATEMENT (of the abstract entered in Block 20, if different from Report)		
18. SUPPLEMENTARY NOTES		
19. KEY WORDS (Continue on reverse side if necessary and identify by block number) Impact Attenuation      Damage Reduction      Ground Recovery Polyurethane Foam      Impact Tests      Test Methods Foam-in-Place      Remotely Piloted Vehicles (RPV)      Cost Analysis Parachute Systems      Plastic Foam Shock Attenuation		
20. ABSTRACT (Continue on reverse side if necessary and identify by block number) An investigation was conducted to determine the feasibility of an advanced deployable impact attenuation system for use with aerospace vehicles. Performance of the system with a boilerplate AQM-34V RPV was quantified through a series of full-scale impact tests. A prototype design and costing analysis is presented. The conclusion was that the Foam Impact Attenuation System (FIAS) could provide the optimum system for the ground recovery of RPV's.		

DD FORM 1 JAN 73 1473

EDITION OF 1 NOV 65 IS OBSOLETE

UNCLASSIFIED

SECURITY CLASSIFICATION OF THIS PAGE (When Data Entered)

012 070

LB



# FOREWORD

This report was prepared by the Aerospace Vehicle Recovery Group of the Recovery and Crew Station Branch of the Vehicle Equipment Division of the Air Force Flight Dynamics Laboratory (AFFDL/FER) under Project 1964, "Recovery System Technology Application to Remotely Piloted Vehicles." This investigation was performed in accordance with a Memorandum of Agreement (MOA) between the Remotely Piloted Vehicle System Program Office (RPV SPO) and the AFFDL dated 15 Nov 76 and 25 Oct 77 (revisions). Volume I of this report documents the investigation results from May 75 through Oct 76. This report (Volume II) documents the investigation results between Nov 76 and May 78 and was submitted for publication in March 1979.

The in-house investigation described in this report was made possible through the collective efforts of a number of organizations and people at Wright-Patterson Air Force Base. Additionally, the personnel of CENTRO Corporation of Dayton, Ohio, who served as the support contractor for the fabrication of the test vehicle and apparatus made this effort possible in a timely manner.

The author wishes to thank Mr. R. H. Walker (AFFDL) and Major R. Johnson (RPV SPO) for their excellent management combination of research and operational considerations into a single investigation. Mr. Michael Higgins, Mr. George Pitts, Mr. Virgil King, and Mr. Paul Coob were instrumental in the accomplishment of the somewhat lengthy test program in a timely and professional manner. Special thanks are due Mrs. Evelyn Yount for her assistance and perseverance in preparing this manuscript.

Accession For	
NTIS	<input checked="checked" type="checkbox"/>
DDC TAB	<input type="checkbox"/>
Unannounced	<input type="checkbox"/>
Justification	<input type="checkbox"/>
By	
Distribution/	
Availability Codes	
Dist	Avail and/or special

TABLE OF CONTENTS

SECTION		PAGE
I	INTRODUCTION AND BACKGROUND	1
	1. Introduction	1
	2. Background and Chronology	1
II	FOAMING SYSTEM AND TESTS NO. 49-57	4
	1. Introduction	4
	2. Foaming System Description	4
	3. Improper Operation of Foaming System	7
	4. Foaming System Preliminary Testing	9
	5. Summary	12
III	BAG DESIGNS	13
	1. Overview	13
	2. Vehicle Recovery Configurations	13
	3. Bag Design Parameters	16
	4. Pods-On Bag Design	23
	5. Pods-Off Bag Design	27
	6. Tail Bags Design	31
	7. Summary	39
IV	VERTICAL TESTS NO. 58-64	40
	1. Test Series Overview	40
	2. IRON PIG Test Facility	40
	3. Data Reduction Technique	42
	4. Test No. 58	43
	5. Test No. 59	43
	6. Test No. 60	43
	7. Test No. 61	46
	8. Test No. 62	52
	9. Test No. 63	56
	10. Test No. 64	60
	11. Summary	64

TABLE OF CONTENTS (CONTINUED)

SECTION	PAGE
V TEST VEHICLE DESCRIPTION	65
1. Test Vehicle Description	65
2. Test Vehicle Inertias	65
3. Modeling Geometry	70
4. Summary	75
VI INSTRUMENTATION AND ANALYSIS TECHNIQUES	78
1. Overview	78
2. Approach	78
3. Hardware	79
4. Analysis Technique	80
VII TEST APPARATUS DESCRIPTION	91
1. Tech Method Selection	91
2. Tower Assembly	91
3. Lower Pendulum Head and Pull Back Winch	95
4. Vehicle Hanging	109
5. Control Station	113
6. Cost and Personnel Requirements	117
VIII HORIZONTAL TESTS NO. 65-71	118
1. Test Conditions	118
2. Test No. 65	119
3. Test No. 66	121
4. Test No. 67	121
5. Test No. 68	122
6. Test No. 69	124
7. Test No. 70	126
8. Test No. 71	127
9. Summary	127
IX HORIZONTAL TESTS NO. 72-82	128
1. Test Series No. 72-82	128
2. Test Results, 0° Yaw, 15 Kts, Mark VIII	130
3. Test Results, 45° Yaw, 15 Kts, Mark VIII	134

TABLE OF CONTENTS (CONCLUDED)

SECTION	PAGE
4. Test Results, 90° Yaw, 15 Kts, Mark VIII	141
5. Test Results, 135° Yaw, 15 Kts, Mark VIII	147
6. Test Results, 180° Yaw, 15 Kts, Mark VIII	153
7. Conclusions	158
X HORIZONTAL TESTS NO. 83-91	161
1. Test Series No. 83-91	161
2. Test Results, 0° Yaw, 15 Kts, Mark IX	162
3. Test Results, 45° Yaw, 15 Kts, Mark IX	169
4. Test Results, 90° Yaw, 15 Kts, Mark IX	172
5. Test Results, 135° Yaw, 15 Kts, Mark IX	181
6. Test Results, 180° Yaw, 15 Kts, Mark IX	186
7. Damage Extrapolation	186
8. Conclusions	190
XI CONCLUSIONS AND RECOMMENDATIONS	192
APPENDIX A MARK VIII AND IX BAG DESCRIPTIONS	193
APPENDIX B FIAS SLIPPER TANK DESIGN	209
REFERENCES	217



LIST OF ILLUSTRATIONS

FIGURE		PAGE
1	FIAS Breadboard Foaming System	5
2	Installed Foaming System	8
3	AQM-34V RPV with AN/ALE-2 Pods	14
4	AQM-34V RPV with AN/ALE-2 Pods	15
5	AQM-34V RPV with AN/ALE-2 Pods	16
6	AQM-34V Clamp Bar	17
7	FIAS Clamp Bar	18
8	Theoretical Performance of Mark VIII FIAS Bag	22
9	Mark IX Bag	25
10	Mark IX Misalignment	26
11	Bag Shape, Test No. 83	28
12	Bag Shape, Test No. 90	29
13	Mark VIII Bag	30
14	Mark VIII Bag Misalignment	32
15	Bag Shape, Test No. 68	33
16	Bag Shape, Test No. 81, Right-Hand	34
17	Bag Shape, Test No. 81, Left-Hand	35
18	Tall Tail Bag, Pre-Test	36
19	Short Tail Bag, Pre-Test	37
20	Short Tail Bag, Test No. 81	38
21	Tall Tail Bag, Test No. 86	39
22	IRON PIG, Test No. 43	41
23	Test No. 58, Acceleration vs Time	44
24	Test No. 58, Energy vs Time	45
25	Test No. 60, Acceleration vs Time	47
26	Test No. 60, Energy vs Time	48
27	Test No. 61, Acceleration vs Time	49
28	Test No. 61, Energy vs Time	50
29	Test No. 61, Bag Damage	51
30	Test No. 62, Acceleration vs Time	53
31	Test No. 62, Energy vs Time	54
32	Test No. 62, Bag Damage	55
33	Test No. 63, Acceleration vs Time	57



LIST OF ILLUSTRATIONS (CONTINUED)

FIGURE		PAGE
34	Test No. 63, Energy vs Time	58
35	Test No. 63, Bag Damage	59
36	Test No. 64, Acceleration vs Time	60
37	Test No. 64, Energy vs Time	61
38	Test No. 64, Bag Damage	62
39	IRON TURKEY Test Vehicle	66
40	Front View, IRON TURKEY	67
41	Side View, IRON TURKEY	68
42	Top View, IRON TURKEY	69
43	Nose Area, IRON TURKEY	72
44	Frangible Wing Tip Joint	73
45	Wing Tip Root Area Modeling	74
46	Horizontal Stabilizer (Test No. 84)	76
47	Horizontal Stabilizer Endplates (Test No. 81)	77
48	Test No. 77, Body Axis Accelerations	82
49	Test No. 77, Body Axis Angular Accelerations	83
50	Test No. 77, Body Axis Angular Velocity	84
51	Test No. 77, Earth Axis Accelerations	85
52	Test No. 77, Earth Axis Velocity	86
53	Test No. 77, Earth Axis Distance	87
54	Test No. 77, Euler Angle Velocity	88
55	Test No. 77, Euler Angles	89
56	Test No. 77, Energy vs Time	90
57	Test Apparatus, Artist's Concept	92
58	Test Apparatus, Dimensions	93
59	Support Facilities	94
60	Parts Layout	96
61	Triangle Assembly	97
62	Beginning of Erection	98
63	Raising First Leg	99
64	Assembly of First Leg	100
65	Assembly of Last Leg	101
66	Hanging Pendulum Tubes	102

LIST OF ILLUSTRATIONS (CONTINUED)

FIGURE		PAGE
67	Lower Pendulum Head	103
68	Cam and Microswitch	105
69	Horizontal Release Assembly	106
70	Pull-Back Winch at Rear Leg	107
71	Breakaway Connector and Yaw Swivel	108
72	Safety Solenoid with Dual Position Indicator	110
73	Electric Brake Assembly	111
74	Truck/Cradle/Vehicle Assembly	112
75	Cradle Detail	114
76	Hand Pump and Slide Block Detail	115
77	Instrumentation Trailer	116
78	FIAS Control Panel	117
79	Test No. 65	120
80	Test No. 67	123
81	Test No. 68	124
82	Test No. 69, Nose-First Slide	125
83	6 DOF Coordinate System	131
84	Mark VIII FIAS, 0° Yaw, 15 Kts	132
85	Test No. 80, Acceleration vs Time	135
86	Mark VIII FIAS, 45° Yaw, 15 Kts	136
87	Test No. 82, Acceleration vs Time	139
88	Test No. 82, Angular Velocity vs Time	140
89	Mark VIII FIAS, 90° Yaw, 15 Kts	142
90	Test No. 81, Acceleration vs Time	145
91	Test No. 81, Angular Velocity vs Time	146
92	Mark VIII FIAS, 135° Yaw, 15 Kts	148
93	Test No. 79, Acceleration vs Time	151
94	Test No. 79, Angular Velocity vs Time	152
95	Mark VIII FIAS, 180° Yaw, 15 Kts	154
96	Test No. 77, Acceleration vs Time	156
97	Test No. 77, Angular Velocity vs Time	157
98	6 DOF Coordinate System	163
99	Mark IX FIAS, 0° Yaw, 15 Kts	164

LIST OF ILLUSTRATIONS (CONTINUED)

FIGURE		PAGE
100	Test No. 87, X Axis Acceleration	166
101	Test No. 87, Y Axis Acceleration	166
102	Test No. 87, Z Axis Acceleration	167
103	Test No. 87, Roll Rotation	167
104	Test No. 87, Pitch Rotation	168
105	Test No. 87, Yaw Rotation	169
106	Mark IX FIAS, 45° Yaw, 15 Kts	170
107	Test No. 89, X Axis Acceleration	173
108	Test No. 89, Y Axis Acceleration	173
109	Test No. 89, Z Axis Acceleration	174
110	Test No. 89, Roll Rotation	174
111	Test No. 89, Pitch Rotation	175
112	Test No. 89, Yaw Rotation	175
113	Mark IX FIAS, 90° Yaw, 15 Kts	176
114	Test No. 90, X Axis Acceleration	178
115	Test No. 90, Y Axis Acceleration	178
116	Test No. 90, Z Axis Acceleration	179
117	Test No. 90, Roll Rotation	179
118	Test No. 90, Pitch Rotation	180
119	Test No. 90, Yaw Rotation	181
120	Mark IX FIAS, 135° Yaw, 15 Kts	182
121	Mark IX Fias, 180° Yaw, 15 Kts	184
122	Test No. 88, X Axis Acceleration	187
123	Test No. 88, Y Axis Acceleration	187
124	Test No. 88, Z Axis Acceleration	188
125	Test No. 88, Roll Rotation	188
126	Test No. 88, Pitch Rotation	189
127	Test No. 88, Yaw Rotation	189
128	Mark VIII Bag	194
129	Mark VIII Wrapper	195
130	Mark VIII Sewing Details	196
131	Seam Construction	197
132	Mark VIII End Panel	199

LIST OF ILLUSTRATIONS (CONCLUDED)

FIGURE		PAGE
133	Mark VIII Diaper	200
134	Mark IX Bag	202
135	Mark IX Wrapper	203
136	Mark IX Tiestring Rigging	204
137	Mark IX End Panel	205
138	Mark IX Belly-Band Attachment	208
139	Slipper Tank, Cross Section	211
140	Slipper Tank, Side View	212
141	Slipper Tank, Top View	213



## SECTION I

### INTRODUCTION AND BACKGROUND

#### 1. INTRODUCTION

This report continues the documentation of an investigation of a Deployable Polyurethane Foam Impact Attenuation System (FIAS) for the surface recovery of a Remotely Piloted Vehicle (RPV). The two previous reports (Volume I and Reference 1) document the initial series of 48 tests and this report contains the results of Tests No. 49 through 91.

The objective of this investigation is to determine a technique to minimize or eliminate damage to an RPV occurring during the ground impact portion of the parachute recovery. The vehicles which were selected as the design vehicles are the AQM-34V and BGM-34C RPV's. However, the technology being developed under this program is directly applicable to the ground impact attenuation of any premeditated aerospace vehicle recovery.

#### 2. BACKGROUND AND CHRONOLOGY

In 1974 the Tactical Air Command issued an operational requirement for the ground recovery of its RPV's. Previous experience has shown both a deficiency in the Mid Air Recovery System's (MARS) ability to recover multiple RPV's and extensive damage to the vehicles which were not MARS'd and were subsequently ground recovered.

In June 1975 the FIAS was begun as a determination of the state-of-the-art of impact attenuation systems which were applicable for RPV recovery. By October 1975 the concept of using a deployable plastic foam had emerged due to advances in the state-of-the-art of foam chemistry. The period from October 1975 through January 1976 was devoted to the selection of a foam compound and initial investigation of how to inject the plastic foam into a fabric bag in a homogeneous and timely manner. On 6 February 1976 the first impact test was performed on freshly deployed foam. This 120 second operating time test (Test No. 12) demonstrated that the plastic foam could achieve the required structural properties in the allotted time. The time period from March 1976 through June 1976 was

dedicated to test preparation and procurement of equipment. Beginning July 1976 a series of tests (No. 12-24) was conducted in which the chemical mixing rates were increased to the required level of over 60 pounds per minute. A series of tests was begun in August (tests No. 25-32) to gain an initial understanding of the foam's behavior during impact. A redesigned fabric bag was tested during the August 1976 through September 1976 time period (Tests No. 33-39) in which the interaction between the foam and the bag was further analyzed.

Also in September 1976 a series of tests (No. 40-42) were conducted to determine the minimum operating time of 60 seconds which was obtainable with this system. Tests No. 43 through 48 were conducted in October 1976 on a refined bag design and resulted in the successful attenuation of a simulated 3500 lb RPV (the maximum design vehicle recovery weight). The results of the initial 48 tests were documented in Volume I in December 1976 and additional work was outlined. The feasibility of the FIAS had been established for vertical impacts but the vehicle stability during combined vertical and horizontal impacts remained. The time period of January 1977 through May 1977 was dedicated to the procurement of the testing apparatus and equipment necessary for the horizontal testing of the FIAS. In June 1977 a series of foam dispensing tests (Tests No. 49-57) were conducted to convert the FIAS foam dispensing system from the large tank, constant pressure arrangement to a simplified small tank, blow down arrangement similar to the original conceptual system. As the FIAS was now being configured for an AQM-34V vehicle application two different bag design concepts (with and without ALE-2 ECM pods) were designed and tested vertically during Tests No. 58 through 64 ending July 1977. The horizontal test facility was completed and approved for operation by the AFFDL Safety Officer on 16 August 1977. A series of procedural and instrumentation checkout tests (Tests No. 65-71) was conducted during August and early September 1977, and resulted in a refinement of the pods-off configuration. Final testing of the pods-off configuration was conducted during Tests No. 72 through 82 and was completed by mid October 1977. The testing of the pods-on configuration was conducted during Tests No. 83 through 91) and was completed on 3 November 1977.

Tests No. 1 through 48 (documented in Volume I) may be considered as the research into the how? what? and why? of an FIAS with Tests No. 49 through 91 representing the development or application of an FIAS for the AQM-34V Remotely Piloted Vehicle. The developmental investigation documented in this report represents approximately 13,000 manhours of effort performed on an in-house basis within the AFFDL with the assistance of a test support contractor.

## SECTION II

### FOAMING SYSTEM AND FOAMING TESTS NO. 49-57

#### 1. INTRODUCTION

The foaming system (tanks, chemical, and mixing head) to be used in this phase of the FIAS program was based on small, blow-down tankage as opposed to the large (125 gallon) constant pressure system used in the early phases of investigation. The foaming system was a commercially available unit modified for the high flow rates required by the FIAS (reference Volume I) and as such represented a breadboard style FIAS foaming system. Some difficulties were noted during testing which were believed to be caused by this unrefined state of development and which should be eliminated in the prototype stage. A series of nine tests (No. 49-57) were required to verify the foaming system's ability to meet the FIAS requirements.

#### 2. FOAMING SYSTEM DESCRIPTION

a. The foaming system used in this phase of the FIAS investigation was based on small, blow down, tankage in which the only mechanical action required was the opening of two valves. Once the valves were opened the foam mixing continued until the chemicals were exhausted and the driving gas pressure reduced to ambient. A complete description of the method of operation and the foaming system requirements is contained in Volume I, Sections V, VII, and IX, but in summary form the FIAS foaming system requirements were to produce 25 cubic feet of a one pound (per cubic foot) polyurethane foam within a dispensing time of thirty seconds and with an operating time from initiation of foaming to hardened foam of 60 seconds.

b. The FIAS foaming system used in the IRON PIG testing is shown in Figure 1. Only one side of the system (one component) is illustrated because both sides are identical insofar as hardware is concerned. Table 1 lists the individual parts description with the total system weights. The foaming system was assembled in place with the 1/8 inch tubing passing through small holes drilled in the skin of the IRON PIG



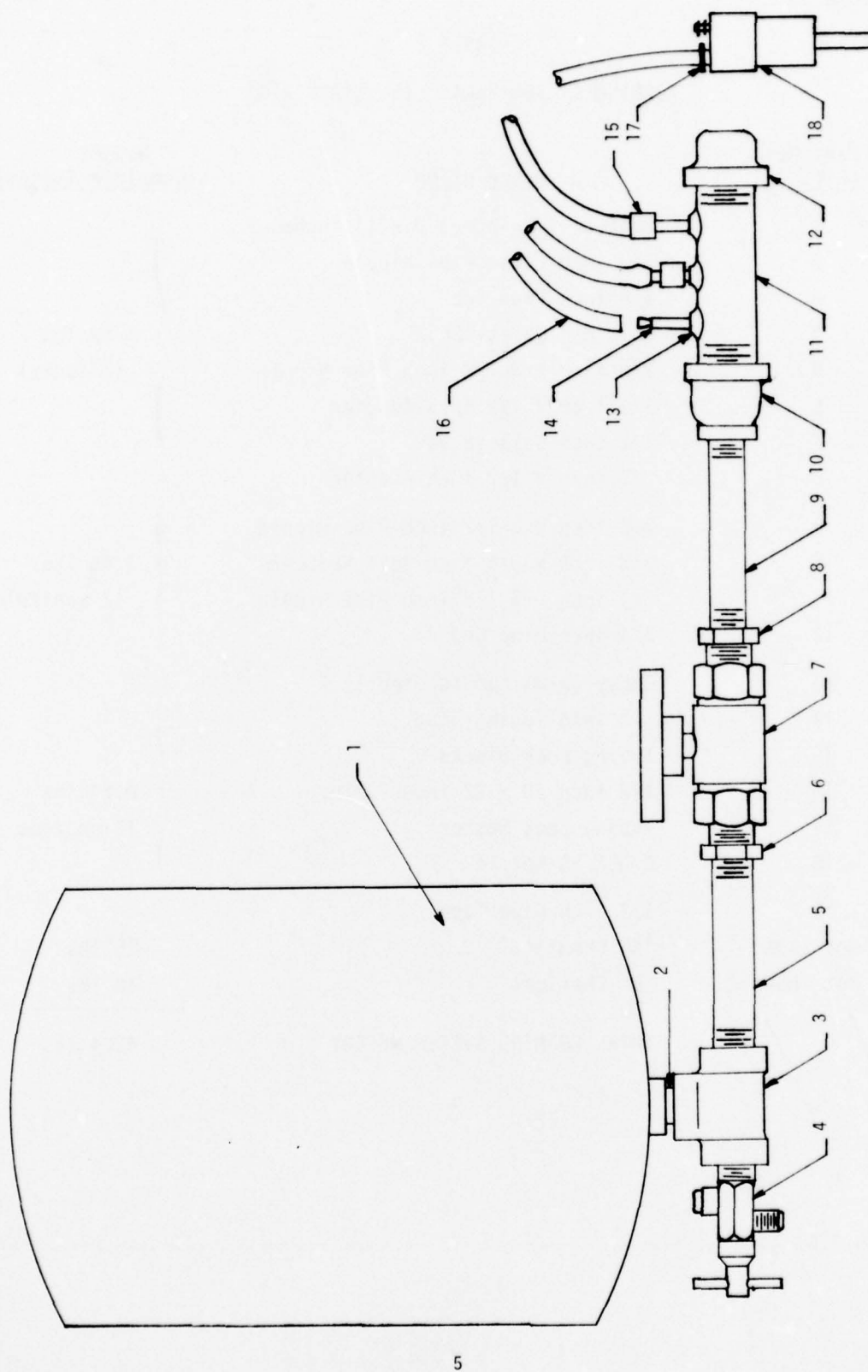


Figure 1. FIAS Breadboard Foaming System

TABLE 1  
FOAMING SYSTEM PARTS LIST (IRON PIG)

<u>Part No.</u> <u>(Fig. 2)</u>	<u>Description</u>	<u>Weight</u> <u>(Complete System)</u>
1	Tank, 7-1/2 inches D x 11 inches H	} 9.40 lbs (2 tanks)
2	3/8 inch Close Pipe Nipple	
3	3/8 inch Pipe Tee	
4	3/8 inch Safety Spud	
5	3/8 inch x 3-1/2 inch Pipe Nipple	
6	3/8 inch x 1/2 inch Adapter	
7	1/2 inch Ball Valve	
8	3/8 inch x 1/2 inch Adapter	
9	3/8 inch x 3-1/2 inch Pipe Nipple	} 1.46 lbs (2 manifolds)
10	3/8 inch x 3/4 inch Bell Reducer	
11	3/4 inch x 3-1/2 inch Pipe Nipple	
12	3/4 inch Pipe Cap	
13	Epoxy (aluminum to steel)	} 0.54 lbs 12 nozzles
14	1/8 inch Tubing Stud	
15	Tubing Lock Blocks	
16	1/8 inch ID x 22 inch Tubing	
17	Tubing Lock Washer	
18	0.062 NS Nozzle	
19	1/2 inch Pipe Tape	
Not shown	"A" Chemical	15 lbs
Not shown	"B" Chemical	16 lbs
TOTAL FOAMING SYSTEM WEIGHT		42.4 lbs

test vehicle (see Section IV) so that the nozzles were located at the bottom center of the vehicle. This passageway for the tubing was a simple curve for the IRON PIG installation and no mixing anomalies were noted. Initially the A chemical tank contained 12.9 pounds of chemical; however, as of Test No. 56 this was increased to 15 pounds. The B tank initially held approximately 14 pounds of chemical and this was also increased to 16 pounds as of Test No. 56. The system described here was purchased in June 1977 at a cost of approximately \$200.00 per foaming system.

c. The foaming system used in the IRON TURKEY (see Section V) testing (Tests No. 65-91) was identical to the IRON PIG version from the tank down to the ball valve. The handle of the ball valve was removed and the valve stud inserted into a modified Jamesbury, Model EL-20, 115 V. AC. valve actuator for remote control operation. To accommodate the geometry of the IRON TURKEY test vehicle the foaming system plumbing between the ball valve and manifold assembly was changed to include a plumbing union and a 90° turn (Figure 2).

The 1/8 inch tubing passageway in the IRON TURKEY was more circuitous than in the IRON PIG and caused the tubing to occasionally become kinked during installation. Although care was taken in the installation of the foaming system, it is believed that this problem led to a number of poor mixing incidents wherein at least one nozzle was deprived of a clean chemical flow.

### 3. IMPROPER OPERATION OF FOAMING SYSTEM

a. There exists a set of conditions whereby the improper operation of the foaming system can start a chain of events which can lead to the autoignition of the foam bag. The required conditions for autoignition are that a quantity (minimum size unknown) of unmixed chemical A exist in the center of a large homogeneous mass of foam and that the foam be undisturbed (i.e., uncrushed) for a relatively long period of time during the exothermic reaction. The presence of unmixed chemical A can be caused by the severing or kinking of a chemical B nozzle feedline (the 1/8 inch tubing) which would result in a nozzle being fed only chemical A.

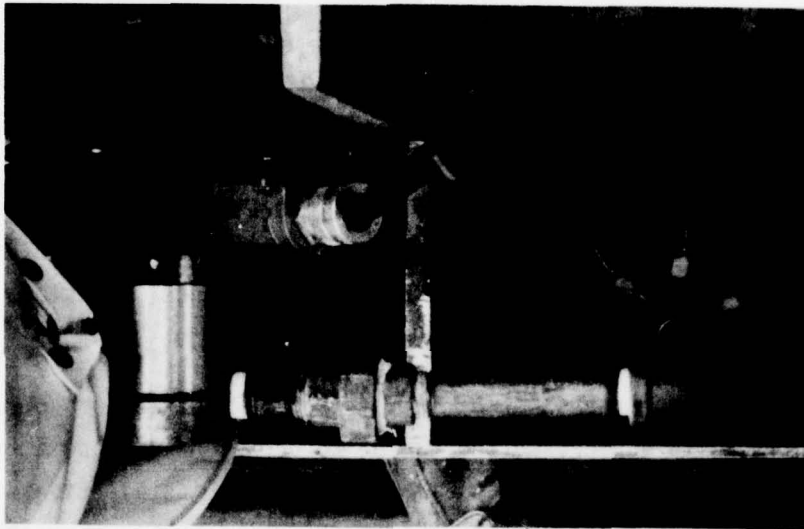


Figure 2. Installed Foaming System



Foreign matter in B tank could also reduce the flow to a nozzle by blockage. The second condition for autoignition is the large homogeneous mass of foam required to sustain the thermal gradient leading to autoignition. Although in the FIAS testing the foam is crushed to a considerable extent there may still remain areas of foam which are relatively intact and large enough to support the required thermal gradient. These two conditions for autoignition of the foam in this manner were met in Tests No. 35, 67, 76, 77, and 78. On 30 August 1977 a training demonstration was conducted to quantify the hazard resulting from allowing the autoignition process to go to completion. With the help of the WPAFB Fire Department a 40 cubic foot bag of polyurethane foam was deliberately set afire. The bag was reduced to ashes within three minutes from ignition and the fire produced temperatures in excess of 1200°F together with large quantities of dense black smoke.

b. The measures which should be taken to prevent the autoignition and/or ignition of the FIAS foam bag are:

(1) The foaming system should be designed so that all of the chemical A is mixed with an excess of chemical B.

(2) The foam mass should be contained within a relatively airtight bag which should be fire resistant up to at least 600°F to prevent ignition from an external source.

It is believed that the incidents which occurred in the FIAS testing happened due to improper mixing of the chemicals caused by the breadboard foaming system.

#### 4. FOAMING SYSTEM PRELIMINARY TESTING

##### a. Test No. 49

Test No. 49 was a foaming test conducted on 24 May 1977 to verify the dispensing flow rates of the new, blow-down, tankage system. The foaming system was configured with 6 nozzles at a nominal tank pressure of 225 psig. The tanks emptied in 32 seconds into a plastic bag and produced an acceptable quality of foam.

b. Test No. 50

Test No. 50 was conducted on 25 May 1977 and was to be the first impact test of the Mark I bag design. The IRON PIG test vehicle was ballasted to a weight of 2000 pounds and was released from a height of 5.2 feet for a total energy of 10450 ft-lbs. The test vehicle rotated violently and all instrumentation was lost. It was noted that only 19 pounds of foam had been produced but the cause of the erratic behavior of the foaming system was unknown.

c. Test No. 51

Test No. 51 was conducted on 27 May 1977 as a repeat of Test No. 50 after a thorough checkout of the test equipment. The impact test was uneventful but it was noted that only 18 pounds of foam had been produced. It was concluded that further testing of the foaming system should be accomplished before further impact testing.

d. Test No. 52

Test No. 52 was conducted on 31 May 1977 in order to determine the quantity of foam being produced by the blow-down tankage arrangement and to verify the "short fills" of the prior two tests. The nozzles were secured within a large plastic bag so that no foam could escape and be lost to weighing. The result was that the nozzles became unfastened, pulled out of the bag, and sprayed foam over the test facility, and the project engineer. This spatial distribution made it impossible to weigh the foam produced and the test would have to be repeated after a cleanup period.

e. Test No. 53

Test No. 53 was repeat of the earlier yield Test No. 52 and was conducted on 13 June 1977. In Test No. 53, 12.90 pounds of chemical A were mixed with 13.37 pounds of chemical B for a total chemical weight of 26.27 pounds. Weighing the resulting mass of foam produced a somewhat surprising result, in that only 17.5 pounds of foam were produced from 26.27 pounds of chemicals. After consultation it was hypothesized that the nozzle plume impingement on the expanding foam mass was causing

severe cell wall damage and that excessive amounts of Freon gas (the expansion agent) were thus escaping into the atmosphere causing the 8.7 pound change in weight.

f. Test No. 54

Test No. 54 was conducted on 15 June 1977 as an attempt to investigate the excessive cell breakage hypothesis. In this test the foaming system was configured with a single nozzle with only a 0.038 inch intake orifice. This arrangement gives a flow rate of approximately 1.4 pounds per minute and would give maximum control of the plume impingement. The foam was manually sprayed in a wide pattern in such a manner that the nozzle plume never impinged on expanding foam. In this manner the maximum yield should have been obtained. After a fifteen minute spraying session it was determined that 24.2 pounds of mixed chemicals had yielded 21 pounds of foam for a yield by weight of 86%.

g. Test No. 55

Test No. 55 was conducted on 21 June 1977 as a confirmatory yield test. After extensive consultation the manufacturer loaned their research chemist to the FIAS investigation. A conclusion of this test was that the chemicals were giving a weight yield of approximately 80-85% with the missing weight being caused by escaping Freon gas. In addition it was determined that the B tank had an unusually large fluctuation in the amount of chemicals contained on a tank-to-tank basis. After discussions with the manufacturer it was determined that a quality control weighing scale on the B tank filling line at the manufacturer's plant had malfunctioned and caused a tank-to-tank weight variation of as large as  $\pm 2$  pounds. The two parts of this problem were solved by first determining what chemical amounts were required to produce the 25 pounds of foam needed and then refilling the remaining sets of chemical tanks to the new chemical loads and pressures.

h. Test No. 56

Test No. 56 was conducted on 22 June 1977 as a foam system yield test. Based on the 80-85% yield previously noted a set of tanks had

been refilled and repressurized so that 31 pounds of chemicals initially at 240 psig would be dispensed. This arrangement yielded 24.8 pounds of foam with a flow-down time of 120 seconds using 6 nozzles and resulted in a final pressure of 30 psig on the A tank. Based on these results it was determined that an initial pressurization of 280 psig and a 12 nozzle configuration (similar to the 6 nozzle configuration) should yield the 25 pounds of foam with a 30 second blow-down time as required for the FIAS. Accordingly the remaining tanks were refilled and repressurized on a makeshift assembly line set up in the IRON PIG test facility.

i. Test No. 57

Test No. 57 was conducted on 30 June 1977 as a confirmatory yield/bag deployment test. A set of refilled, repressurized tanks was used to deploy a Mark I bag (see Section III) to determine blow-down time and bag shape after deployment. The results were that the foaming system met the FIAS requirements with satisfactory bag deployment.

5. SUMMARY

Following Test No. 57 the foaming system was considered ready for vertical impact testing of the Mark I and Mark II bag designs. The following lessons learned are based on this experience with the breadboard foaming system and were incorporated into the prototype slipper tank FIAS design.

a. The chemical A (isocyanate) shall always be mixed with an excess of chemical B (polyols).

b. The polyurethane chemicals used (A and B) give a foam yield by weight of 80-85% due to the escaping Freon gas.

In addition to these guidelines the difficulties encountered with the kinking of the flexible nozzle feedlines in the breadboard foaming system were to be designed out of the FIAS prototype for the AQM-34V RPV application.



### SECTION III

#### BAG DESIGNS

##### 1. OVERVIEW

This phase of the FIAS investigation is concerned with the adaptation of the FIAS to the AQM-34V Remotely Piloted Vehicle (RPV). The AQM-34V is currently undergoing a similar attenuation investigation using an air-bag approach and as a result much of the preliminary integration work has already been accomplished for this vehicle (Reference 2). This integration work is considered as a given parameter in the FIAS adaptation effort. The knowledge gained from the initial phase of the FIAS investigation (Volume I) was used to design two different FIAS bag concepts: with and without pods. These concepts were tested in both the vertical and horizontal modes with relatively minor modifications being incorporated in their design in an evolutionary process. For clarification the bag design for use with pods on was initially named the Mark I bag. As each modification was introduced and sent for fabrication the name was changed so that the Mark I bag evolved as the Mark I, Mark III, Mark IV, Mark V, and finally the Mark IX. Similarly the bag designed for use without pods started as the Mark II design and evolved through the Mark VII into the final Mark VIII configuration. The Mark VI nomenclature was used for the tailbag. Although this nomenclature tends to be confusing it was necessary to adopt this system to keep the bag fabricators and bookkeepers cognizant.

##### 2. VEHICLE RECOVERY CONFIGURATIONS

a. The vehicle to which the FIAS is to be adapted is the AQM-34V RPV as shown in Figures 3, 4, and 5. The nominal recovery configuration is with the ALE-2 or ALE-38 chaff pods mounted on the wing pylons as shown. These pylons are mounted at 3° nose down relative to the RPV's longitudinal axis. This mounting arrangement results in the pods hanging below the engine nacelle and contacting the ground first in an unprotected ground landing. A laboratory investigation has determined the feasibility of removing these pods prior to ground impact (and this current FIAS investigation later determined the advisability of so doing).

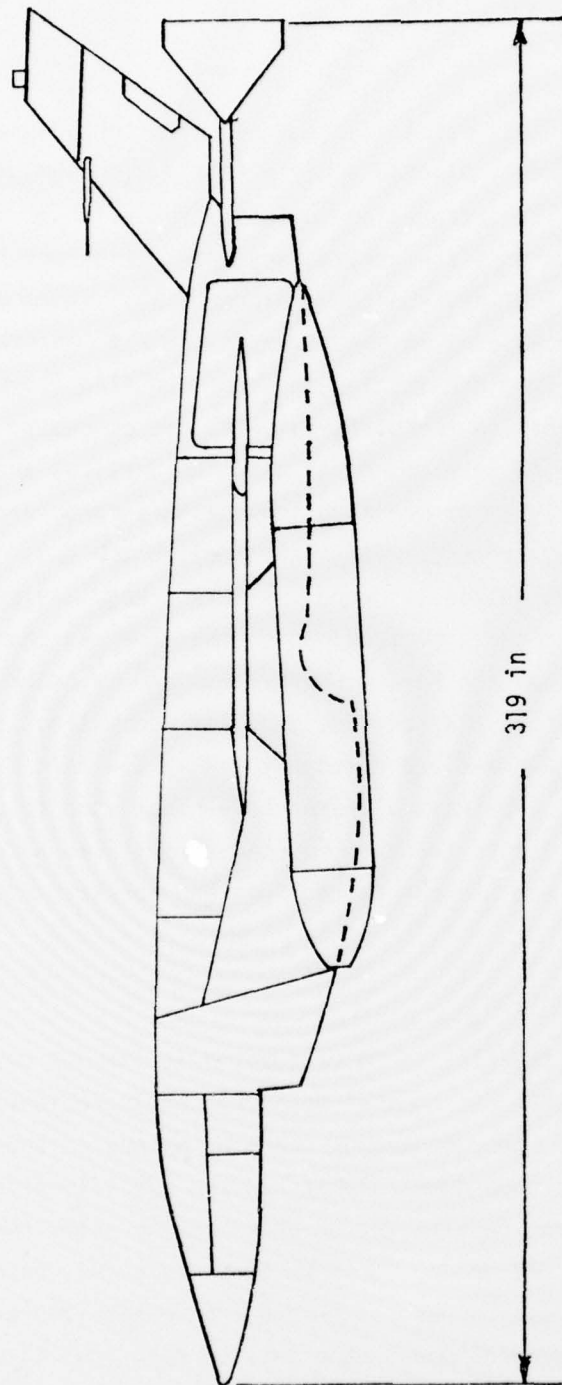


Figure 3. AQM-34V RPV with AN/ALE-2 Pods

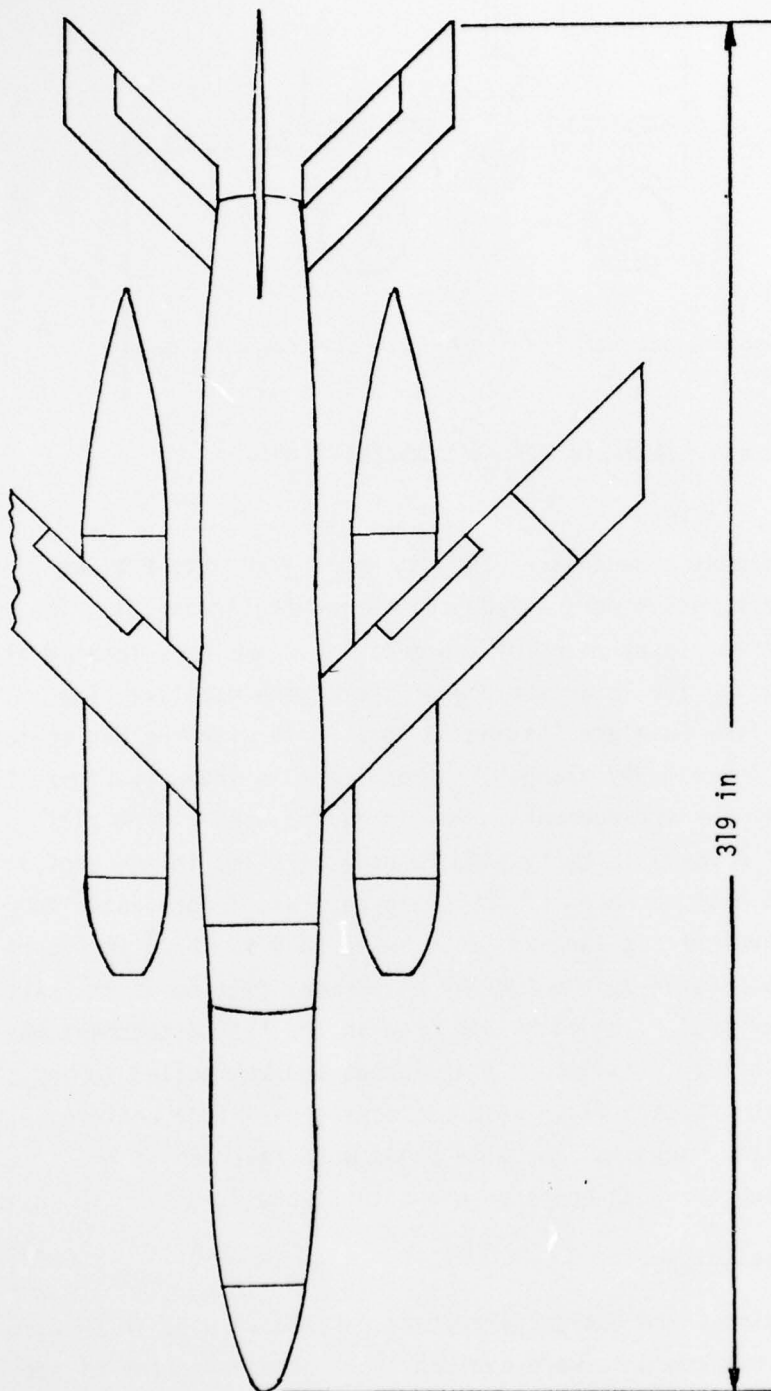


Figure 4. AQM-34V RPV with AN/ALE-2 Pods

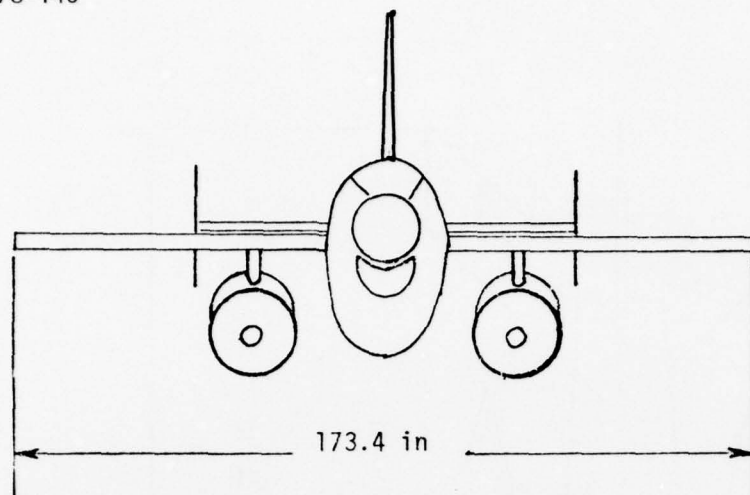


Figure 5. AQM-34V RPV with AN/ALE-2 Pods

b. The attachment between the FIAS bag and the AQM-34V RPV was provided by the integration work already performed (Reference 2). The vehicle/bag attachment is by means of two metallic clamp bars located at butt line  $\pm 9$  inches on the lower surface of the engine nacelle. The clamp bars extend from Fuselage Station 35 to F.S. 75 with the bag centerline at F.S. 55. The AQM-34V clamp bar arrangement is shown in Figure 6 with the FIAS clamp bar arrangement shown (installed with a Mark VIII bag) in Figure 7. A metallic belly band running parallel to the vehicle Y axis and supported at each end of the clamp bars was incorporated to support the longitudinal bag forces. This belly band is shown in Figure 7 and was later incorporated in the AQM-34V attachment fitting as the airbag investigation progressed. The clamp bar used in the FIAS attachment was mild steel, 3/16 inch x 1-1/4 inches x 42 inches and was bolted to the engine nacelle with 1/4 inch flush head cap screws on 4 inch centers. The ends of the clamp bars and the belly bands were fastened to the engine nacelle using 1/2 inch bolts as shown in Figure 7.

### 3. BAG DESIGN PARAMETERS

a. The guidelines and design parameters which were used in the design of the two bag concepts were derived from the experiences of the initial series of 48 tests. Using these bits and pieces of data and



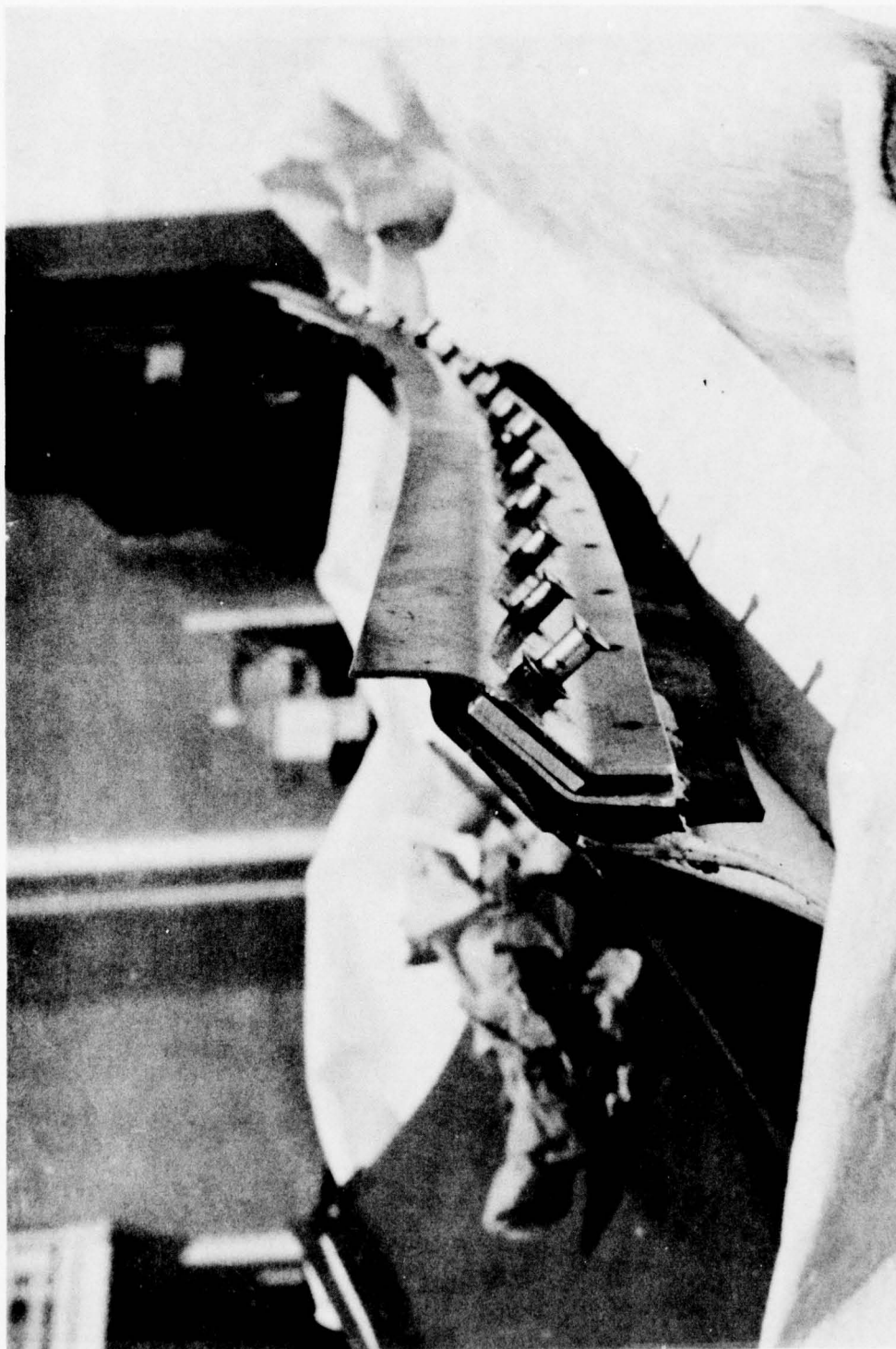


Figure 6. AQM-34V Clamp Bar

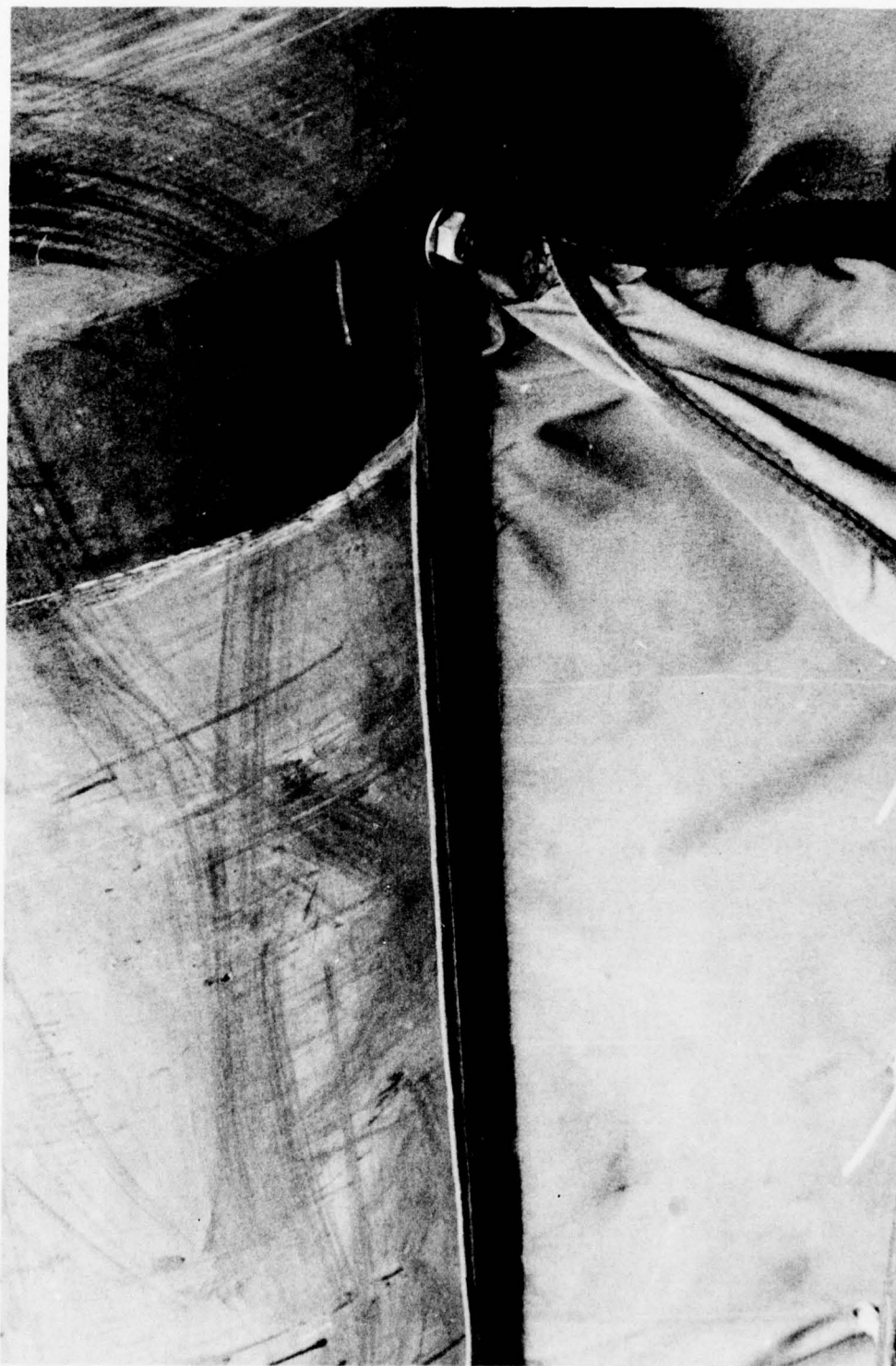


Figure 7. FIAS Clamp Bar

theory an inductive reasoning process was used to design the initial Mark I and Mark II bags. Although future, more extensive, investigation may render the bag design process a deductive exercise, the state-of-the-art as described below still applies to this current investigation:

State-of-the-Art

"... attenuation system designs frequently evolve from the experience of individual designers. Design concepts often reflect personal preferences and include features which affect landing performance in, at best, only a partially understood manner."

NASA Monograph, 1970

By combining some known parameters, some hypothesized theories, and some engineering judgment, together with extensive full-scale testing, the bag designs were evolved into workable systems.

b. The following design parameters were considered as knowns in the bag design process.

(1) The AQM-34V RPV possessed a maximum vertical energy level of 27,200 ft-lbs at the full pods weight condition of 3230 pounds.

(2) The AQM-34V RPV in the pods-off weight condition of 2000 pounds possessed a vertical energy level of 10,450 ft-lbs.

(3) Twenty-five cubic feet of the one pound per cubic foot polyurethane foam was capable of attenuating 28,000 ft-lbs.

(4) It was known that the vertical impact test represented a worse case condition for the bag energy attenuation process. In the vertical testing all the vertical energy was transmitted into the bag during the initial impulse. In the horizontal testing to follow some of the vertical impact energy would be transferred into a pitch rotation of the vehicle and into other angular and linear 6-DOF movements. This transformation of the vertical energy results in a lesser amount of energy being transmitted into the main bag during the initial impulse than in the vertical test condition.

(5) The bag attachment fitting and hence the initial bag/vehicle contact area were specified as part of an integration analysis. Additionally the geometric constraints posed by the presence of the pods were known.

(6) The primary stress axis of the generic FIAS bags was known to be perpendicular to the vehicle longitudinal axis and a rudimentary understanding of the total bag stress distribution had been obtained from earlier testing.

c. The data from the earlier 48 tests had been hypothesized into a theory which sought to predict the bag force versus bag deflection (hence energy transmittal). The following procedures and assumptions were used in this effort to predict the bag performance.

(1) A total bag volume of uncrushed foam was selected. In this investigation a volume of  $25 \text{ ft}^3$  was chosen for this volume (called  $V_1$ ).

(2) A bag shape was selected for analysis. The important features of this shape are the total depth (allowable stroke), initial contact area and total volume.

(3) Based on the bag shape and the impacting vehicle's shape an estimate of the contact area versus deflection distance is made. In this instance where the vehicle geometry is a cylinder crushing into a bag of some shape the projected area (vertical axis) is used as the basis for design.

(4) Based on the contact area versus deflection curve, a curve of volume crushed ( $V_2$ ) versus deflection curve may be obtained.

(5) The foam compressive stress is hypothesized as behaving as if it were a perfect gas initially pressurized at its mechanical compressive stress level at its initial volume. In this instance the foam properties are a compressive stress of between 5 and 5.5 psi at an initial volume ( $V_1$ ) of  $25 \text{ ft}^3$ . A range of compressive stress properties is specified because the foam has a rated stress of 5 psi perpendicular to



the direction of rise and 5.5 psi parallel to its direction of use. In the FIAS application these two directions are somewhat random in regards to the direction of crush.

(6) The foam's pressure versus deflection curve can be obtained through the use of the perfect gas law.

$$P_2 = \frac{V_1}{(V_1 - V_2)} P_0$$

where  $P_2$  = pressure at a deflection level  
 $V_1$  = initial bag volume  
 $V_2$  = volume crushed at the deflection level  
 $P_0$  = initial foam pressure (5 -5.5 psi)

(7) The bag force versus deflection curve can now be obtained by multiplying the contact area versus deflection and the apparent pressure versus deflection curves.

(8) The energy transmitted to the bag versus deflection distance can now be computed by integrating the force versus deflection curve (force through a distance).

(9) Once the energy versus deflection curve is computed the bag performance for any given impact condition (energy level) is readily obtained. Starting with the total impact energy level the maximum force (hence acceleration) and bag deflection may be read off the plots. This is shown for a general case in Figure 8. Some possible defects in this theory are that the stretching of the bag is not taken into consideration and that the foam is capable of sustaining apparent pressure gradients due to its shear stress capability.

d. It had been determined that the fabric bag was capable of storing a portion of the impact energy in the form of fabric stretch and then returning this energy to the vehicle resulting in excessive rebound and bouncing. It was theorized that this energy storage mechanism could be designed out of the problem by a careful consideration of the required

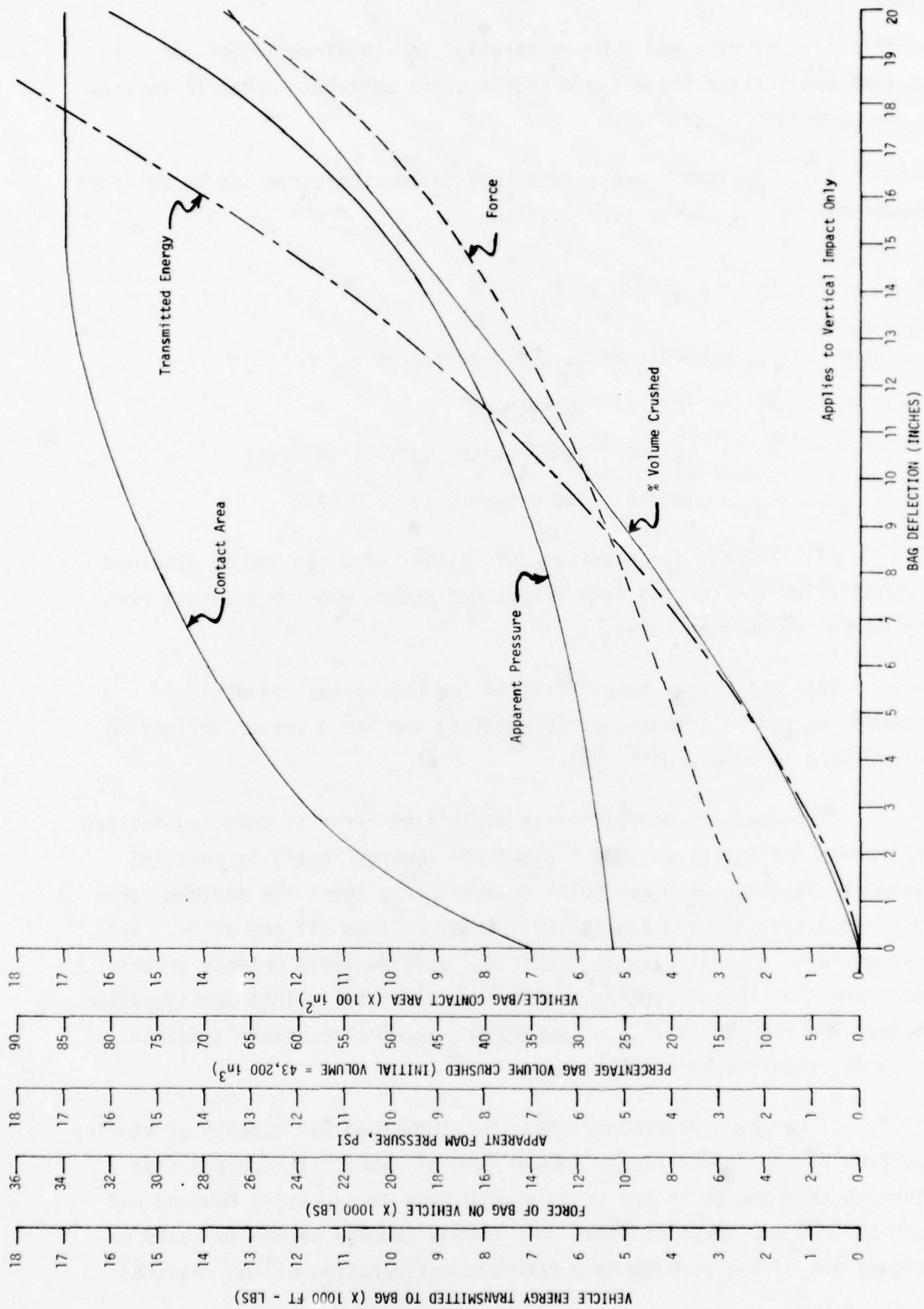


Figure 8. Theoretical Performance of Mark VIII FIAS Bag

bag circumference versus deflection during the crushing phase. Because the major stress axis was perpendicular to the longitudinal axis of the vehicle and because this appeared to be the major energy storage location (maximum stress = maximum strain energy) the problem could be reduced to the circumference in a cross-sectional plane. The circumference of the uncrushed bag in any cross-sectional plane must be equal to or larger than the circumference of the crushed bag in the same cross-sectional phase. In this manner "fullness" was designed into the bag in order to prevent excessive fabric strain and subsequent rebound due to the fabric energy storage mechanism.

e. Since the purpose of the FIAS bag is to provide a stable slideout cradle for the horizontal slideout of the RPV as well as the attenuation of the vertical energy, the question of how to design a bag for sliding over a random terrain at random yaw angles arose. Engineering judgment indicated that the vehicle center of gravity should be kept as close to the ground as possible for stability. The bag should form large foam shoulders which wrap around the engine nacelle, as an aid to roll stability, and the bag should have a large footprint area to minimize the surface bearing pressure. Colloquially, the final bag shape should resemble a large hot dog bun with a flat bottom cradling the RPV engine nacelle in such a manner that the engine nacelle would never come in direct contact with the ground. This design philosophy of a hot dog bun shape was followed as far as possible giving consideration to the geometric constraints of the "pods on" recovery configuration. The presence of the pods indicated that not only should the engine nacelle be prevented from touching the ground but that the pods should also be kept off the ground to prevent excessive loading of the wing pylons and wing structure.

#### 4. PODS-ON BAG DESIGN

a. The previously stated design guidelines were utilized in the design of a FIAS bag for use with the pods mounted on the wing pylons. This bag design originated as the Mark I bag and then evolved through the Mark III, Mark IV, and Mark V design changes into the final Mark IX design. The detailed design layouts and fabrication requirement of the

Mark IX bag are contained in Appendix A and only a general discussion will be presented here.

b. The general geometry of the Mark IX bag is shown in Figure 9. The 27,200 ft/lb energy level required a thirty inch bag height based on a volume of 25 ft<sup>3</sup>. The top of the bag is sized to fit the engine nacelle attachment points. The bag length of 40 inches is about the maximum length which can be securely fastened by the 40 inch clamp bar attachment fittings. The bag width of 40 inches is the maximum that can be obtained with the pods on board the vehicle. The bag wrapper is a single piece of cloth which is seamed together between the attachment flaps. In this manner there are no seams or splices along the major stress axis of the bag. The girdles serve to both carry the horizontal stress across the bag ends as well as to maintain the bag crushed shape within the 40 inch width constraint posed by the pods. The expansion pleats in the bag ends serve to allow fullness in these localized areas. The longitudinal reinforcing bands transmit loading from the bag lower surface into the metallic bag attachment belly bands and thus reduce the stress at the corners of the bag attachment flaps.

c. Although this bag geometry performed quite adequately in the vertical testing there were reservations about its ability to perform in an oblique horizontal impact. This concern arose from the angle of the velocity vector during a 90° yaw impact condition. At first contact with the ground the lower surface of the bag essentially stopped moving due to frictional forces, while the upper surface tended to follow the velocity vector. It was not known to what extent the foam's shear stress would keep the bag from deforming in shear and coming into contact with pods. As long as the velocity vector yaw angle was longitudinal (0° or 180° yaw) there was no interference with the pods. But a yaw angle of 90° with a high horizontal velocity vector could possibly push the bag over into the pods. The worst case test condition for this configuration is with the vehicle being recovered with empty pods in a 15 knot drift rate at a 90° yaw angle. This condition gives the lowest vertical velocity component coupled with the 15 knot horizontal drift rate as shown in Figure 10.



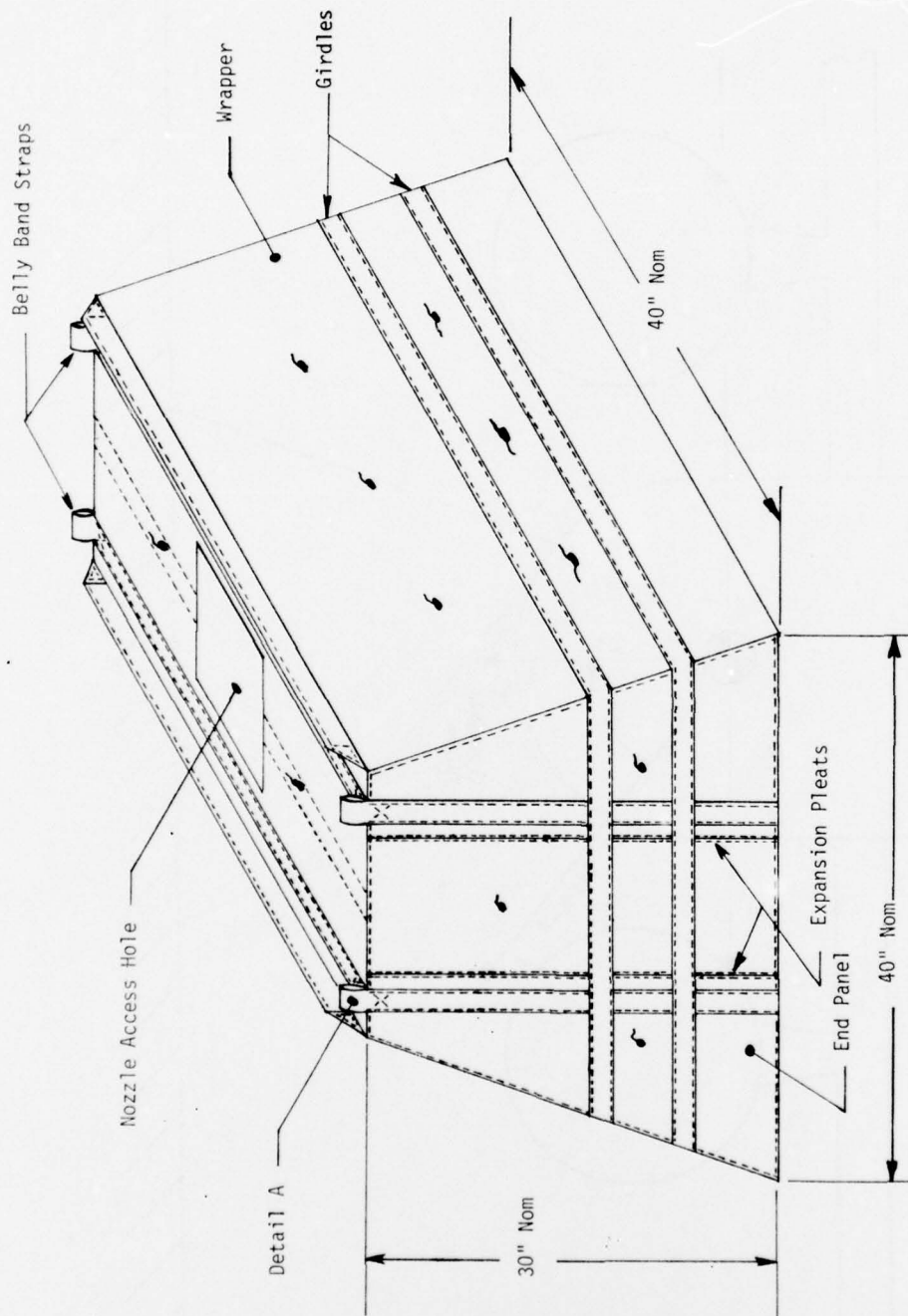


Figure 9. Mark IX Bag

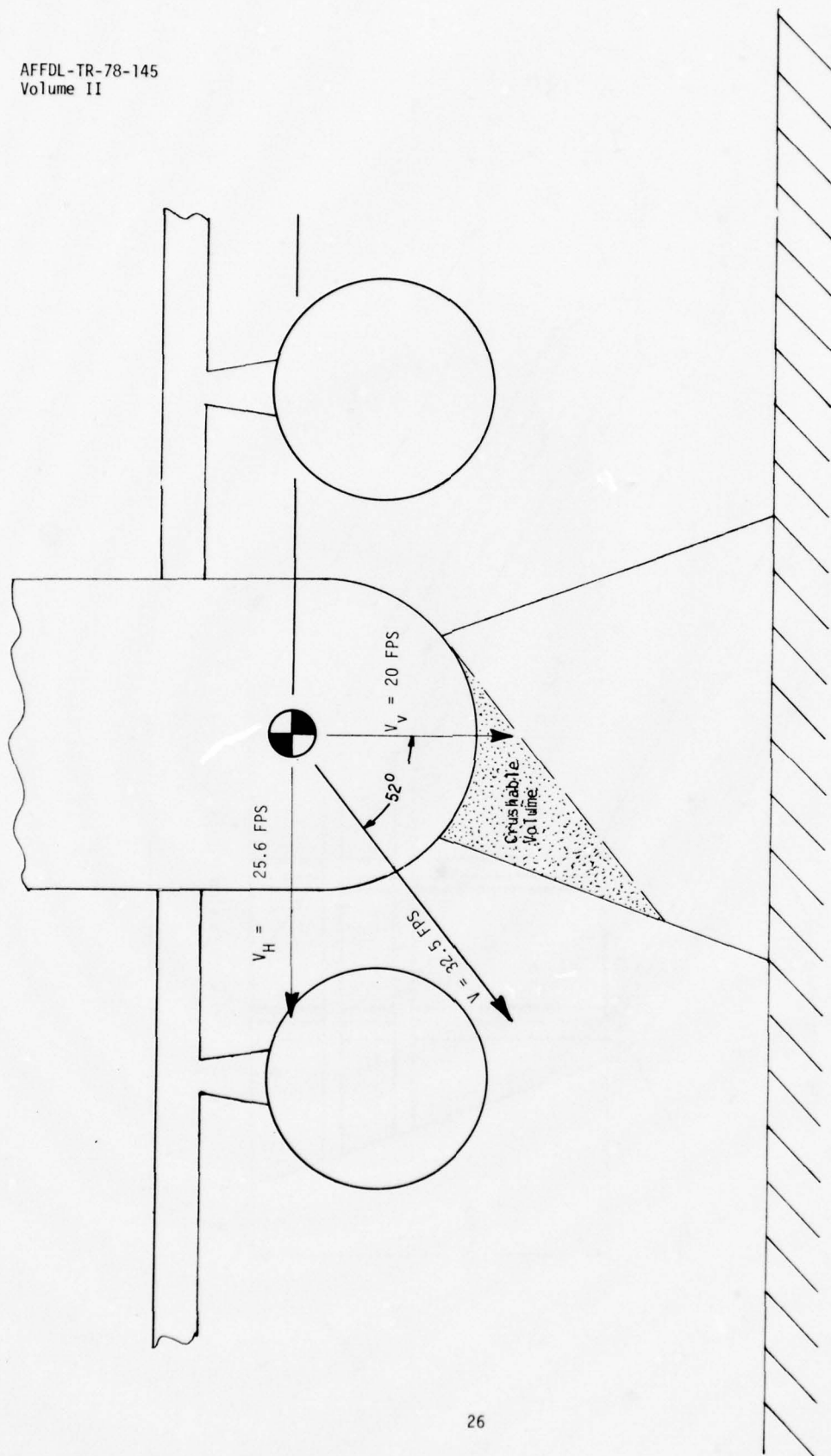


Figure 10. Mark IX Misalignment

This misalignment of approximately  $52^\circ$  between the velocity vector and the centerline of the bag causes the engine nacelle to literally "miss" the bag. The bag crushed shape for a vertical impact (Test No. 83) is shown in Figure 11. The result of the severe vector misalignment is shown in Figure 12 (Test No. 90) in which the worst case conditions for this misalignment problem (see above) were tested. Although the foam did exhibit some shear resistance, the bag still contacted the pod. Solutions to this problem of not loading the pods while maintaining the bag under the engine nacelle were not readily obvious and were not pursued during this phase of the FIAS investigation.

#### 5. PODS-OFF BAG DESIGN

a. The design guideline presented in part 3 of this section were used in the design of a FIAS bag for use with the pods removed from the wing pylons. The pods were considered as having been either jettisoned and recovered under a separate pod recovery system or as having been lowered on long tethers so that they struck the ground some time before the main vehicle and thus were not part of the ground impact attenuation problem. This bag design was originally known as the Mark II bag and it evolved into the Mark VII and finally the Mark VIII bag design. The detailed design layout and fabrication requirements for the Mark VIII bag design are contained in Appendix A and only a general description will be included here.

b. The general arrangement of the Mark VIII bag is shown in Figure 13. This bag has the same engine nacelle attachment fittings as the Mark I series and is also 40 inches long. Because this bag was designed for use without pods it has a total width of 60 inches. The lightened vehicle (without pods) requires only a 20 inch bag depth to accommodate the 10,450 ft-lbs of impact energy based on a bag volume of  $25 \text{ ft}^3$ . Essentially the "extra" foam was used to create the foam shoulders for additional slideout stability. The modification distinguishing the Mark VIII bag from the initial Mark II bag is the longitudinal diaper which was added to transmit the longitudinal slideout loads into the vehicle structure and thus bridge around a stress concentration at the corners of the bag attachment flaps.

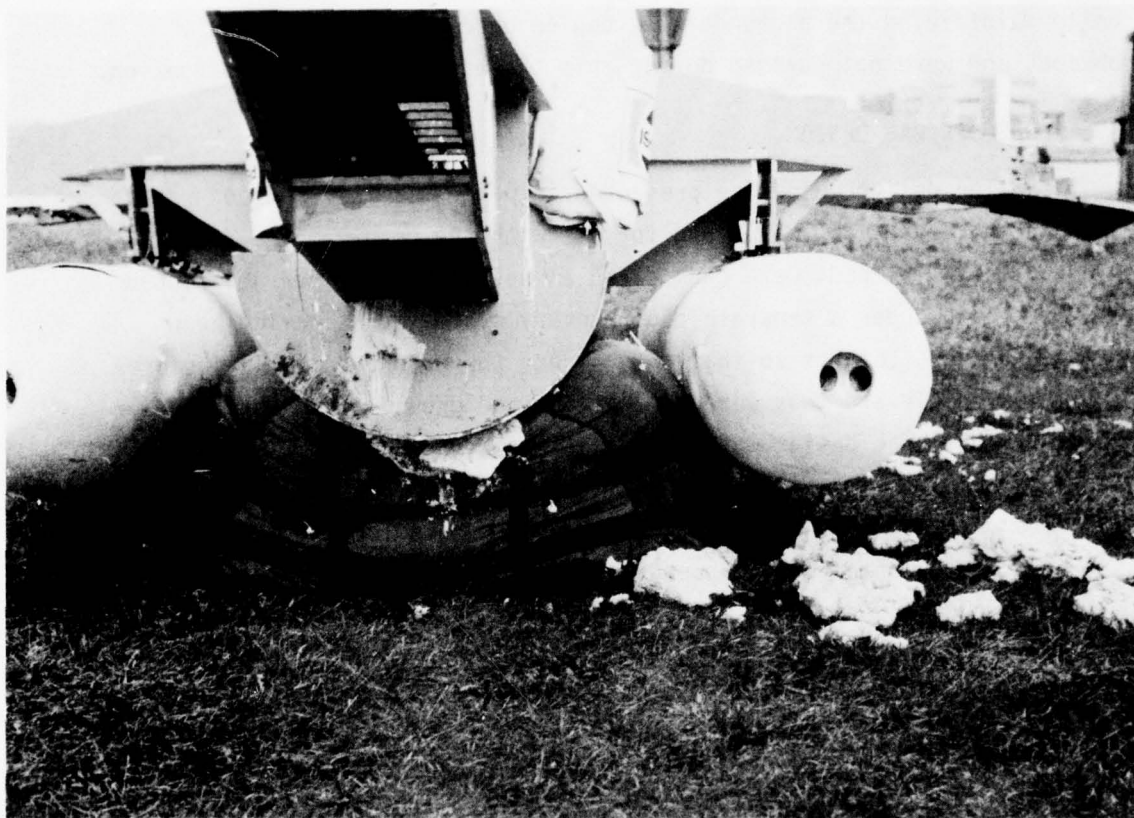


Figure 11. Bag Shape, Test No. 83





Figure 12. Bag Shape, Test No. 90

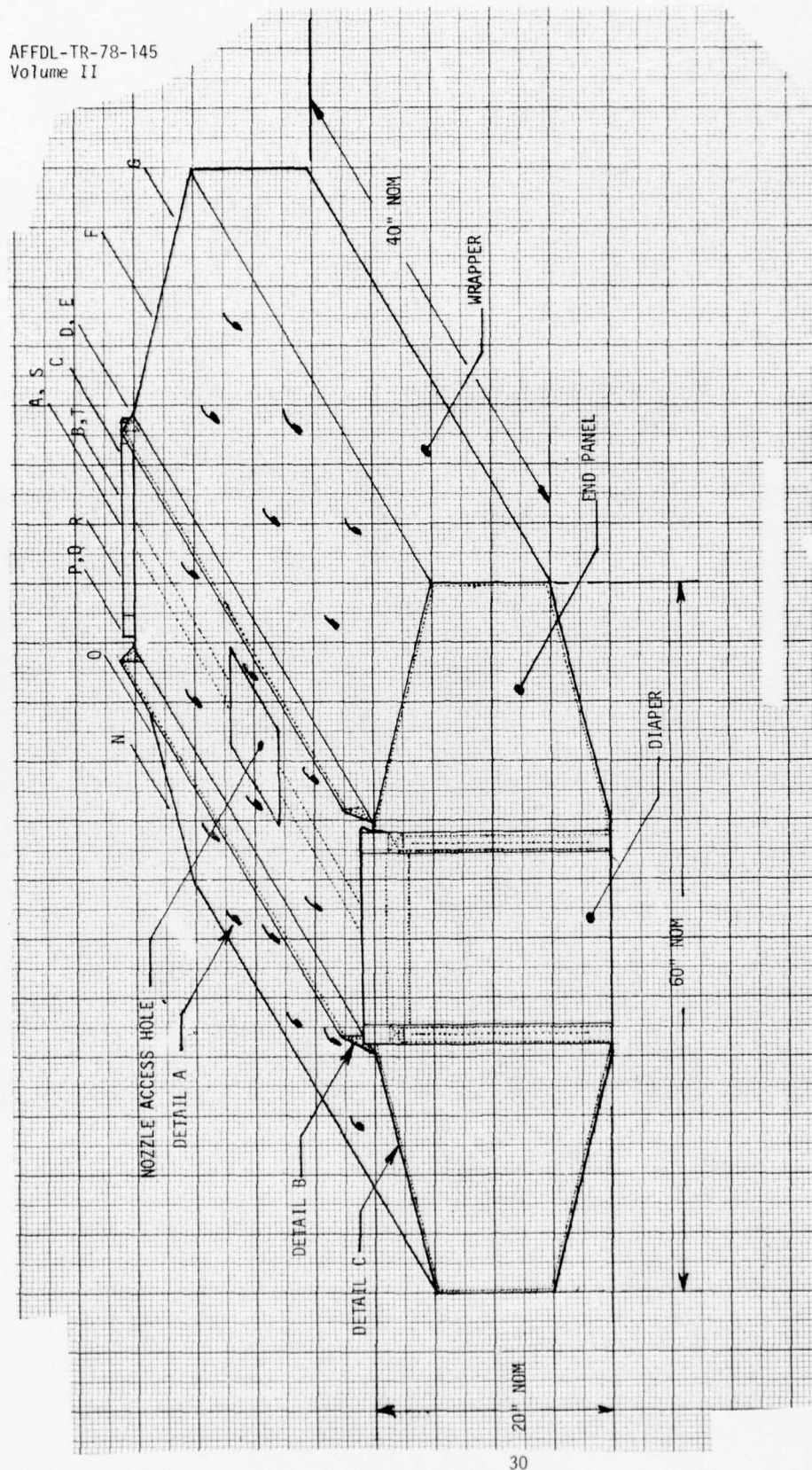


Figure 13. Mark VIII Bag

c. The large foam wings in the Mark VIII design served to aid the performance in high oblique angle impacts. Again, the worst case of velocity vector misalignment occurs in a 15 knot drift at a  $90^\circ$  yaw angle as shown in Figure 14. Due to the lightened weight of the vehicle the misalignment is approximately  $54^\circ$  between the velocity vector and the bag centerline. The bag wings, however, compensate for this misalignment and as shown in Figures 15, 16, and 17 form a "leading edge foam shoulder" even at this high misalignment angle. Test No. 81 shown in the pictures was at the worst case conditions of 15 knots drift rate at a  $90^\circ$  yaw angle. Although the bag is bulged out on the trailing side of the engine nacelle a substantial leading edge shoulder has been formed in front of the engine nacelle. The hot dog bun shape is clearly evident in Figure 15 where the test conditions were a 7-1/2 knot horizontal drift at  $180^\circ$  yaw. The Mark VIII bag design proved successful at forming the desired foam cradle and thereby preventing the engine nacelle from coming into contact with the ground.

#### 6. TAIL BAGS DESIGN

Because the center of the main FIAS bags was at F.S. 55 while the vehicle center of gravity lie between F.S. 78 and F.S. 80, a tail pitch down was expected. Accordingly a tail bag was designed to accommodate this pitch axis rotational energy. The tail bag arrangement used from Tests No. 65 through 84 was an oblate spheroid 15 inches thick by 30 inches in diameter. Starting with Test No. 85 and going through Test No. 91 this geometry was changed to that of a cylinder 16 inches in diameter by 26 inches in height. These two bags are shown in Figures 18 and 19. These tail bags were prefoamed and bolted onto the test vehicle prior to test. The short tail bag (15 inches) performed adequately in conjunction with the Mark VIII FIAS main bag as shown in Figure 20 where the frangible horizontal stabilizer endplate has been broken. The tail bag height was increased to 26 inches for Test No. 85 in conjunction with the taller Mark IX FIAS main bag in an attempt to provide more clearance for the pods. At the oblique yaw angles, however, this taller bag tended to roll out from under the vehicle as shown in Figure 21 after Test No. 86.

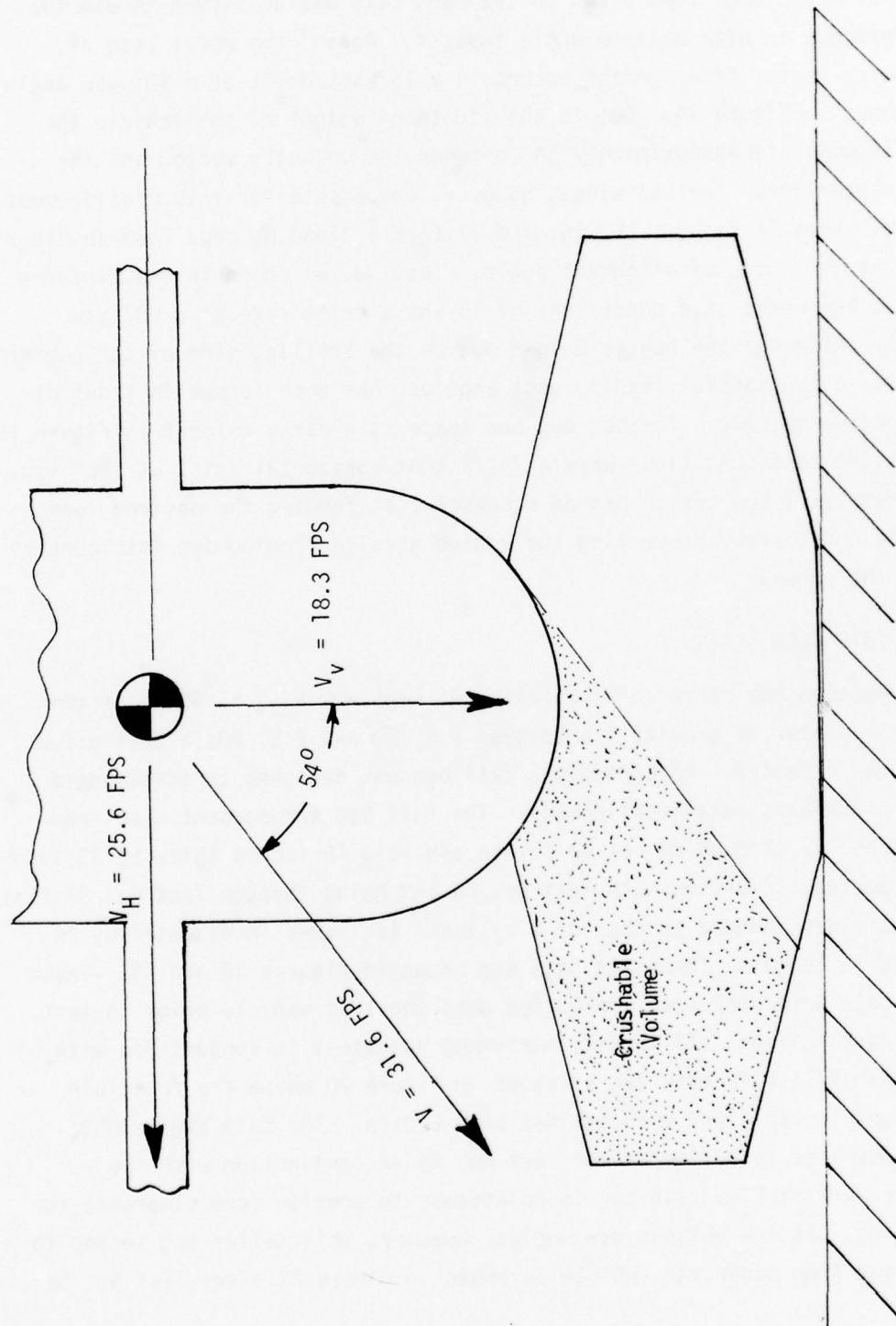


Figure 14. Mark VIII Bag Misalignment



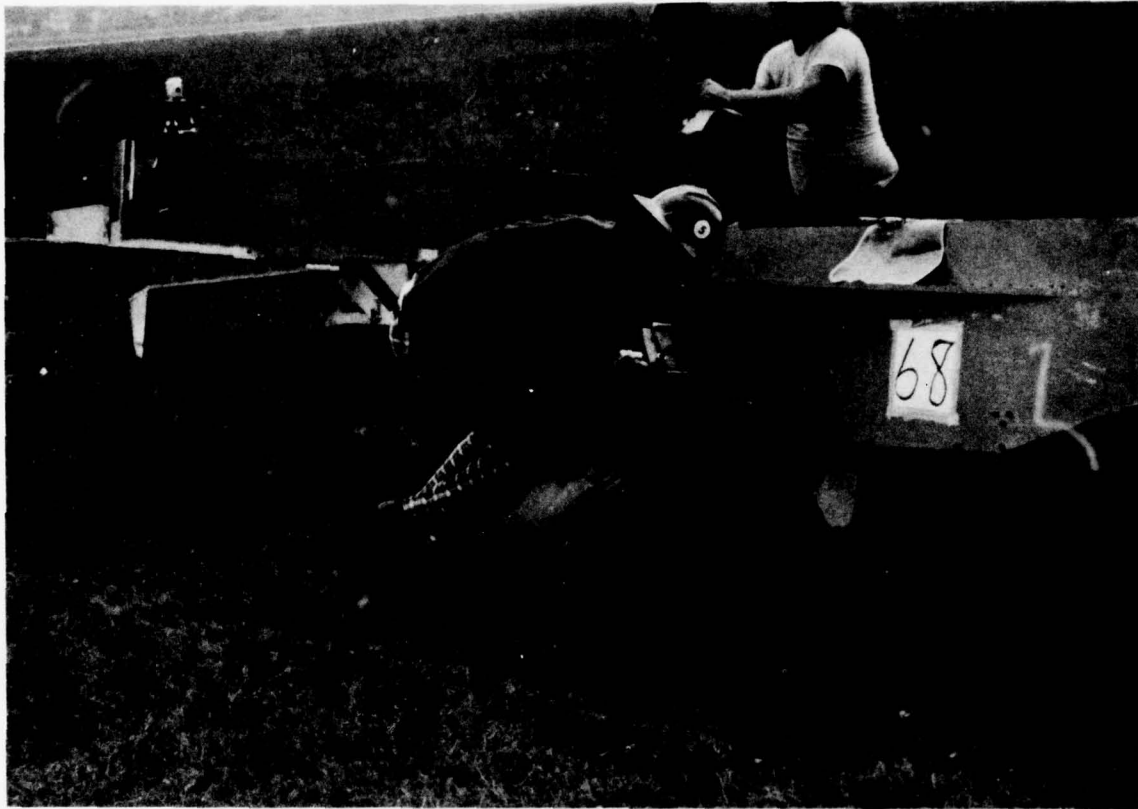


Figure 15. Bag Shape, Test No. 68

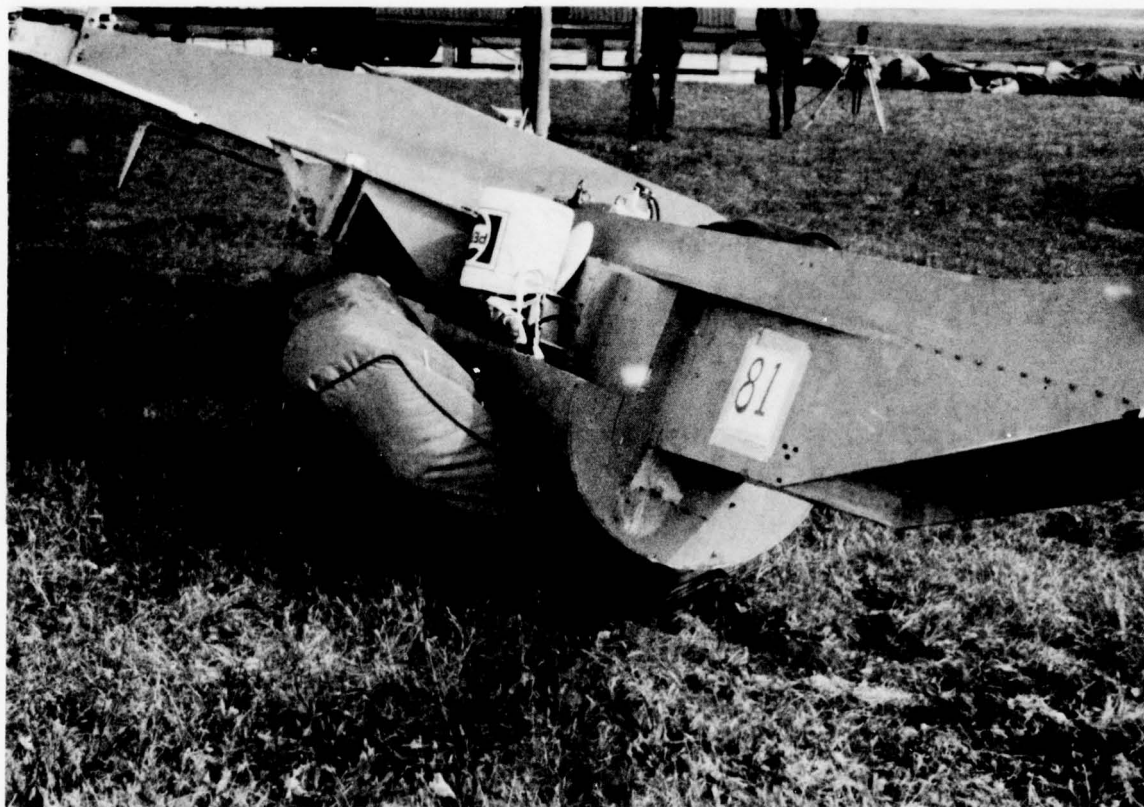


Figure 16. Bag Shape, Test No. 81, Right-Hand

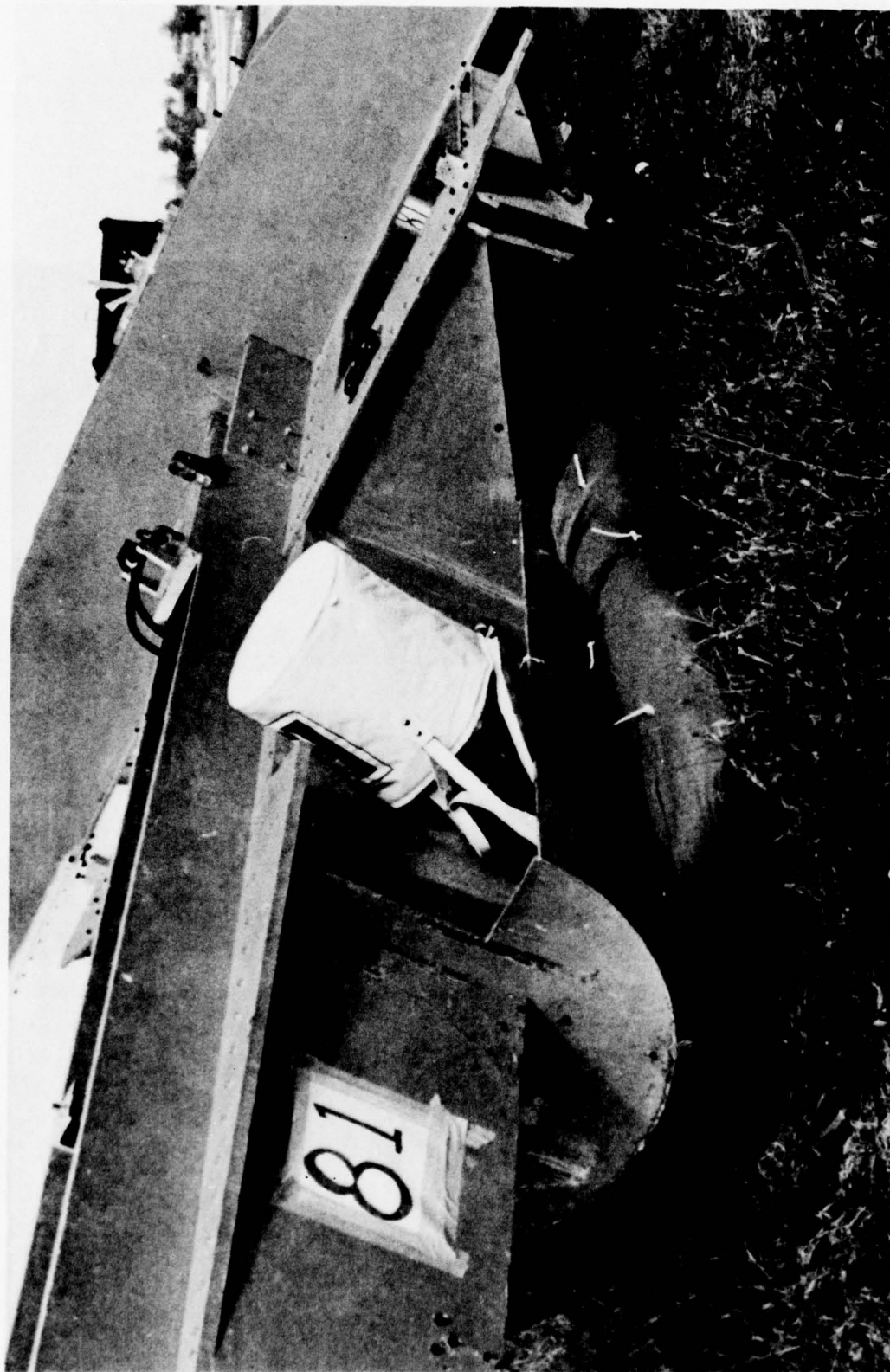


Figure 17. Bag Shape, Test No. 81, Left-Hand

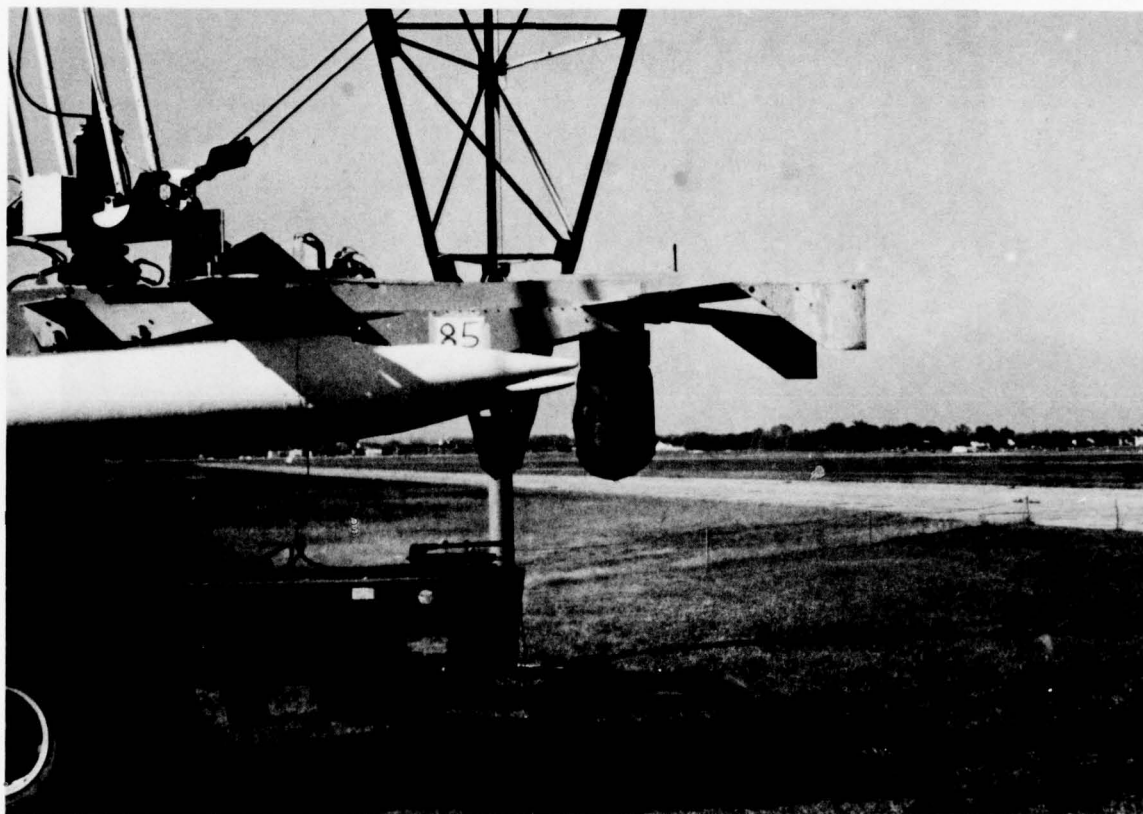


Figure 18. Tall Tail Bag, Pre-Test





Figure 19. Short Tail Bag, Pre-Test

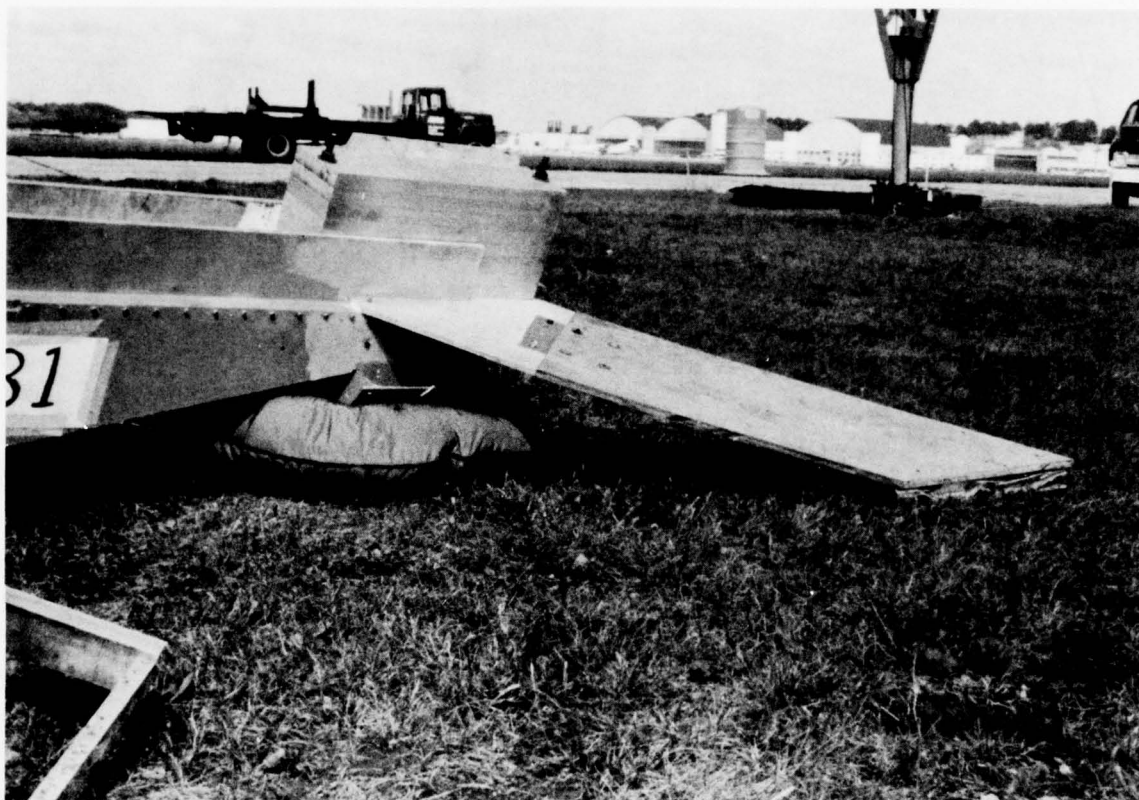


Figure 20. Short Tail Bag, Test No. 81

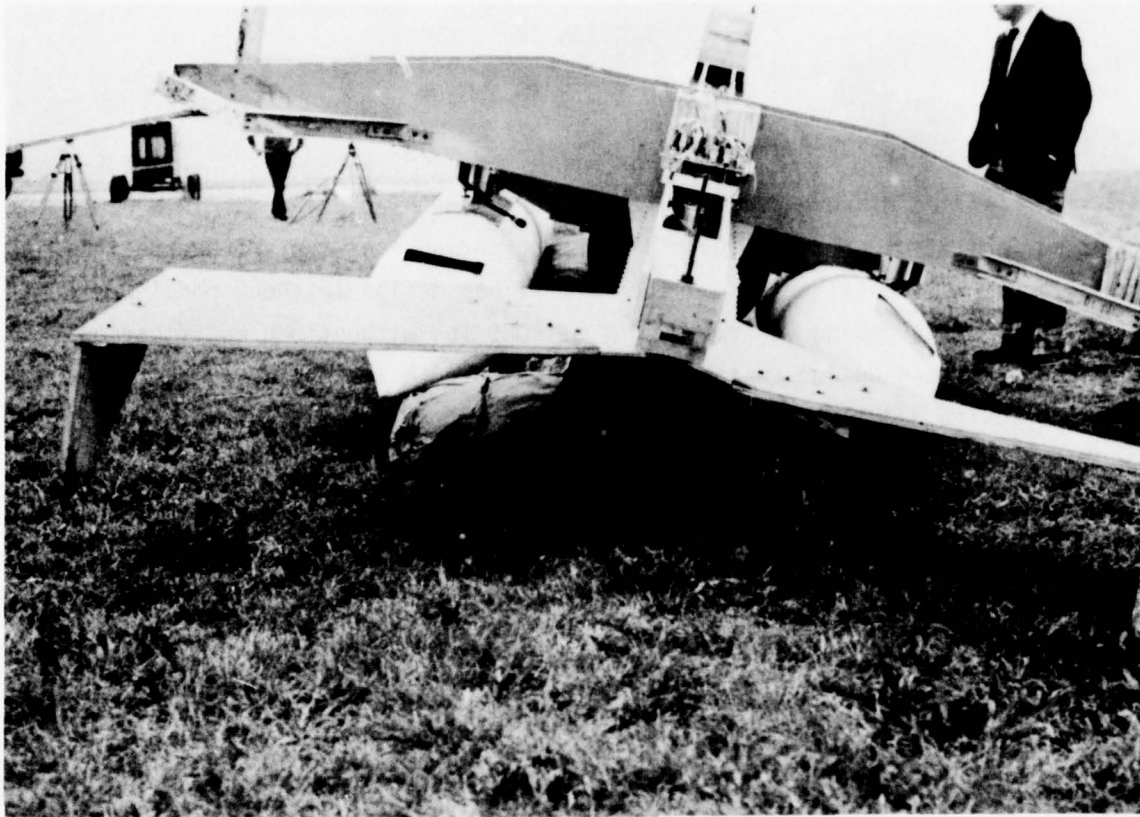


Figure 21. Tall Tail Bag, Test No. 86

## 7. SUMMARY

In the adaptation of the FIAS to the AQM-34V RPV two different bag designs were conceived and tested. These bag designs (the Mark VIII and Mark IX) are considered to be in the prototype stage of development, because they are ready for incorporation into the prototype slipper tank FIAS design. The detailed design and fabrication requirements for these bags are contained as Appendix A to this report. The performance of these bag designs (presented later in this report) serve to establish the validity of the inductive design guidelines which were gleaned from earlier testing in this investigation.

SECTION IV  
VERTICAL TESTS NO. 58-64

1. TEST SERIES OVERVIEW

A series of seven vertical tests were conducted using the IRON PIG test facility in order to quantify the performance of the two bag designs prior to horizontal testing. The Mark II bag design (without pods) was tested at its design vehicle weight of 2000 lbs without bag modification. The Mark I bag design (with pods) was tested with vehicle weights from 2000 lbs to 3230 lbs and required modification in order to sustain the higher weight condition. The Mark I bag thus evolved into the Mark III, the Mark IV, and finally the Mark V bag design which was considered ready for horizontal testings.

2. IRON PIG TEST FACILITY

a. The IRON PIG test facility is designed for the vertical testing of the FIAS, using a simulated engine nacelle (IRON PIG). A complete description of the facility is contained in Volume I and an abbreviated version is presented here for the clarification of the test results. The major components are shown in Figure 22, which shows the IRON PIG and an early version of the FIAS bag design. This facility was used to conduct the initial 48 tests prior to this current effort.

b. The IRON PIG is an all-steel, welded structure with a lower radius of 15 inches, which approximates the 14 inch radius of the AQM-34V engine nacelle. The IRON PIG's tare weight of 1300 lbs can be increased to 3230 lbs by the addition of lead shot bags in the weight chambers in each end of the vehicle. The vehicle is tethered at each of the four corners in such a manner that vertical movement is unimpeded but horizontal movement is limited to the confines of the impact pad for safety of test. The vehicle is suspended and released from a bomb rack/overhead crane assembly which is remotely controlled from outside the test cell.

c. The impact pad consists of an 8 feet x 9 feet rectangle of 2-1/2 inches aluminum plate backed by plywood and the concrete floor. This



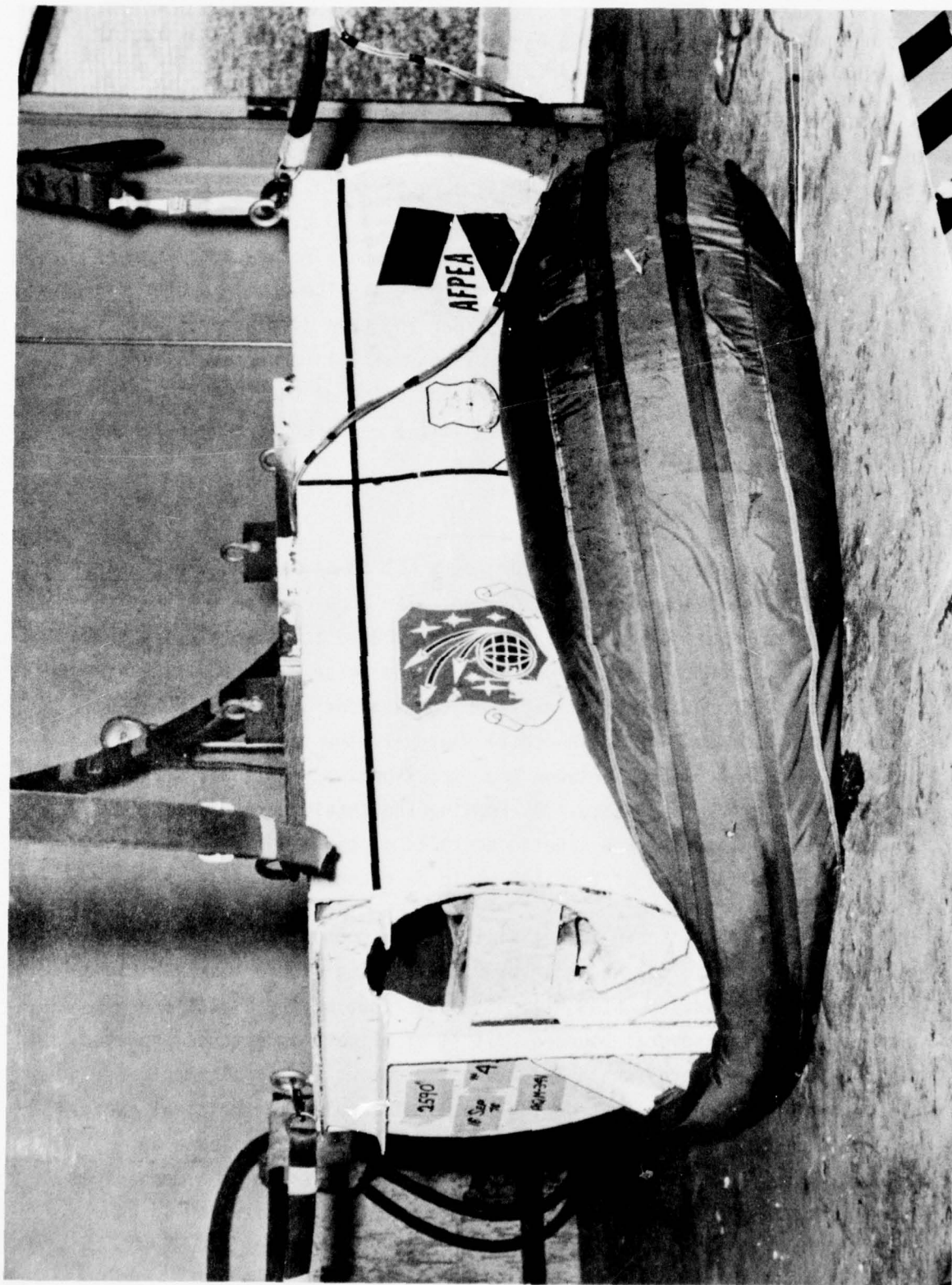


Figure 22. IRON PIG, Test No. 43

arrangement was chosen as being a worst case landing surface, in that it approximates an "infinitely hard" landing surface.

d. The IRON PIG instrumentation consisted of a three-axis accelerometer package located at the vehicle's center of gravity and connected by an umbilical cable to a magnetic tape recorder in an adjacent test cell. The Z axis (vertical) accelerometer was a 50 g, piezoresistive accelerometer, linear to 500 Hz and calibrated on a rotary accelerator at g levels of 0, 5, 10, 20, 30, 40, and 50 g's. The accelerometer signal was hard-wired to a magnetic tape recorder and then displayed on a visicorder for data reduction. The data was normally interpreted filtered at 300 Hz, but in those instances where bottoming of the IRON PIG on the impact pad occurred, a lower frequency filter was used to eliminate the high frequency ringing of the transducer.

### 3. DATA REDUCTION TECHNIQUE

a. The accelerometer data from Tests No. 58-64 was analyzed, using a simplified energy management technique. The acceleration versus time visicorder trace was digitized and then integrated to give velocity versus time and distance travelled versus time. From these plots the kinetic and potential energy versus time traces for the energy of the IRON PIG vehicle could be obtained. The total energy in the test was determined by measuring the distance between the impact pad and the lower surface of the IRON PIG prior to release. By knowing the total energy and the instantaneous potential and kinetic energies of the IRON PIG during the impact, the performance of the FIAS could be quantified.

b. The FIAS is known to act similar to a mechanical damping system with a damping ratio on the order of 0.8. So long as the test vehicle does not bottom out, the FIAS will attenuate 100% of the impact energy eventually, after several bounces. It is of primary importance, however, to determine the energy which is attenuated during the first impulse. The ratio of the energy lost during the first impulse to the total energy of the impact is the measure of performance of the FIAS in Tests No. 58-64. This ratio may be thought of as the damping ratio of a mechanical damping system or as unity minus the coefficient of restitution in an impact situation.

4. TEST NO. 58

Test No. 58 was conducted on 11 July 1977, using the IRON PIG test facility. The purpose of this test was to assess the performance of the Mark I bag design (with pods) at the lowest energy level of 10,450 ft-lbs. These test conditions simulate the Mark I bag design being impacted in an off-design pods-off condition. The IRON PIG was ballasted to a weight of 2000 lbs and released from a height of 5.2 feet for a total impact energy of 10,450 ft-lbs. The acceleration versus time trace (Figure 23) shows a relatively mild impact with a maximum acceleration of 4.5 g's and an onset rate of approximately 28 g's/second. The energy versus time plot (Figure 24) shows an energy after first impulse of 4200 ft-lbs which would indicate a first impulse attenuation ratio of 0.6. However, the test vehicle came to stop approximately eleven inches (0.93 feet) above the impact pad. Thus, of the 4200 ft-lbs remaining after the first impulse, approximately 1860 ft-lbs was due to potential energy. Subtracting this portion gives a residual energy of 2340 ft-lbs or a first impulse attenuation ratio of 0.78. At this off design test condition the Mark I bag (designed for use with pods) brought the podless vehicle to a stop approximately a foot above the surface while not exceeding an acceleration level of 4.5 g's.

5. TEST NO. 59

Test No. 59, on 12 July 1977, was to be with the Mark II bag design (without pods), impacting at its design vertical energy level of 10,450 ft-lbs. This test was aborted prior to release when the Mark II bag failed to fully deploy. Examination revealed a pressure leak in the "A" chemical tank which had allowed the pressurized nitrogen to escape during storage. The cause of the leak appeared to be a cross-threaded connection between the safety valve and 3/8 inch plumbing tee at the base of the tank. A check of the remaining tanks showed that this was a unique condition and testing was resumed.

6. TEST NO. 60

Test No. 60, on 12 July 1977, was with the Mark II bag design (without pods) impacting at its design vertical energy level of 10,450 ft-lbs. The IRON PIG was ballasted to a weight of 2000 pounds and



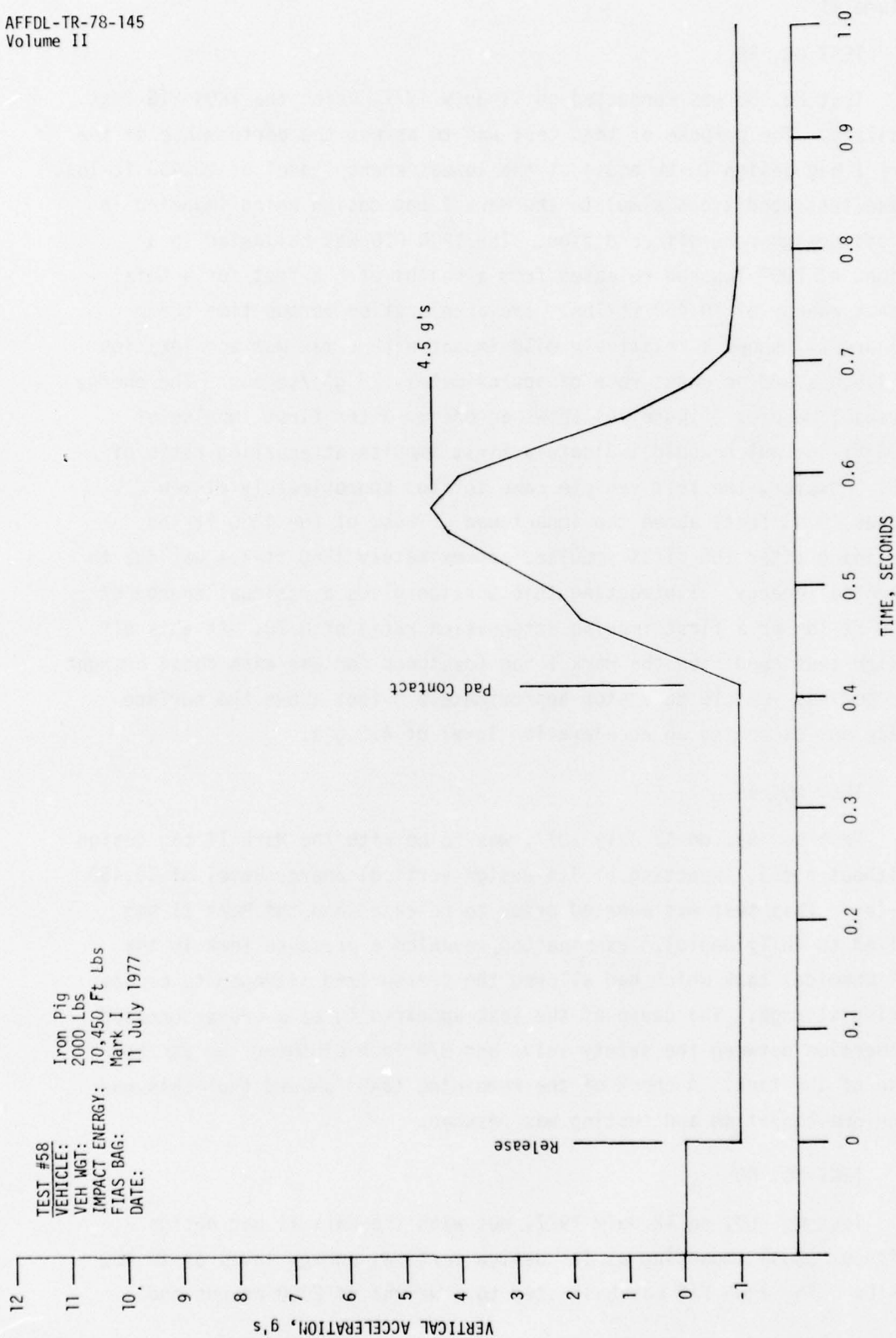


Figure 23. Test No. 58, Acceleration vs Time



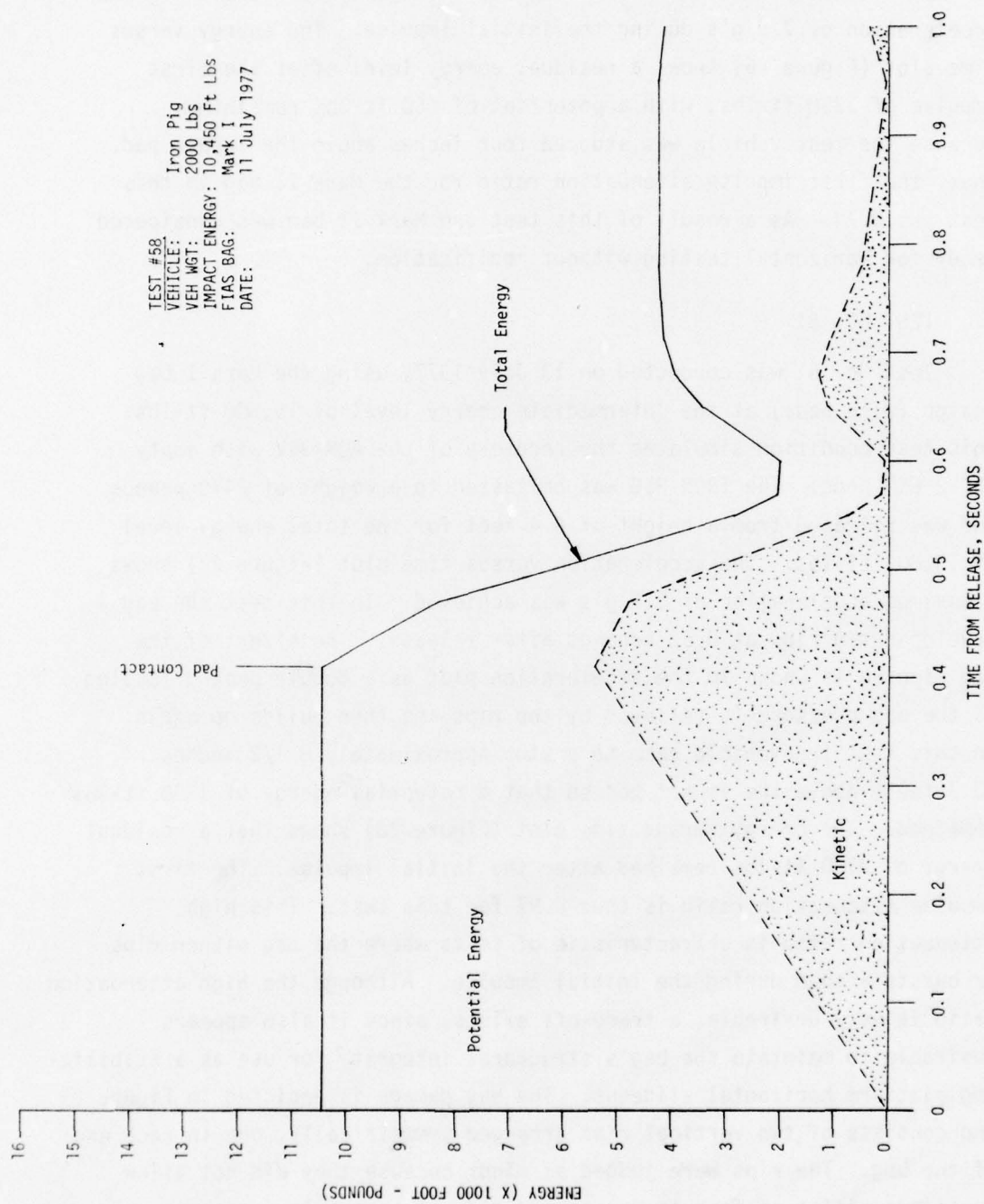


Figure 24. Test No. 58, Energy vs Time

released from a height of 5.2 feet for the total energy level of 10,450 ft-lbs. The acceleration versus time trace (Figure 25) shows a maximum acceleration of 7.9 g's during the initial impulse. The energy versus time plot (Figure 26) shows a residual energy level after the first impulse of 3350 ft-lbs, with a potential of 660 ft-lbs remaining because the test vehicle was stopped four inches above the impact pad. Thus, the first impulse attenuation ratio for the Mark II bag in this test was 0.74. As a result of this test the Mark II bag was considered ready for horizontal testing without modification.

#### 7. TEST NO. 61

Test No. 61 was conducted on 13 July 1977, using the Mark I bag design (with pods) at the intermediate energy level of 15,800 ft-lbs. This test condition simulates the recovery of the AQM-34V with empty ALE-2 ECM pods. The IRON PIG was ballasted to a weight of 2470 pounds and was released from a height of 6.4 feet for the total energy level of 15,800 ft-lbs. The acceleration versus time plot (Figure 27) shows a maximum acceleration of 5.8 g's was achieved. In this test the bag developed two rips at 0.62 seconds after release. The effect of the bag ripping is shown in the acceleration plot as a double peak g loading as the bag pressure is relieved by the rips and then builds up again. In this test the vehicle came to a stop approximately 8-1/2 inches (0.7 feet) above the impact pod so that a potential energy of 1730 ft-lbs remained. The energy versus time plot (Figure 28) shows that a residual energy of 2180 ft-lbs remained after the initial impulse. The first impulse attenuation ratio is thus 0.97 for this test. This high attenuation ratio is characteristic of tests where the bag either rips or bursts a seam during the initial impulse. Although the high attenuation ratio is very desirable, a trade-off exists, since it also appears desirable to maintain the bag's structural integrity for use as a stabilizing platform horizontal slideout. The bag damage is depicted in Figure 29 and consists of two vertical rips arranged symmetrically, one in each end of the bag. The rips were judged as minor because they did not allow large quantities of foam to escape and did not appear to jeopardize the bag's attachment to the vehicle.

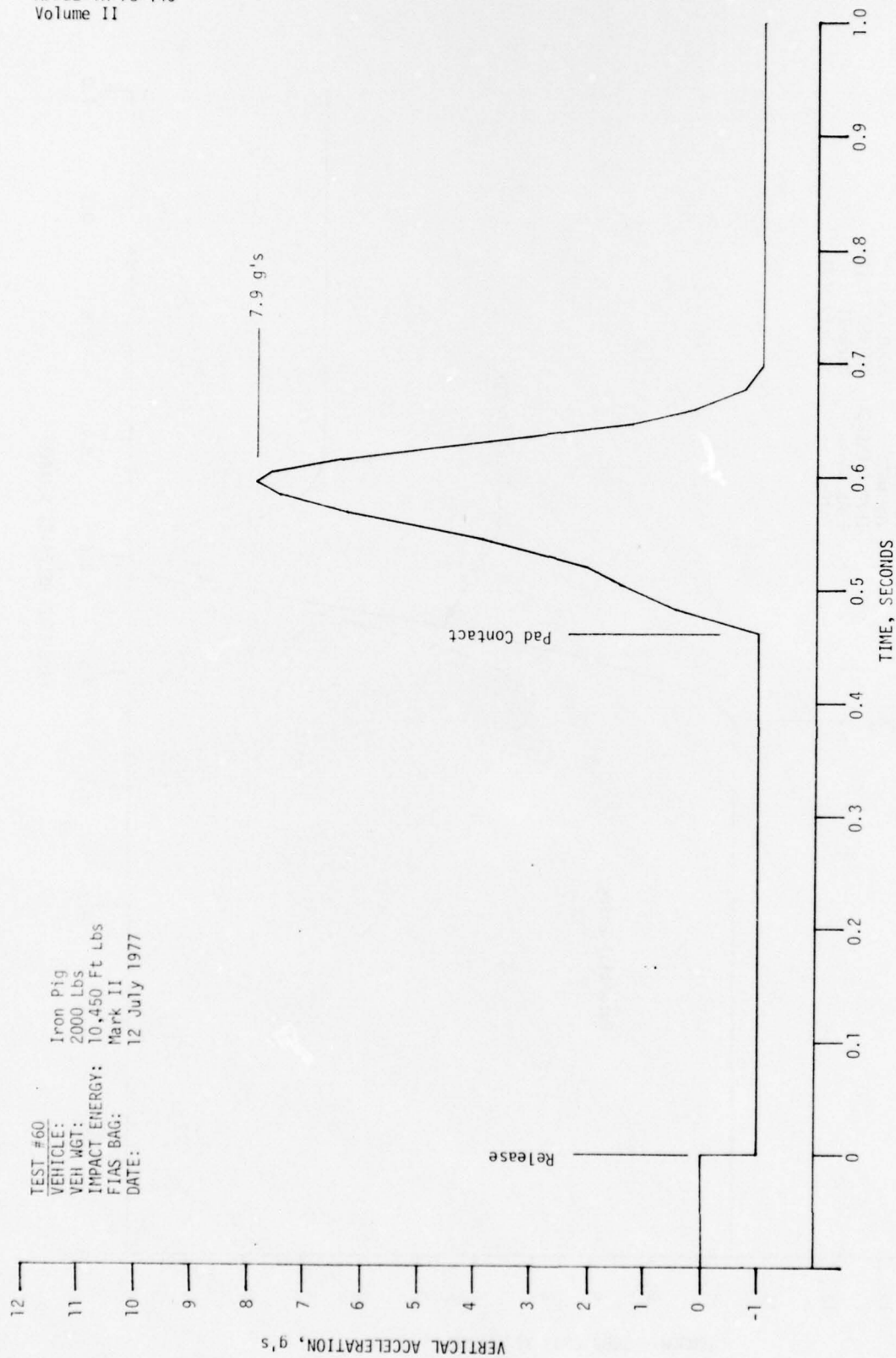


Figure 25. Test No. 60, Acceleration vs Time

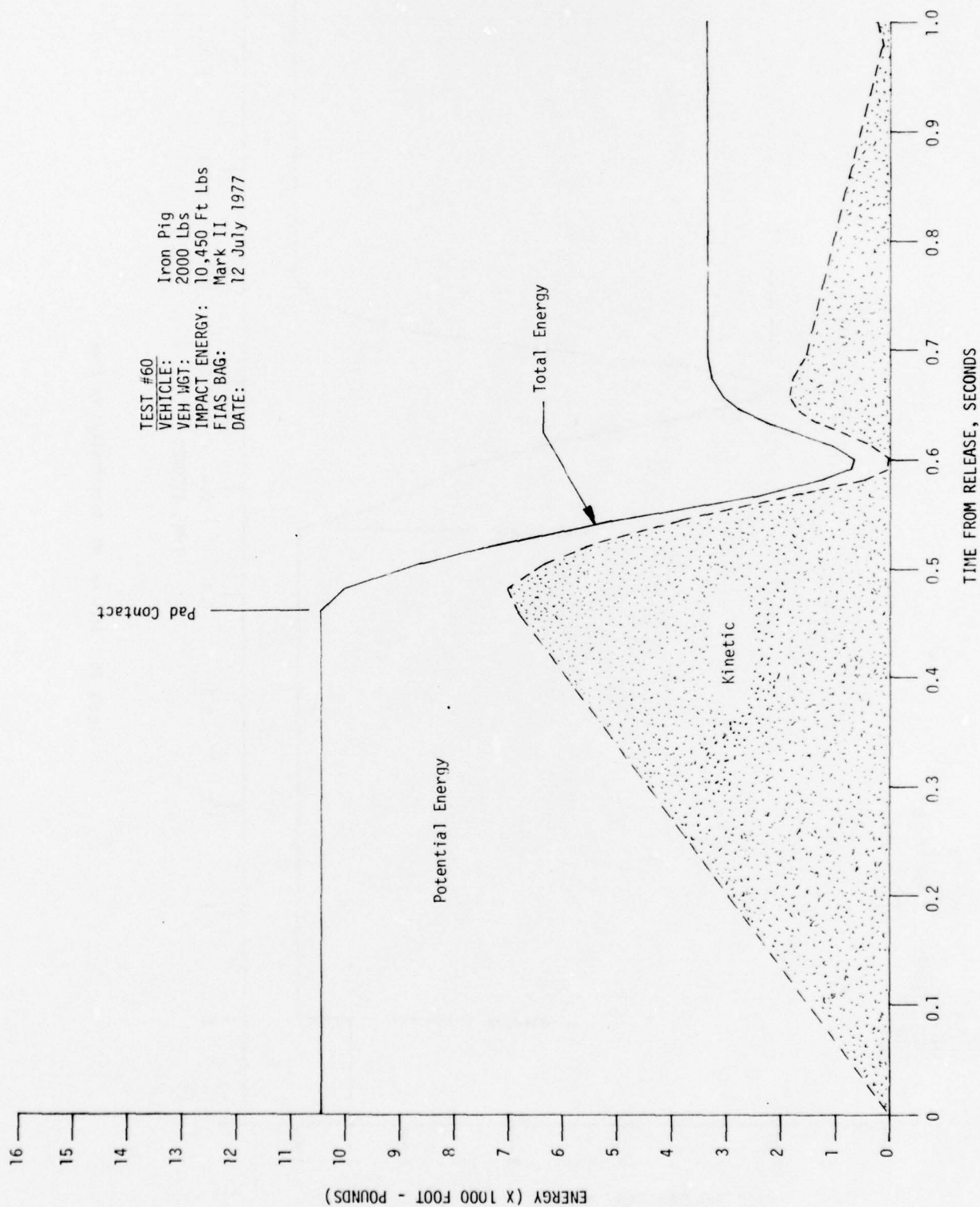


Figure 26. Test No. 60, Energy vs Time



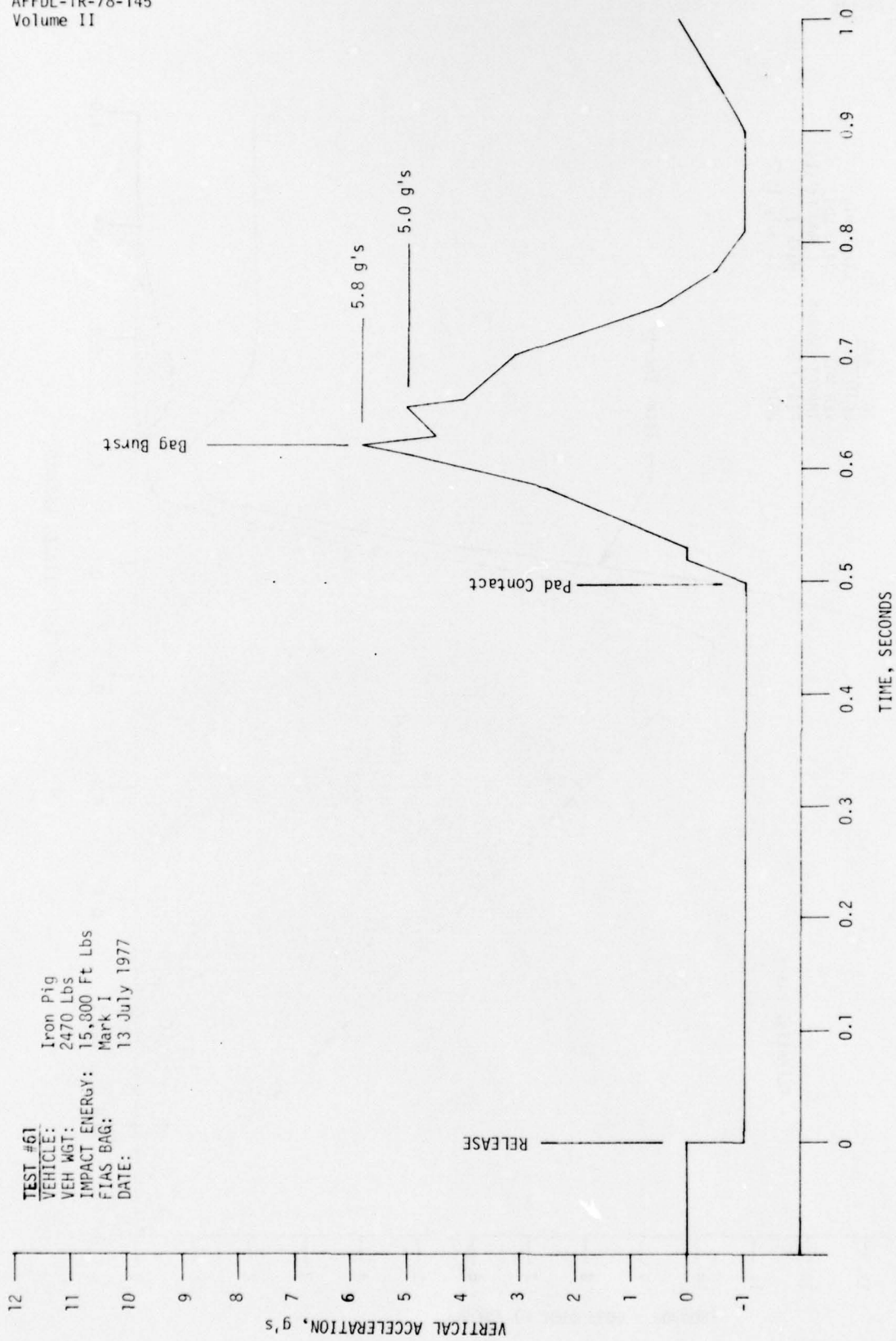


Figure 27. Test No. 61, Acceleration vs Time

TEST #61  
VEHICLE: Iron Pig  
VEH WGT: 2470 Lbs  
IMPACT ENERGY: 15,800 Ft Lbs  
FIAS BAG: Mark I  
DATE: 13 July 1977

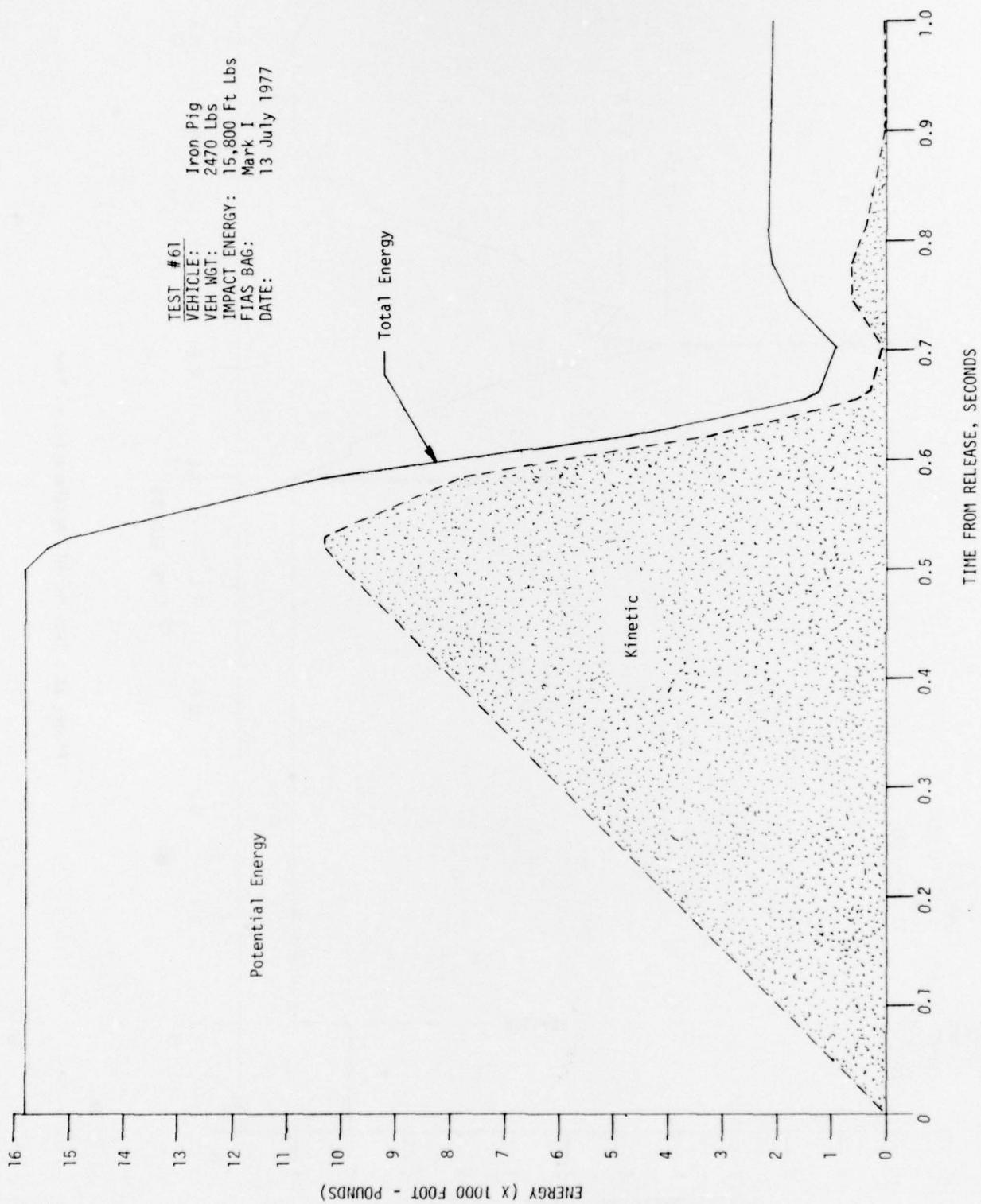


Figure 28. Test No. 61, Energy vs Time

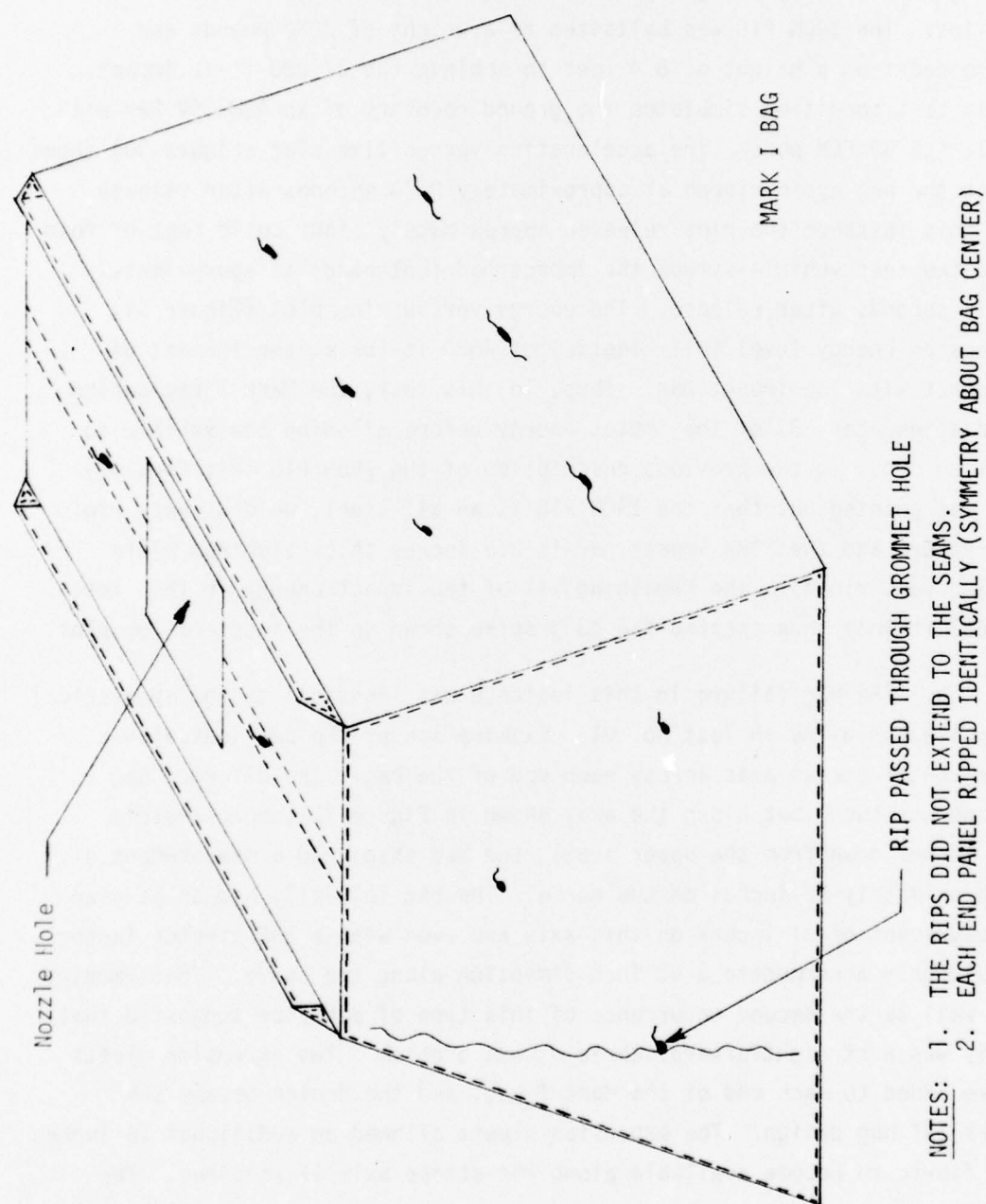


Figure 29. Test No. 61, Bag Damage

8. TEST NO. 62

a. Test No. 62 was conducted on 13 July 1977, with the Mark I bag design (with pods) being impacted at its maximum design level of 27,200 ft-lbs. The IRON PIG was ballasted to a weight of 3230 pounds and released from a height of 8.4 feet to achieve the 27,200 ft-lb impact. This test condition simulates the ground recovery of an AQM-34V RPV with full ALE-38 ECM pods. The acceleration versus time plot (Figure 30) shows that the bag again ripped at approximately 0.70 seconds after release. In this instance the rips released approximately eight cubic feet of foam and the test vehicle struck the impact pad (bottomed) at approximately 0.75 seconds after release. The energy versus time plot (Figure 31) shows an energy level (all kinetic) of 4660 ft-lbs at the instant of contact with the impact pad. Thus, in this test, the Mark I bag design had attenuated 83% of the impact energy before allowing the vehicle to bottom out. In the previous description of the IRON PIG test facility it was pointed out that the IRON PIG is an all-steel, welded, very rigid structure and that the impact pad is 2.5 inches thick aluminum plate (also very rigid). The remaining 17% of the impact energy in this test (4660 ft-lbs) thus created the 43 g spike shown in the acceleration plot.

b. The bag failure in this instance was identical to the symmetrical ripping exhibited in Test No. 61. Examination of the bag indicated a horizontal stress axis across each end of the bag. The deformed bag shape was such that along the axis shown in Figure 32 (approximately 17 inches down from the upper seam), the bag shape had a measurement of approximately 52 inches on the curve. The bag initially had an as-sewn measurement of 31 inches on this axis and even with a 30% stretch factor could only accommodate a 40 inch dimension along the curve. The symmetry as well as the second occurrence of this type of behavior suggested that this was a straightforward fabric stress problem. Two expansion pleats were added to each end of the Mark I bag, and the design became the Mark III bag design. The expansion pleats allowed an additional 16 inches of fabric to become available along the stress axis if required. The pleats were sewn in so that the stress would govern how much of the sewn



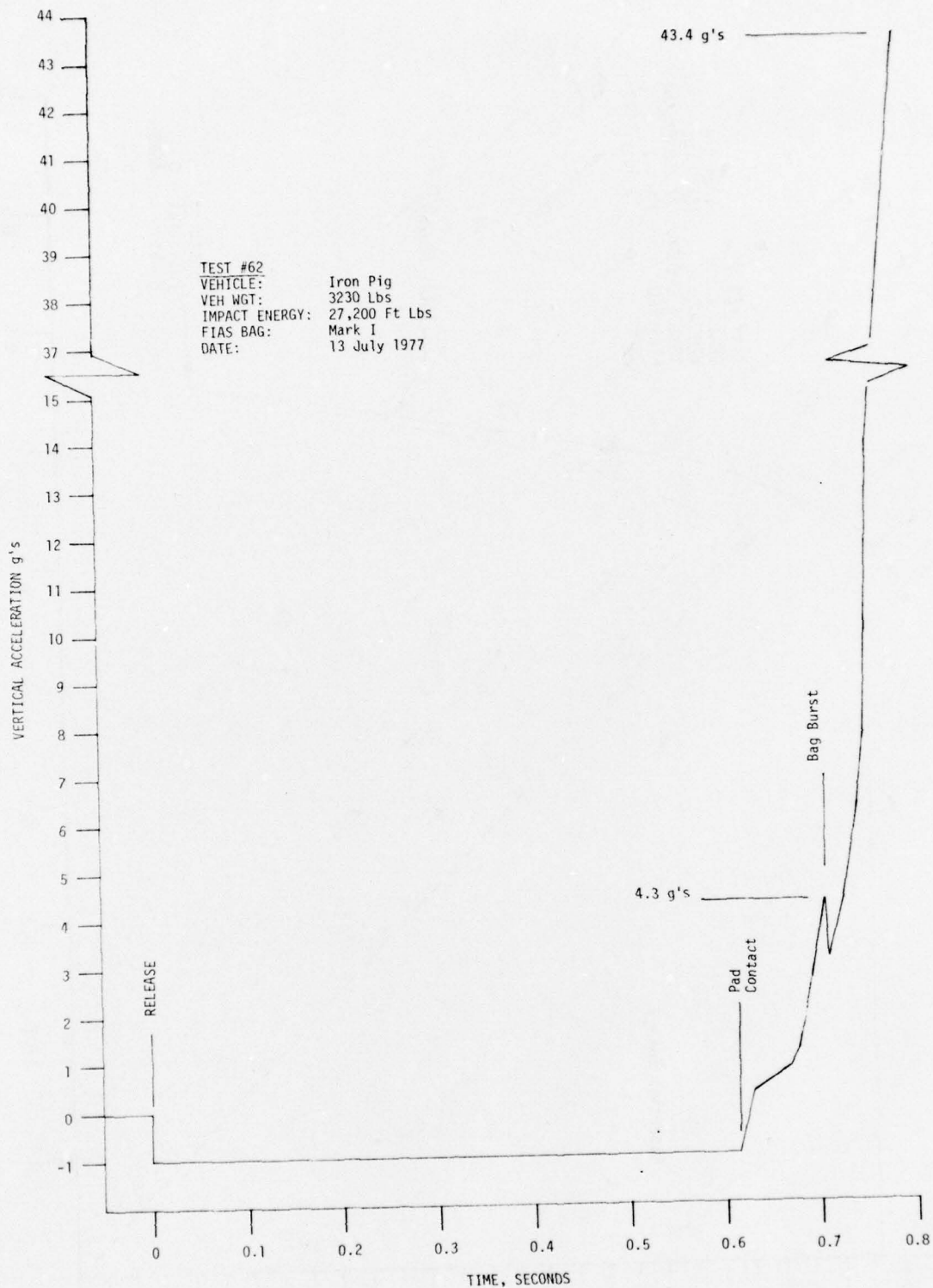


Figure 30. Test No. 62, Acceleration vs Time

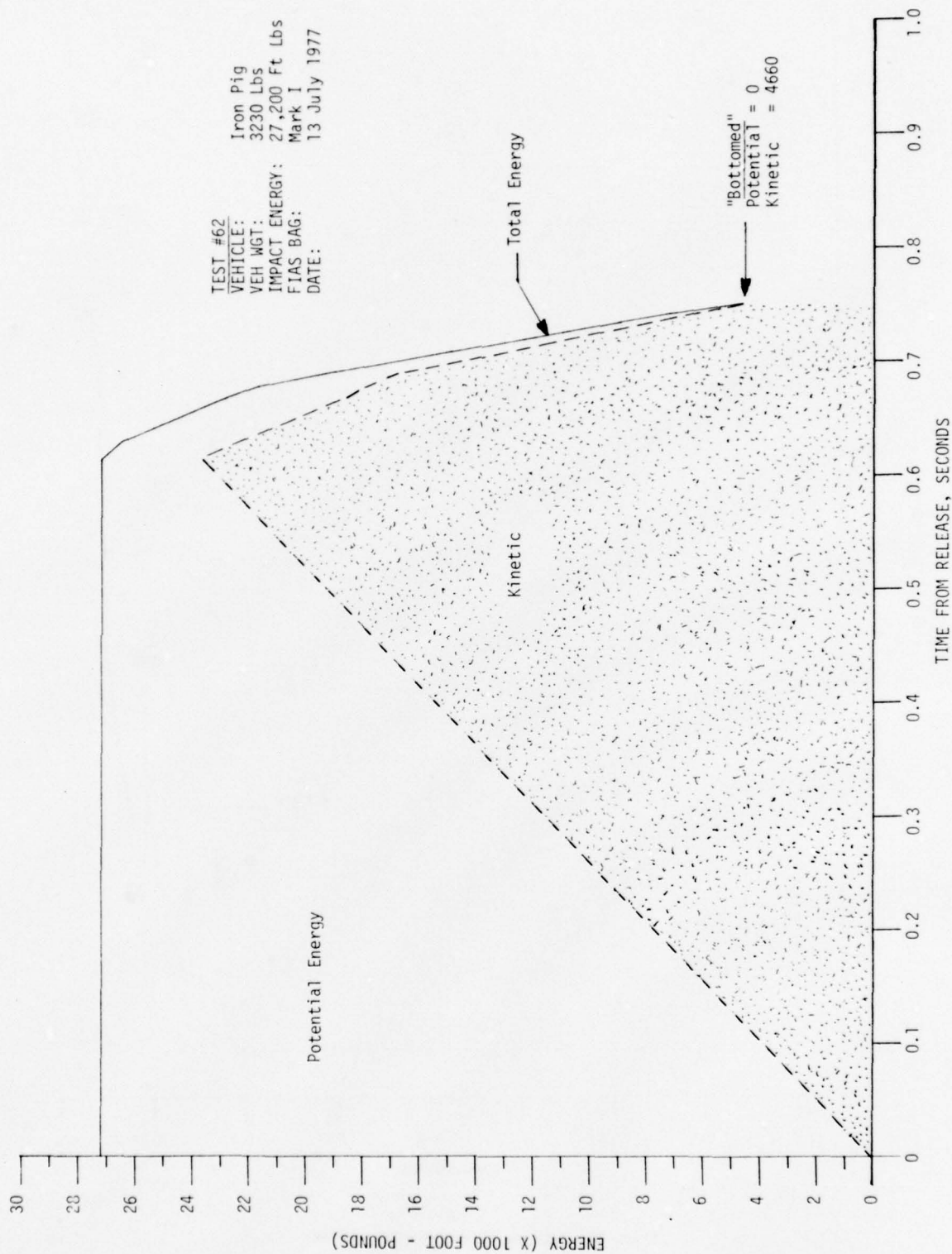


Figure 31. Test No. 62, Energy vs Time

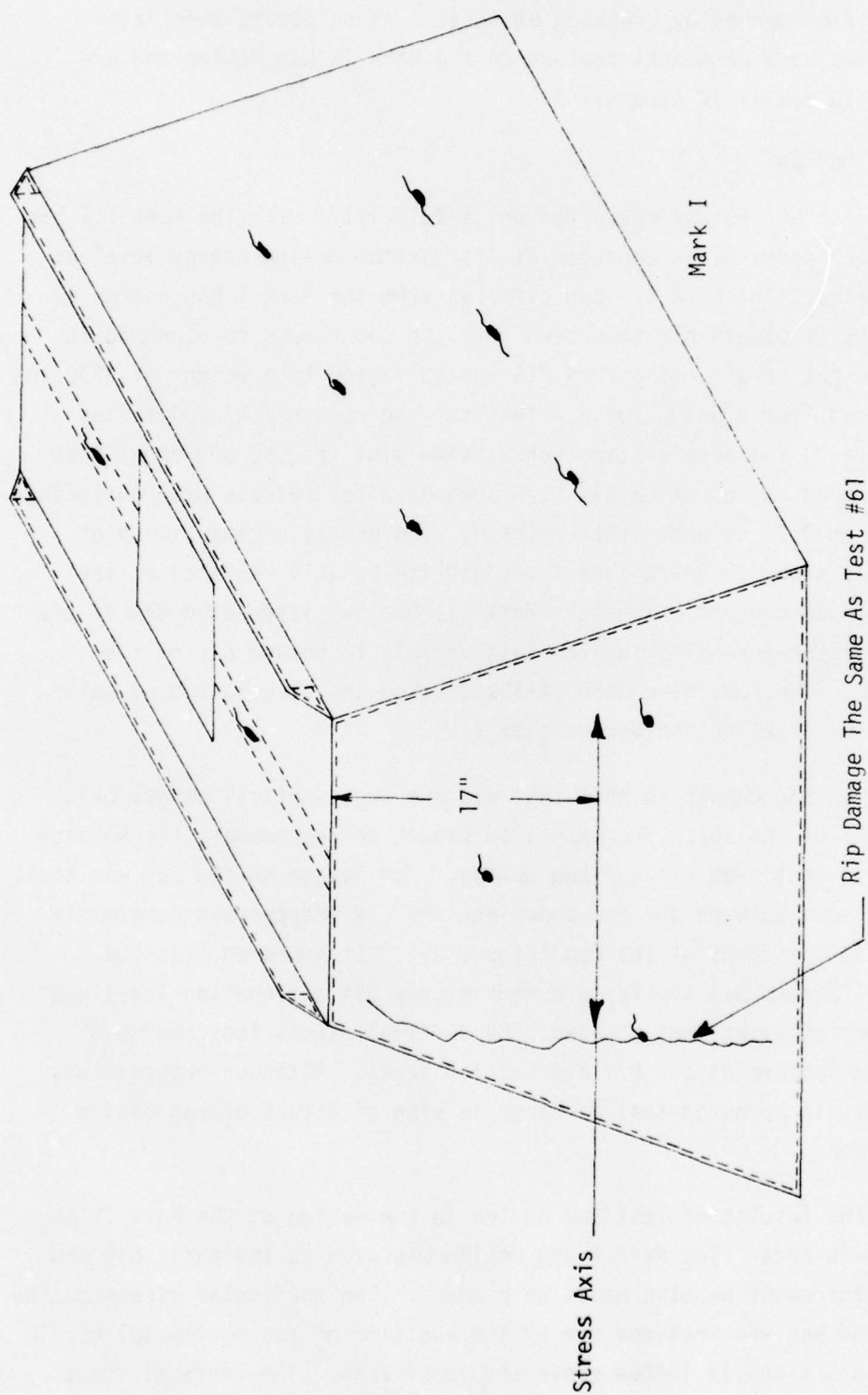


Figure 32. Test No. 62, Bag Damage

pleat would be opened by breaking stitches. These pleats were later incorporated as a permanent feature on the Mark IX bag design and are described in detail in Appendix A.

9. TEST NO. 63

a. Test No. 63 was conducted on 14 July 1977, with the Mark III bag design (with pods) being impacted at its maximum design energy level of 27,200 ft-lbs. The Mark III bag differed from the Mark I bag design in that expansion pleats had been sewn into the end panels to accommodate the horizontal strain. The IRON PIG was ballasted to a weight of 3230 lbs and released from a height of 8.4 feet for the required 27,200 ft-lbs energy level. The acceleration versus time plot (Figure 33) shows that the bag ripped at approximately 0.70 seconds after release with bottoming occurring at 0.74 seconds after release. The energy versus time plot (Figure 34) shows an energy level of 3650 ft-lbs (all kinetic) at the instant of pad contact. Thus the Mark III bag had attenuated 87% of the impact energy before allowing the test vehicle to bottom out on the impact pad. The remaining 3650 ft-lbs created the 38 g bottoming spike shown in the acceleration versus time plot.

b. The bag damage in this test was due to a vertical stress axis on the ends of the bag. The expansion pleats to accommodate the horizontal strain functioned without bag damage. The damage to the bag was that the lower seam between the end panel and the bag wrapper was completely torn out on both ends of the bag (Figure 35). It appeared that the horizontal stress was the failure mode at the 83% attenuation level and that after resolving that problem, the vertical stress took over and caused bag failure at the 87% attenuation level. Although progress was being made, it appeared that a change in plan of attack of bag design was in order.

c. The results of Test No. 63 led to the design of the Mark IV bag for use with pods. The Mark I bag design was used as the basic bag and four reinforcement webbing bands were added. The horizontal stress on the ends of the bag was provided for by the addition of two horizontal girdle bands 6 inches and 15 inches above the lower seam. The vertical stress



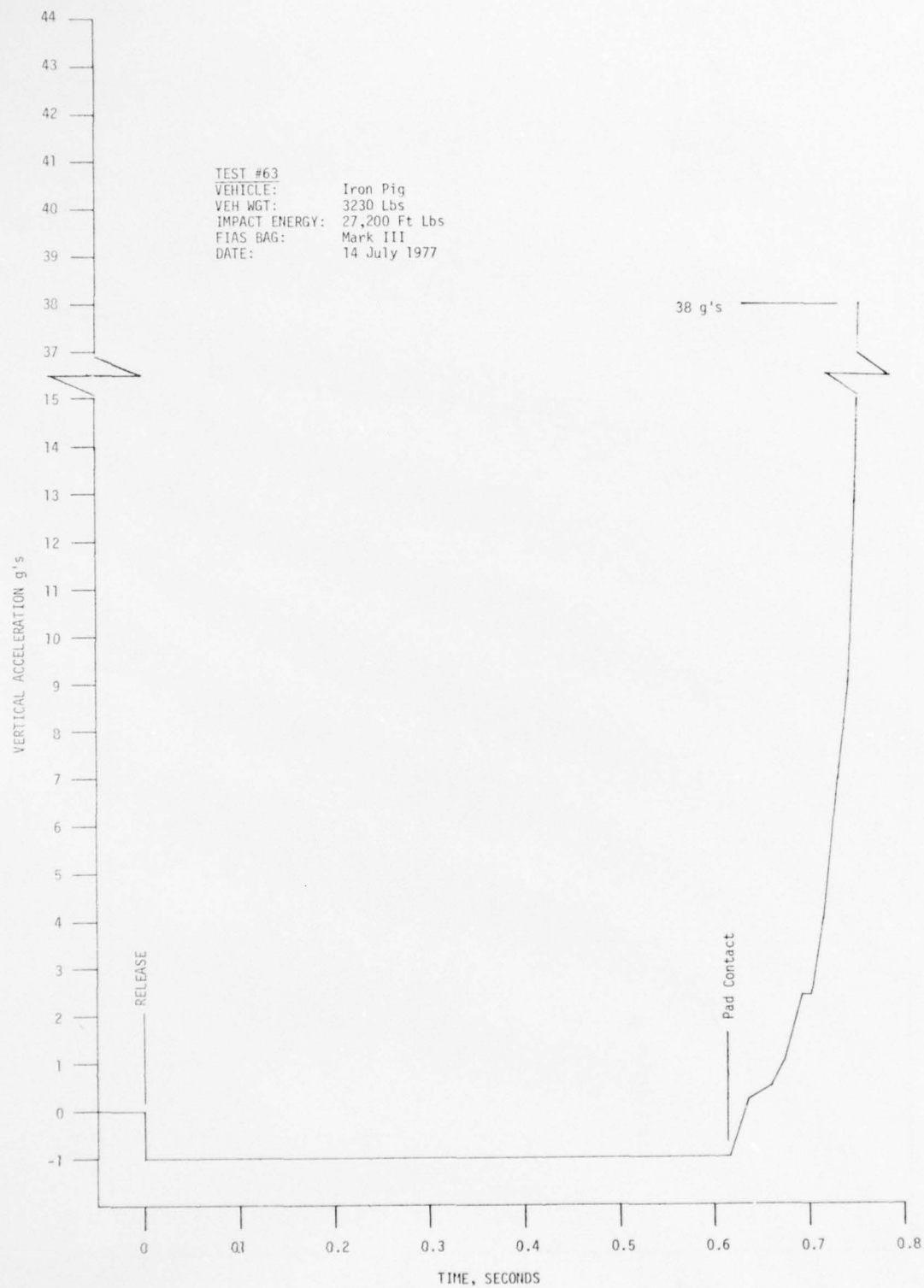


Figure 33. Test No. 63, Acceleration vs Time

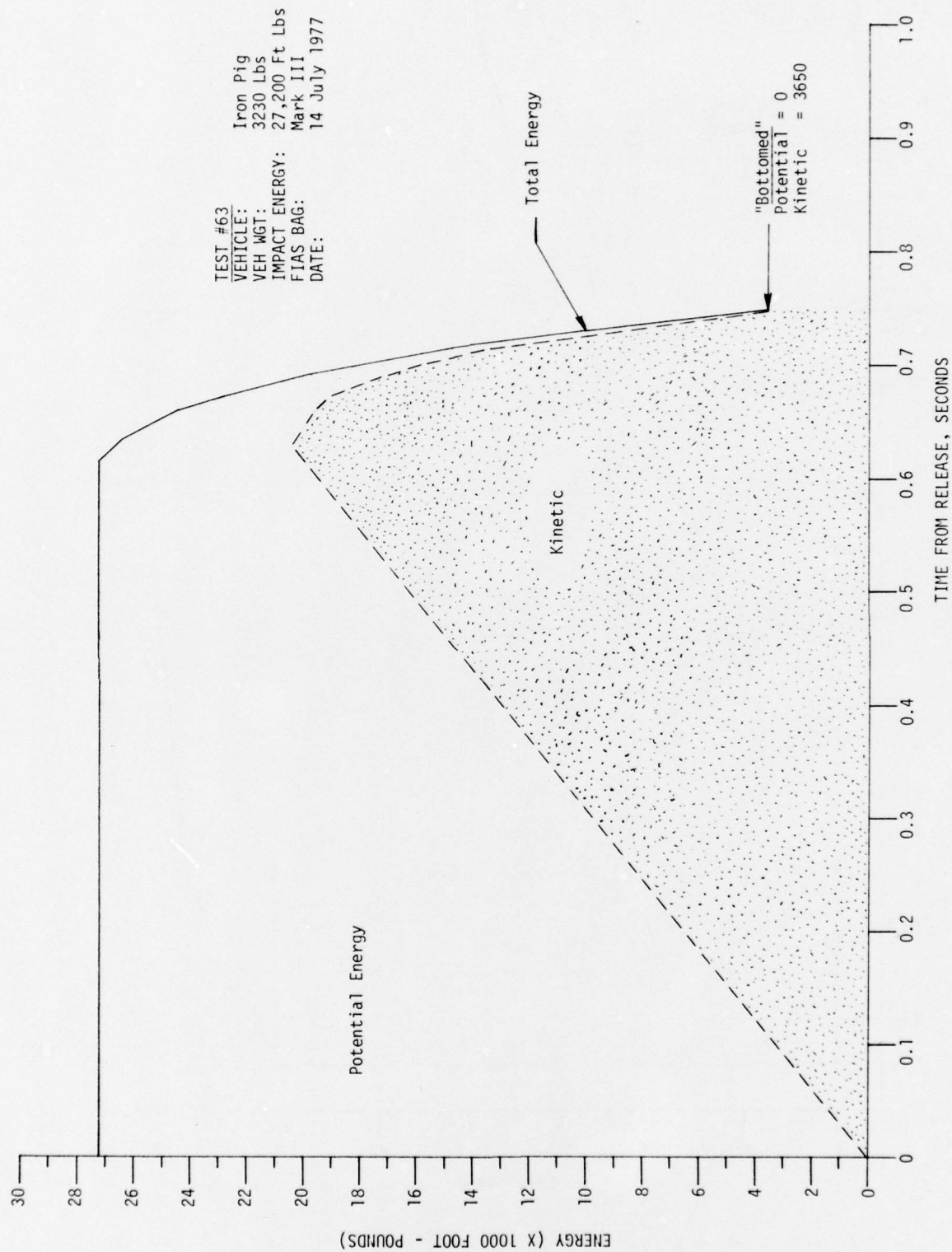


Figure 34. Test No. 63, Energy vs Time

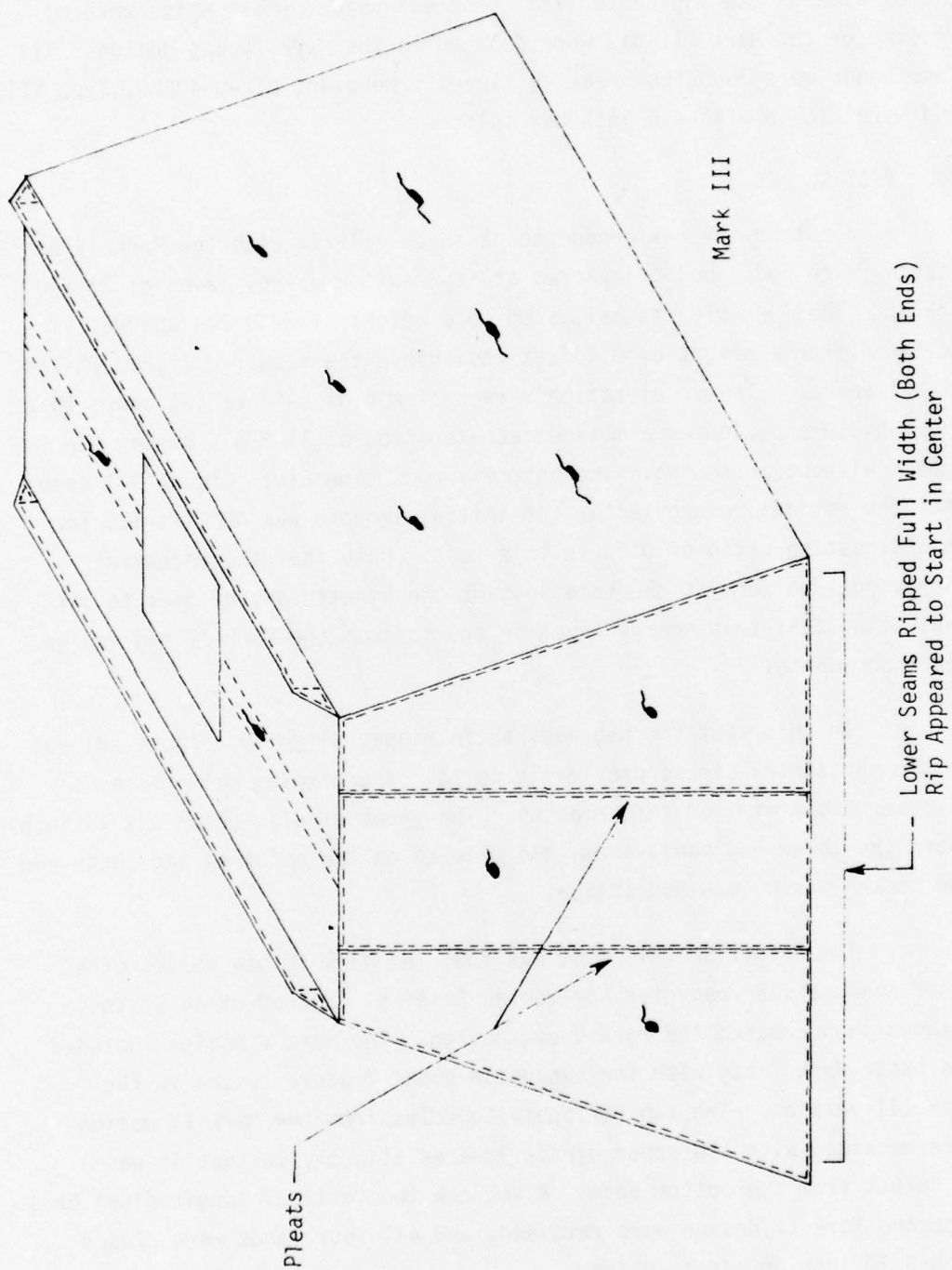


Figure 35. Test No. 63, Bag Damage

was accommodated with two vertical longitudinal bands placed 6 inches on either side of the bag centerline. The expansion pleats which were a feature of the Mark III bag were deleted in the Mark IV bag design. All four bands were 3600 lbs breaking strength webbing, MIL-W-4088G, Type VIII, and were closed with a 6 inch box splice.

10. TEST NO. 64

a. Test No. 64 was conducted on 18 July 1977, with the Mark IV bag design (with pods) being impacted at its maximum energy level of 27,200 ft-lbs. The IRON PIG was ballasted to a weight of 3230 lbs and was released from a height of 8.4 feet to achieve the required 27,200 ft-lbs impact energy. The acceleration versus time plot (Figure 36) shows that the vehicle experienced a maximum acceleration of 11.3 g's during the impact without bottoming. The energy versus time plot (Figure 37) shows that the residual energy after the initial impulse was 4620 ft-lbs for an attenuation ratio of 0.83 in this test. Note that the potential energy goes to zero at the same instant the kinetic energy goes to zero, indicating that this energy level is the maximum the Mark IV bag design can accommodate.

b. In this test the bag ends again ripped slightly (Figure 38) due to the horizontal stress previously noted. The girdles held the ends together and minimized this ripping. The upper girdle, which was 15 inches above the lower end panel seam, had slipped on the deformed bag shape and had broken its 6 inch box splice.

c. The result of this test was that the Mark IV bag design with minor changes was ready for horizontal testing. Introduction of these changes thus created the Mark V bag design. The Mark V design included the basic Mark I bag with the expansion pleat feature tested in the Mark III version. The two horizontal girdles from the Mark IV design were retained with the upper girdle lowered slightly so that it was 12 inches from the bottom seam. Also, the two vertical longitudinal bands from the Mark IV design were retained, and all four bands were closed with a 10 inch double-X splice.



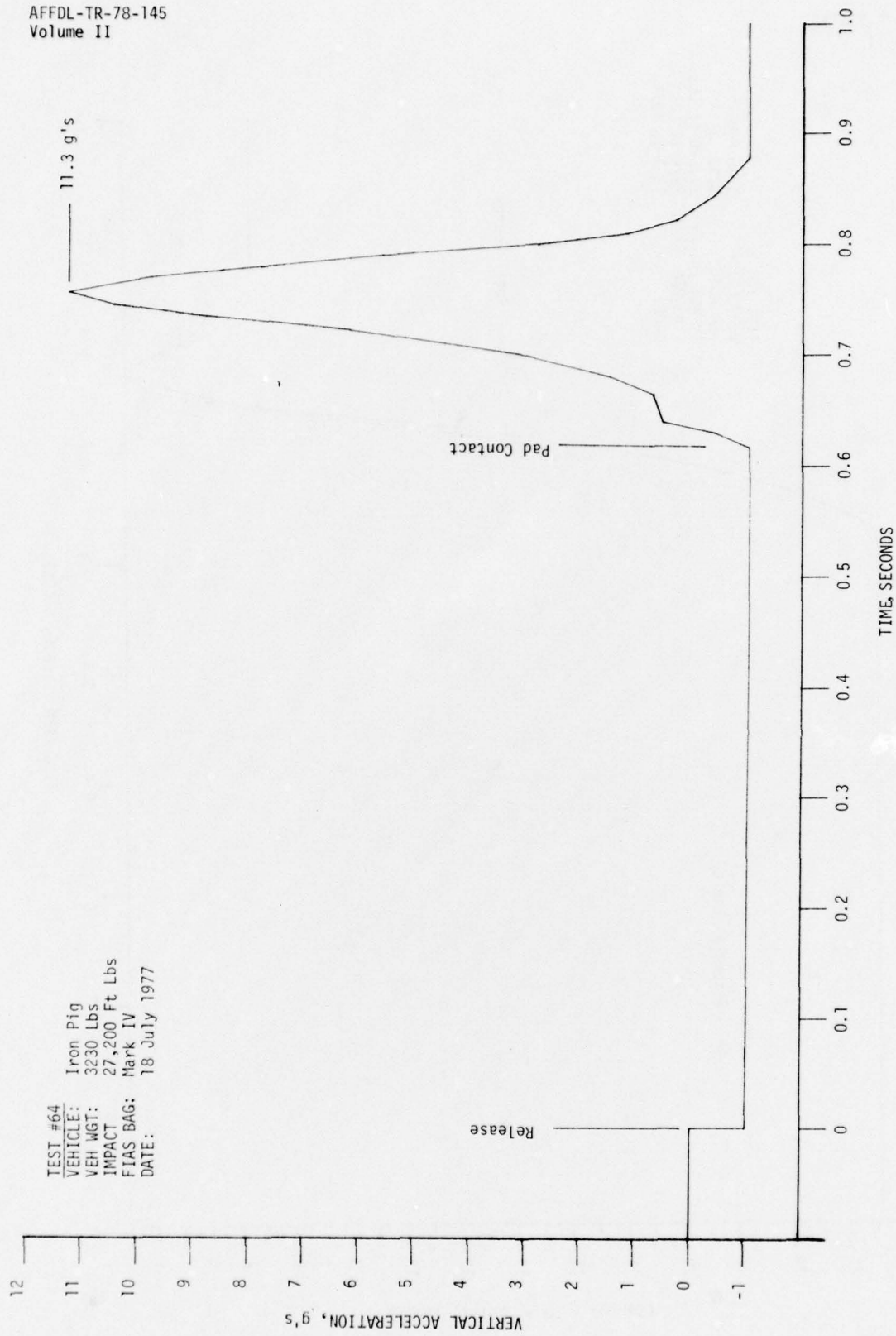


Figure 36. Test No. 64, Acceleration vs Time

TEST #64  
VEHICLE: Iron Pig  
VEH WGT: 3230  
IMPACT ENERGY: 27,200 Ft Lbs  
FIAS BAG: Mark IV  
DATE: 18 July 1977

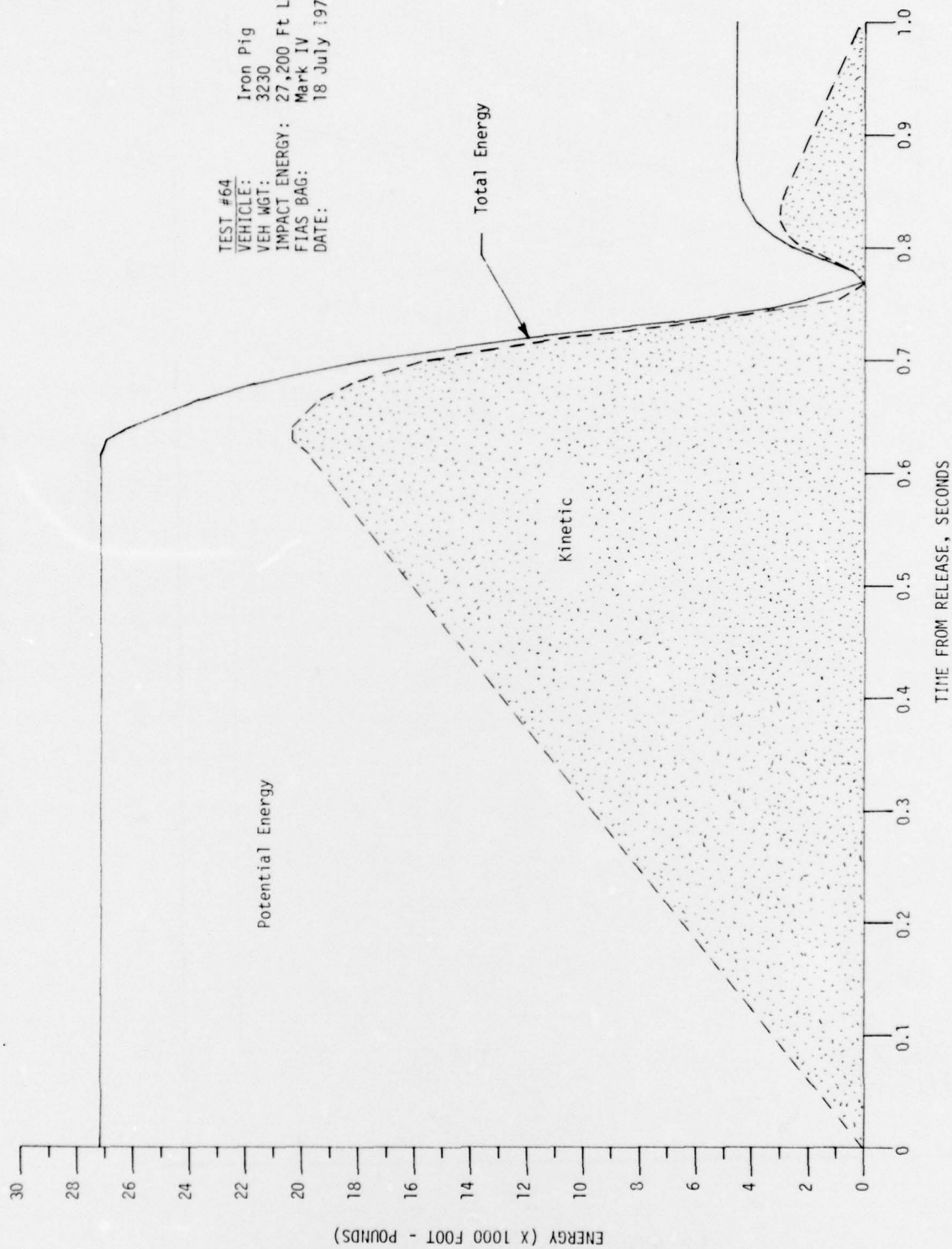


Figure 37. Test No. 64, Energy vs Time

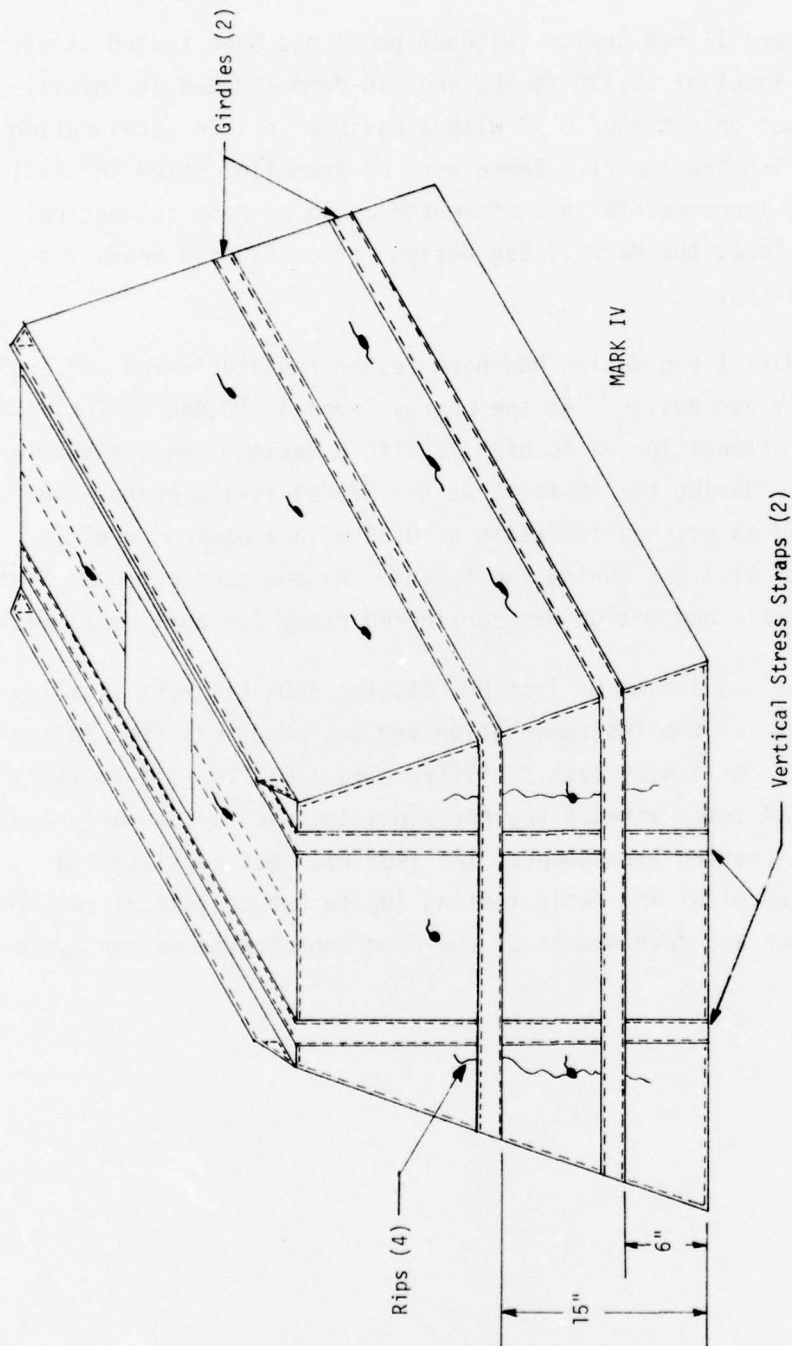


Figure 38. Test No. 64, Bag Damage

11. SUMMARY

a. The Mark II bag design (without pods) had been tested at its design energy level of 10,450 ft-lbs and had demonstrated an initial impulse attenuation ratio of 0.74 with a maximum vehicle acceleration of 7.9 g's during the impact. There were no anomalies noted in testing, and no obvious improvements in performance could be made in vertical testing; therefore, the Mark II bag design was considered ready for horizontal testing.

b. The Mark I bag design had been tested repeatedly and had evolved into the Mark V bag design. At the energy level of 10,450 ft-lbs, this design had an attenuation ratio of 0.78 with a maximum vehicle acceleration of 4.5 g's during the impact. At the 27,200 ft-lbs energy level, this design had an attenuation ratio of 0.83 with a maximum vehicle acceleration of 11.3 g's during the impact. At the conclusion of Test No. 64, the Mark V bag design was considered ready for horizontal testing.

c. At the conclusion of Test No. 64, the IRON PIG test facility was dismantled, and the instrumentation and equipment was used in the building of the horizontal test facility. The IRON PIG test facility has withstood 64 tests without any personnel injuries or property damage. As an in-house testing arrangement, the IRON PIG test facility had allowed the economical and rapid testing (up to two tests/day) required for the research and development of the Foam Impact Attenuation System.



## SECTION V

### TEST VEHICLE DESCRIPTION

1. A full-scale, dynamically similar, ground-impact model of the AQM-34V RPV (dubbed the IRON TURKEY) was used for the horizontal testing of the FIAS. A vehicle was desired which would have a realistic rigid body behavior during ground impact but which would also be rugged and durable enough to withstand a long test program without major repairs. The model was built in full scale to avoid the uncertainties of scaling an impact situation. Dynamic similarity was assured through careful design which maintained a realistic weight, CG, and mass moments of inertia. The IRON TURKEY was a ground-impact model, in that those portions of the actual vehicle which contacted the ground during a surface landing were realistically modeled as to position and geometry. Within these strict guidelines the model was designed to be as rugged and strong as possible, and it is conservatively estimated that the IRON TURKEY can withstand a static load of 50 g's without yielding. The IRON TURKEY (shown in Figures 39, 40, 41, and 42) is built of 1/2 inch and 3/4 inch 7075-T6 aluminum plate held together with cap screws. The frangible features (wing tips and end plates) were made of 3/4 inch plywood with easily replaceable splice plate fasteners.

2. Because the AQM-34V RPV can be recovered in three different configurations (clean wing, empty, or full pods) it was desired to model the vehicle in the clean wing configuration and then add pods (empty or full) to achieve the alternate configurations. The parameters of dynamic behavior which were chosen as representative of the AQM-34V RPV in the clean wing recovery configuration and the associated modeling tolerances are shown below in vehicle body coordinates.

Vehicle Weight	= 2000 lbs $\pm 25$ lbs
	X = 78.1 $\pm 1.0$ inches
CG Location	Y = 0.0 $\pm 0.5$ inches
	Z = 20.0 $\pm 0.5$ inches
Rolling Moment:	Ixx = 3,730 in-lb-sec <sup>2</sup> $\pm 10\%$
Pitching Moment:	Iyy = 61,900 in-lb-sec <sup>2</sup> $\pm 10\%$
Yawing Moment:	Izz = 62,000 in-lb-sec <sup>2</sup> $\pm 10\%$
Cross Product:	Ixz = 8,050 in-lb-sec <sup>2</sup> $\pm 10\%$

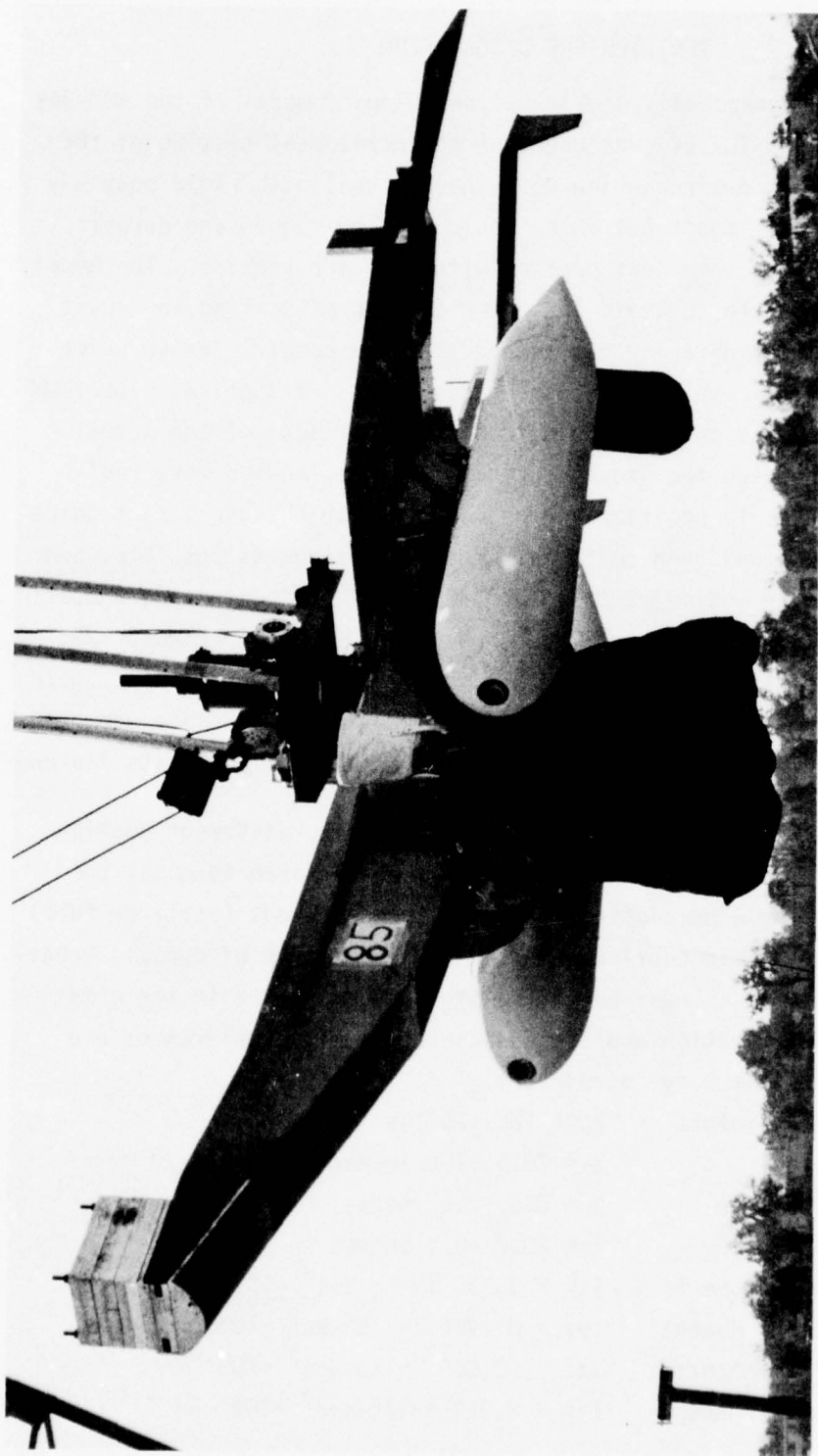
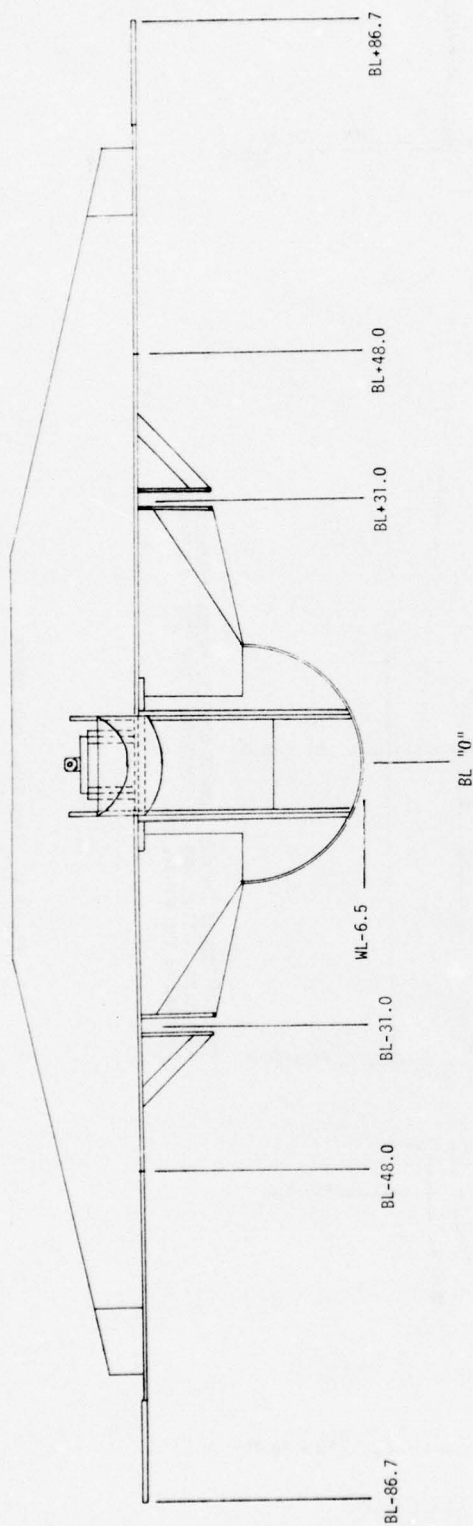
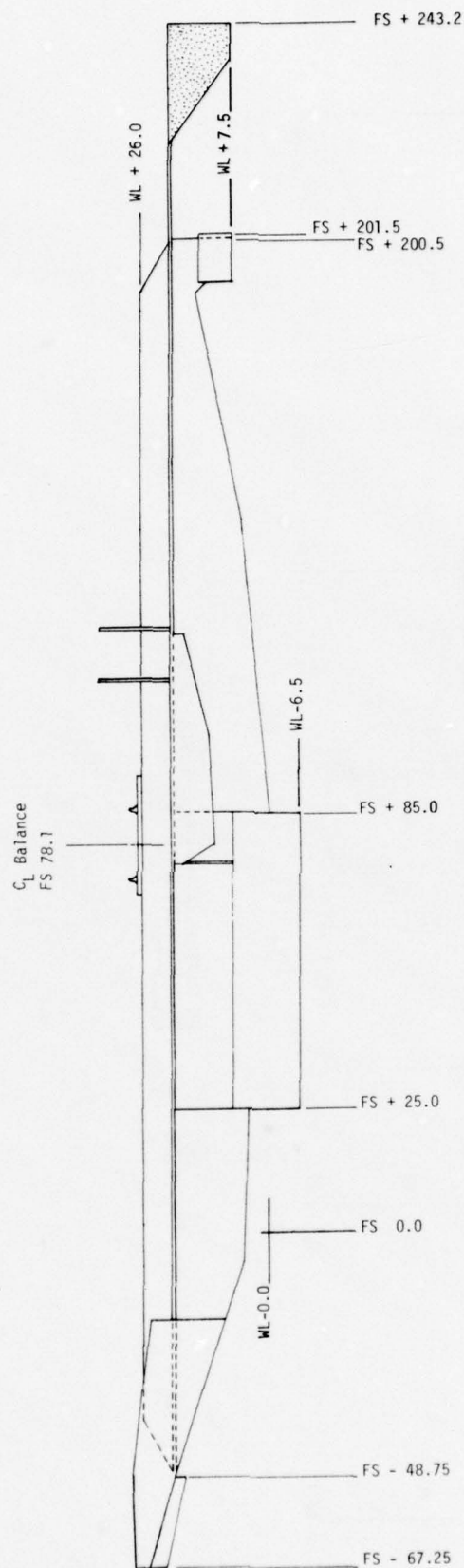


Figure 39. IRON TURKEY Test Vehicle



THE LOCATIONS OF THE WING TIPS, WING TIP ROOTS,  
PYLON AND ENGINE NACELLE ARE THE SAME AS THE  
AQM-34V RPV.

Figure 40. Front View, IRON TURKEY



THE LOCATIONS OF THE NOSE, ENGINE MACELLE, PYLONS, PARACHUTE CAN ATTACHMENT FITTING, AND THE HORIZONTAL STABILIZER ENDPLATES ARE THE SAME AS THE AQM-34V RPV.

Figure 41. Side View, IRON TURKEY



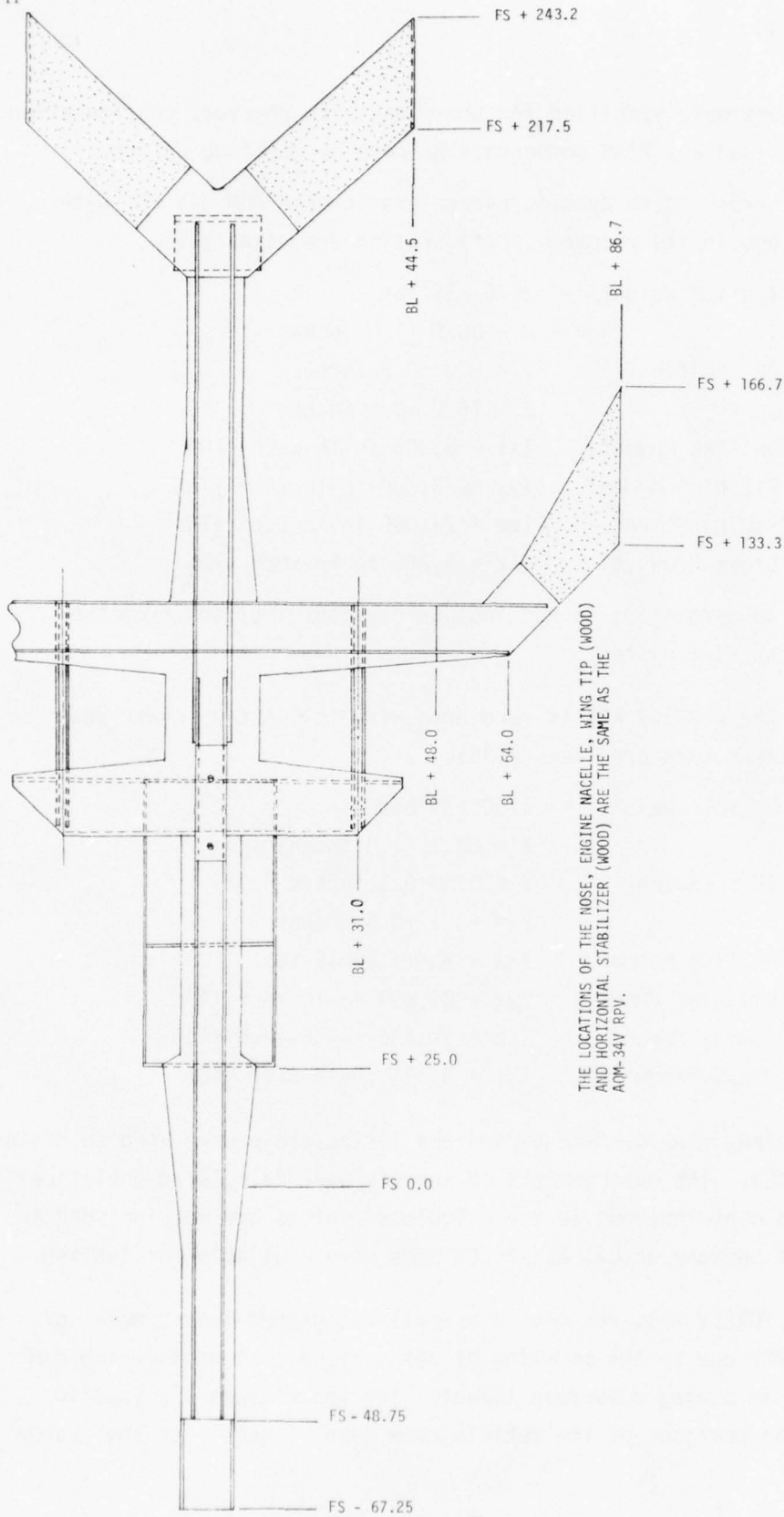


Figure 42. Top View, IRON TURKEY

These values were specified for the clean wing recovery configuration and do not include any FIAS components or pods or mounting pylons.

a. The corresponding dynamic parameters for the AQM-34V RPV with empty ALE-2 pods in its recovery configuration are given below:

Vehicle Weight	=	2470 $\pm$ 25 lbs
		X = 80.5 $\pm$ 1.0 inches
CG Location		Y = 0.0 $\pm$ 0.5 inches
		Z = 16.8 $\pm$ 0.5 inches
Rolling Moment:	Ixx =	5,005 in-lb-sec <sup>2</sup> $\pm$ 10%
Pitching Moment:	Iyy =	73,200 in-lb-sec <sup>2</sup> $\pm$ 10%
Yawing Moment:	Izz =	73,000 in-lb-sec <sup>2</sup> $\pm$ 10%
Cross Product:	Ixz =	8,200 in-lb-sec <sup>2</sup> $\pm$ 10%

Again these parameters do not include any contributions from the presence of the FIAS system.

c. When the AQM-34V RPV is recovered with full ALE-38 chaff pods the dynamic parameters are (sans FIAS):

Vehicle Weight	=	3230 $\pm$ 25 pounds
		X = 82.2 $\pm$ 1.0 inches
CG Location		Y = 0.0 $\pm$ 0.5 inches
		Z = 13.3 $\pm$ 0.5 inches
Rolling Moment:	Ixx =	6,965 in-lb-sec <sup>2</sup> $\pm$ 10%
Pitching Moment:	Iyy =	89,500 in-lb-sec <sup>2</sup> $\pm$ 10%
Yawing Moment:	Izz =	91,100 in-lb-sec <sup>2</sup> $\pm$ 10%
Cross Product:	Ixz =	8,880 in-lb-sec <sup>2</sup> $\pm$ 10%

d. The clean wing dynamic parameters listed above were used to design the IRON TURKEY. The mass moments of inertia were calculated analytically. The ALE-2 pod contributions to the calculated values are not included in this analysis because actual ALE-2 ECM pods were available for testing.

3. The IRON TURKEY test vehicle is a realistic ground-impact model of the AQM-34V RPV due to the modeling of the vehicle components which contact the ground during a surface impact. The vehicle was analyzed to determine what portions of the vehicle came into contact with the ground

during a "normal" impact. It was decided that only the lower surfaces of the vehicle would be modeled because ground contact of the upper surface (e.g., the vertical stabilizer) would not be a normal (hopefully) impact condition. The portions of the vehicle which were chosen as ground contact areas and which were modeled are listed below.

- (1) Nose
- (2) Frangible wing tips
- (3) Frangible wing tip root area
- (4) Horizontal stabilizer endplates
- (5) Engine nacelle (lower surface)
- (6) Parachute can attachment fitting
- (7) Pods

a. The nose of the AQM-34V RPV is located at coordinates  $X = 75.5$ ;  $Y = 0$ ; and  $Z = 24.5$ . Because the contour of the RPV nose is a loft line contour and because engineering drawings were not available, a copycat approach was used to model the nose area. An actual fiberglass nose from a BGM-34A RPV was installed in a reproducing milling machine and a solid aluminum replica was carved out and bolted onto the IRON TURKEY (Figure 43).

b. The frangible wing tips were located so that the outermost portions (the edge striking the ground first) were parallel to the X axis at a Y coordinate of  $\pm 86.7$  inches; a Z coordinate of  $Z = 20$  inches and extended from  $X = 133.3$  inches to  $X = 166.7$  inches. The frangible wing tips were attached at these root areas by means of a  $3/4$  inch plywood splice plate as shown in Figure 44.

c. The frangible wing tip root area was not initially modeled during Tests No. 65 through Test No. 74. Beginning with Test No. 75 this area was modeled by adding a 1 inch x 2 inch x 24 inch aluminum bar to simulate the wing cross sectional area after departure of the frangible wing tip (Figure 45). The importance of this cross-sectional area in determining vehicle slideout stability had not been anticipated in the initial design, so this modeling feature was added during testing.

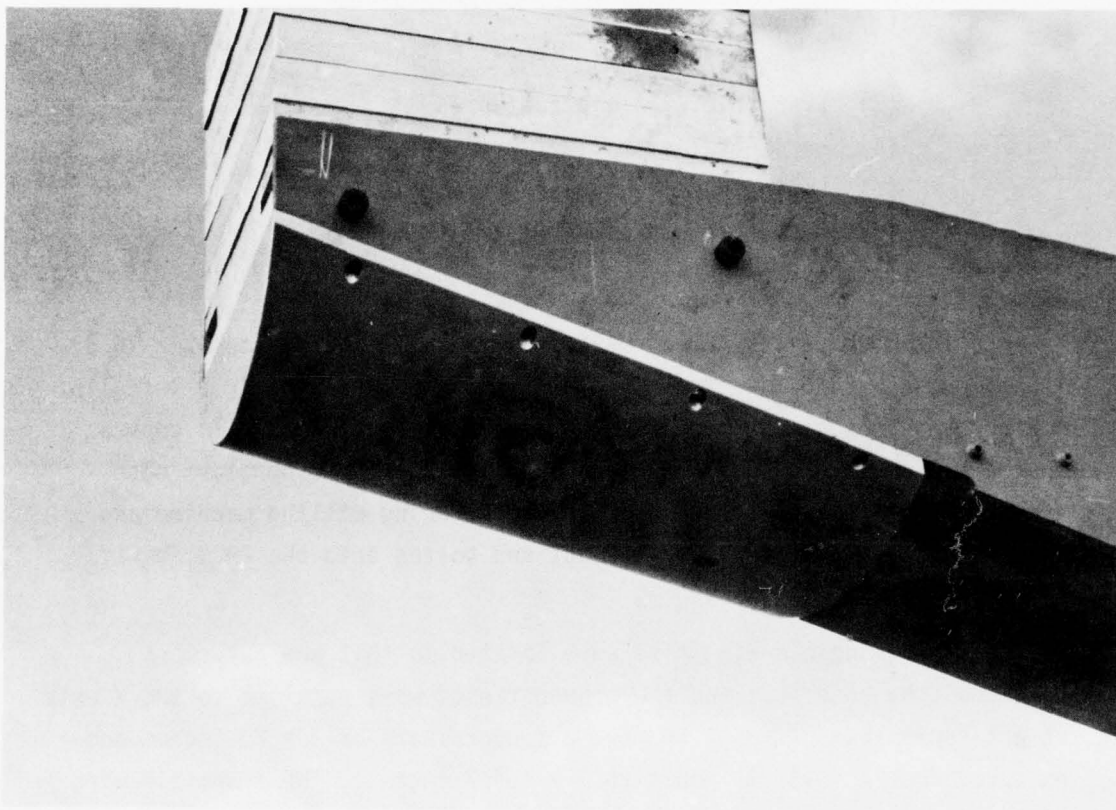


Figure 43. Nose Area, IRON TURKEY



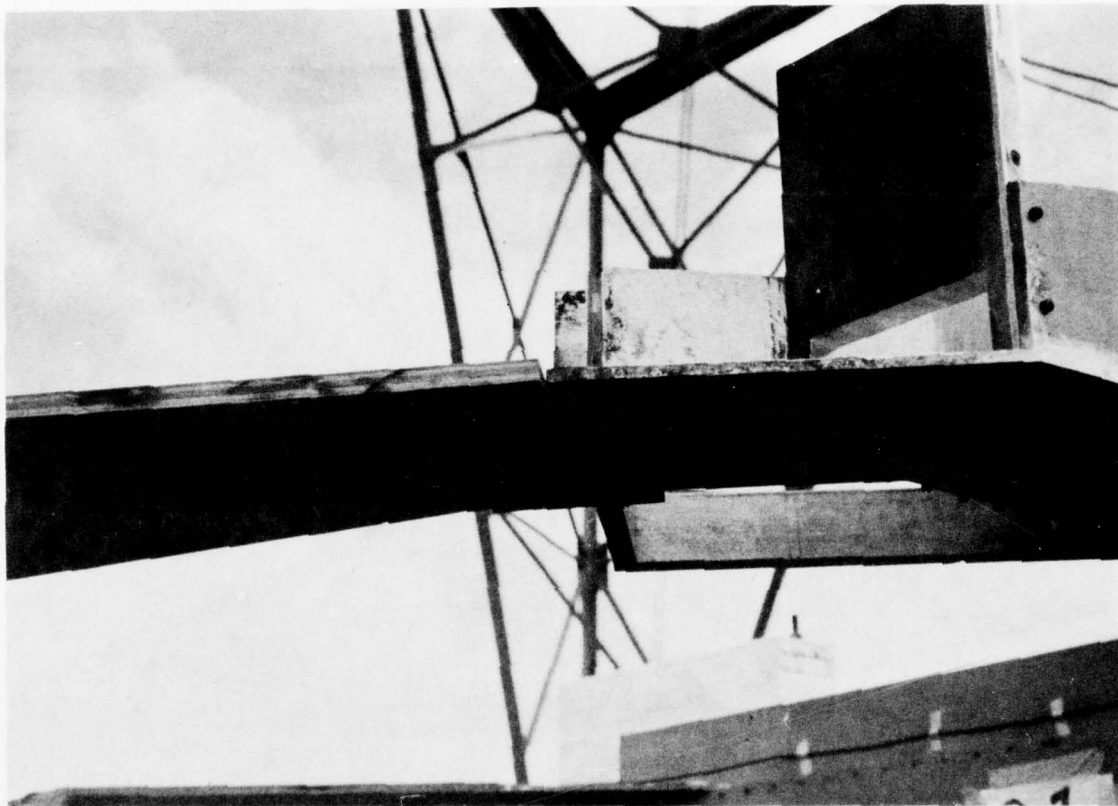


Figure 44. Frangible Wing Tip Joint

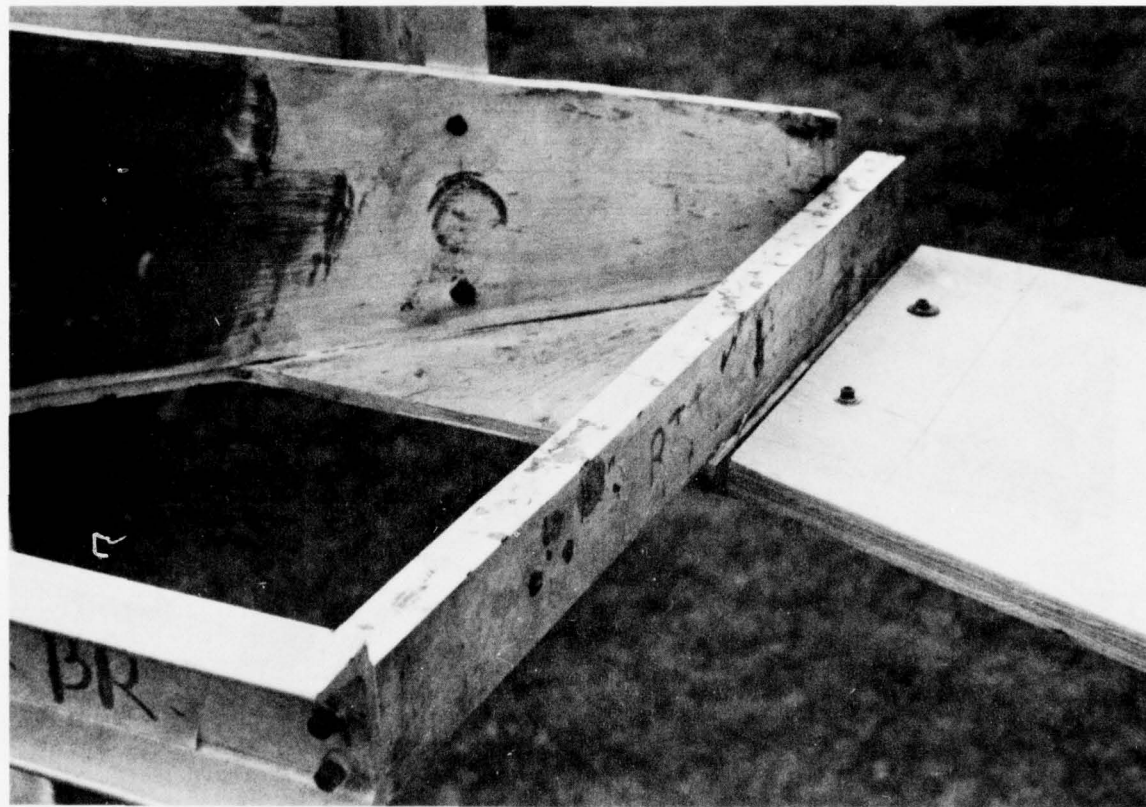


Figure 45. Wing Tip Root Area Modeling

d. The frangible horizontal stabilizer endplates were located at a Y coordinate of  $\pm 44.5$  inches with the first contact edge at  $Z = 7.5$  inches. Only the lower half of the endplates were modeled, so that the upper edge extended from  $X = 217.5$  to  $X = 243.2$  inches. The endplates were joined to the plywood horizontal stabilizer by short pieces of aluminum at an angle as shown in Figures 46 and 47.

e. The engine nacelle was modeled as a cylindrical surface 14 inches in radius with the lowermost portion at  $Z = -6.5$  inches and extended from  $X = 25$  inches to  $X = 85$  inches. The nacelle was modeled as a simply curved surface in lieu of the actual compoundly curved surface, because the nacelle would only be in contact with the FIAS bag and would not receive any ground contact reactions. The engine nacelle as modeled is shown in Figure 39.

f. After the main parachute can was removed from the vehicle during the recovery process a "scoop like" ground contact area was created. This area was modeled in the IRON TURKEY vehicle at an X coordinate of 201.5 inches and a Z coordinate of 7.5 inches. This semi-circular scoop is ten inches in radius with a 2 inch protruding lip and extends over  $Y = \pm 8$  inches, as shown in Figure 47.

g. The pods which were used for the IRON TURKEY testing were actual ALE-2 ECM pods which had been salvaged by the 6514th Test Squadron at Hill Air Force Base. They were mounted on the wing pylons ( $Y = \pm 31.0$  inches) at a  $3^\circ$  nose down relation to the X axis so that the lowermost portion of the pod was at  $Z = -11.0$  inches, as shown in Figure 39.

4. Although the IRON TURKEY does not physically look like an RPV, it is a realistic tool for the study of the ground impact of the AQM-34V RPV. The test vehicle proved to be durable and capable of being refurbished for the next test in one eight hour day without difficulty. The IRON TURKEY was designed and fabricated by the test support contractor during the time period of late April 77 through July 77, with a delivered price of \$39,118.00 (without pods and instrumentation).



Figure 46. Horizontal Stabilizer (Test No. 84)



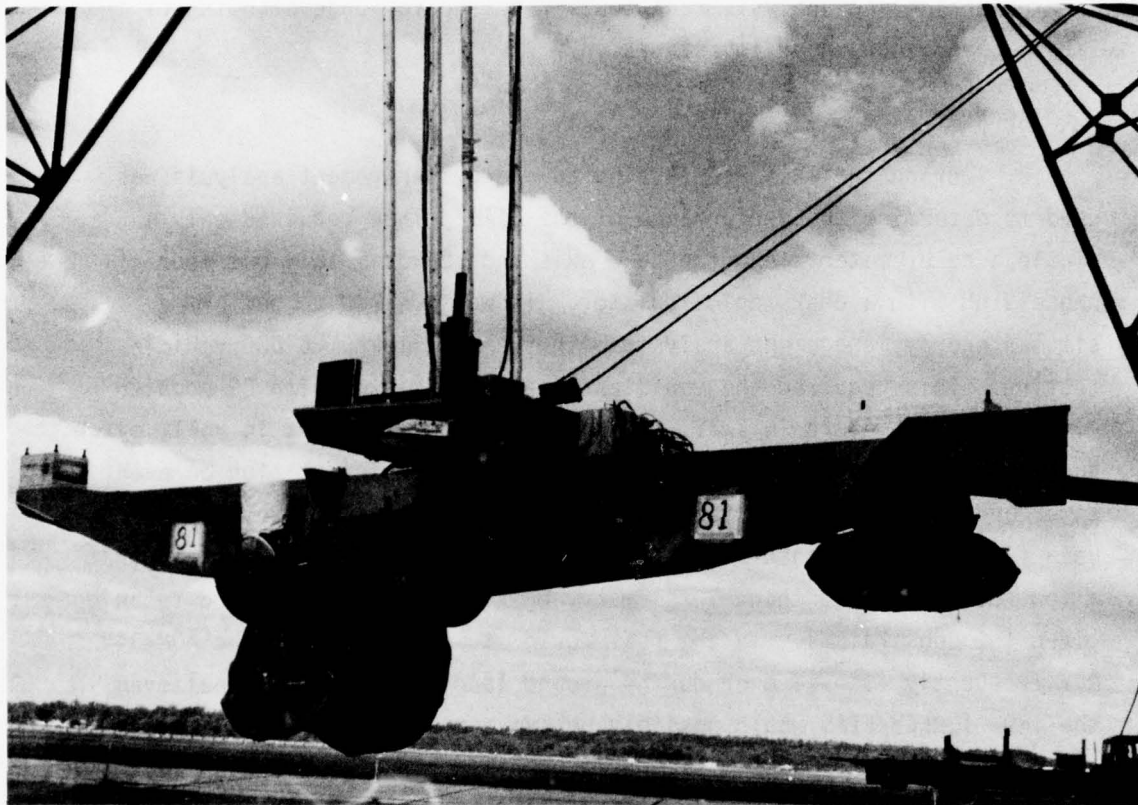


Figure 47. Horizontal Stabilizer Endplates (Test No. 81)

SECTION VI  
INSTRUMENTATION AND ANALYSIS TECHNIQUES

1. OVERVIEW

The transition from the one degree-of-freedom (DOF) IRON PIG testing to the six DOF IRON TURKEY testing required a major effort to upgrade the data gathering and analysis techniques required for understanding of the impact phenomenon under investigation.

2. APPROACH

a. During the IRON PIG testing an energy management analysis was used to determine the performance of the FIAS. This required only a single accelerometer along the CG-Z axis and approximately one hour of processing with a desk top calculator. It was desired to perform a similar energy management analysis with the IRON TURKEY 6 DOF vehicle testing. This required the vehicle to be instrumented with CG mounted linear accelerometers in X, Y, and Z as well as rate gyros in roll, pitch, and yaw. In addition to these channels additional information on event times and instrumentation functioning was required. To transmit the raw data from the test vehicle to a recording station it was determined that a low cost, multiple channel telemetry unit would provide a good technique given the constraints. In the real world it was known that the AQM-34V RPV frequently flipped over during ground landings and it was believed the IRON TURKEY/FIAS would possibly behave similarly. If an umbilical cable (hard wire) were used, it would probably be damaged during a vehicle flipover and would require new wiring (\$1500/set) and extensive labor to recalibrate the sensors. The telemetry unit (\$9,600) removed this problem and allowed for a simpler testing process as well. During refurbishment of the vehicle between tests it was taken to a location several miles from the test site which would have required continual connecting and disconnecting of the umbilical cable. Another feature of the telemetry was that in order to determine if everything was working properly it was simply a matter of turning the unit on and driving the truck/vehicle around in circles within range of the receiving antennae (a non-precise but simple procedure).

b. At the test site the received data was permanently recorded on a magnetic tape which was compatible with the computerized processing required.

c. The overall goal of the data gathering and processing was an energy management analysis with a resolution of  $\pm 100$  ft-lbs. It was known that at the beginning of a test the 2,140 pound vehicle was 15.15 feet above the ground and so had an energy level of 32,420 ft-lbs and at the end of the test the vehicle was at rest atop the FIAS bag. The purpose of the energy management analysis was to determine where the energy went and how it got there. Further, the energy management allowed for the examination of the quality of the data being recorded. By starting at vehicle release and tracking the energy using the recorded data it was possible to determine the overall level of error in the data gathering system. For example, if by open loop integration the energy management analysis shows the vehicle to be 10 feet in the air at the conclusion of the test when it is known that the vehicle is at rest on the ground then an estimation of the collective errors in the data gathering system may be made. This energy management technique was a powerful tool during the testing and revealed performance parameters which would have been hidden using just acceleration traces.

### 3. HARDWARE

a. The accelerometers used during the IRON TURKEY testing were KULITE Model GA-E-813-50 which had a range of  $\pm 50$  g's with linear response to 500 Hz. Each accelerometer was calibrated on a turntable at loadings of -50, -40, -30, -20, -10, -5, 0, 5, 10, 20, 30, 40, and 50 g's. Further, the output voltages were calibrated through the entire data gathering system (telemetry transmission and recording) for each test.

b. The rotational rates were sensed by three axis rate transducers, Model No. RT02-0203-1 and -2, manufactured by Humphrey Inc., San Diego, CA. These transducers were capable of  $\pm 400^\circ/\text{sec}/\text{axis}$  and were also calibrated on the turntable and through the entire system similarly to the linear accelerometers.

c. The telemetry system employed for the data transmission was a custom modification of a standard PCM-16 Telemetry System manufactured by Inmet Inc., Indian Harbour Beach, FL. The specifications for this unit are as follows:

Modified PCM-16 Telemetry System

System to consist of three units:

- (1) Transmitter
- (2) Receiver
- (3) Demodulator/Decommutator

Number of channels: 16 maximum

Data work: 8 bits

Frame: 16 channels (data words)

Range: 200 feet nominal

Sample rate: 6,000 samples per second

Accuracy through system:  $\pm 1.5\%$  of full scale

Carrier Frequency range: 88 - 108 MHz

Transmitter:

- (1) Input to be +5 VDC full scale, single ended, unipolar.
- (2) Power source: 20-28 VDC
- (3) Weight: 46 oz
- (4) Output format: PCM with frame and channel sync.
- (5) Transmission mode: NRZ - PCM/FM
- (6) Temperature range: 0°C to +65°C
- (7) Transmitter to be shock mounted to 20 g's.

Receiver: Model R-10A

- (1) Output: 5 volts at 5 MA
- (2) Sensitivity: 2 microvolts for 20 dB quieting
- (3) Power requirements: 105-125 VAC at 50-60 Hz

d. The recording equipment used was the same Bell and Howell magnetic tape unit and signal conditioners used during the IRON PIG testing.

#### 4. ANALYSIS TECHNIQUE

Once the acceleration and rate data were recorded, the energy management analysis was performed using the CDC 6600 computer complex at



WPAFB. The energy management technique was analyzed, programmed, and performed by Mr. Michael W. Higgins and was based on the technique of Lagrangian Dynamics. Lagrangian techniques (which themselves are based on an energy approach) readily lent themselves to the energy management analysis of this problem and thus "simplified" the analysis. The results of this analysis are the complete time histories of the vehicle in both a body fixed and an earth fixed coordinate system and the time histories of the two coordinate systems as well as the vehicles energy vs time (translational, rotational, and potential) history in the earth fixed coordinate system as shown in Figures 48 through 56 for Test No. 77.

Application of this powerful technique requires a great degree of mathematical expertise due to the nature of the testing. The testing borders on impact phenomena, and as such the data frequently contains discontinuities and non-linearities due to the transducer limitations. Additionally, any small errors in the data sensing or processing will be magnified by the multiple integrations and manipulations required by the energy management analysis. However, when this energy management technique is intelligently applied it is most revealing of the phenomena under investigation.

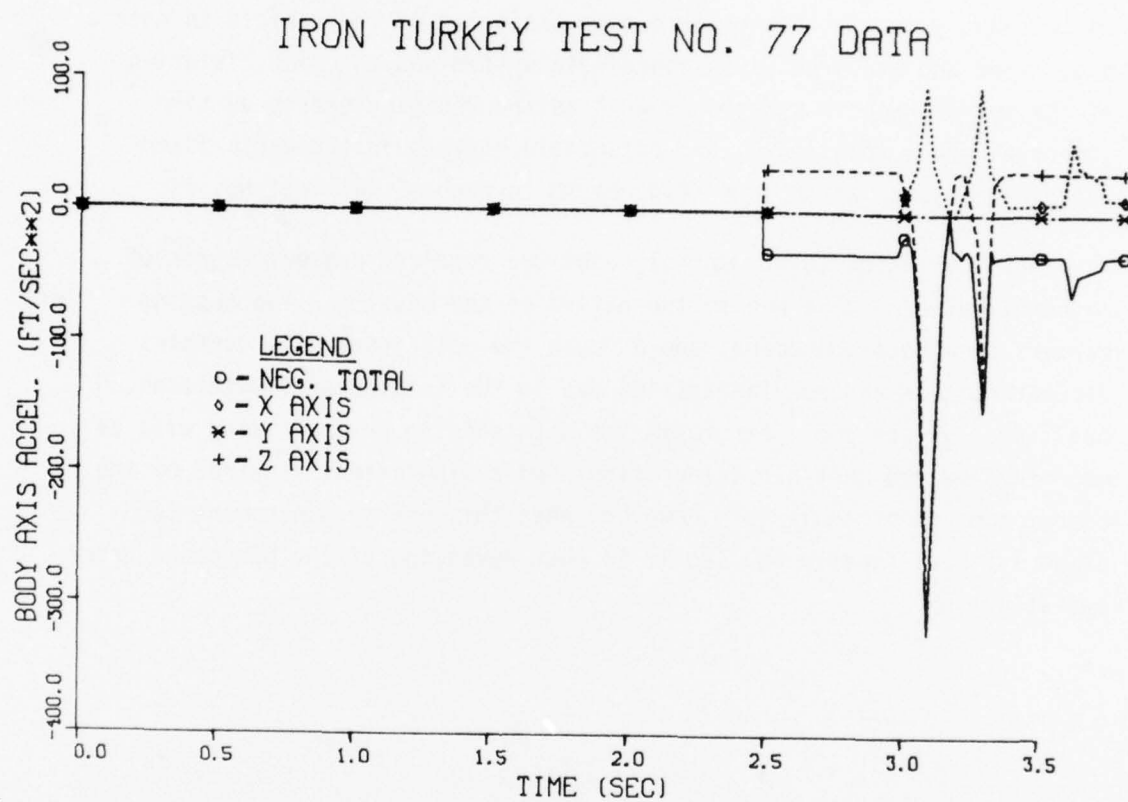


Figure 48. Test No. 77, Body Axis Accelerations

# IRON TURKEY TEST NO. 77 DATA

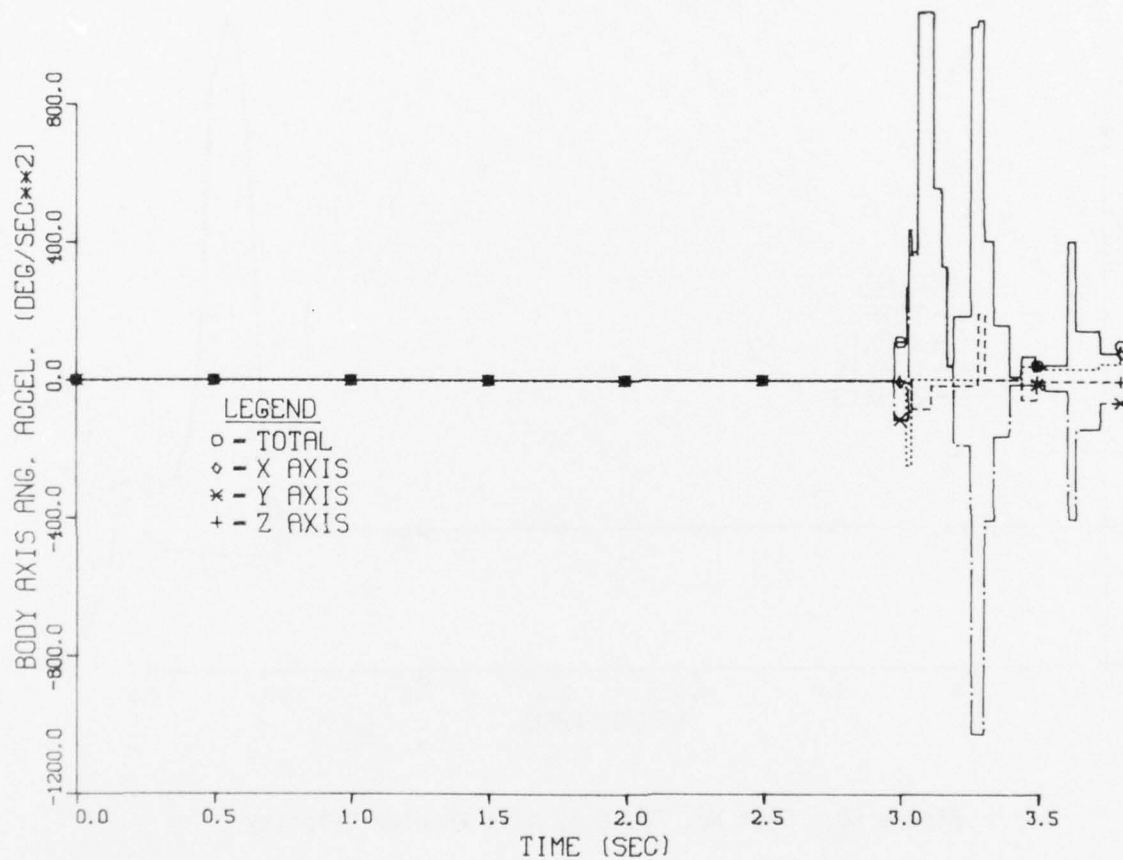


Figure 49. Test No. 77, Body Axis Angular Accelerations

# IRON TURKEY TEST NO. 77 DATA

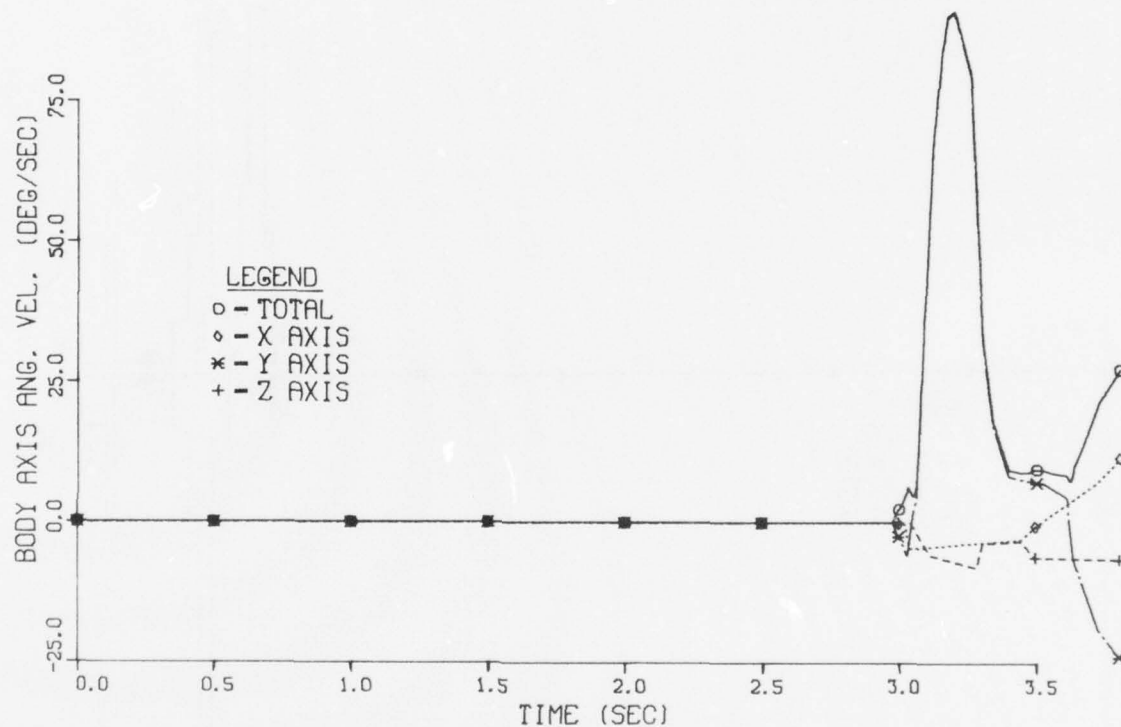


Figure 50. Test No. 77, Body Axis Angular Velocity



AD-A075 658

AIR FORCE FLIGHT DYNAMICS LAB WRIGHT-PATTERSON AFB OH  
INVESTIGATION OF A DEPLOYABLE POLYURETHANE FOAM GROUND IMPACT A--ETC(U)  
JUL 79 S R MEHAFFIE

F/O 22/2

IMPACT A--ETC(U)

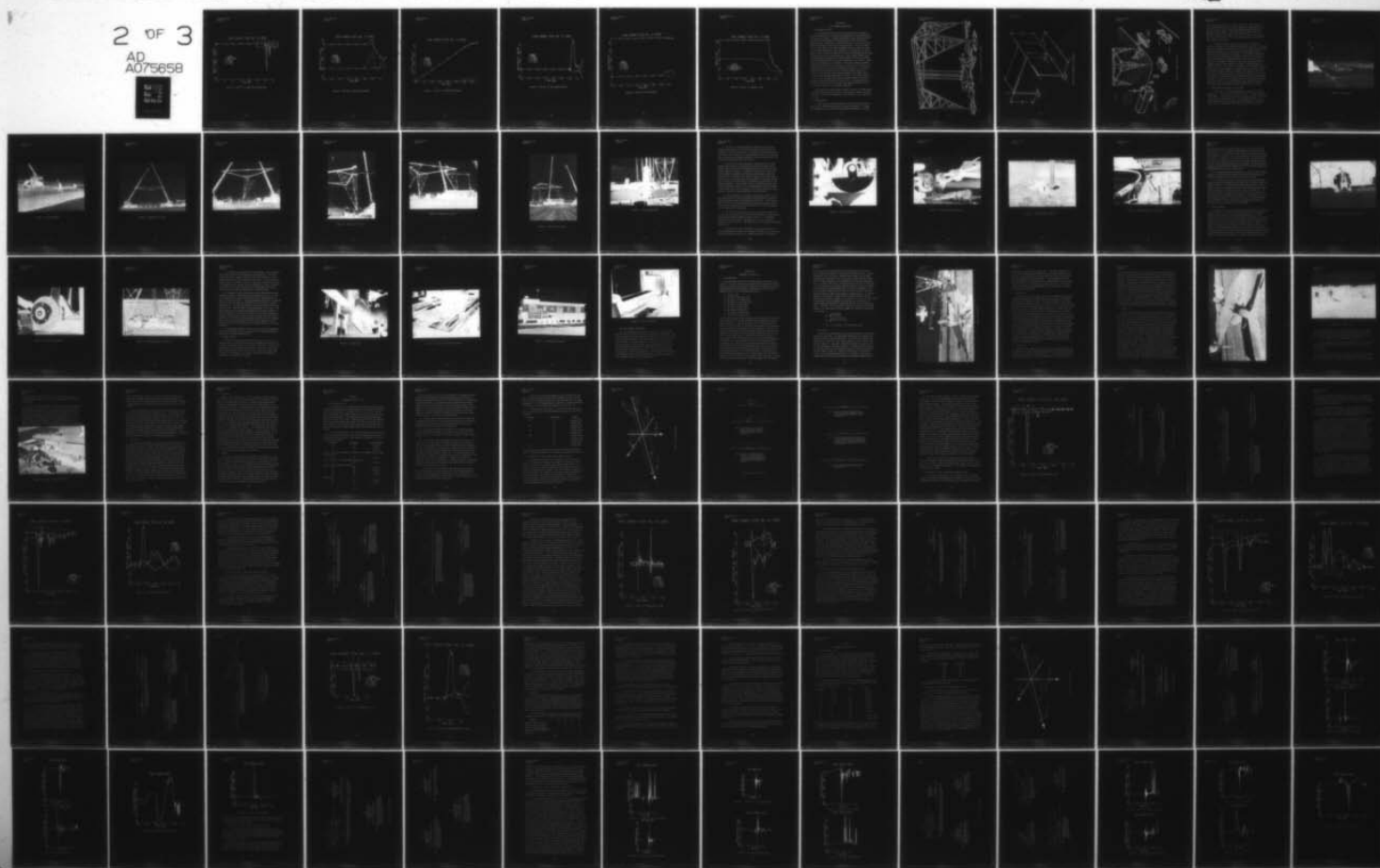
UNCLASSIFIED

AFFDL-TR-78-145-VOL-2

NL

2 OF 3

AD  
A075658





IRON TURKEY TEST NO. 77 DATA

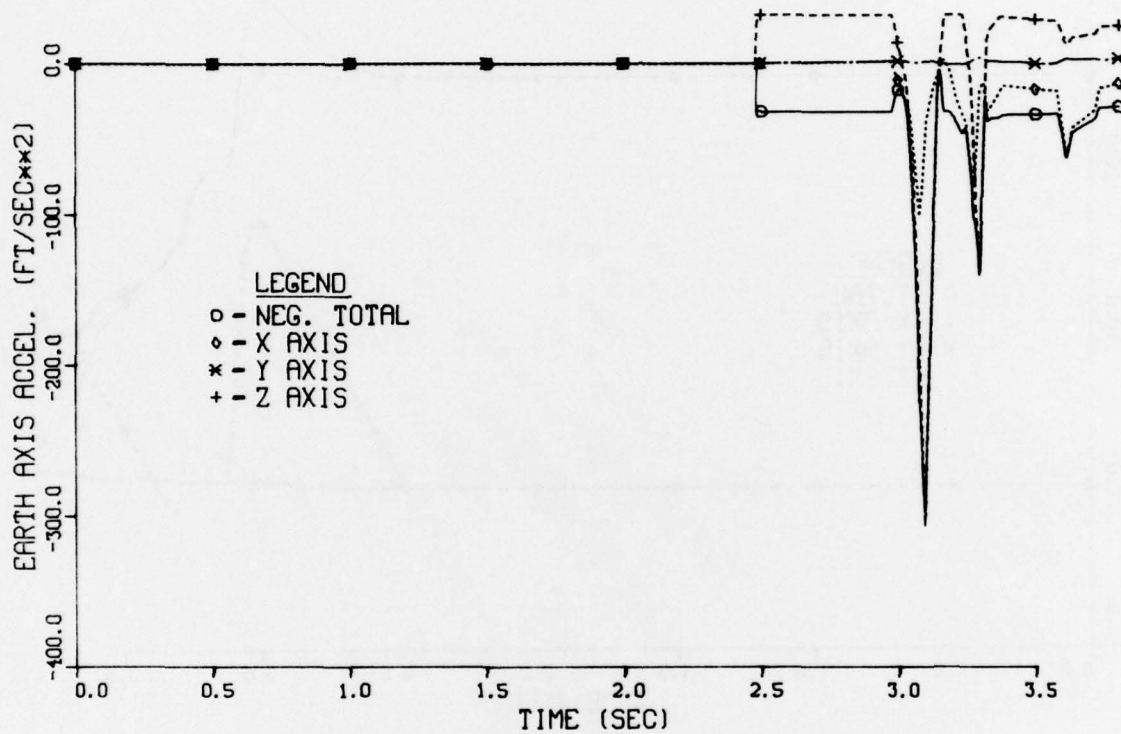


Figure 51. Test No. 77, Earth Axis Accelerations

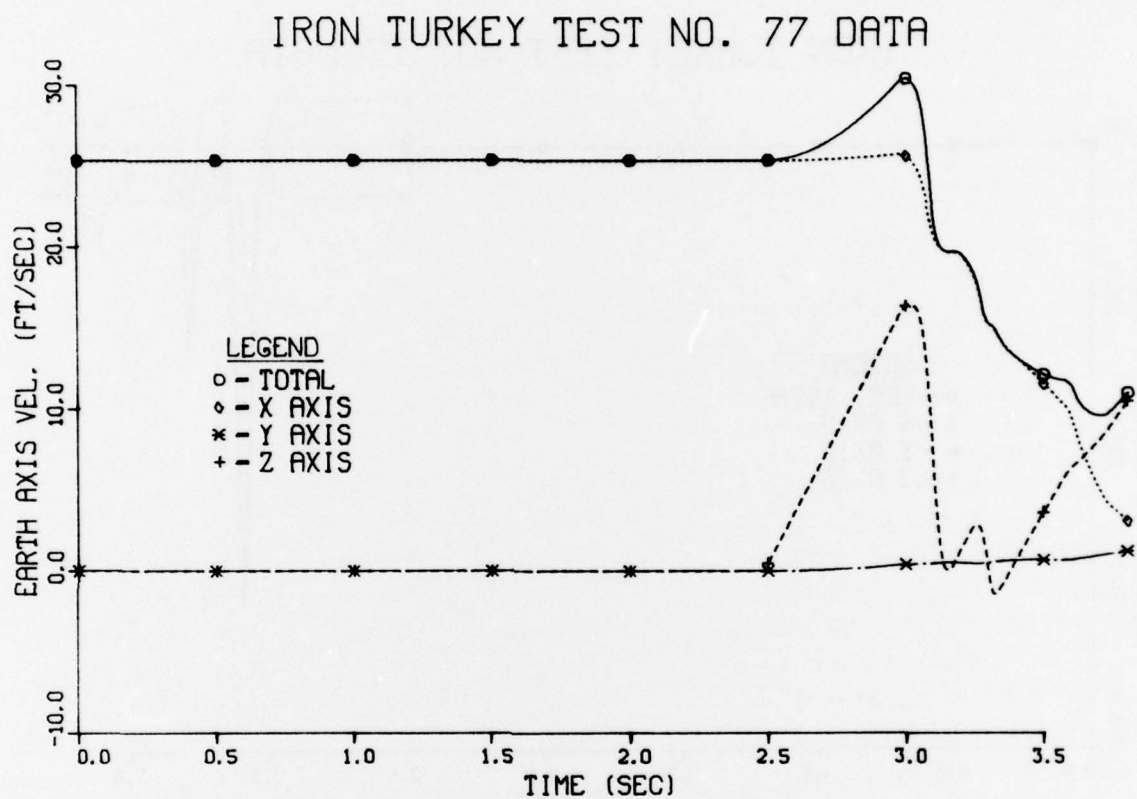


Figure 52. Test No. 77, Earth Axis Velocity



# IRON TURKEY TEST NO. 77 DATA

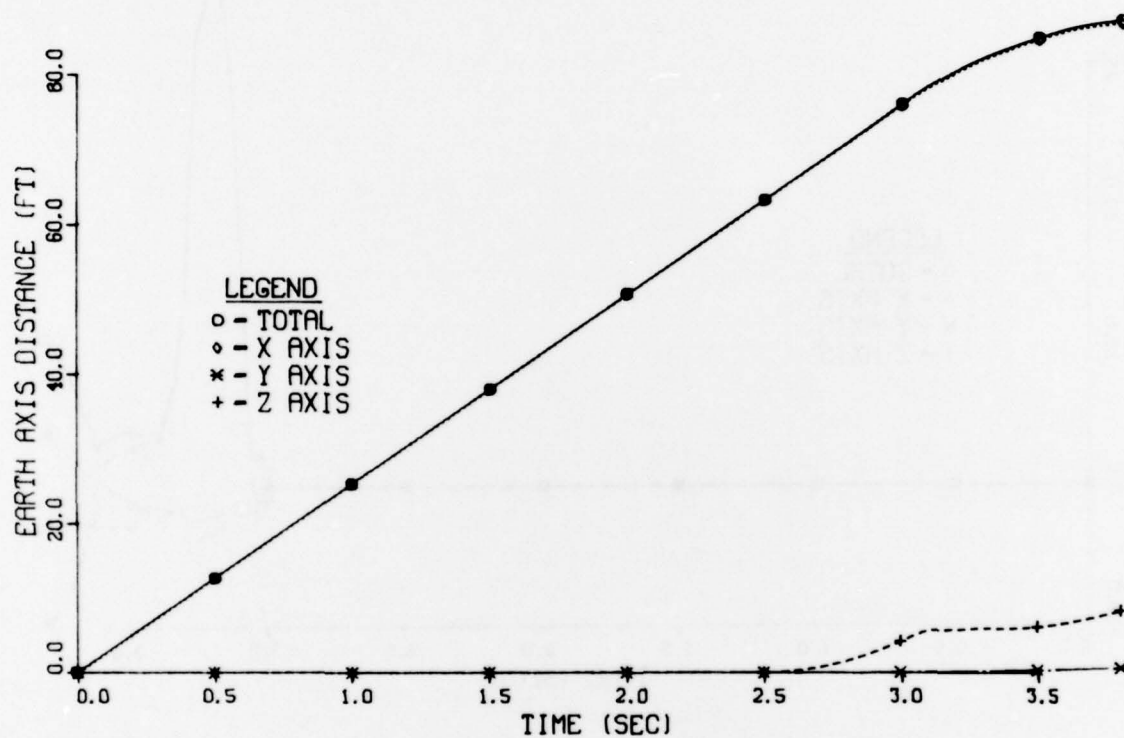


Figure 53. Test No. 77, Earth Axis Distance

# IRON TURKEY TEST NO. 77 DATA

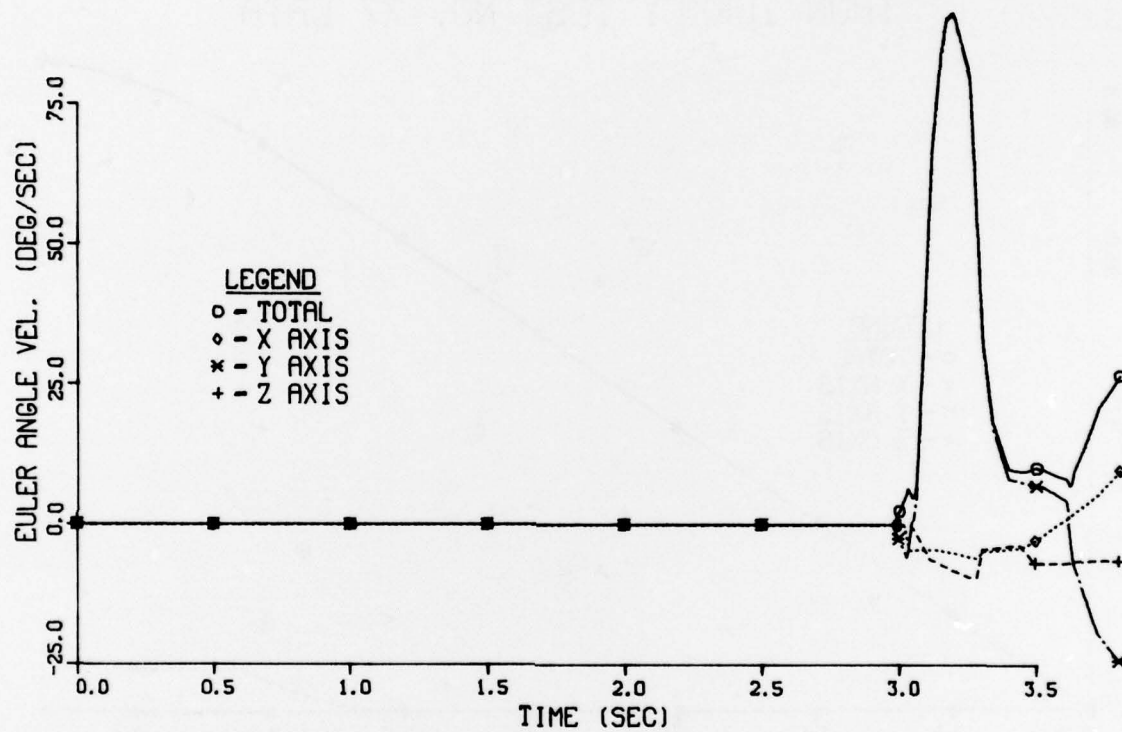


Figure 54. Test No. 77, Euler Angle Velocity

IRON TURKEY TEST NO. 77 DATA

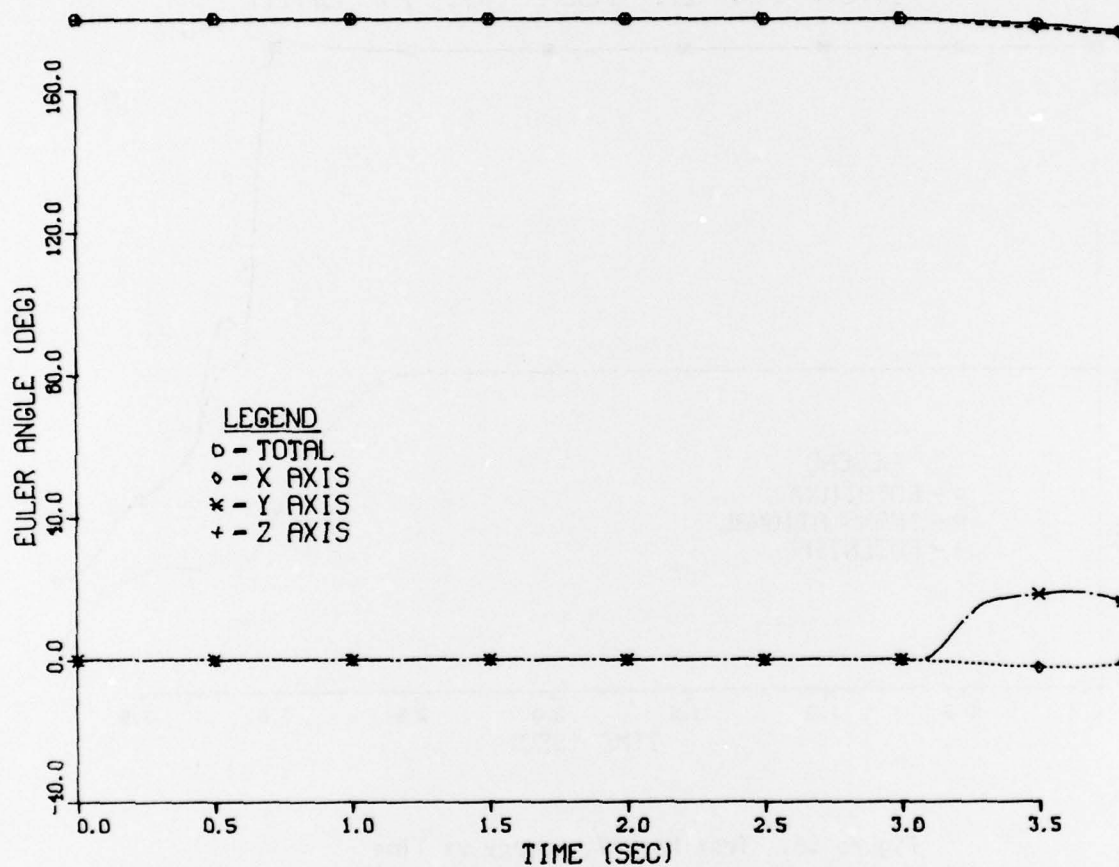


Figure 55. Test No. 77, Euler Angles

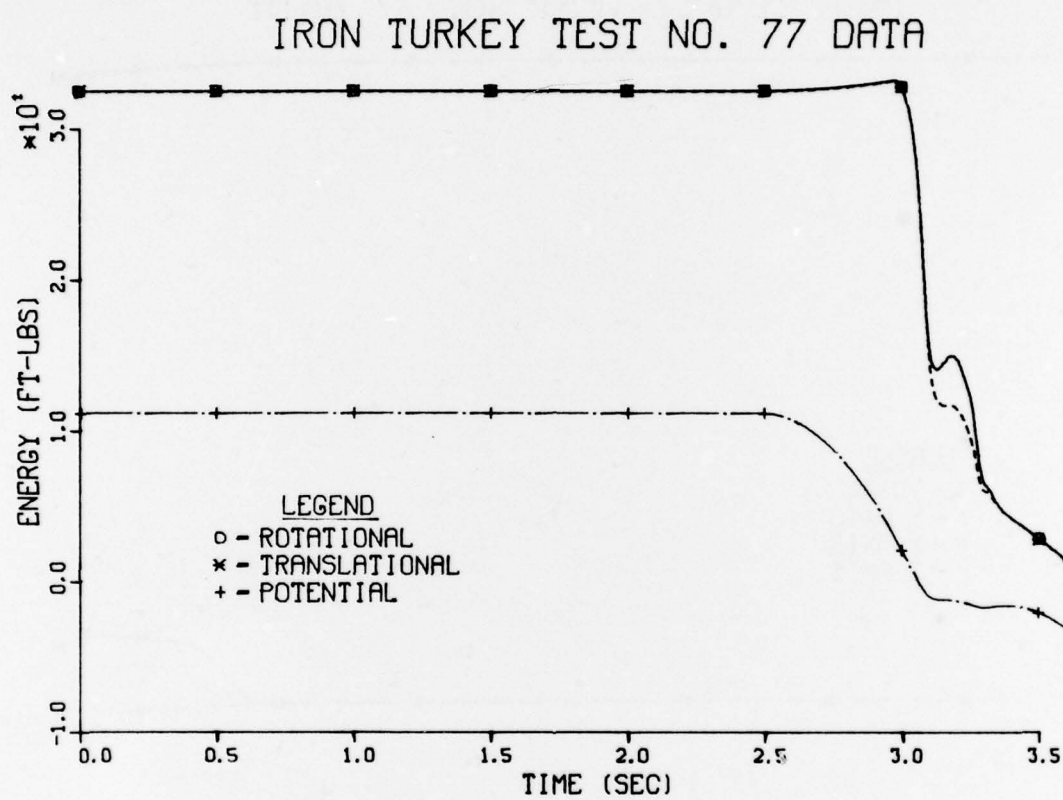


Figure 56. Test No. 77, Energy vs Time



## SECTION VII

### TEST APPARATUS DESCRIPTION

#### 1. TEST METHOD SELECTION

a. The horizontal testing of the FIAS required that a method of testing which would yield the maximum knowledge for a minimum expenditure of resources be devised. The test method should offer maximum control of the vertical and horizontal velocities and the vehicle orientation at ground contact. Additionally, a sustained test rate of one test per day should be achievable using only a single work shift. Due to the nature of full-scale impact testing and the hazards which can arise, the safety of test was considered as a major parameter in the selection of a test method. After an extensive analysis of various test methods and nationally available facilities, it was decided that a test method incorporating a four-bar pendulum suspended from a tower assembly and located at Wright-Patterson AFB would offer the optimum combination of test control, safety, speed, and minimum resources required. The four-bar pendulum assembly (Figures 57 and 58) was to be a temporary structure which could be disassembled and moved as the FIAS investigation progressed. A flat grassy meadow was chosen as being typical of the RPV recovery area terrain conditions and therefore a test site was located in the WPAFB, Area B airfield, which had been deactivated for flying. The site was chosen at a corner of the East-West Taxiway and a cross-over ramp so that there was paved access on two sides of the test site. The pendulum tower was oriented so that the test vehicle was aimed toward the middle of the field with at least 1/2 mile clearance downrange.

The location thus chosen became a remote test site, since there were no available hookups to any utilities including power, water, sanitation, steam, etc. The overall arrangement at the FIAS test site is depicted in Figure 59.

#### 2. TOWER ASSEMBLY

a. The purpose of the tower assembly is to serve as the mounting point for the upper head assembly of the four-bar pendulum. The tower was designed so that it could be disassembled and moved with a minimum

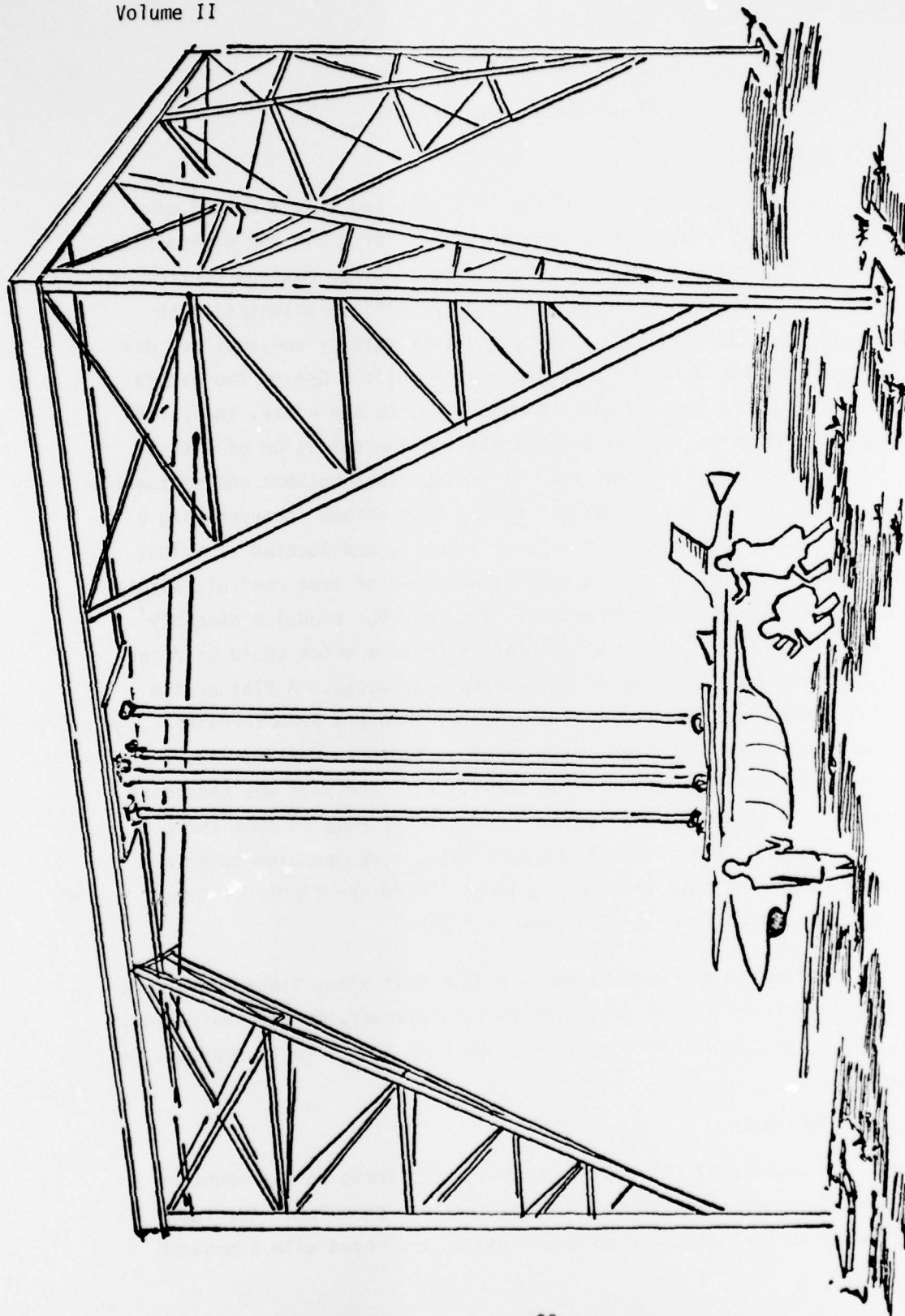


Figure 57. Test Apparatus, Artist's Concept

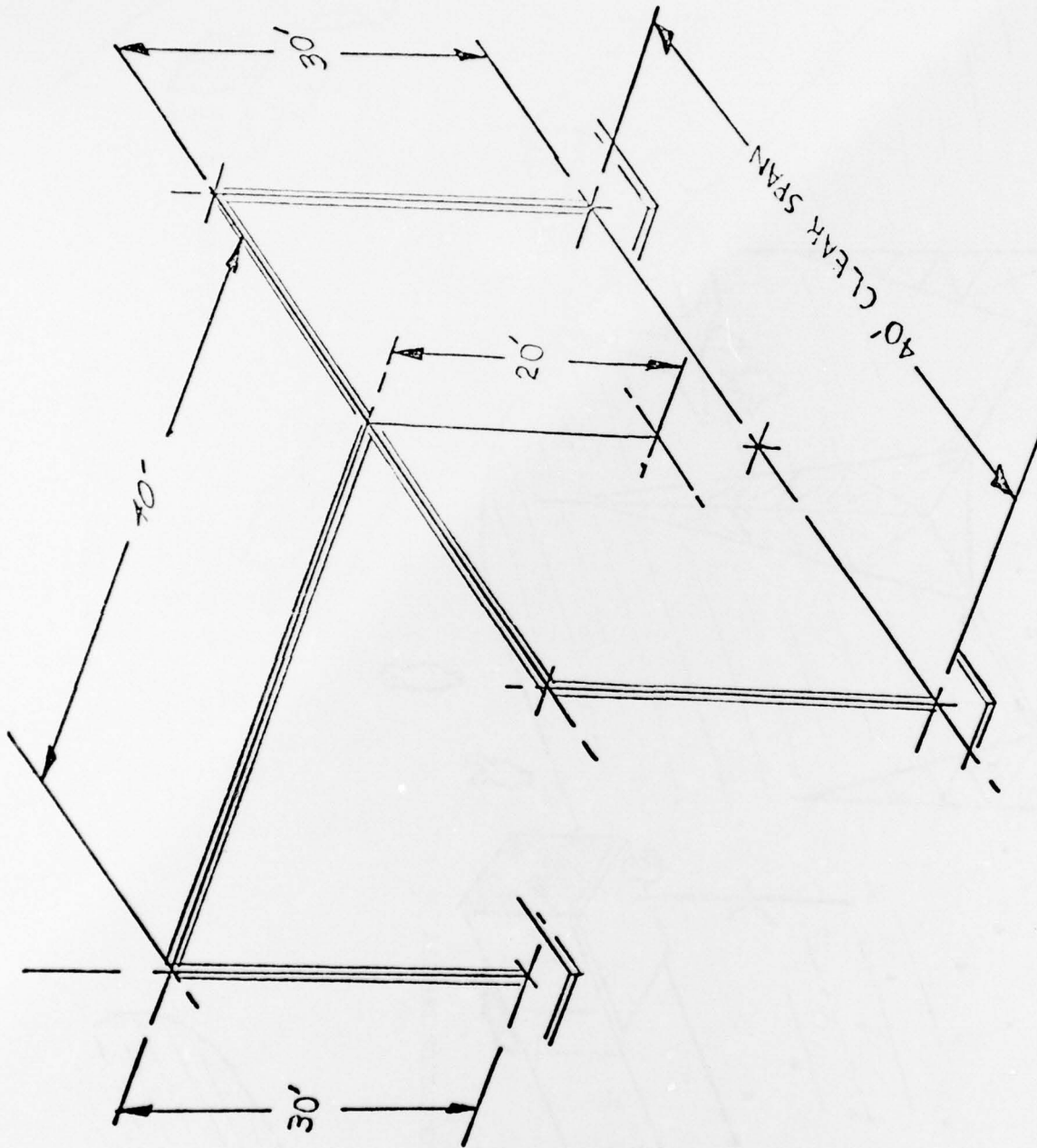


Figure 58. Test Apparatus, Dimensions

Figure 59. Support Facilities



of site preparation so as not to overly disturb the impact terrain. A three-legged triangular steel structure capable of withstanding a maximum live pendulum load of 10,000 pounds applied anywhere within the pendulum arc was designed. The site preparation consisted of the permanent placement of 3 footers, each 4 feet x 4 feet x 3 feet deep, set flush with the terrain so as not to interfere with other activities after removal of the tower.

b. The tower assembly consists of nine pieces of structure: 3 legs, 2 tie beams, 1 main beam, and three braces, as shown in Figure 60. The tower is assembled by first joining the two tie beams, the main beam, and the three braces into the major triangle subassembly shown in Figure 61, using eighteen nuts and bolts. This triangular subassembly is then raised to a height of approximately 35-40 feet (Figure 62) so that a crane hook can be lowered through a corner to place a leg in position for attachment (Figure 63). The leg is then attached to the triangle using the 6 nuts and bolts provided (18 required total) as shown in Figure 64. This process is repeated for the remaining two legs (Figure 65) until the assembly is complete and the tower lowered onto the concrete footers where it is secured by four studs per leg. The final step in the tower assembly is to mount the upper head of the four-bar pendulum to the main beam (Figure 66) using the four nuts and bolts provided. The total on-site assembly time for this process is approximately four hours at a cost (professional steel riggers) of \$1845. To disassemble the tower assembly the above steps should be reversed.

### 3. LOWER PENDULUM HEAD AND PULL-BACK WINCH

a. The heart of the four-bar pendulum test method is the lower pendulum head with its multiplicity of functions. The lower pendulum head (shown with the vehicle installed in Figure 67) consists of vertical and horizontal release mechanism, a Z axis height adjustment, a yaw angle adjustment, a vehicle safety mechanism (redundant), a pendulum brake, and a pull-apart umbilical power cable to the test vehicle.

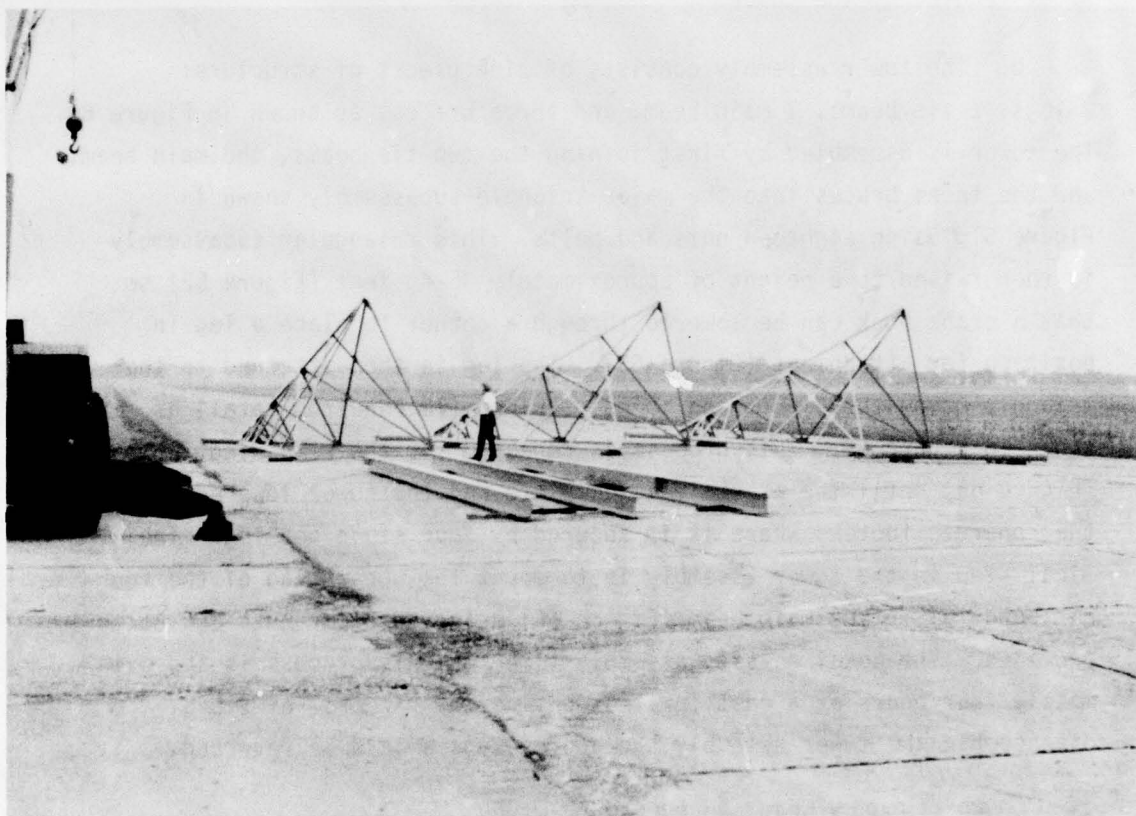


Figure 60. Parts Layout

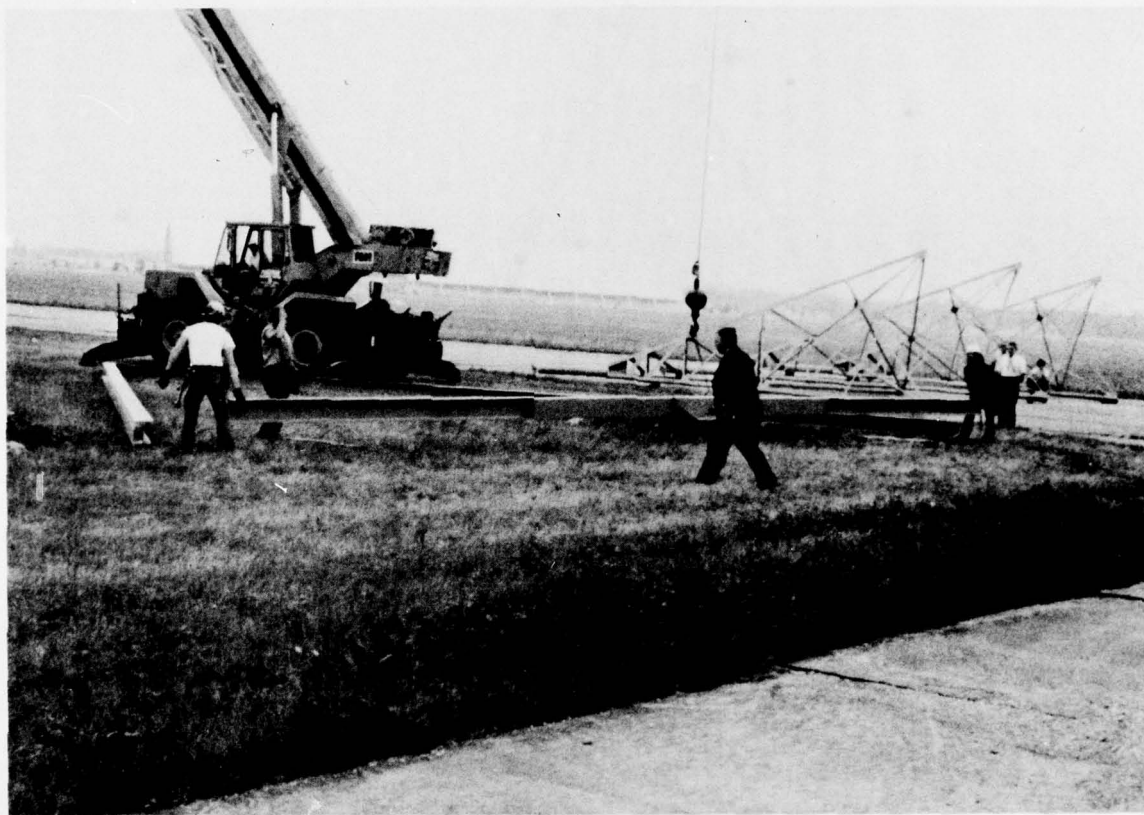


Figure 61. Triangle Assembly

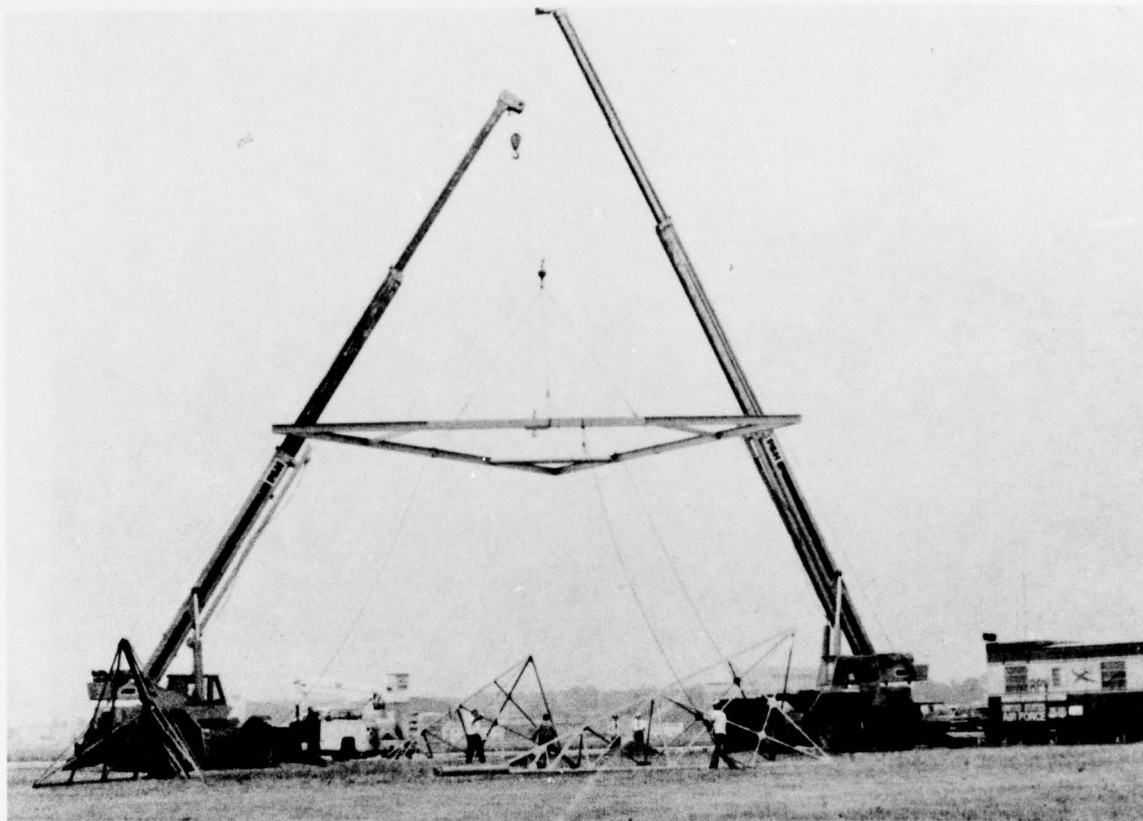


Figure 62. Beginning of Erection



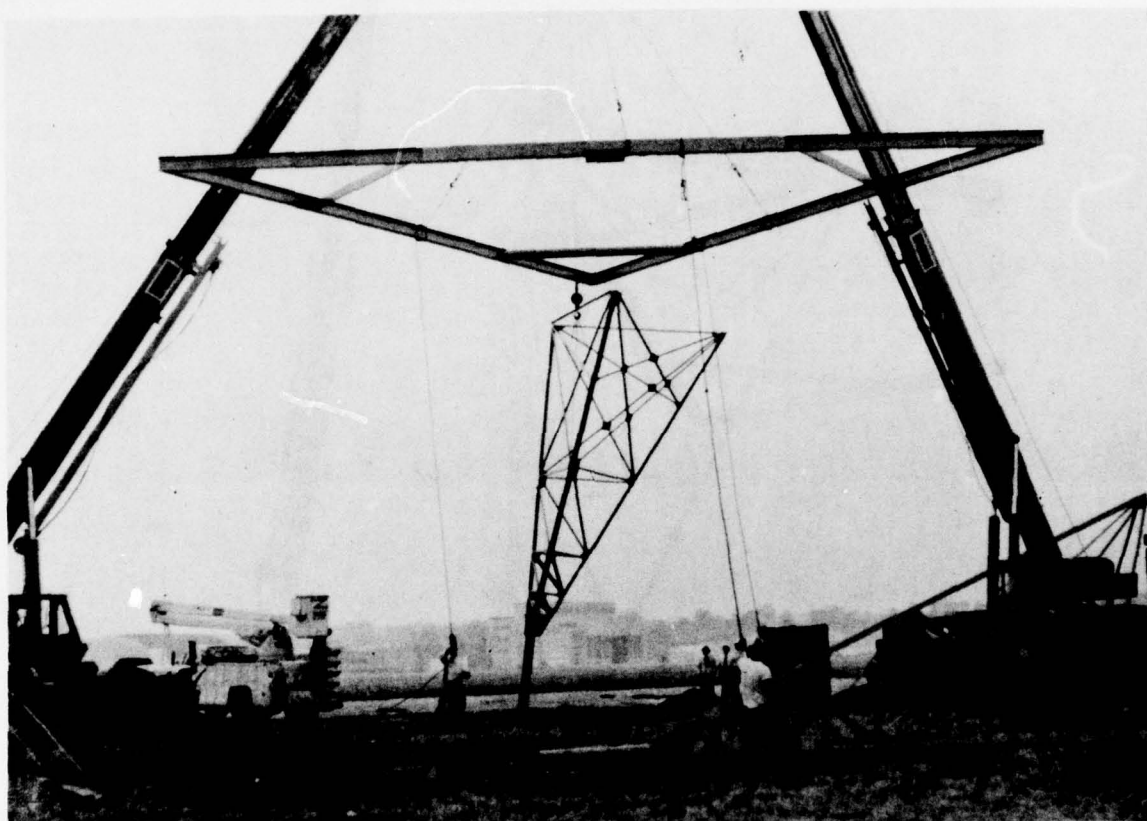


Figure 63. Raising First Leg



Figure 64. Assembly of First Leg

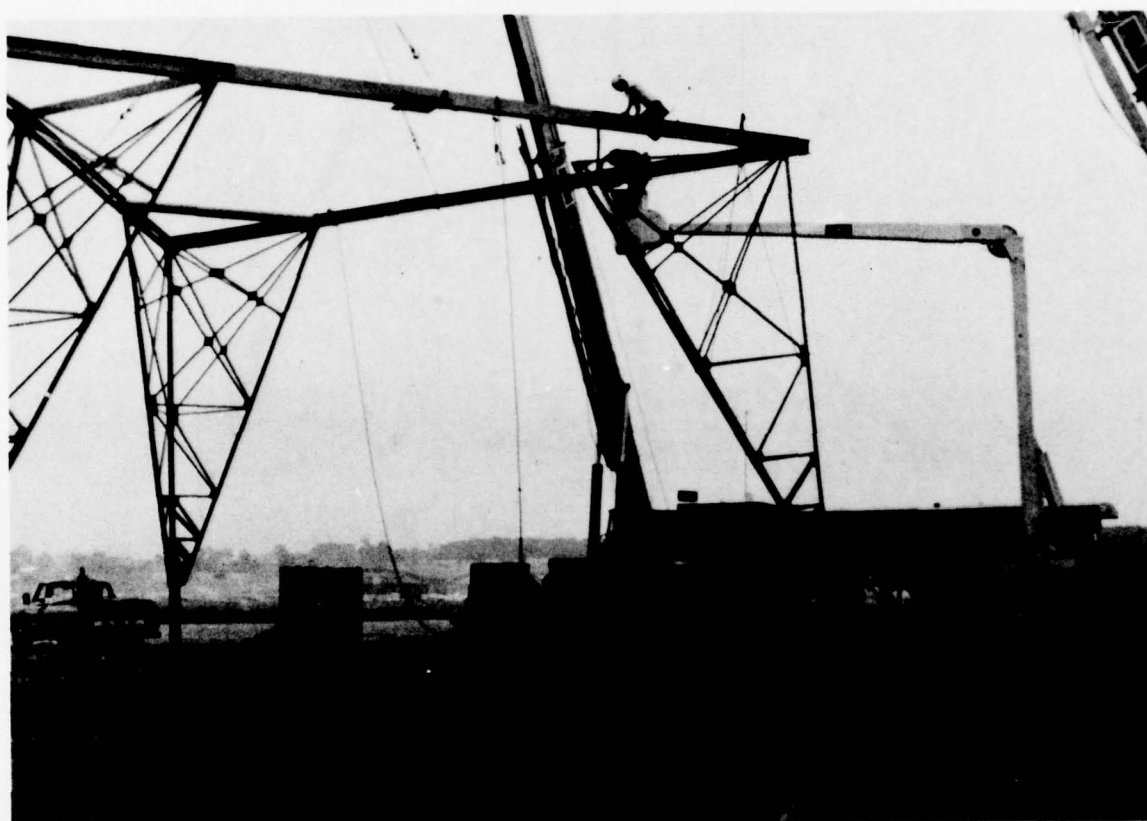


Figure 65. Assembly of Last Leg

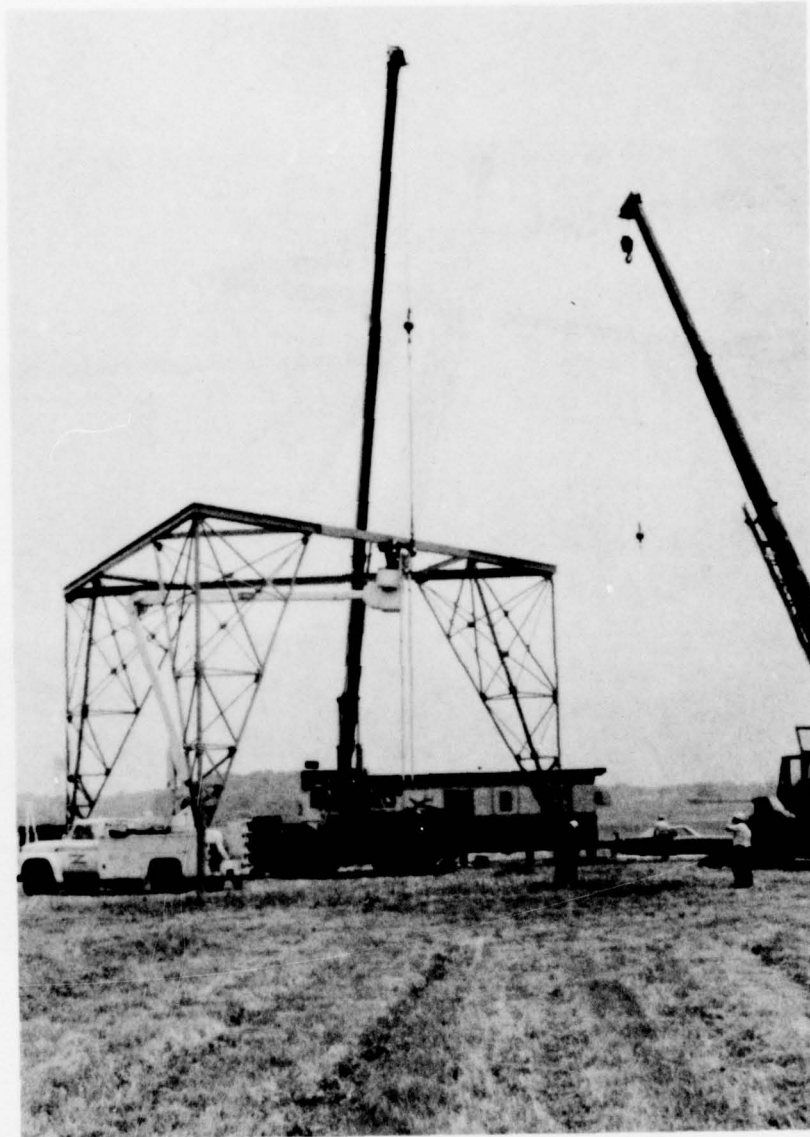


Figure 66. Hanging Pendulum Tubes



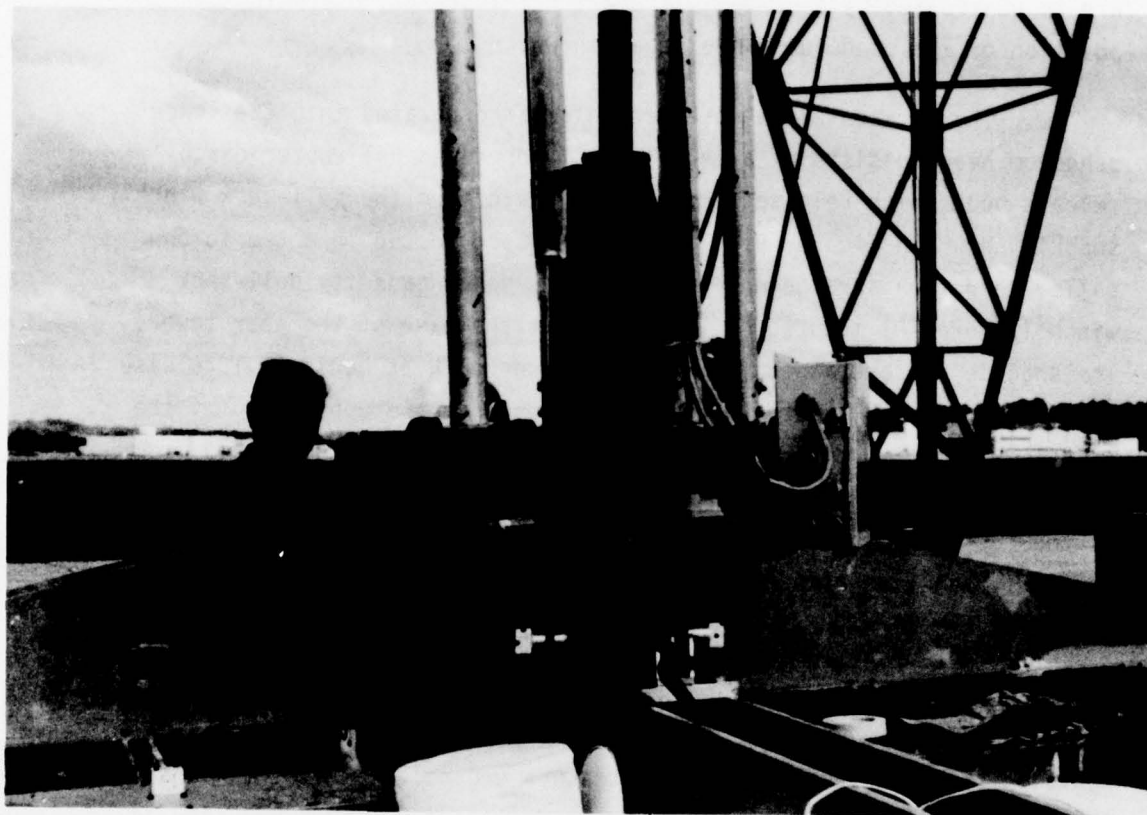


Figure 67. Lower Pendulum Head

b. The vertical release mechanism incorporated into the lower pendulum head consists of an electrically operated aircraft bomb rack (Type MA-4) into which the vehicle is secured by conventional bomb lugs. The release of this bomb rack at the bottom dead center of the pendulum arc is controlled by a cammed microswitch (Figure 68) operating off the position of the pendulum arm axle as shown.

c. The horizontal release mechanism incorporated into the lower pendulum head consists of an electrically operated helicopter cargo release hook which releases the pendulum head from the pull-back winch shackle shown in Figure 69. The shackle is connected in a two to one pulley reduction arrangement with the 3000 pound capacity pull-back winch (Figure 70) mounted on the footer at the base of the rear tower. The shackle is restrained from excessive snapback at horizontal release by a 1/2 steel cable tether which is fastened at the upper head of the pendulum assembly. The horizontal release is remotely controlled from the test controllers station in the instrumentation trailer and serves as the initiation of vehicle release as the vertical release will automatically function at bottom dead center on the cam switch.

d. Fine adjustments in the pendulum height above ground (Z axis) are accomplished by a manually operated jackscrew (shown in Figure 67) with an adjustment range of approximately eight inches. Course adjustments in the pendulum length (height above ground) are made by means of the telescoping pendulum legs which are drilled for 6 inch adjustments over an approximate 10 foot range.

e. The vehicle yaw angle can be set at any position by means of a lockable swivel bearing set into the index head between the jackscrew and the bomb rack mounting assembly (shown in Figure 71). The pendulum wiring was installed so that a yaw angle of up to 180° was possible without rerouting the wiring. The mechanism itself is capable of unlimited yaw travel.

f. Two mechanical safety mechanisms were incorporated into the lower pendulum head to prevent the inadvertent release of the test vehicle. Each safety mechanism consists of a solenoid-operated 1 inch diameter

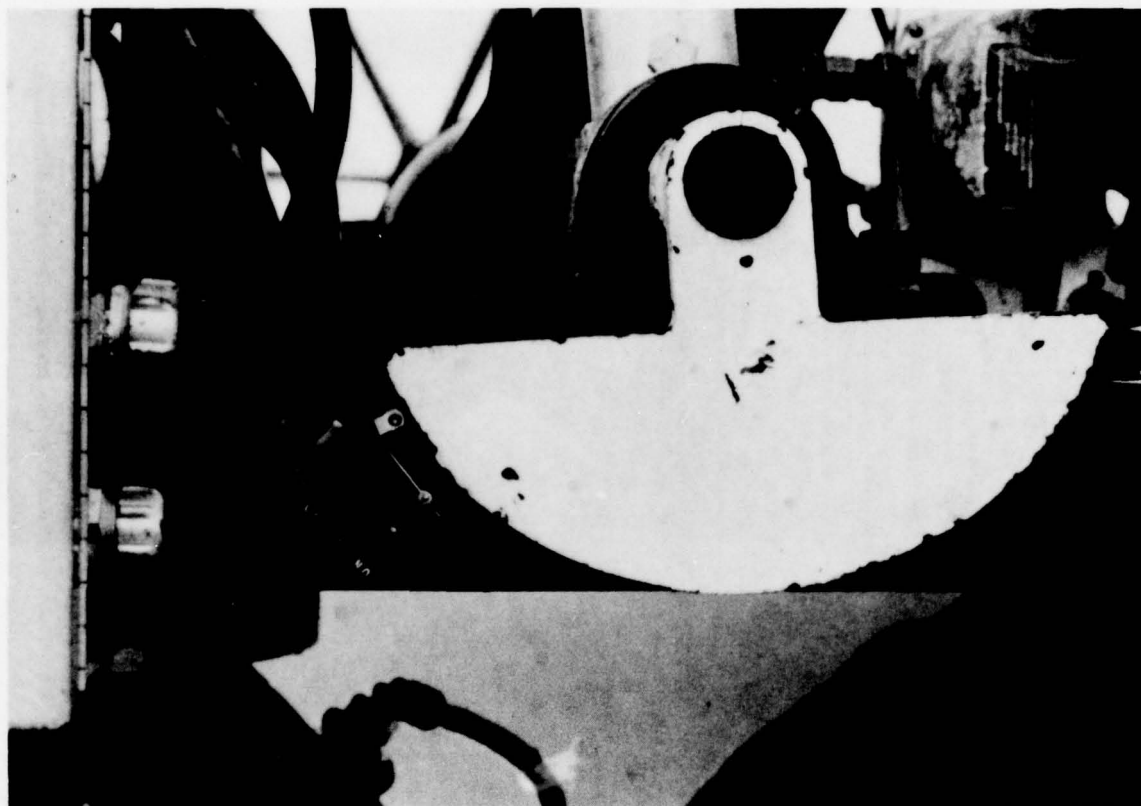


Figure 68. Cam and Microswitch

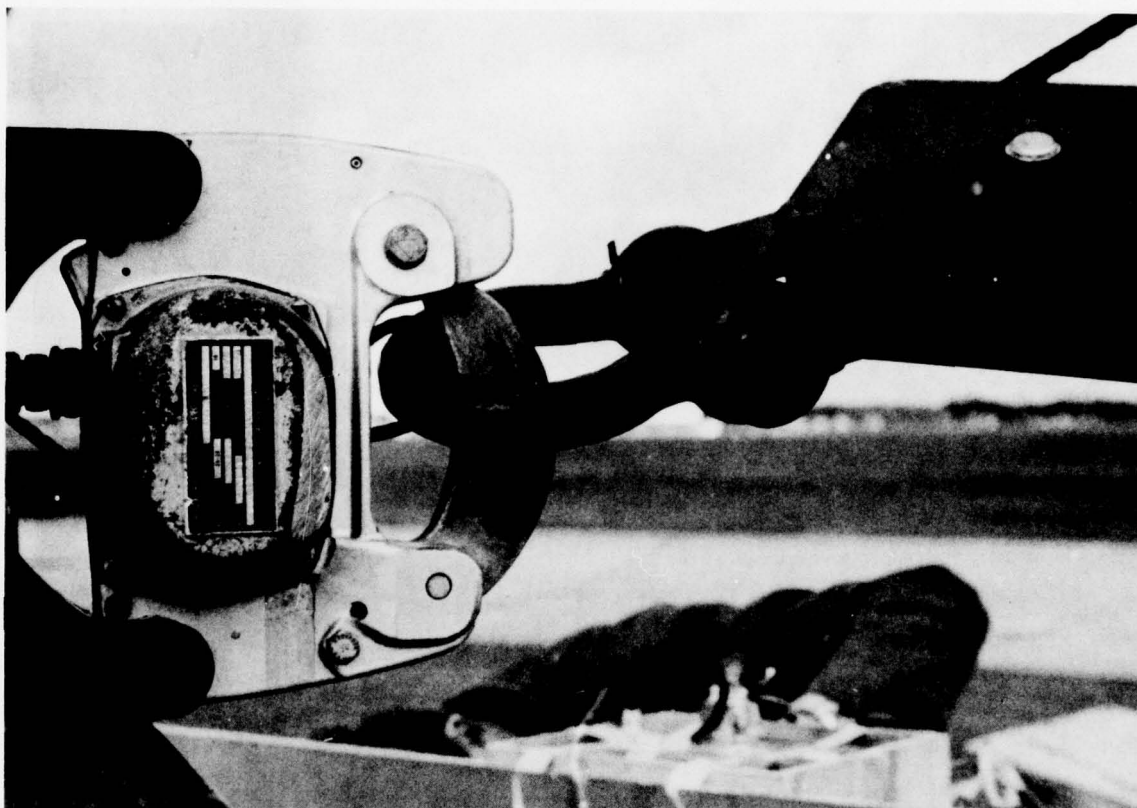


Figure 69. Horizontal Release Assembly





Figure 70. Pull-Back Winch at Rear Leg

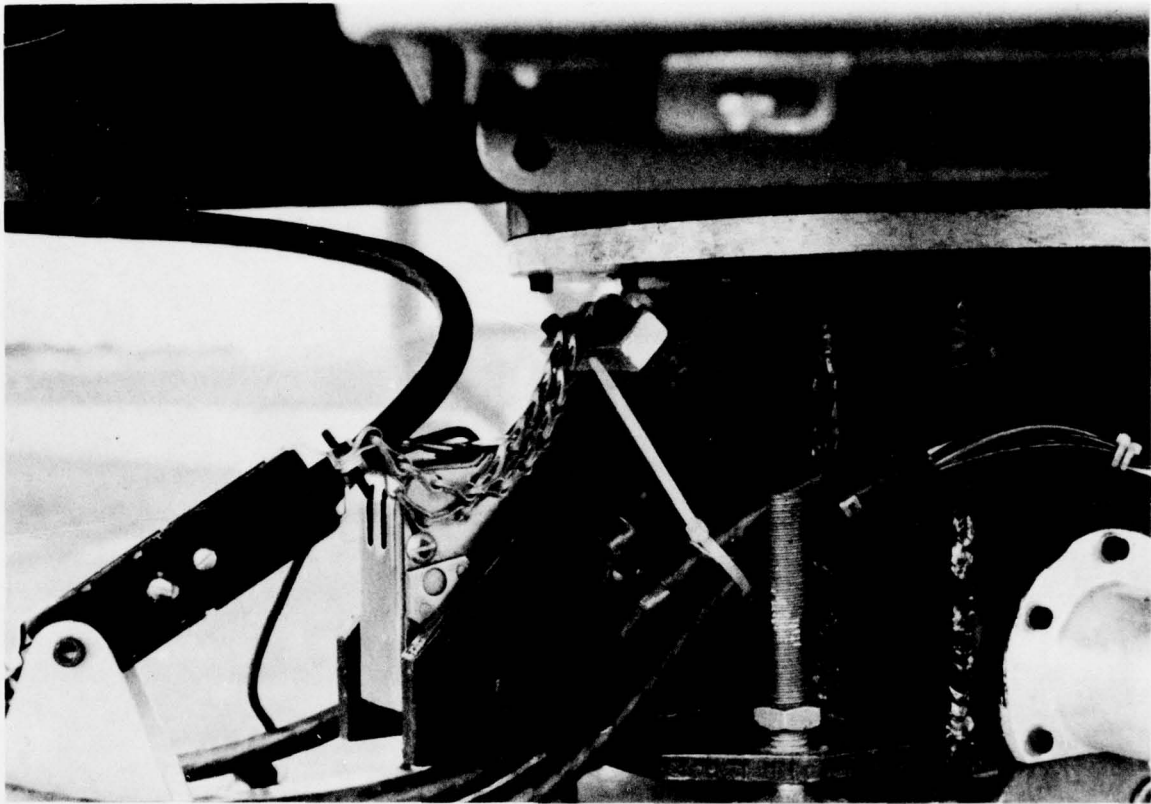


Figure 71. Breakaway Connector and Yaw Swivel

steel shear pin which protruded through a hole in the test vehicle and pinned the vehicle to the pendulum independently of the bomb rack mechanism (Figure 72). The positions of these safety pins were monitored by an independent microswitch circuit which depended on the physical position of the pin. The solenoids were wired so that in the de-energized state the safety pins engaged the test vehicle (fail-safe) and the vehicle was free for release only upon energizing the solenoids. The possibility of an energized solenoid with an engaged pin (due to friction) prompted the independent monitoring of the pins position.

g. The pendulum assembly was braked to a halt after vehicle release by means of an electric brake mounted on the axle of the pendulum arm (Figure 73) and operated from the test controllers station.

h. The FIAS valve actuators located onboard the IRON TURKEY were powered and controlled through the pull-apart umbilical cable connection shown in Figure 71. Although great effort was made to limit all the electrical power on the pendulum head to 28 VDC (considered non-lethal), the valve actuators circuitry was 115 V.A.C. due to availability. The male half of this six conductor pull-apart connection was mounted in a two direction swivel onboard the test vehicle. The female half of this connection was tethered on a stress relief chain to the pendulum head. This arrangement functioned perfectly and showed no signs of wear or degradation at the conclusion of the test program.

#### 4. VEHICLE HANGING

The hanging of the test vehicle from the lower pendulum head required that the bomb lugs on the vehicle and the bomb rack on the pendulum be brought into alignment with an approximate tolerance of  $\pm 1/8$  inch. Additionally, the vehicle was to be garaged and refurbished at a location remote from the test site. Both of these operations were made possible through the use of the truck/cradle arrangement shown in Figure 74. The twenty foot stake bed truck with power lift gate was outfitted with a vehicle cradle assembly which allowed the easy transport of the vehicle and which allowed for the vehicle hanging tolerance requirements (the truck was leased due to non-availability from local government sources). After testing, the vehicle was replaced in the cradle with a portable crane.

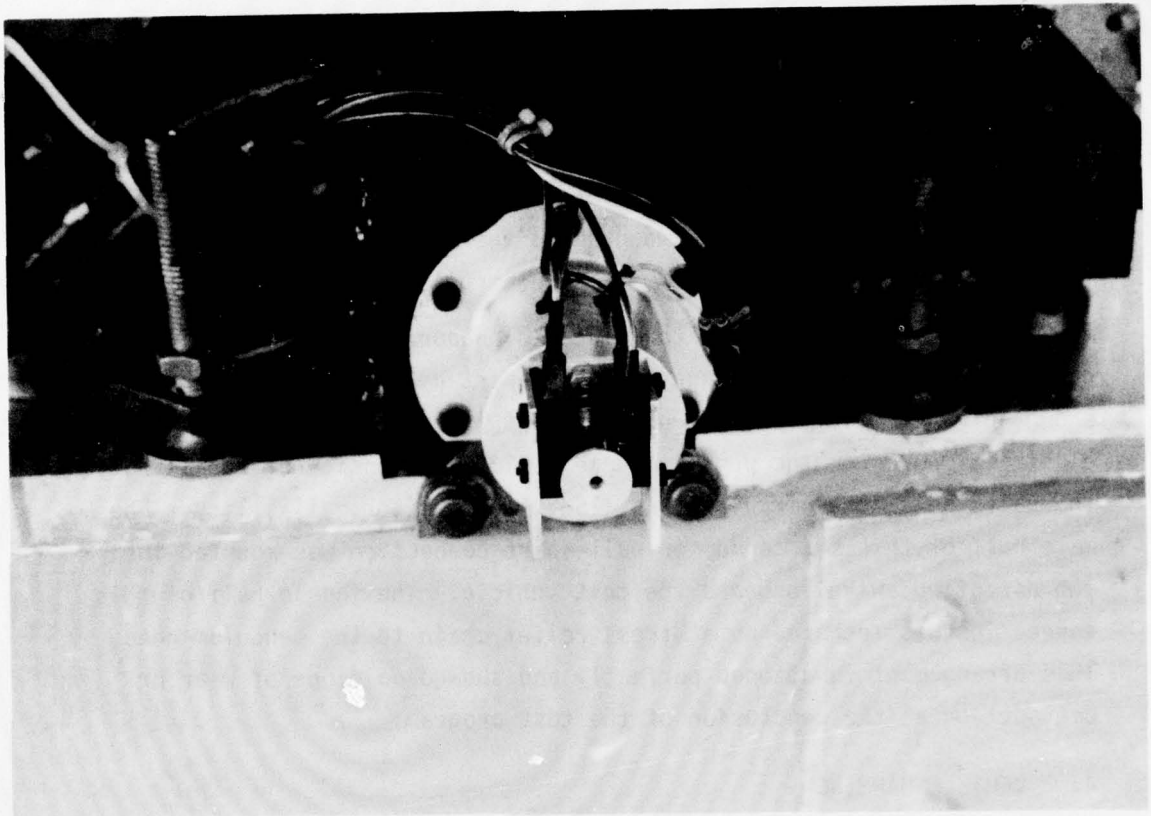


Figure 72. Safety Solenoid with Dual Position Indicator



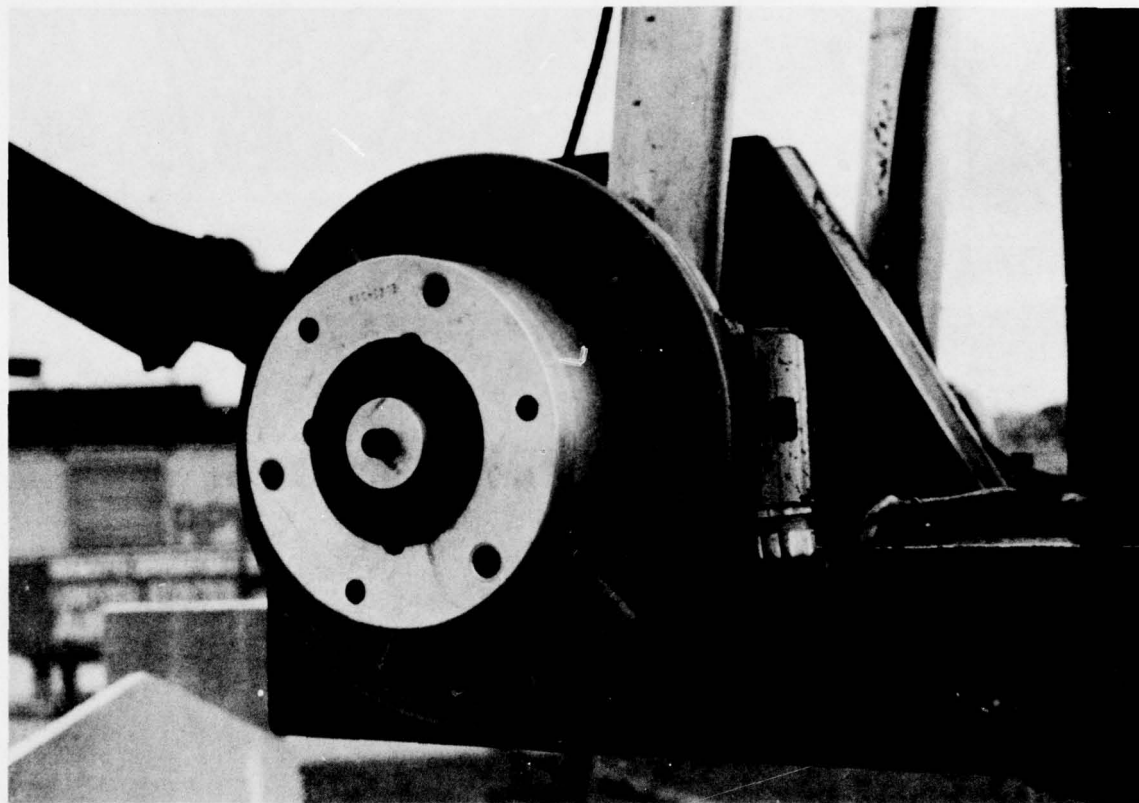


Figure 73. Electric Brake Assembly

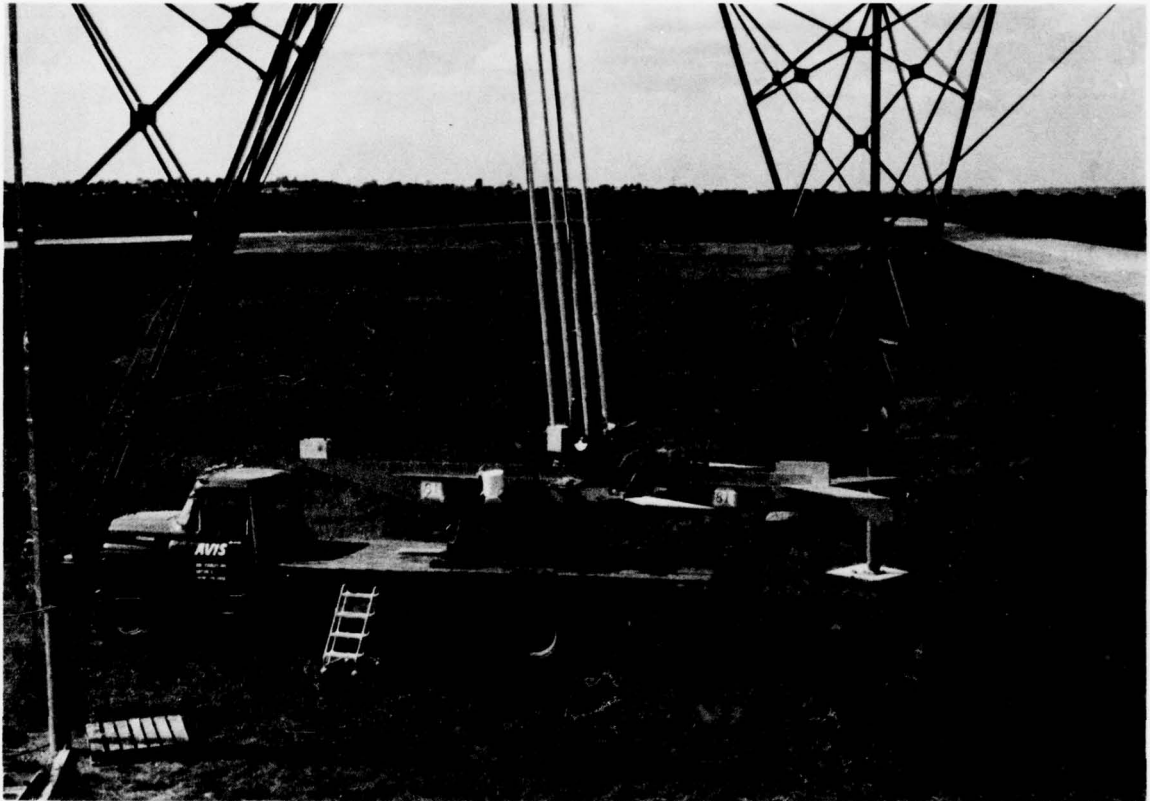


Figure 74. Truck/Cradle/Vehicle Assembly

a. The vehicle cradle (Figure 75) is adjustable so that the approximate height required for pendulum mating may be obtained. The vehicle is secured to this "floating" portion of the cradle by means of three safety chains for the safe transport of the vehicle. This portion of the vehicle cradle is "floating" in that it rests on slide blocks controlled by a manual hydraulic pump and cylinder arrangement as shown in Figure 76. In this manner, the cradle provided the fine adjustments necessary in the X and Y axis to mate the vehicle with the pendulum head.

b. The process of mating the vehicle to the pendulum head was thus reduced to a series of coarse and fine adjustments in the X, Y, Z and yaw orientation of the vehicle (the pitch and roll orientation was correctly fixed by the cradle). The mating procedure consisted of a judicious parking of the truck under the pendulum arc so as to obtain a coarse X and Y location. The pull-back winch was used to lower the pendulum head along its arc in order to obtain a coarse adjustment in the Z axis. The swivel bearing in the pendulum head allowed for the ready alignment of the yaw orientation. The cradle's hydraulic slide block arrangement was used as a fine adjustment in the X-Y plane to center the vehicle under the bomb rack while the pendulum jackscrew allowed the final fine adjustment in the Z axis for mating of the vehicle to the bomb rack. With practice, the test crew could perform this mating operation in less than 10 minutes.

c. An additional important feature of the truck/cradle arrangement was that the truckbed served as a convenient, safe working platform at the height of the lower pendulum head.

#### 5. CONTROL STATION

A 10 foot x 40 foot house trailer was placed at the test site as a control station for the pendulum and as an instrumentation station. The trailer was furnished for use by the RPV SPO. The trailer (Figure 77) was equipped with a Test Controller Station which included a two way radio, public address system, warning lights, and the FIAS Control Board shown in Figure 78. Additionally, the trailer contained an instrumentation station for the recording of test data.

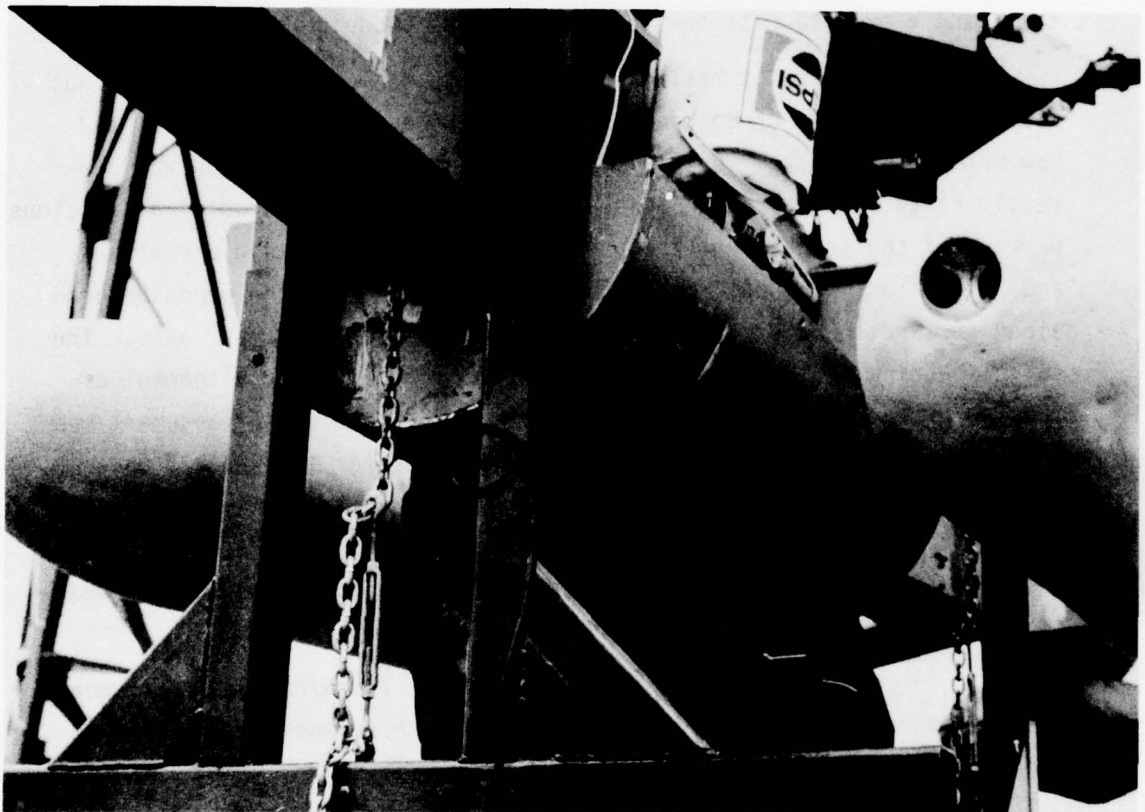


Figure 75. Cradle Detail





Figure 76. Hand Pump and Slide Block Detail



Figure 77. Instrumentation Trailer

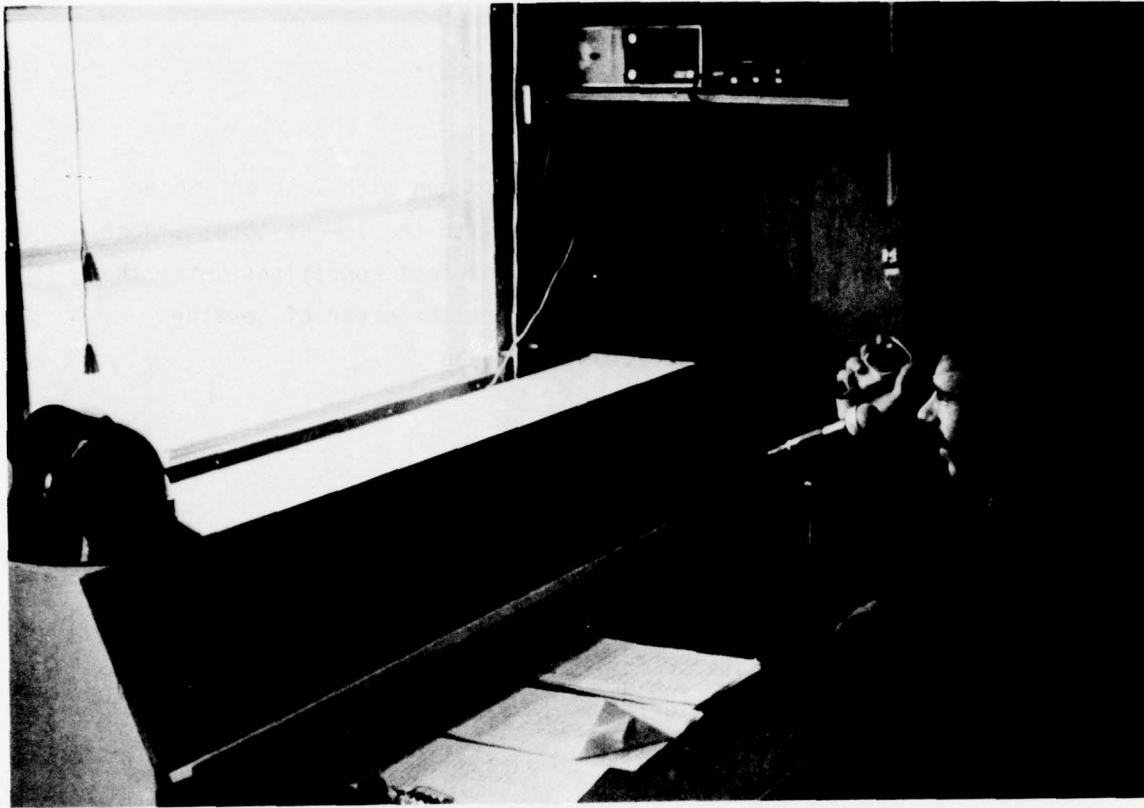


Figure 78. FIAS Control Panel

#### 6. COST AND PERSONNEL REQUIREMENTS

The four-bar pendulum horizontal test facility erected at Wright-Patterson AFB proved to be a dependable, economical research tool. The four-bar pendulum and tower assembly were erected on site at a delivered price of \$49,937.00 with an additional charge of \$7,147 for the truck/cradle assembly. The normal operation of this facility during this test program required two engineers, two electronics technicians, and two junior mechanical technicians to maintain a sustained test rate of one test per day (weather permitting). In addition to these full time personnel, a crew of approximately 10 other personnel were utilized on an as-needed basis (includes photographers, generator maintenance, crane operators, refueling truck operator, etc.).

## SECTION VIII

### HORIZONTAL TESTS NO. 65-71

#### 1. TEST CONDITIONS

The horizontal testing of the FIAS was begun with Test No. 65 on 18 Aug 77. The test schedule was to begin with the lowest total impact energy and gradually increase the severity of test conditions until the maximum energy level was obtained. Therefore the order of testing conditions for a single configuration was to be:

- a. Vertical drop
- b. 0° yaw at 7-1/2 knots drift
- c. 90° yaw at 7-1/2 knots drift
- d. 180° yaw at 7-1/2 knots drift
- e. 0° yaw at 15 knots drift
- f. 45° yaw at 15 knots drift
- g. 90° yaw at 15 knots drift
- h. 135° yaw at 15 knots drift
- i. 180° yaw at 15 knots drift

As testing progressed and more knowledge was obtained about the vehicle's impact behavior, this testing progression was rearranged to preserve physical resources. Test No. 65 was to be the vertical drop on the Mark II bag with the vehicle configured without pods with the following tests to proceed to higher energy levels as indicated. The results of Tests No. 65 through 71 were that the Mark II bag design evolved into the Mark VII and finally into the Mark VIII design which was to be the final "without pods" design. Because this series of tests was the initial usage of the horizontal test facility a period of debugging was anticipated. An extensive checkout of the facility was done using a 50 pound weight to check facility operation and operation procedures. Although the facility performed adequately during this series of tests the instrumentation system fell prey to several anomalies and almost no usable acceleration or rate data was obtained. Although most of the instrumentation anomalies were isolated, identified, and corrected, there were still some transient type problems which occasionally resulted in loss of data which were never isolated throughout the test program.



This difficulty lead to the repetition of some tests and the lack of data on other test conditions. Due to the constraints of time, resources and weather, the 15 knot drift conditions were judged to be the more important while the vertical and 7-1/2 knot test conditions were judged to be of lesser importance in the determination of the FIAS performance. This test series from Test No. 65 through 68 constitutes the vertical and 7-1/2 knot portion of the without pods configuration testing and although no acceleration data was obtained these tests were not repeated. Tests No. 69 through 71 were the initial tests at the 15 knot drift condition and were repeated to obtain the necessary engineering data. The vertical component of the vehicle's impact energy is determined by the height above ground at vertical release (e.g., 2140 lbs x 5.2 feet = 11,100 ft-lbs). The horizontal velocity component is determined by the difference in height between the horizontal release ( $R_H$ ) and the vertical release ( $R_V$ ) points. For the 7-1/2 knot wind drift condition ( $V_H$ ) with the horizontal release at 7.7 feet and the vertical release at 5.2 feet the calculation is as follows:

$$V_H = \sqrt{2 g (R_H - R_V)}$$

$$V_H = \sqrt{2 (32.2) (7.7 - 5.2)}$$

$$V_H = 12.7 \text{ ft/sec} = 7\text{-}1/2 \text{ knots drift rate}$$

## 2. TEST NO. 65

Test No. 65 was conducted on 18 Aug 77 with the Mark II main bag and the Mark VI-A tail bag. The IRON TURKEY weighed 2140 lbs complete with pylons (no pods) and attenuation system. The vehicle was released from a height of 5.2 feet for a total impact energy of 11,100 ft-lbs in this vertical drop test. Upon impact the vehicle pitched tail down until the tail bag contacted the ground as expected. The vehicle rolled slightly so that the right wing tip contacted the ground to stabilize the vehicle position shown in Figure 79. (Note that the vehicle is not stable in a level roll attitude when balanced on its cylindrical engine nacelle.) Although the wing tip touched the ground the frangible plywood portion

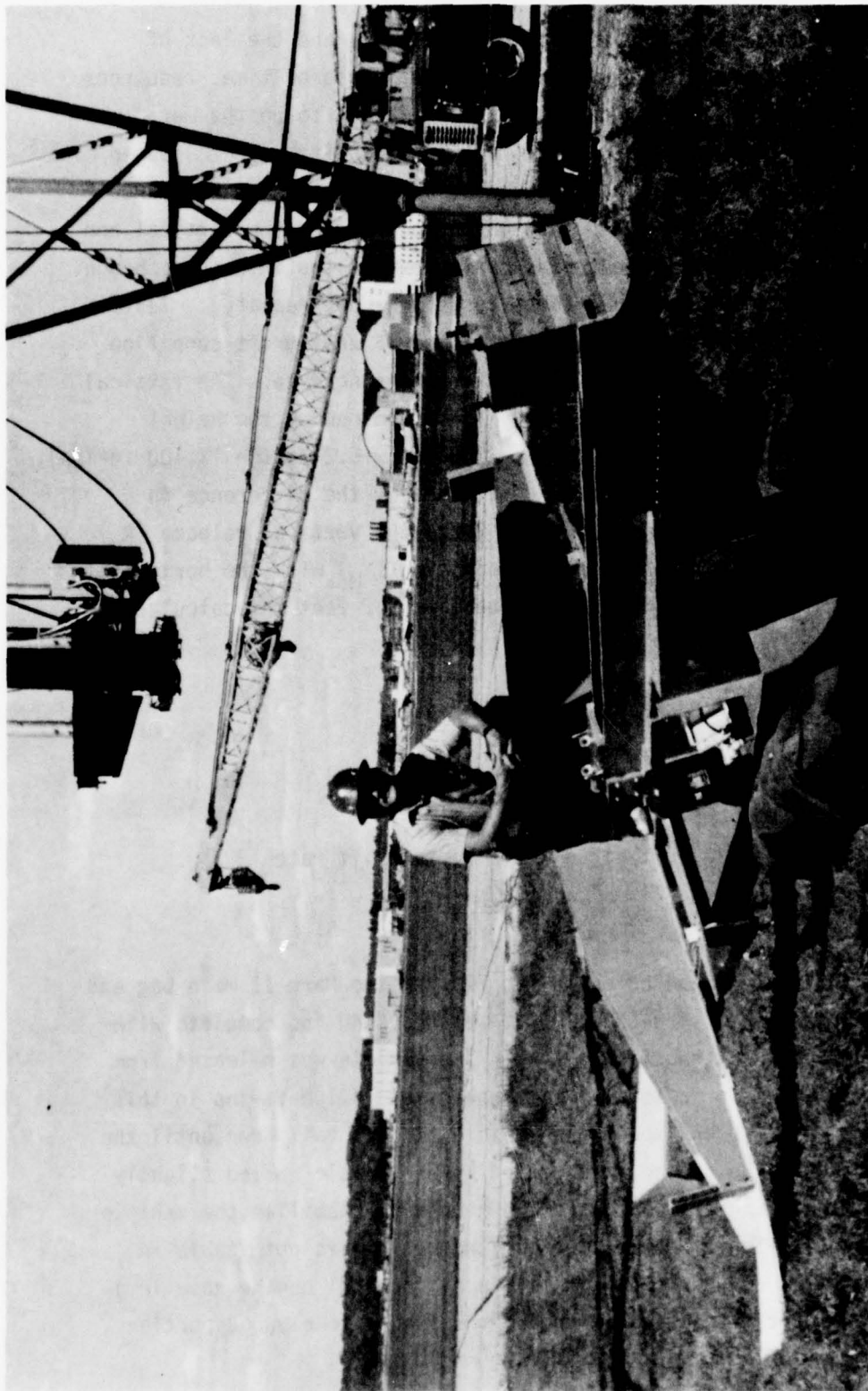


Figure 79. Test No. 65

did not break, indicating a low force level. The impact appeared to be less severe than the equivalent IRON PIG test conducted previously (Test No. 60). The acceleration and rate data were lost on this test so that only the photographic data was obtained. It was determined that the electronic data was not obtained due to a mismatch between a 5 VDC signal and a  $5\mu$  VDC gate in a recording tape signal conditioner. In this test the Mark II bag behavior appeared normal and it was decided to continue testing without modification.

3. TEST NO. 66

Test No. 66 was conducted on 24 Aug 77 with the Mark II main bag and the Mark VI-A tail bag. The IRON TURKEY was at a weight of 2140 pounds with pylons and attenuation system. The test conditions were a  $0^\circ$  yaw vehicle attitude (nose first) at a 7-1/2 knot drift rate. These conditions were obtained by setting the horizontal release at 7.7 feet and the vertical release at 5.2 feet. The total impact energy was thus 16,480 ft-lbs, of which 11,100 ft-lbs was vertical, with the remaining 5380 ft-lbs being taken up by the 7-1/2 knot horizontal drift velocity. The results of the test were that the vehicle appeared to settle into the Mark II bag smoothly, skidded approximately two feet, and then sat back (pitched) onto the tail bag as the forward motion stopped. Although the instrumentation system had provided a clean signal prior to test, severe noise all but obliterated the actual impact data. Although it was possible to discern the presence of a recorded signal it was considered impossible to attempt to digitize any of the traces. In general the test was smooth, without bag anomalies, and without any vehicle damage to the frangible parts, therefore, the decision was made to continue testing. The electronics crew was now engaged in the double checking of all the onboard electrical connectors and other suspected noise sources.

4. TEST NO. 67

Test No. 67 was conducted on 25 Aug 77 with the Mark II main bag and the Mark VI-A tail bag. The test conditions were a  $90^\circ$  yaw angle orientation with a 7-1/2 knot horizontal drift rate. The 2140 pound vehicle was released horizontally at 7.7 feet and vertically at 5.2 feet for a total

impact energy of 16,480 ft-lbs. At impact the vehicle rolled strongly (leading wing down) with the leading frangible wing tip and horizontal stabilizer endplate contacting the ground and breaking off as shown in Figure 80. The main bag still cradled the engine nacelle and exhibited no damage. Although the instrumentation had been thoroughly checked out and functioned perfectly prior to test, no usable acceleration data was recorded. At five seconds prior to release a broadband noise obscured all sixteen channels and then disappeared approximately ten seconds after release. The time sequencing of this electronic noise pointed towards the electric motor in a high speed motion picture camera mounted on the roof of the trailer within approximately 15 feet of the telemetry receiving antennae. During the test sequence this camera was turned on 5 seconds prior to release and thus caused the loss of data. The camera was relocated immediately after confirmation and testing were continued.

5. TEST NO. 68

Test No. 68 was conducted on 26 Aug 77 using the Mark II main bag and the Mark VI-A tail bag. The test conditions were a 180° yaw angle (tail first) at a 7-1/2 knot horizontal drift rate. The 2,140 pound vehicle was released horizontally at 7.7 feet and vertically at 5.2 feet for a total impact energy of 16,480 ft-lbs. The vehicle had a pronounced tail down pitch rotation at impact and proceeded to skid approximately three feet with both the main and tail bags in contact with the ground, as shown in Figure 81. Although the instrumentation was functioning correctly prior to test, no usable data was recorded. At the moment of vertical release of the vehicle, the vehicle was experiencing a two g pull-through on the pendulum arc. As the bomb rack release was triggered, the vehicle bomb lugs were suddenly released from a tension load of approximately 4280 pounds. This action was exciting the vehicle into a high frequency vibration (ringing) which was being picked up by the accelerometers. This situation was apparently being aggravated by loose bolts (incorrectly torqued) on the bomb lug mounting plate which allowed this 16 pound plate to slam back onto the vehicle. This phenomena was confirmed by observing the accelerometer output while hitting the test vehicle with a large hammer. The solution to this problem was to isolate



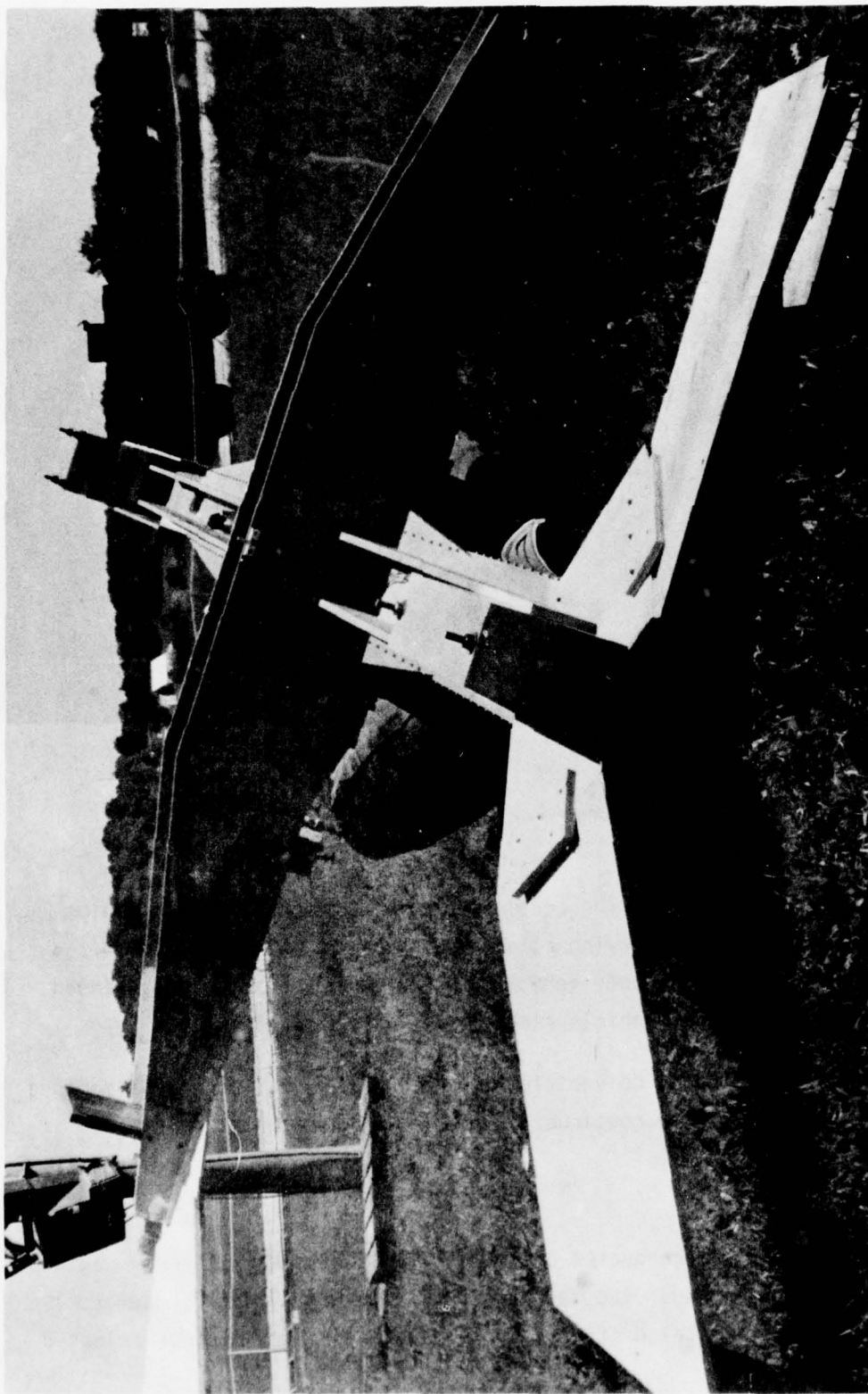


Figure 80. Test No. 67

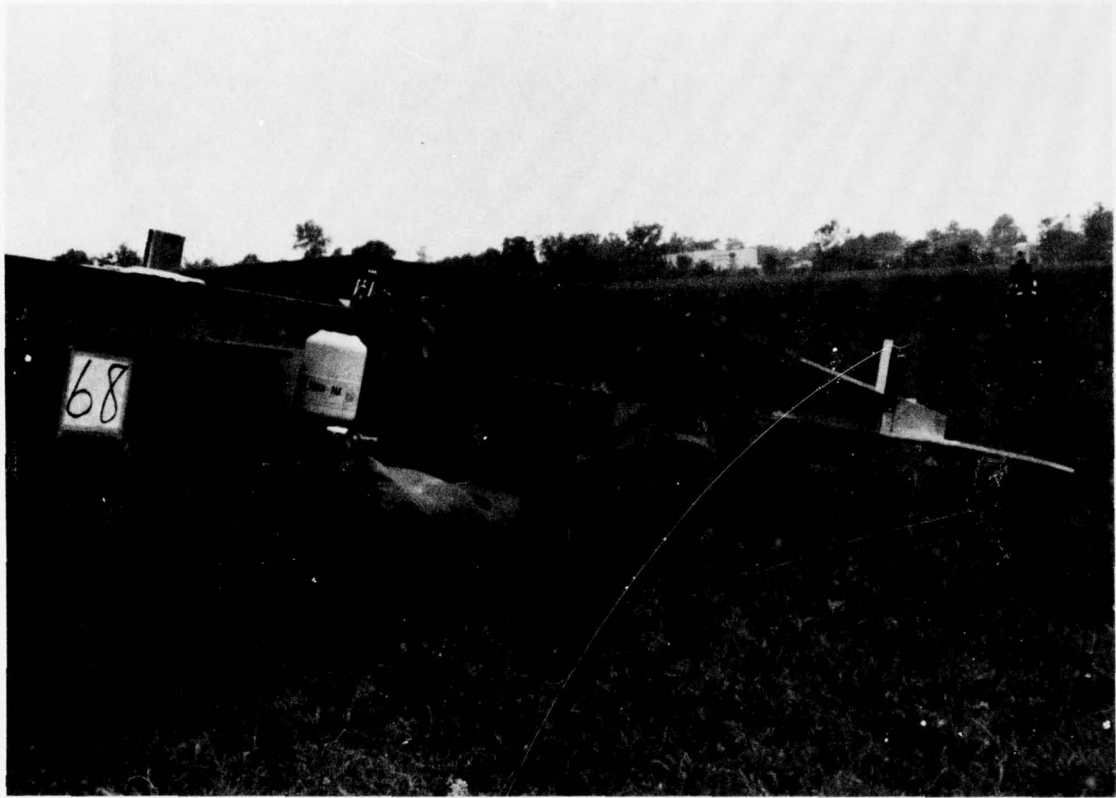


Figure 81. Test No. 68

the excitation force from the accelerometers by means of a low modulus of elasticity material serving as a high frequency mechanical filter. By this means the rigid body vehicle motions would be accurately sensed but the high frequency vehicle ringing would be blocked out.

This test produced no vehicle or FIAS bag damage, and it was decided that the testing should continue at the 15 knot horizontal drift rate energy levels.

#### 6. TEST NO. 69

Test No. 69 was conducted on 31 Aug 77 with the Mark II main bag and the Mark VI-A tail bag. The testing conditions were 0° yaw (nosefirst) at a 15 knot horizontal drift rate. The 2140 pound vehicle was released

from a horizontal release height of 15.15 feet and from the normal vertical release height of 5.2 feet for a total impact energy level of 32,400 ft-lbs.

The results of this test were that the vehicle contacted and moved forward relative to the Mark II bag. The bag leading edge attachment points failed in tension so that the vehicle slid over the bag tearing the bag off the length of the engine nacelle (see Figure 82). Some usable data was recorded on this test which indicated that the vehicle had experienced a maximum acceleration of approximately 14 g's at the CGZ axis sometime after bag rupture. Although some data was being obtained the quality of signal was poor with strong noise still existent.

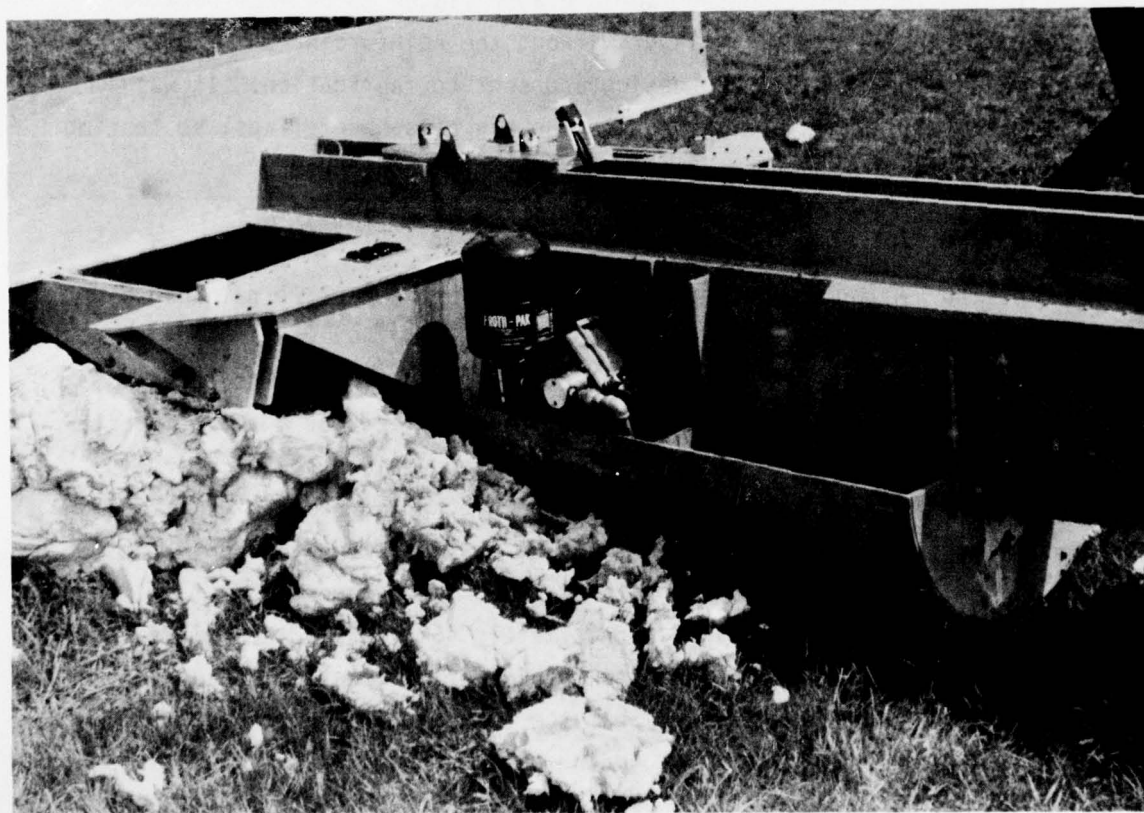


Figure 82. Test No. 69, Nose-First Slide

It was believed that the noise in this test was due to a loss in telemetry signal strength caused by changing "look" angles between the transmitting and receiving antennas during the vehicle motion. Therefore a longer transmitting antenna was installed on the vehicle prior to the next test.

The bag attachment point failure in this test was caused by a stress concentration at the end of the attachment flaps. The attachment flaps had been primarily designed for lateral bag stresses and the effect of longitudinal stress had not been previously quantified. At the 7-1/2 knot drift condition there had been no bag damage noted in the longitudinal direction but at the 15 knot condition the bag had been torn off. A bag modification incorporating the fabric diaper (later to be incorporated into the Mark VIII bag design) but without the reinforcing webbing was conceived as the Mark VII bag design and sent to fabrication. It was desired to test the lateral stress on the bag attachment flaps, so testing at a 90° yaw angle on the Mark II bag design was continued.

#### 7. TEST NO. 70

Test No. 70 was conducted on 2 Sep 77 with the Mark II main bag and the Mark VI-A tail bag. The test conditions were a 90° yaw angle at a horizontal drift rate of 15 knots. The 2140 pound vehicle was released horizontally at 15.15 feet and vertically at 5.2 feet for a total impact energy level of 32,400 ft-lbs. Upon impact the vehicle rolled sharply with the leading wing tip digging into the ground and serving as a pivot point. The vehicle pivoted (rolled) about this point so that both the main and tail bags lost contact with the ground. Recovering from this roll maneuver the vehicle yawed approximately 45° towards the original velocity vector (the nose swung into the impact) and settled back onto the Mark II bag. During this rollout the transmitting antenna whipped against the vehicle structure grounding out, and thus caused the loss of all data. This longer antenna was immediately scheduled for replacement by a long, stiff, antenna (a piece of welding rod was finally used). The lack of data at these test conditions caused the repetition of this test in Tests No. 76 and 81.



8. TEST NO. 71

Test No. 71 was conducted on 7 Sep 77 with Mark VII main bag and the Mark VI-A tail bag. The test conditions were a 180° yaw angle (tailfirst) with a 15 knot horizontal drift rate. The Mark VII bag represented an increase in longitudinal load carrying ability of 5000 pounds over the original Mark II design. The 2140 pound vehicle was released horizontally at 15.15 feet and vertically at 5.2 feet for a total impact energy level of 32,400 ft-lbs. The results of the test were that the vehicle again exhibited the pronounced tail down pitch rotation due to the misalignment between the vehicle's CG velocity vector and the Mark VII bag force vector. The Mark VII bag tore off the vehicle although not as severely as on Test No. 69. The 5000 pound diaper attachment appeared to have some effect on the bag stress concentrations and the failure made on this test was primarily at the attachment bolt fittings. The accelerometer data on this test was recorded and was readable; however, it was not yet of a quality which would allow for the energy management processing required. The CG accelerometer data indicated that the vehicle experienced a maximum acceleration of 8 g's even though the bag attachments failed and the vehicle rolled over the bag. As a result of this test 7500 pounds breaking strength webbing was added at the edges of the diaper to aid in carrying the longitudinal loads from the lower bag surface into the vehicle structure. This modification resulted in the Mark VIII bag design which became the final design for the "without pods" condition.

9. SUMMARY

This series of seven FIAS tests resulted in the final Mark VIII bag design for use with the AQM-34V in the "without" pods recovery configuration. In general the data recorded on this test series consists only of the photographic records. The instrumentation system had exhibited several levels of problems which had been isolated and resolved only with difficulty. The team of Mr. King and Mr. Coob exhibited great skill and perseverance during this portion of the test program and their fortitude is greatly appreciated. Due to the constraints of time, money, and weather the project engineer decided that the emphasis would be placed on obtaining data on the 15 knot drift conditions and that the vertical and 7-1/2 knot testing would not be repeated in order to obtain data.

## SECTION IX

### HORIZONTAL TESTS NO. 72-82

#### 1. TEST SERIES NO. 72-82

a. Test condition - The purpose of this series of eleven tests was to obtain engineering data on the performance of the Mark VIII FIAS bag at five different yaw angles. Yaw angles of 0°, 45°, 90°, 135° and 180° were to be tested at a horizontal velocity of 15 KTS with the Mark VIII/ clean wing configuration. The horizontal and vertical release heights were at 15.15 feet and 5.2 feet respectively, so that the 2140 pound test vehicle had a total impact energy level of 32,400 ft-lbs at each of the five yaw angles. Difficulties in data collection required that eleven tests were necessary to obtain useable data on the five desired test conditions.

b. Chronological History - This series of tests was performed during the time period of 8 Sep 77 to 14 Oct 77 with occasional delays due to weather and testing anomalies. These tests were performed in the following chronological order.

<u>Test Number</u>	<u>Yaw Angle</u>	<u>Date Performed</u>
72	0°	8 Sep 77
73	45°	12 Sep 77
74	135°	13 Sep 77
(Vehicle configuration change in the area of the frangible wing tip root, see Section V).		
75	135°	16 Sep 77
(Rain and repair of telemetry power supply card)		
76	90°	23 Sep 77
(Extensive Instrumentation Checking)		
77	180°	29 Sep 77
78	135°	30 Sep 77
79	135°	4 Oct 77
80	0°	5 Oct 77
(Rain delay)		
81	90°	13 Oct 77
82	45°	14 Oct 77

The time period of 26-28 Sep 77 was devoted to instrumentation work. Although the instrumentation system had been exhaustively tested and examined, unacceptable noise was still interfering with the interpretation of the recorded data. The problem had been narrowed down to the time frame beginning at horizontal release and lasting approximately three seconds. To isolate this problem a scheme was proposed in which a large number of old, used FIAS bags were laid on the ground, and the IRON TURKEY was repeatedly dropped on them while the instrumentation problem was being studied. It was finally determined that:

(1) When the vehicle was pulled back for a horizontal release the pull-back cable was under a significant tension load which was partially transmitted to the tower structure by the directional change pulley, mounted on the upper portion of the aft tower leg.

(2) At horizontal release of the vehicle this tower loading was almost instantaneously reduced to zero, thus exciting the tower frame-work and causing it to vibrate at its natural frequency of approximately 8.3 Hz.

(3) The telemetry receiving antennae had been moved to one of the front legs of the tower about 10 feet off the ground in an attempt to improve the look angle between the transmitting and receiving antennae. This receiving antennae was connected to its coaxial cable by a defective connector. When mechanically vibrated this connector would ground out the telemetry signal through the tower leg. The interpretation of the voltage running through this connector was such that a reading of 2.5 VDC indicated 0 g's from the accelerometer. Voltages of 0 and 5 volts indicated 50 and -50 g's, respectively. Therefore, whenever the connector momentarily grounded out, the recorded signal would start to indicate a 50 g acceleration of the test vehicle.

The result of these conditions was that the true data signal had superimposed upon it a noise signal with an amplitude approaching 50 g's and with a frequency of approximately 8 Hz. Because the noise frequency was approximately the same as the true signal frequency it had been very difficult to isolate the problem.

That this in fact was the problem was verified when the same noise signal was recorded while the tower framework was being excited into its natural frequency through the liberal application of a 16 pound sledgehammer. This instrumentation work resulted in a great improvement in the quality of the recorded data beginning with Test No. 77.

c. Presentation of Test Results - The results of testing at the five yaw angle conditions were obtained and are presented in the following manner:

<u>Yaw Angle</u>	<u>Test Numbers</u>	<u>Remarks</u>
0°	72	Unuseable data
	80	Useable data
45°	73	Unuseable data
	82	Useable data
90°	76	Unuseable data
	81	Useable data
135°	74	Unuseable data
	75	Unuseable data
	78	Unuseable data
	79	Useable data
180°	77	Useable data

The tests results are presented in the order of increasing yaw angle with all data being recorded in the coordinate system shown in Figure 83.

## 2. TEST RESULTS, 0° YAW, 15 KNOTS DRIFT, MARK VIII FIAS

a. The landing conditions of a 0° yaw angle at a 15 knot drift rate with the Mark VIII FIAS were investigated in Tests No. 72 and 80. Test No. 72 resulted in unuseable data due to extraneous noise. On Test No. 80 the 3 axis rate gyro package failed so that only the 3 axis linear accelerometer data is useable. Due to the relative smoothness of the vehicle dynamics in rotation in this landing condition additional testing to obtain rotation data was not warranted. Examination of the photographic coverage of the two tests shows no major differences in vehicle dynamics with the result that Test No. 80 is considered as typical performance under the landing conditions.



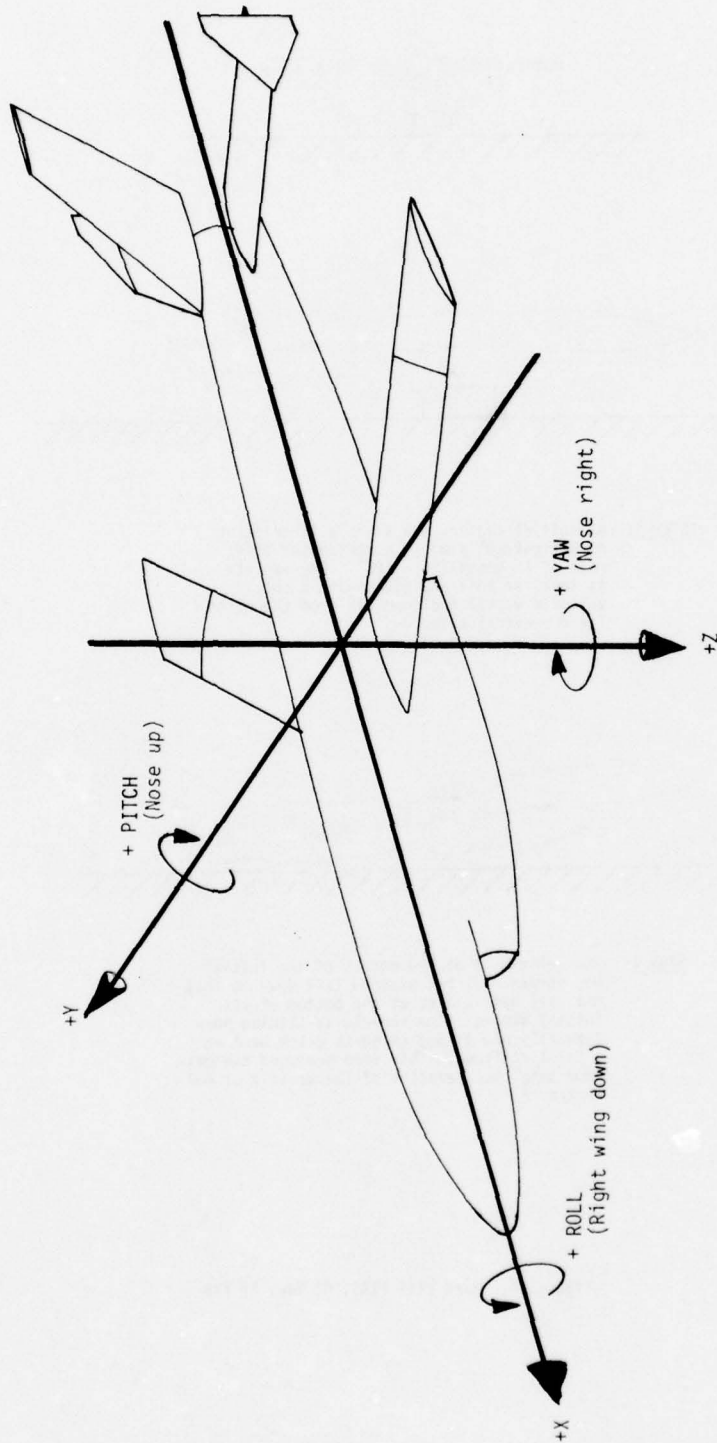
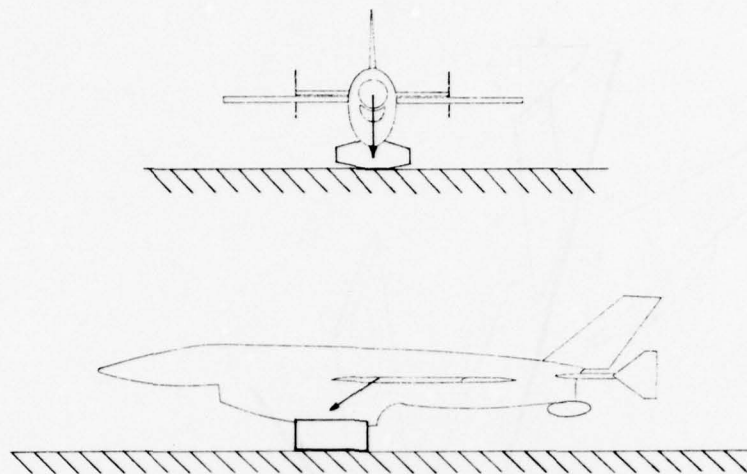
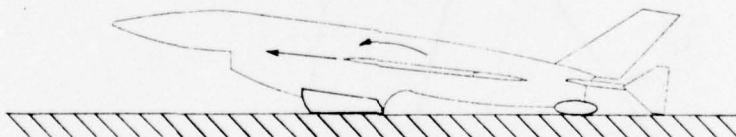


Figure 83. 6 DOF Coordinate System

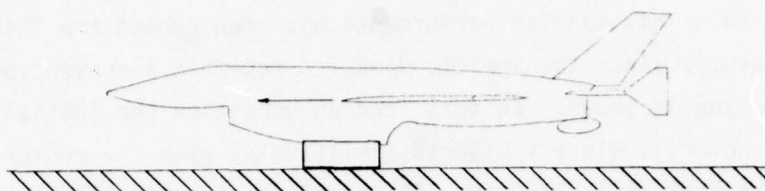


STEP 1: At initial contact the vehicle is drifting nose first ( $0^\circ$  yaw) at a horizontal drift rate of 15 knots (25.6 FPS). The vehicle is level on roll and pitch with a total velocity vector inclined  $54^\circ$  from the earth fixed vertical axis.

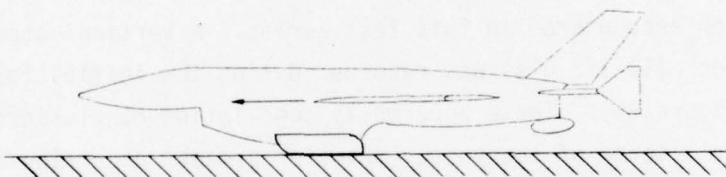


STEP 2: The vehicle is at the bottom of the initial bag stroke. It has pitched tail down so that the tail bag is also at the bottom of its initial stroke. The vehicle is sliding horizontally and is beginning to pitch back to a level attitude. This step produced the maximum total acceleration of the vehicle of 437 feet/sec<sup>2</sup>.

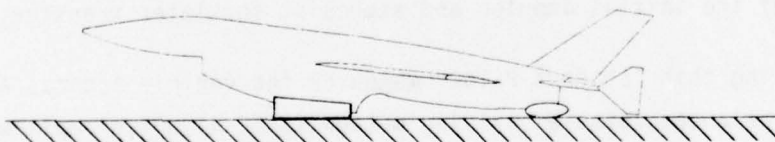
Figure 84. Mark VIII FIAS,  $0^\circ$  Yaw, 15 Kts



STEP 3: The vehicle has rebounded off the MARK VIII bag so that the bag is barely grazing the ground. The vehicle is in a level pitch and roll attitude and is moving horizontally. The Z axis accelerometer is indicating a freefall condition.



STEP 4: The vehicle has landed on the bag for the second time and is still moving horizontally in a level attitude. This second impulse recorded an acceleration of 66 feet/sec<sup>2</sup>. The vehicle is now in a stable slide with the tail bag off the ground. Although the vehicle remains in contact with the ground an additional "heaving" acceleration of 21 feet/sec<sup>2</sup> was recorded.



STEP 5: As the horizontal velocity decays due to friction the vehicle settles back (pitch) onto the tail bag and stops all movement.

b. The vehicle dynamics during a 15 knot,  $0^\circ$  yaw landing are shown in Figure 84. This landing performance has been dubbed the "Student Pilot" maneuver since the vehicle dynamics resemble a conventional one bounce landing as shown. In this landing condition the initial total velocity vector is closely aligned (relatively) with the center of pressure of the Mark VIII FIAS bag. The result is a negligible transfer of energy into roll and yaw and evidence of only a mild pitching motion. This vector alignment and resulting "smoothness" of the vehicle dynamics results in two conclusions of a "good news/bad news" nature. The "good news" is that no vehicle damage was encountered (i.e., none of the fragile wing tip or horizontal stabilizer end plates were broken off). The "bad news" is that this landing condition resulted in the highest vertical acceleration encountered in this test series. A vertical acceleration of  $437 \text{ feet/sec}^2$  ( $13\text{-}1/2 \text{ g's}$ ) was recorded during the initial touchdown impulse (Figure 85). These apparently conflicting conclusions are quite compatible in terms of the energy transfer process occurring during this maneuver. Due to the vector alignment significant quantities of energy were not transferred into rotational storage during the initial impulse. Therefore, this energy was involved in the initial vertical impulse causing the large acceleration loading. This is more easily understood by examining the other four landing conditions ( $45^\circ$ ,  $90^\circ$ ,  $135^\circ$ , and  $180^\circ$  yaw) in which the vector misalignment causes the initial impulse to be accompanied by a large rotational buildup which effectively transfers energy out of the initial impulse and stores it for later transfer.

During this "Student Pilot" maneuver the vehicle assumes a dynamically balanced, stable sliding motion (STEP 4) which implies that there is no critical velocity which would cause vehicle flipover at this yaw angle. In this regard this maneuver is very similar to a conventional piloted aircraft landing.

### 3. TEST RESULTS, $45^\circ$ YAW, 15 KNOTS DRIFT, MARK VIII FIAS

a. The landing conditions of a  $45^\circ$  yaw angle with a 15 knot horizontal drift rate were investigated during Tests No. 73 and 82. The data obtained during Test No. 73 was unuseable due to extraneous signals and



# IRON TURKEY TEST NO. 80 DATA

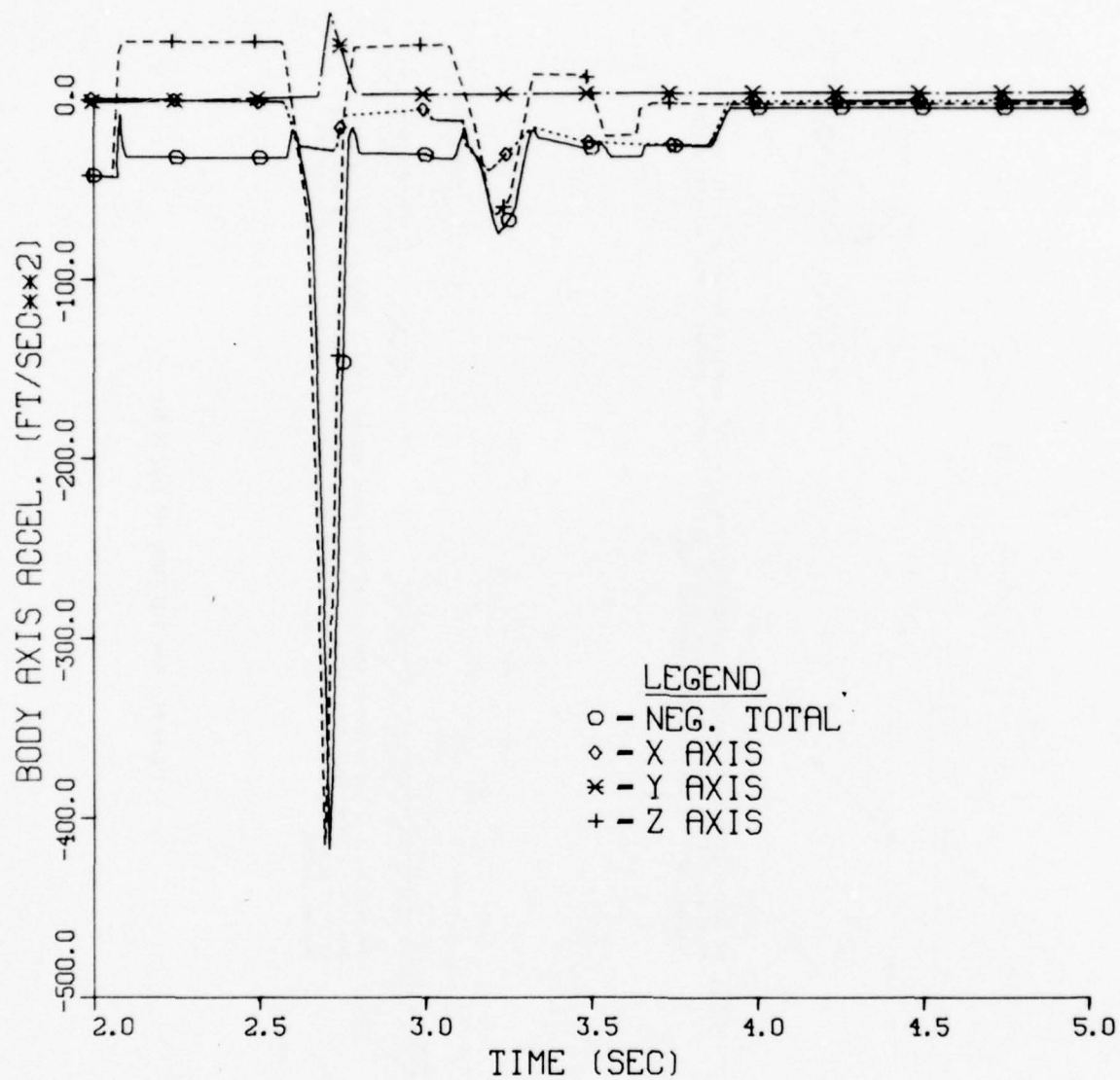


Figure 85. Test No. 80, Acceleration vs Time

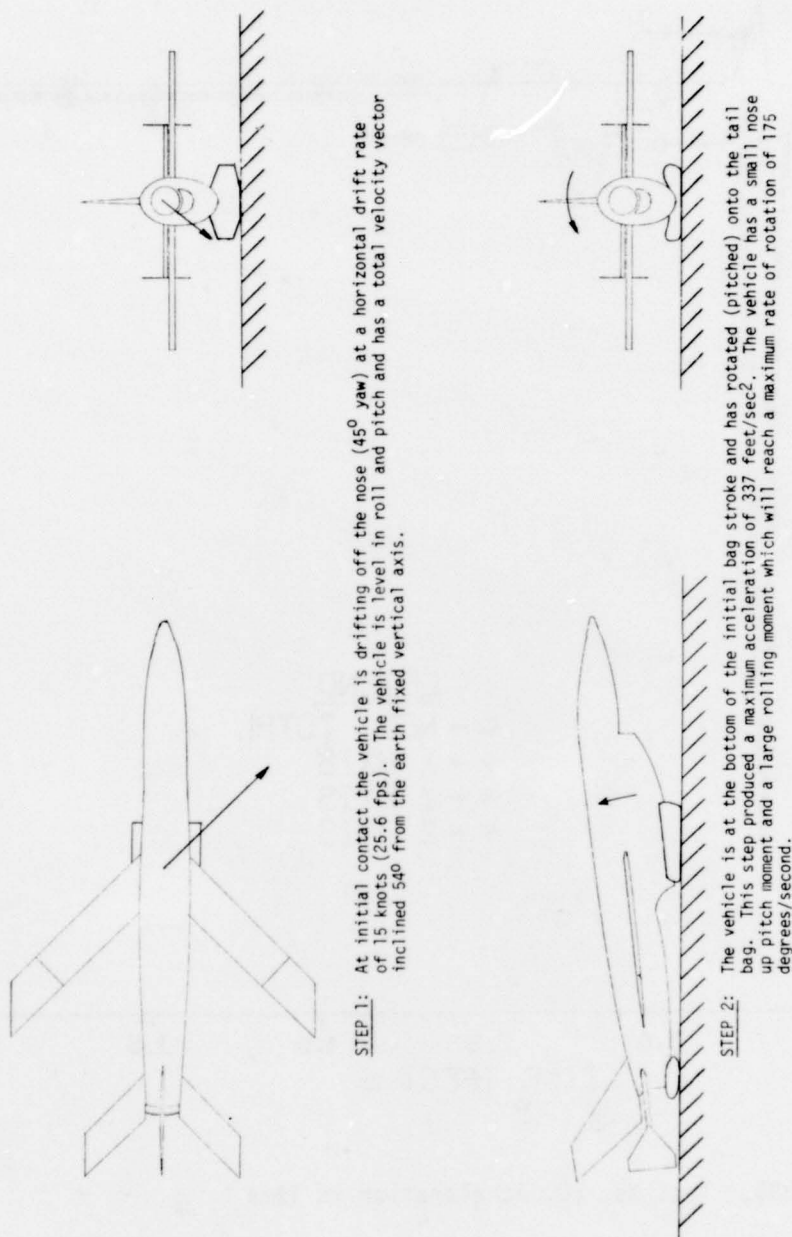
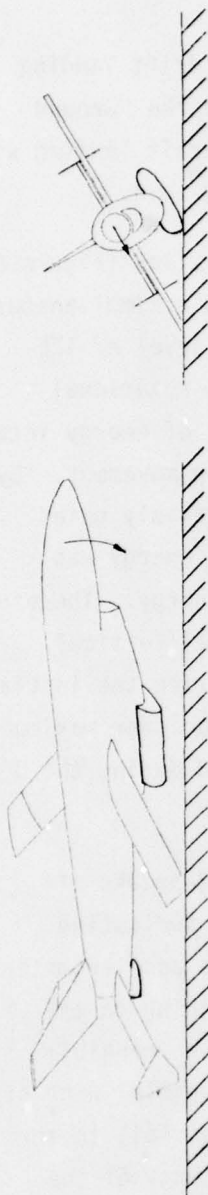


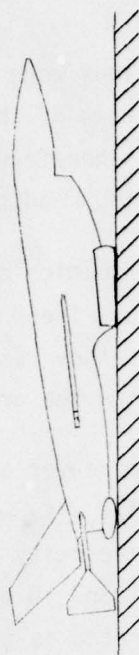
Figure 86. Mark VIII FIAS,  $45^\circ$  Yaw, 15 Kts



STEP 3: As the wing tip contacts the ground due to the rolling movement the frangible wing tip breaks off. The vehicle starts a positive yawing movement due to the dragging wing tip similar to a conventional ground loop. At the peak of the rolling arc the vehicle is approximately 30° off the ground.



STEP 4: As the vehicle rotates it pivots back onto the bag recording an acceleration of 77 feet/sec<sup>2</sup>. As the vehicle continues to rotate about the wing tip and the bag the nose (due to the rotation) comes to a stop barely off the ground (all rate gyros record zero rotation at this point).



STEP 5: The vehicle reverses its rotation and settles back onto the main and tail bags.

so the landing conditions were repeated in Test No. 82. Examination of the photographic coverage of the two tests revealed no major differences in vehicle behavior. Therefore, the results of Test No. 82 are considered typical for this landing condition.

b. The vehicle dynamics during a 45° yaw, 15 knot drift landing are shown in Figure 86. These dynamics have been dubbed the "Ground Loop" maneuver because they resemble a conventional aircraft landing with one low wingtip striking the ground and causing a yawing spin.

During this maneuver an initial impulse acceleration (Figure 87) of 337 feet/sec<sup>2</sup> (10-1/2 g's) was recorded together with a simultaneous buildup of rotational velocity (Figure 88) to a maximum level of 175 degrees/second in roll and 28 degree/sec in pitch. This rotational buildup can be interpreted as the transfer of 650 ft-lbs of energy into rolling motion and an additional 280 ft-lbs into pitching movement. By observing that the X and Y accelerometer traces are relatively quiet during this rotational buildup, it is inferred that this energy was transferred from the initial vertical (Z axis) kinetic energy. Therefore, it can be concluded that approximately 8.4% of the initial vertical kinetic energy was transformed into rotational energy during the initial impulse. The overall effect of this energy transfer is a lower maximum acceleration during the initial impulse than was observed during the 0° yaw landing condition.

As the frangible wing tip strikes the ground and breaks off (STEP 3) the rolling velocity is seen to reduce sharply, indicating dissipation of the 650 ft-lbs of roll energy. The Y axis accelerometer shows a typical double spike during this period corresponding to the contact of the frangible wing tip; the breaking off of the frangible portion; and the ground contact of the remaining (nonfrangible) wing tip. At the peak of this rolling arc the vehicle rotation rates fall to zero as the rotational energy is transferred into potential energy of the vehicle C. G.



## IRON TURKEY TEST NO. 82 DATA

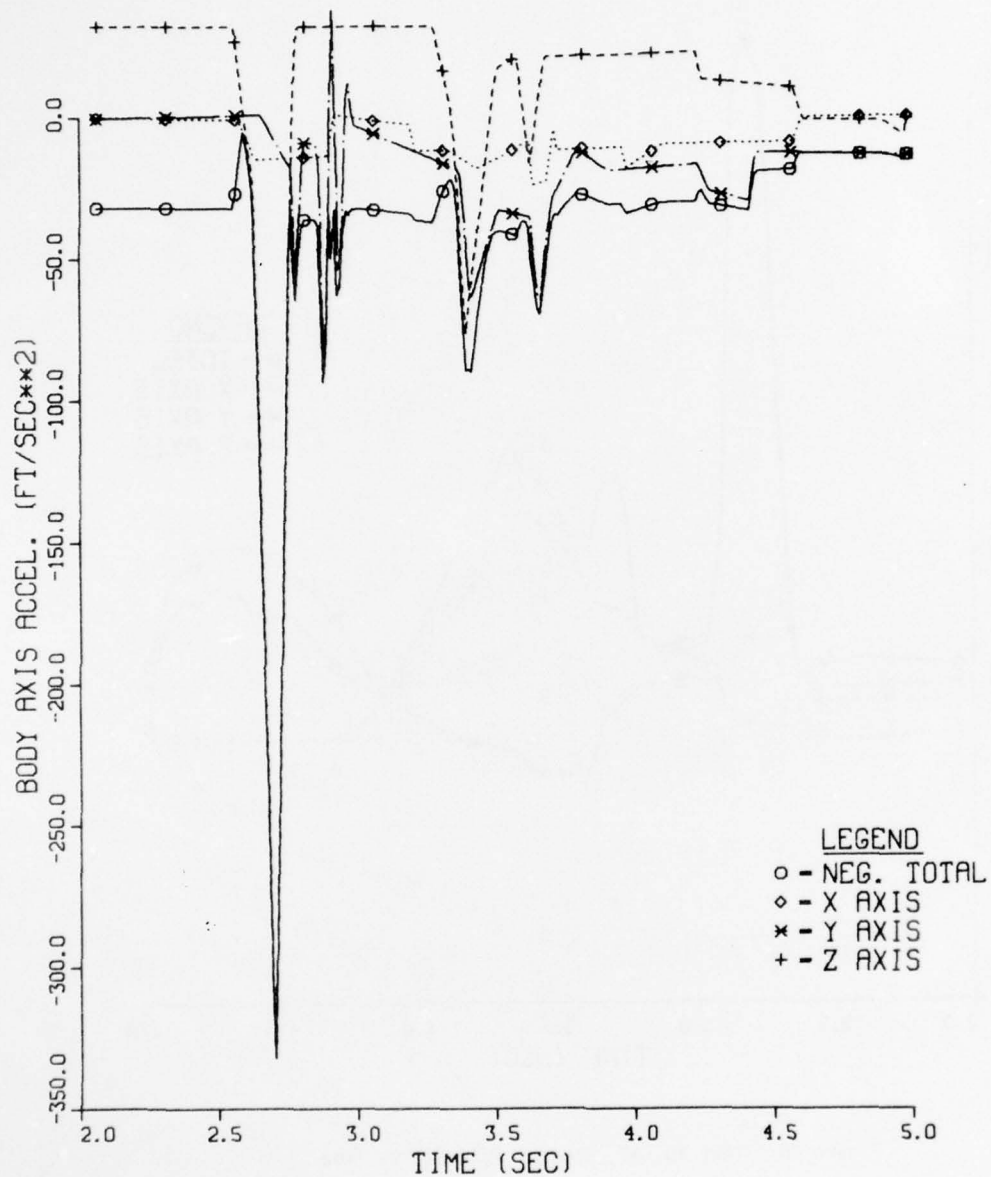


Figure 87. Test No. 82, Acceleration vs Time

# IRON TURKEY TEST NO. 82 DATA

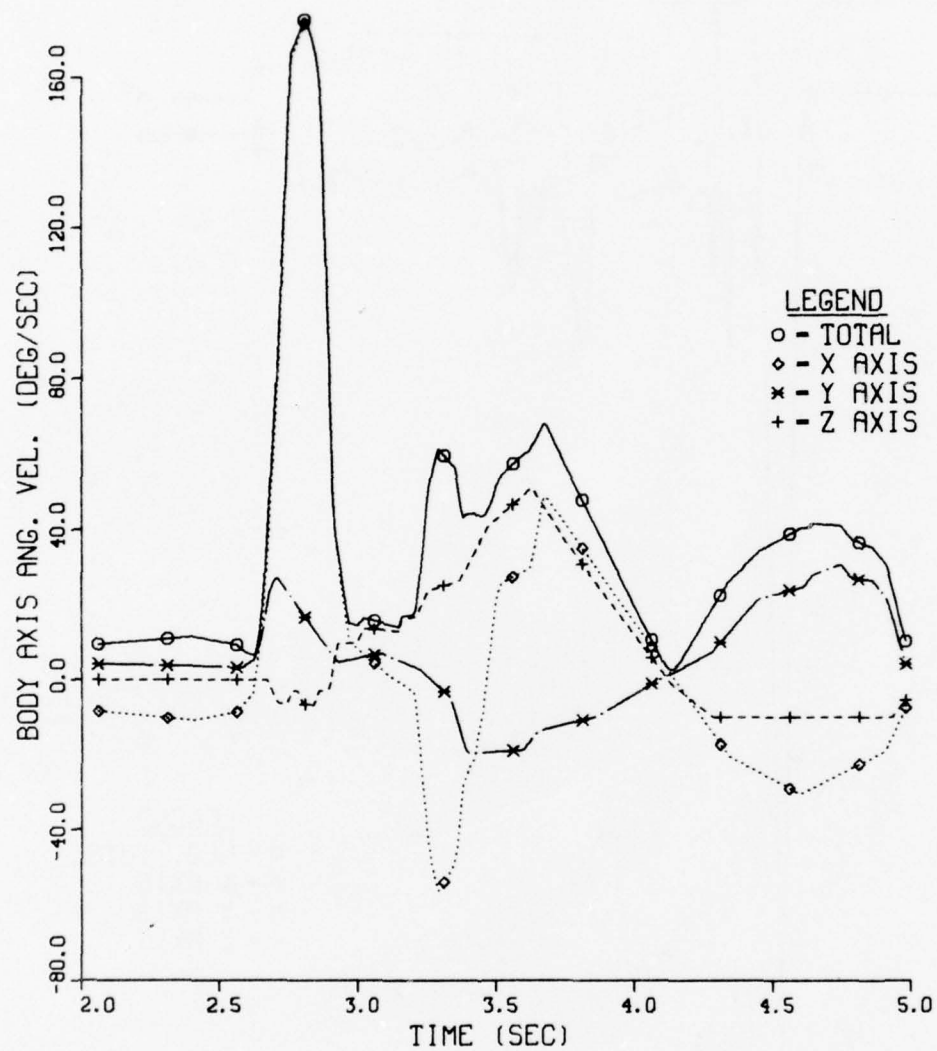


Figure 88. Test No. 82, Angular Velocity vs Time

As the vehicle falls through from the peak of its arc all three rotations are seen to reverse their direction indicating a transformation from potential energy back to rotational energy. When the vehicle again contacts the FIAS bag (STEP 4) maximum accelerations of 77 feet/sec<sup>2</sup> and 65 feet/sec<sup>2</sup> are recorded in the Z and Y axis, respectively. The final settling of the vehicle on the FIAS bag takes the form of damped oscillations in all three rotational axes as well as the linear Z axis.

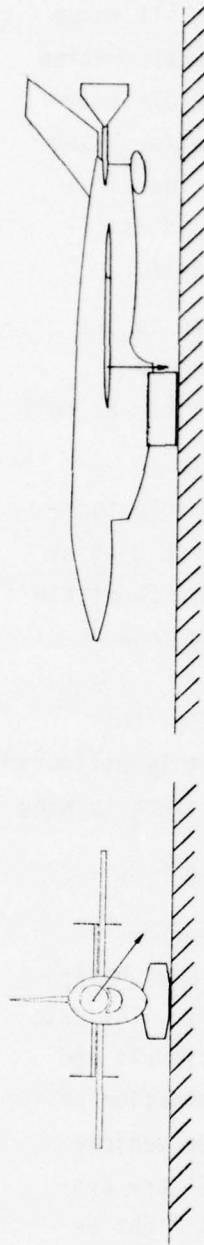
In this landing condition the vehicle sustained damage to the leading frangible wing tip caused by the unattenuated (uncontrolled) transfer of an estimated 650 ft-lb of energy which had been stored as roll rotational energy during the initial impulse.

It does not appear feasible to predict a critical vehicle turn-over horizontal drift rate for this landing condition due to the digging in behavior of the leading wing tip. Although the wing tip did penetrate the soil it was more of a slicing action than it was a digging in and stopping motion. At this yaw angle the wing presents a sloping surface to the ground (see plan view, STEP 1) which tends to rise out of the ground rather than to dig in deeper as the vehicle slides. It is estimated that as the horizontal drift rate increases the ground loop effect (yawing spin) will become more pronounced.

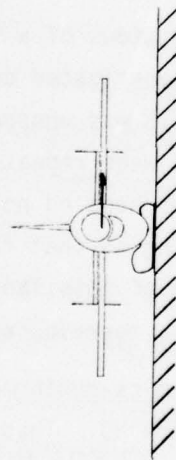
#### 4. TEST RESULTS, 90° YAW, 15 KNOTS DRIFT, MARK VIII FIAS

a. The landing conditions of a 90° yaw angle with a 15 knot horizontal drift rate were investigated during Tests No. 76 and 81. The data obtained during Test No. 76 was unuseable due to extraneous signals and so the landing conditions were repeated in Test No. 81. Examination of the photographic coverage revealed no major differences in the vehicle dynamics during the landing so that the results of Test No. 81 are considered as representative of this landing condition except as might be modified by differences in terrain, as will be discussed.

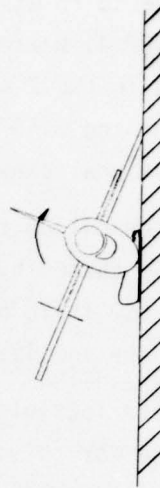
b. The vehicle dynamics during a 90° yaw, 15 knot horizontal drift landing are shown in Figure 89. These dynamics have been dubbed the "Cartwheel" maneuver, in that they resemble a gymnastic cartwheel, albeit somewhat poorly executed.



STEP 1: At initial contact the vehicle is drifting sideways towards the left wing ( $90^\circ$  yaw) at a horizontal drift rate of 15 knots (25.6 fps). The vehicle is level in both roll and pitch and has a total velocity vector inclined  $94^\circ$  from the earth fixed vertical axis.



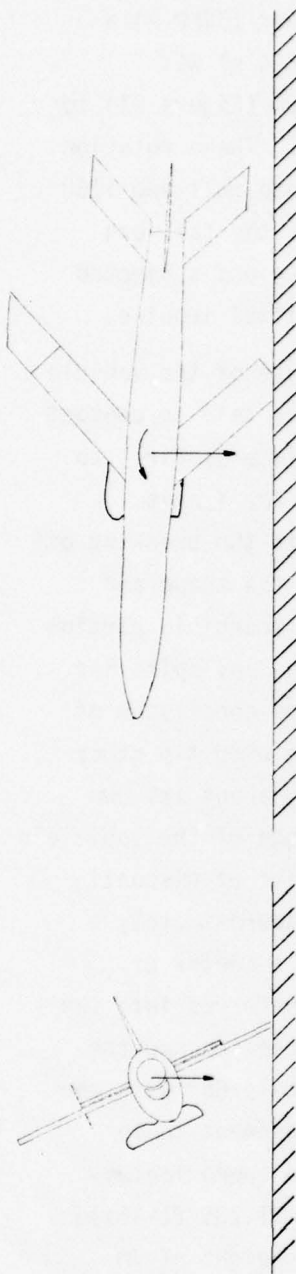
STEP 2: The vehicle is at the bottom of the initial bag stroke. It has pitched tail down slightly so that the tail bag is also crushed. This initial impulse recorded a maximum total acceleration of 308 feet/sec<sup>2</sup>. At this step the vehicle is still level in roll but with a large rolling moment created.



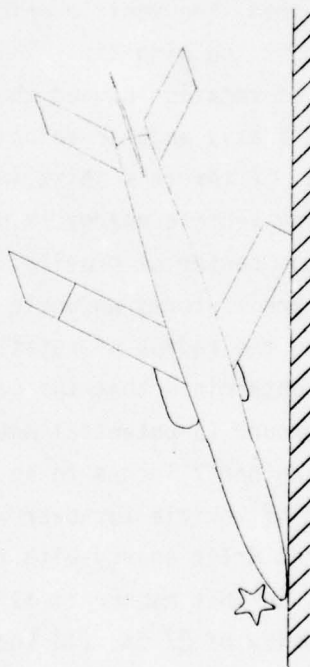
STEP 3: The vehicle has rotated (rolled) at a maximum speed of 230 degrees/sec up till the time when the wing makes contact with the ground. During this rotation the leading horizontal stabilizer endplate breaks off followed by the frangible wing tip. As the remaining wing tip penetrates the ground 6" - 12" the center of vehicle rotation shifts to the wing tip as shown on the X axis rotation.

Figure 89. Mark VIII FIAS,  $90^\circ$  Yaw, 15 Kts

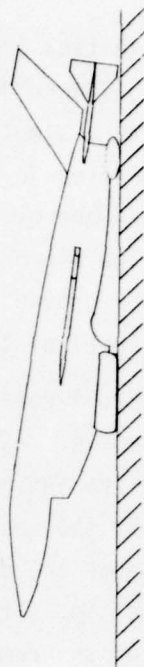




**STEP 4:** The vehicle has rotated approximately  $65^\circ$  in roll about the wing tip at the peak of the arc. At this time the weight vector becomes dominate and causes a yawing movement with rotation about the wing tip. This yaw rotation due to the weight vector will reach a maximum rate of  $77^\circ/\text{second}$ . From the vehicle dynamics during this stage it is estimated that a horizontal drift rate of  $27 \text{ feet/sec}$  ( $16 \text{ knots}$ ) with soft ground and the  $90^\circ$  yaw condition will produce vehicle flipover. (Note that the energy required is based on the square of the velocity).



**STEP 5:** The vehicle yaw rate abruptly drops to zero as the vehicle nose slams into the ground recording a maximum acceleration (Y direction) of  $477 \text{ feet/sec}^2$  on a short duration spike. This acceleration was partially caused by the rigidity of the test vehicle and it is estimated that an actual AQM-34V would have suffered nose damage thus reducing the spike amplitude.



**STEP 6:** The vehicle has rotated in roll and pitch back onto the main bag. The vehicle "rocks" over the main bag onto the tail bag and thus records Z axis accelerations of  $45 \text{ feet/sec}^2$  and  $34 \text{ feet/sec}^2$  as it settles.

During the initial impulse phase of this maneuver (STEP 2) a maximum acceleration (Figure 90) of  $308 \text{ feet/sec}^2$  ( $9\frac{1}{2} \text{ g's}$ ) was recorded together with a simultaneous buildup in rotation (Figure 91) to maximum values of  $230^\circ/\text{sec}$  in roll and  $57^\circ/\text{sec}$  in pitch. These rotation rates correspond to an energy transfer of 1120 ft-lbs into roll and 1160 ft-lbs into pitch. The pitch rotation rapidly decays as the tail bag makes contact with the ground, implying that the tail bag was subjected to an impact energy level of 1160 ft-lbs during this initial impulse.

The vehicle roll rotation is the dominant feature of the vehicle dynamics in STEPS 3 and 4. As the vehicle rolls with the tail in contact with the ground, the leading horizontal stabilizer endplate is first to break off, followed by the leading frangible wing tip. The Y axis acceleration trace shows the double spike associated with the breaking off of the frangible wing tip. It is of importance to note the shape and direction of travel of the remaining wing tip after the frangible portion has departed (see plan view, STEP 4). A pointed, digging in, spike has been created which proceeded to penetrate the soft ground conditions of this test to a depth estimated at one foot. Because the wing tip stuck in the ground and stopped, the vehicle which was rolling about its own C.G. began rolling about the wing tip. This sudden change of the vehicle's instantaneous center of rotation caused the apparent point of discontinuity observed in the X axis angular velocity curve at approximately  $t$  equal to 2.75 seconds. After this shift in the vehicle's center of rotation, the remaining vehicle energy is primarily transferred into the potential energy of the center of gravity. As the vehicle reached the peak of this rolling arc it forms an angle of approximately  $65^\circ$  with the ground. By estimating the radius of rotation in this movement to be 70 inches, it can be determined that the C.G. was raised approximately 63 inches above the ground (a potential energy level of 11,235 ft-lbs). By raising the C.G. another 7 inches to an above ground height of 70 inches, the threshold of vehicle turnover would have been reached. By ratioing the horizontal drift energy with the potential energy associated with raising the C.G. in this manner it is possible to predict a critical vehicle turnover velocity of 27 fps (16 knots) under these landing conditions. Note that this only holds for the case of a soft terrain where

# IRON TURKEY TEST NO. 81 DATA

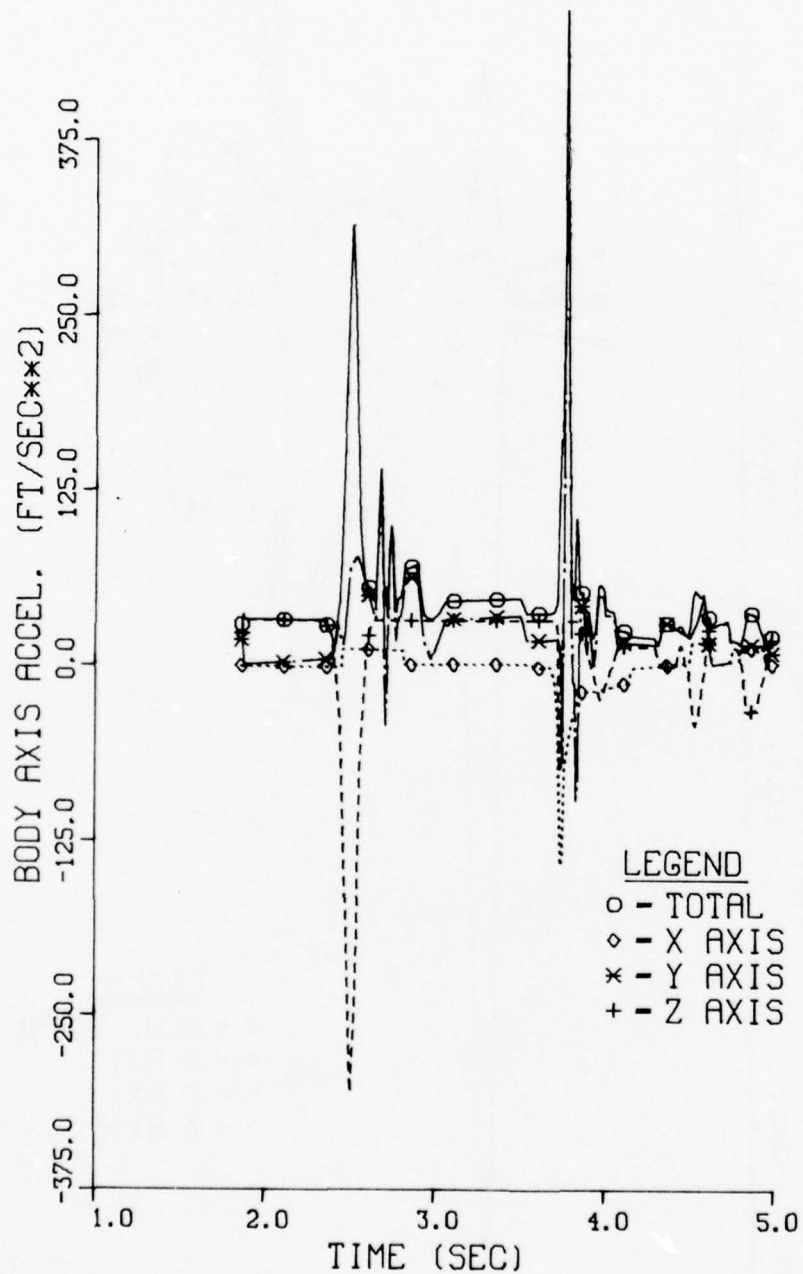


Figure 90. Test No. 81, Acceleration vs Time

# IRON TURKEY TEST NO. 81 DATA

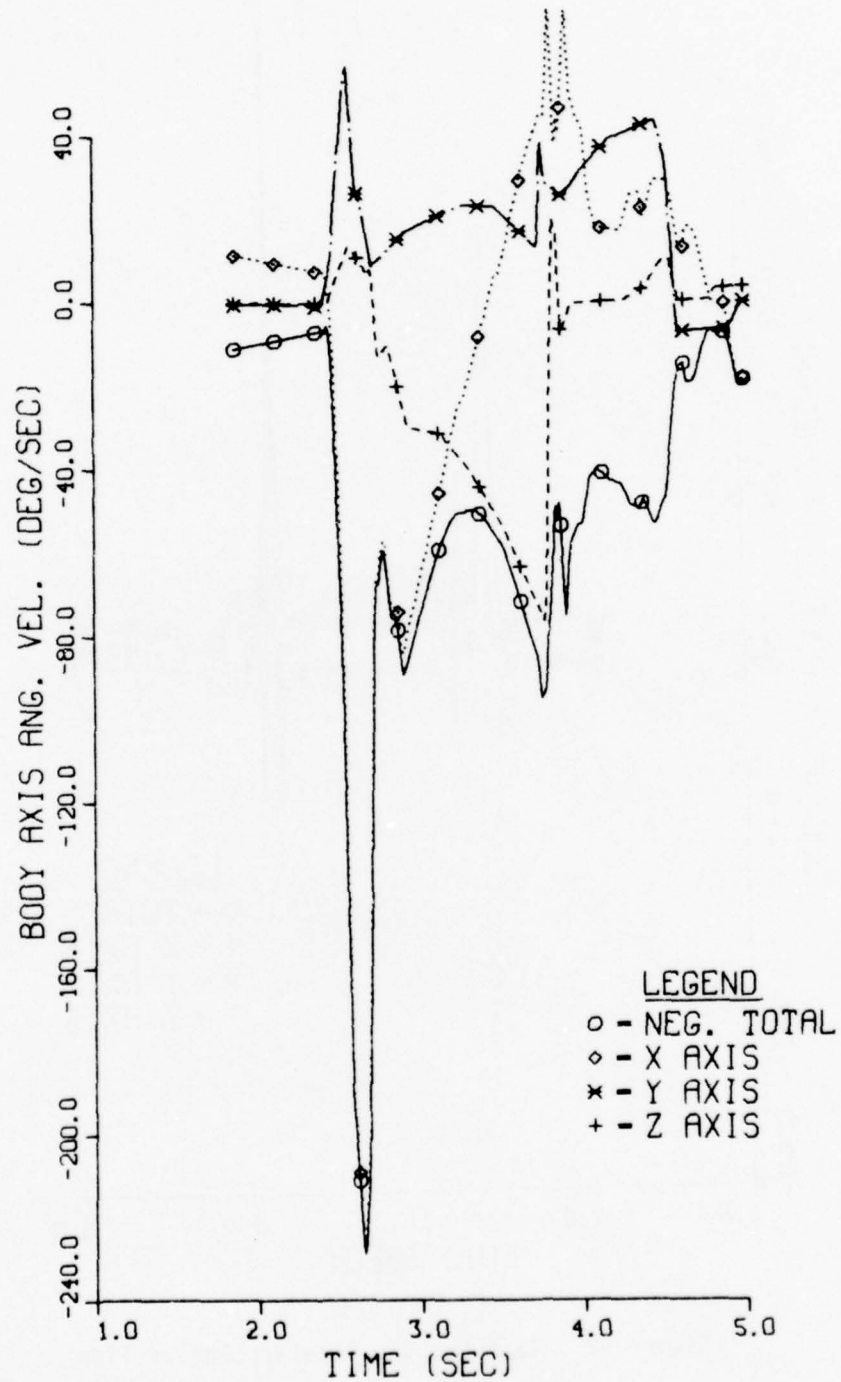


Figure 91. Test No. 81, Angular Velocity vs Time



the wing tip sticks and stops instantaneously. If the ground had been hard (e.g., concrete) then the wing tip would have slid for some distance radically changing the vehicle's subsequent dynamic behavior.

As the vehicle starts back down from the peak of its rolling arc the weight vector comes into play creating a yawing moment which builds up to a  $77^\circ/\text{sec}$  yaw rate (or a 2170 ft-lb yaw energy level). This yaw movement abruptly ends as the vehicle nose strikes the ground more or less sideways. This action is recorded as a Y axis accelerometer spike of 447 feet/sec<sup>2</sup>. The spike was recorded on the IRON TURKEY test vehicle but it is believed that it would not be recorded on an actual AQM-34V. In the case of the real vehicle, damage to a greater or lesser extent would have occurred in the nose area, thus reducing the overall rigid body acceleration. From this step it may be inferred that the unattenuated (uncontrolled) transfer of an estimated 2170 ft-lbs through the nose of the RPV will cause some level of damage under these landing conditions.

After the vehicle nose has contacted the ground the vehicle rotates about the nose and wing tip back onto the main FIAS bag. A damped rocking motion in pitch occurs as the vehicle settles to a stop.

##### 5. TEST RESULTS, $135^\circ$ YAW, 15 KNOTS DRIFT, MARK VIII FIAS

a. The landing conditions for a  $135^\circ$  yaw angle with a 15 knot horizontal drift rate were investigated during Tests No. 74, 75, 78, and 79. During Test No. 74 the leading wing dug in deeply after separation of the frangible wing tip. This test led to the retrofit of a realistic frangible wing tip root area as described in Section V. Retesting during Test No. 75 showed that the vehicle dynamics did depend upon the realistic modeling of this area. During Test No. 75 the wing tip slid approximately 6 feet (on hard ground) instead of digging in and stopping. This sliding motion reduced the severity of the dynamics compared to Test No. 74 (reduced the arc angle shown in STEP 4, Figure 92) but did not otherwise change the vehicle landing performance. The data recorded during Test No. 75 was unuseable due to extraneous noise and so the landing conditions were repeated during Test No. 78.

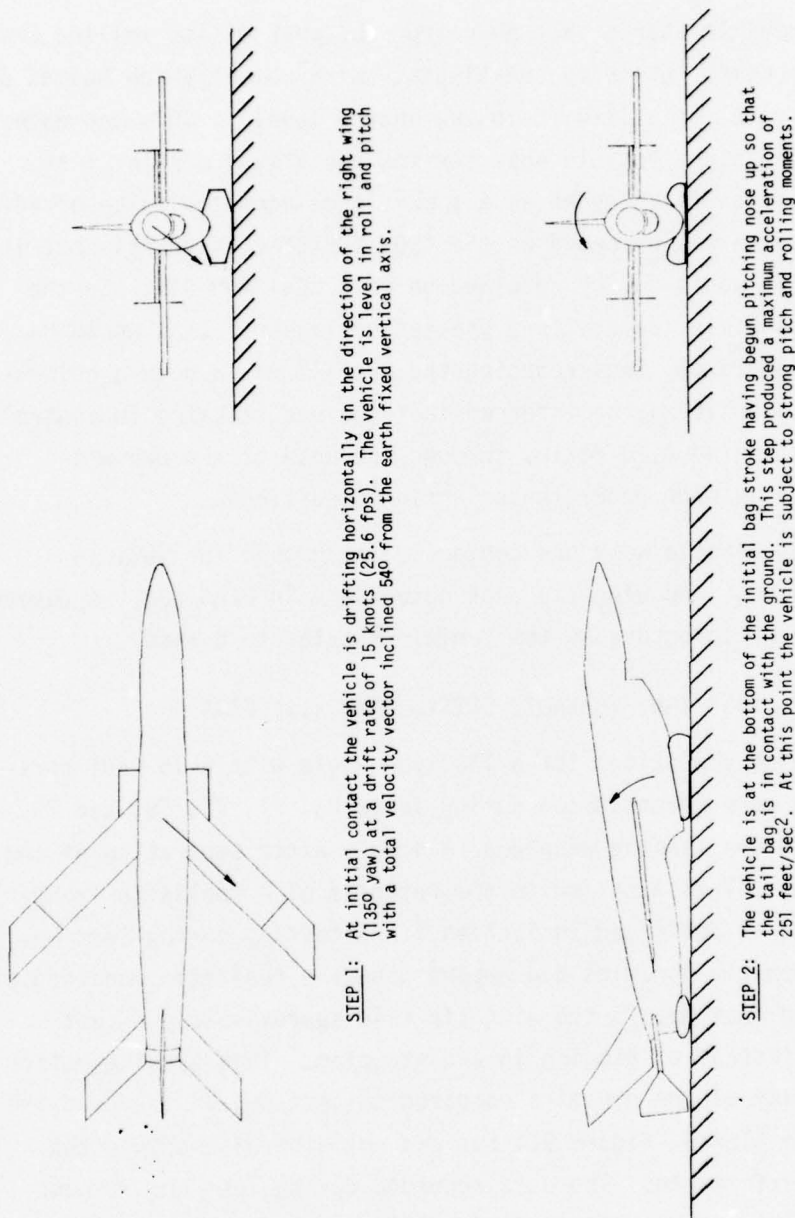
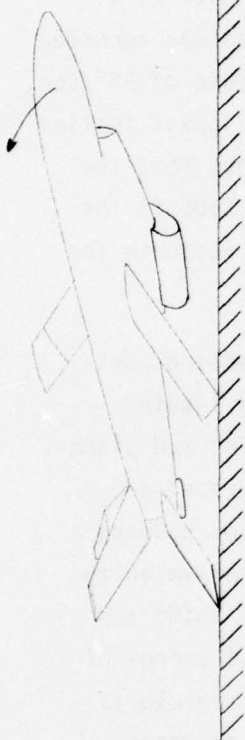
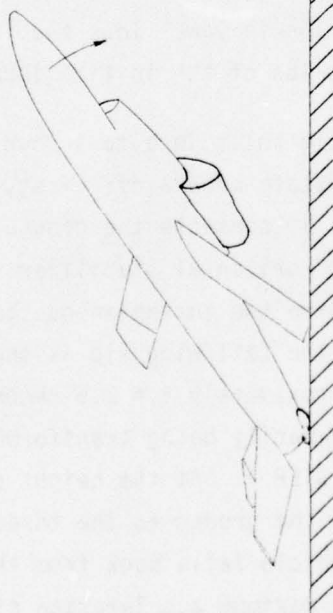
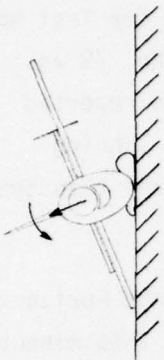


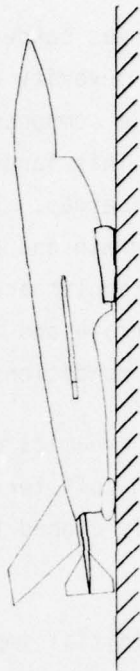
Figure 92. Mark VIII FIAS, 135° Yaw, 15 Kts



STEP 3: As the vehicle rolls with the tail in contact with the ground the leading horizontal stabilizer endplate breaks off first. Further rotation causes the leading frangible wingtip to break off as the wing contacts the ground. Note in the angular velocity curves the point of discontinuity as the vehicle changes its instantaneous center of rotation from the FIAS bag to the wingtip and tail.



STEP 4: As the vehicle continues to rotate in roll and pitch the leading horizontal stabilizer breaks off. At the peak of this arc the vehicle is approximately 50° off the ground. Coming down from this peak the wing tip starts sliding causing rotation in yaw as well as roll and pitch.



STEP 5: The vehicle has rotated (3 axis) back onto the main bag where it rocks and settles causing a maximum acceleration of 148 feet/sec<sup>2</sup>. During this rocking/settling moment note that the angular velocity curves take the general form of a damped sine wave.

Test No. 78 was conducted on Friday afternoon and again exhibited sliding and reducing severity due to the hard terrain at the time of test. Unfortunately a simple component failure resulted in the loss of useable data from the test. This landing condition was rescheduled for Test No. 79 on the following Tuesday. It rained all weekend. Test No. 79 was conducted on soft terrain and exhibited the vehicle dynamics reported herein. These test results are considered typical for this landing condition on soft terrain and are similar to (but more severe) than the hard terrain landing conditions.

b. The vehicle dynamics during a  $135^\circ$  yaw angle, 15 knot horizontal drift rate landing on soft terrain are shown in Figure 92. This maneuver has been descriptively dubbed the "One-arm Pushup" primarily for lack of a better name.

During the initial impulse phase of this maneuver (STEP 2) a maximum acceleration (Figure 93) of  $251 \text{ feet/sec}^2$  ( $7\text{-}3/4 \text{ g's}$ ) was recorded together with a roll rate of  $138^\circ/\text{sec}$ , (Figure 94) a pitch rate of  $84^\circ/\text{sec}$ , and a yaw rate of  $35^\circ/\text{sec}$ . This acceleration level was the lowest initial impulse level recorded during this test series. Note however, that the induced rotations account for 400 ft-lbs of energy in roll, 2500 ft-lbs in pitch, and 450 ft-lbs in yaw. Thus the induced rotation accounts for approximately 3500 ft-lbs of the initial impact energy.

As the vehicle rolls in a tail down attitude the leading horizontal stabilizer endplate breaks off first, followed by the leading frangible wing tip as it contacts the ground. Further rolling and pitching cause the leading horizontal stabilizer to contact the ground and break off. At this time the instantaneous centers of rotation undergo a shift from the CG to the tail/wing tip as shown on the angular velocity vs time curves at approximately  $t = 2.6$  seconds. After this shift the vehicles energy is primarily being transformed into potential energy of the C.G. as shown in STEP 4. At the height of this arc the vehicle is approximately  $50^\circ$  off the ground as the three-axis rotation reverses direction. As the vehicle falls back from this arc, back onto the FIAS bag, it experiences a maximum acceleration of  $148 \text{ feet/sec}^2$  ( $4\text{-}1/2 \text{ g's}$ )



# IRON TURKEY TEST NO. 79 DATA

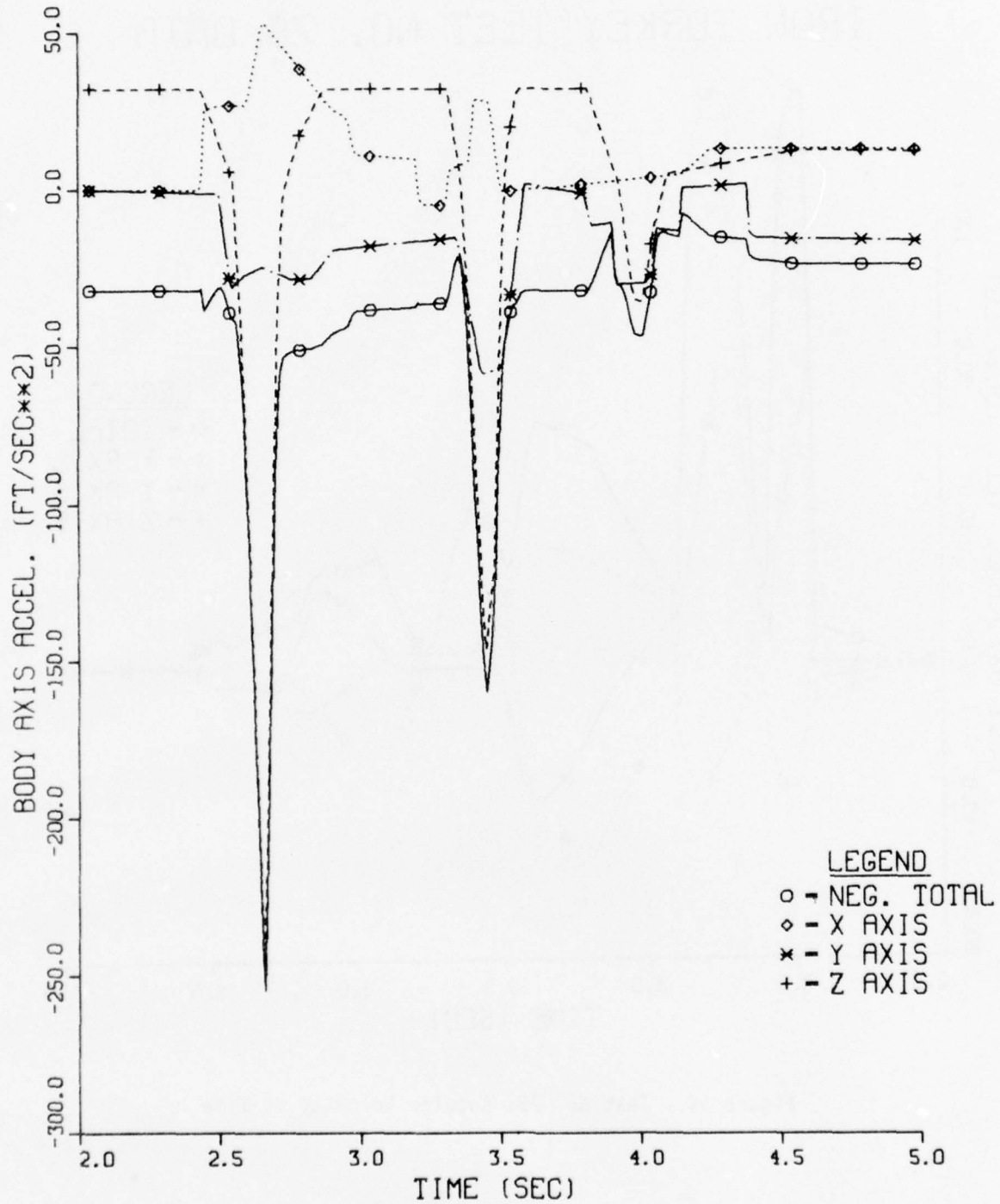


Figure 93. Test No. 79, Acceleration vs Time

## IRON TURKEY TEST NO. 79 DATA

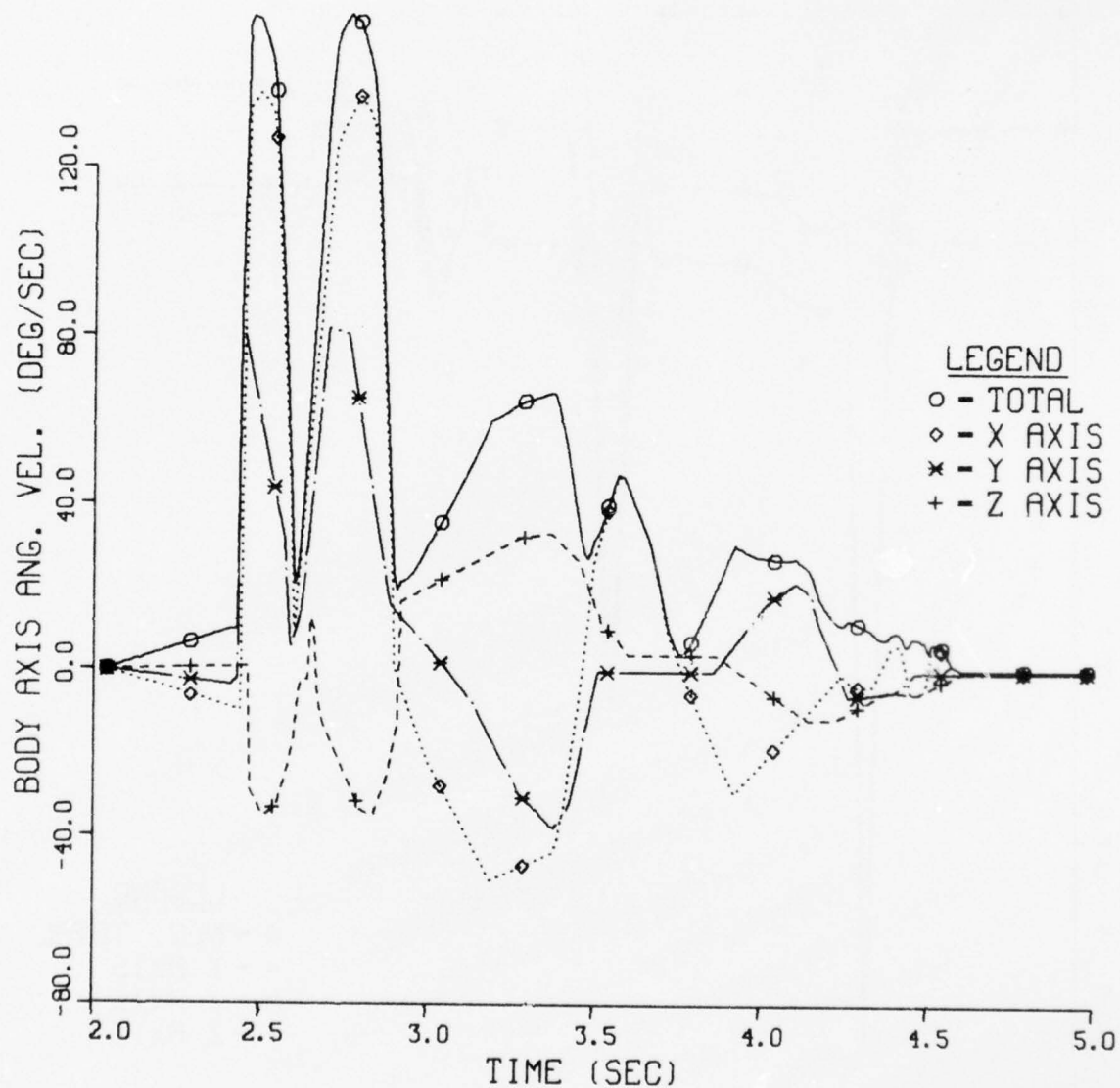


Figure 94. Test No. 79, Angular Velocity vs Time

which is the highest second impulse rate recorded during this test series. As the vehicle settles onto the FIAS bag a third impulse of  $36 \text{ feet/sec}^2$  (1 g) is recorded together with a damping out of the rotational velocities.

c. The landing condition of a  $135^\circ$  yaw angle at 15 knots drift produced the seemingly paradoxical conclusion that this test saw the lowest accelerations and the highest damage level reported during this test series. This is readily explained by the transference of the impact energy into rotation during the initial impulse, followed by the subsequent ground contact of the damaged portions due to the rotation and the retransference of this "stored" energy back into the second impulse.

#### 6. TEST RESULTS, $180^\circ$ YAW, 15 KNOTS DRIFT, MARK VIII FIAS

a. The landing conditions for a  $180^\circ$  yaw angle with a 15 knot horizontal drift rate were investigated during Test No. 77. The recorded data from Test No. 77 is considered as useable even though a massive, all channel, electronic noise signal obliterated the secondary impulse readings. (This noise also affected Test No. 78 when the defective component finally failed completely.) The test results are considered as typical of the vehicle performance under these landing conditions.

b. The vehicle dynamics during a  $180^\circ$  yaw (tail first) 15 knot drift landing are shown in Figure 95. This maneuver has been descriptively dubbed the "wheelie" because it involves a dynamic balance similar to a motorcycle wheelie during the slideout portion.

During this maneuver an initial impulse acceleration (Figure 96) of  $318 \text{ feet/sec}^2$  (10 g's) was recorded together with a buildup in pitch (Figure 97) to a rate of  $91^\circ/\text{second}$ . This pitch rate implies an energy transfer of 2960 ft-lbs into the pitch rotation. When the vehicle's tail slapped down (STEP 3), an acceleration level of  $145 \text{ feet/sec}^2$  (4-1/2 g's) was recorded. The vehicle continued to pitch up to an angle of approximately  $20^\circ$  above the ground while sliding on the tail/tail bag. During the tail slapdown both of the horizontal stabilizer end plates contacted the ground and broke off. As the vehicle slid on the tail it came into a dynamic balance between the tail friction vector and the weight vector as

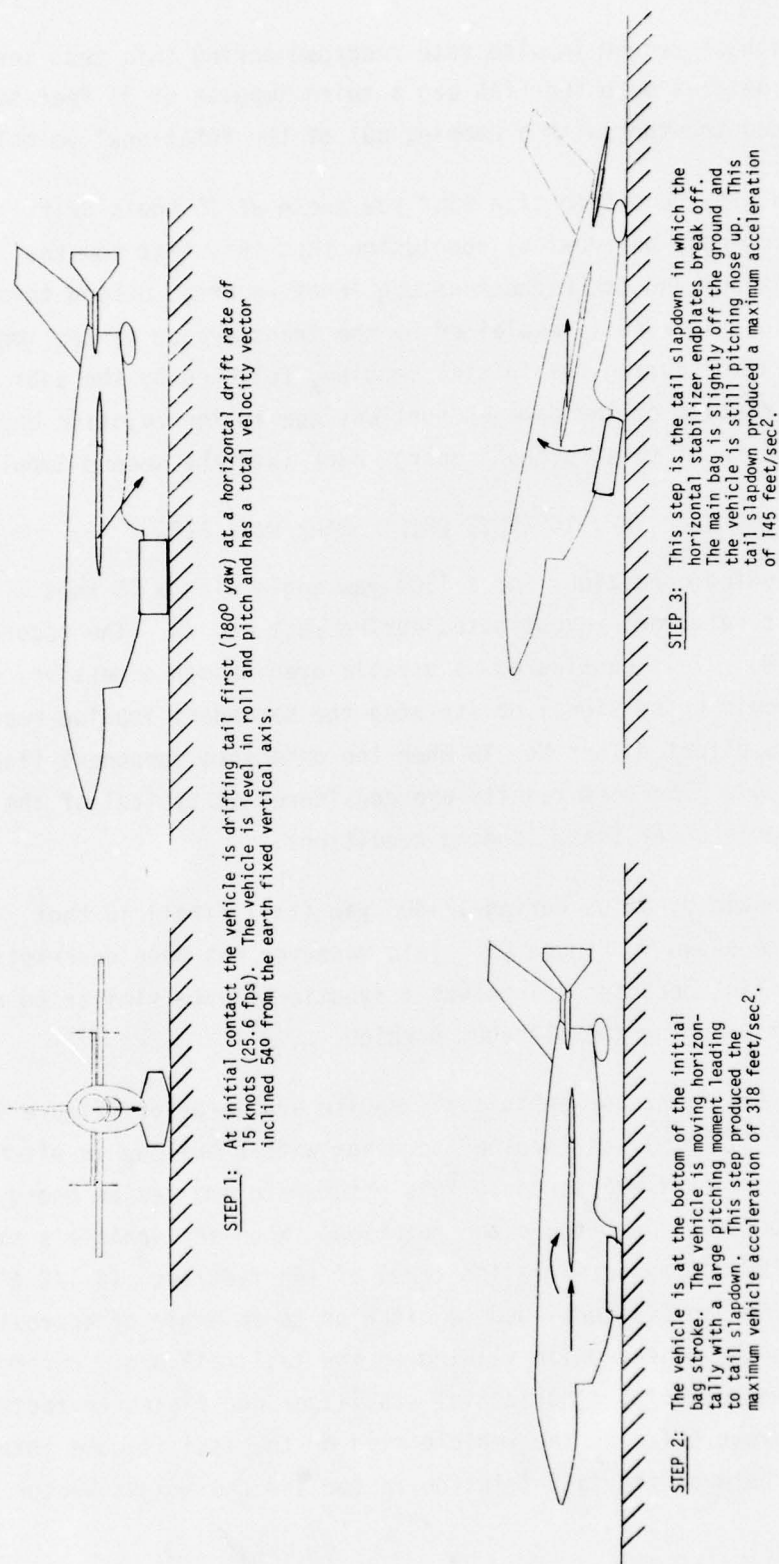
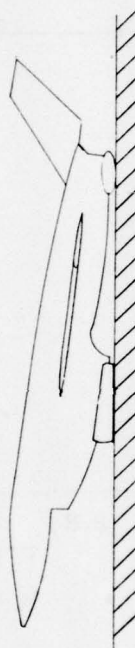


Figure 95. Mark VIII FIAS,  $180^\circ$  Yaw, 15 Kts





STEP 4: The vehicle has pitched to its maximum arc of  $20^\circ$  and is sliding horizontally. This dynamic balance is maintained for some time and is similar to a motorcycle "wheelie". During this slideout the tail bag rolls under the tail allowing the aft parachute can fitting to scoop dirt causing an X-axis acceleration of  $56 \text{ feet/sec}^2$ . This tail bag movement also allows the horizontal stabilizer to contact the ground and break off.



STEP 5: As the horizontal velocity decays due to friction the vehicle pitches down back onto the main bag and settles to a stop.

## IRON TURKEY TEST NO. 77 DATA

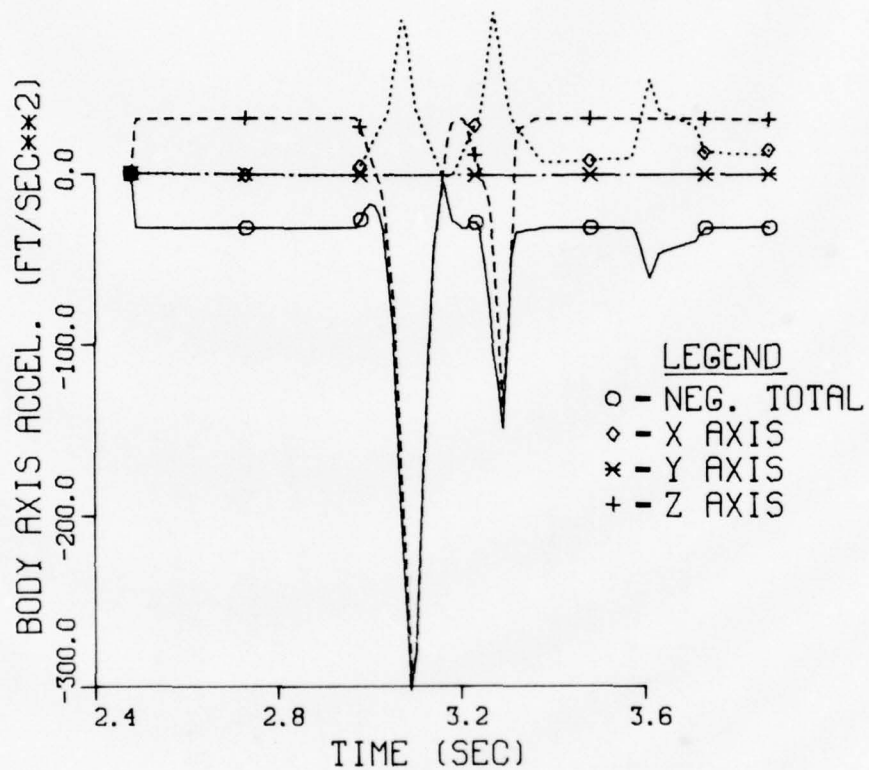


Figure 96. Test No. 77, Acceleration vs Time

# IRON TURKEY TEST NO. 77 DATA

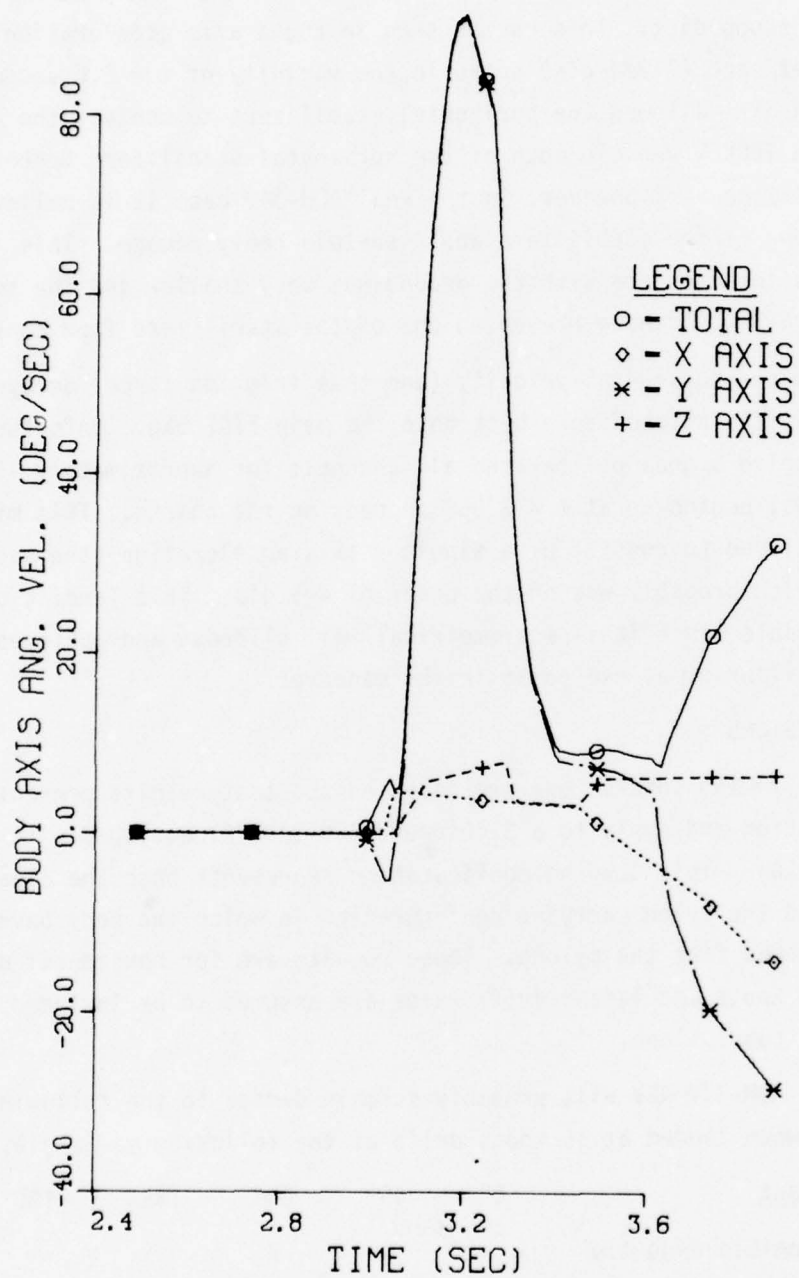


Figure 97. Test No. 77, Angular Velocity vs Time

indicated by the leveling off of the Y axis (pitch) rotation rate vs time curve. The horizontal slide caused the vehicle tail to "runover" the tail bag and allowed the parachute can attachment fitting to contact the ground and scoop dirt. This can be seen in the X axis acceleration trace as a 56 feet/sec<sup>2</sup> (1-3/4 g's) spike in the vicinity of t = 3.6 seconds. This motion also allowed the horizontal stabilizers to contact the ground. In the IRON TURKEY vehicle both of the horizontal stabilizers broke off during this maneuver; however, in the real AQM-34V case it is believed that only one of the stabilizers would sustain heavy damage. This is because the interference with the ground was very shallow and the smallest amount of roll would have prevented one of the stabilizers from contact.

As the horizontal velocity (and thus friction force) decayed to zero the vehicle pitched down back onto the main FIAS bag. Unfortunately a massive noise signal obliterated all channels for approximately 155 milliseconds, beginning at t = 3.950 seconds on the charts. This missing data is believed to consist of a single Z axis acceleration (the second impulse) which probably was on the order of 4-5 g's. This landing condition is notable since it is a symmetrical tail slideout and achieves a dynamic equilibrium at one point in the maneuver.

## 7. CONCLUSIONS

The following conclusions are based on the test results presented in this section and apply to a 2140 pound AQM-34V PRV equipped with a Mark VIII FIAS. This landing configuration represents both the clean wing RPV and the pylon carrying configuration in which the pods have been jettisoned from the pylons. These results are for horizontal drift rates of 15 knots and lesser drift rates are assumed to be included under these conclusions.

a. An AQM-34V RPV will probably sustain damage to the following components when landed at 15 knots drift at the following yaw angles.

<u>Component</u>	0°	45°	90°	135°	180°
Leading frangible wing tip		X	X	X	
Leading frangible endplate			X	X	X
Trailing frangible endplate					X
Leading horizontal stabilizer				X	X
Nose area			X		



b. The damage which was sustained is not directly traceable to the vehicle accelerations encountered. Test No. 80 (0° yaw) had the highest acceleration level and the lowest damage level. Test No. 79 (135° yaw) had the lowest acceleration level and the highest damage level. Damage during the vehicle landing is not a function of accelerations but rather of energy flux and flow paths.

c. In every test the vehicle received at least two major impulses from the FIAS bag. The ability of the FIAS to withstand multiple impacts has been demonstrated. It is known that the FIAS has a damping ratio of approximately 85%. The 15% rebound accounts for the double hit only on Test No. 80 (0° yaw). The other four test conditions (45°, 90°, 135°, 180°) would have experienced a double hit, even if the FIAS bag had a 100% damping ratio. The initial vector misalignment in the four cases caused the vehicle to rotate onto one of its extremities and then fall back onto the FIAS bag, producing the double hit.

d. This configuration of vehicle/FIAS has a vehicle turnover horizontal velocity threshold of 16 knots which occurs at a 90° yaw angle.

e. The vehicle will be more stable when landing on a hard terrain than on a soft terrain. The soft terrain allows the vehicle extremities to dig in and become instantaneous centers of rotation. The hard terrain will force the extremity to slide/gouge and thus will not provide a pivot point. This is especially applicable to the 90° and 135° yaw angle landings.

f. The vehicle stability during the 90° and 135° yaw angle landings could possibly be improved by changes to the digging in mechanism.

(1) Wing bags: a wing bag which can both attenuate the maximum roll energy of 1100 ft-lbs and present a large bearing area to the ground should be effective in preventing dig in.

(2) Wing tip changes: if the wing tip area could be reshaped so as to eliminate any sharp bladelike geometry then the digging in would be lessened.

g. Tail slapdown appears to be only of major significance in the 180° yaw landing condition. In Test No. 77 a maximum tail slapdown energy of 2960 ft-lbs was encountered. In the other landing conditions the tail bag played a relatively minor role. Whether or not a tail bag for this vehicle is cost-effective is a question outside the scope of this analysis.

h. A nose bag for this vehicle would be effective only in the 90° yaw/soft ground landing condition. Wing tip changes may negate even this landing criteria by reducing dig in.

i. Because the vehicle is the most stable during a 0° yaw landing condition it would be desirable to drive the vehicle to this yaw angle by means of a gliding parachute recovery system (Hi-glide type canopy) and then optimize a new FIAS bag for this relatively controlled landing condition. This combination would possibly yield a no-damage recovery system for this vehicle.

j. The maximum initial impulse acceleration during these five landing conditions were 13-1/2 g's, 10-1/2 g's, 9-1/2 g's, 7-3/4 g's, and 10 g's respectively. On Test No. 60 the same FIAS was tested vertically with the IRON PIG vehicle and recorded 7.9 g's. What is causing the higher accelerations onboard the IRON TURKEY vehicle is not fully understood but is believed to be related to bag distortion caused by the horizontal movement of the vehicle. Test No. 65 was to be a comparative check of vertical FIAS performance but unfortunately the data was not obtained and resources did not permit retesting.

k. The problem of the ground impacting of an RPV has now been turned into a problem in dynamics rather than a problem in impact. Only one major instance of uncontrolled energy transfer (impact) occurred during this test series and that was the nose slam during the 90° landing, Test No. 81.

l. Although data collection was a recurring problem throughout this test series it should be obvious by inspection that very little noise was required to render the 6-axis curves presented unuseable.

SECTION X

HORIZONTAL TESTS NO. 83-91

1. TEST SERIES NO. 83-91

a. Test Conditions - The purpose of this series of nine tests was to obtain engineering data on the performance of the Mark IX FIAS bag at five different yaw angles and at varying horizontal velocities. Yaw angles of 0°, 45°, 90°, and 180° were to be tested at horizontal velocities of 7-1/2 and 15 knots with the Mark IX/empty pods configuration. The horizontal and vertical release heights were at 6.4 and 8.9 feet, respectively, for the 7-1/2 knot conditions. For the 15 knot condition these heights were 6.4 and 16.4 feet, respectively. Thus, the 2640 pound test vehicle had a total impact energy of 23,500 ft-lbs at the 7-1/2 knot conditions and 43,300 ft-lbs at the 15 knot conditions.

b. Chronological History - This series of tests was performed during the time period 19 Oct 77 to 3 Nov 77. These tests were performed in the following chronological order:

<u>Test Number</u>	<u>NH</u>	<u>Yaw</u>	<u>Date</u>
83	0 Kts	-	19 Oct 77
84	7-1/2	0°	20 Oct 77
85	7-1/2	180°	21 Oct 77
86	7-1/2	90°	27 Oct 77
87	15	0°	31 Oct 77
88	15	180°	1 Nov 77
89	15	45°	2 Nov 77
90	15	90°	3 Nov 77 (AM)
91	15	135°	3 Nov 77 (PM)

The order of the test conditions was estimated to be in increasing severity of damage based on the results of Tests No. 72-82. At this point in the investigation the combination of time, money, and weather did not allow

for the repetition of any test conditions. Fortunately the testing process had been debugged to the point where intelligible data was obtained on 6 of the 9 tests.

c. Presentation of Test Results - The results of this test series are presented in the following manner for comparison with the Mark VIII results. The tests are grouped by yaw angle similarly to the Mark VIII discussions.

<u>Yaw Angle</u>	<u>Test Number</u>
0°	87
45°	89
90°	90
135°	91
180°	88

The data and discussions are presented in accordance with the coordinate system shown in Figure 98.

## 2. TEST RESULTS, 0° YAW, 15 KNOTS DRIFT, MARK IX FIAS

a. The landing conditions of a 0° yaw angle at a 15 knot drift rate with the Mark IX FIAS were investigated during Test No. 87.

b. The vehicle dynamics during a 15 knot, 0° yaw landing are shown in Figure 99. Under these landing conditions the initial velocity vector is relatively closely aligned with the center of pressure of the Mark IX FIAS bag. As the bag contacts the ground (STEP 2) it starts to develop shearing forces due to friction and deforms along the ground track as shown. These shearing forces are seen by the vehicle as a nose down pitching moment which starts before the initial Z axis impulse. At the bottom of the initial bag stroke the leading edge area of the bag ruptures, resulting in a maximum acceleration of only 5-1/3 g's (Figures 100 through 105). At this point the vehicle is sliding and gaining momentum in pitch. The vehicle's pitch movement continues until at the peak of the arc the vehicle's nose is barely touching the ground. This movement caused the nose of the pods to contact the ground somewhat heavily producing a 6 inch diameter dent in the nose of both pods. It is extrapolated that this



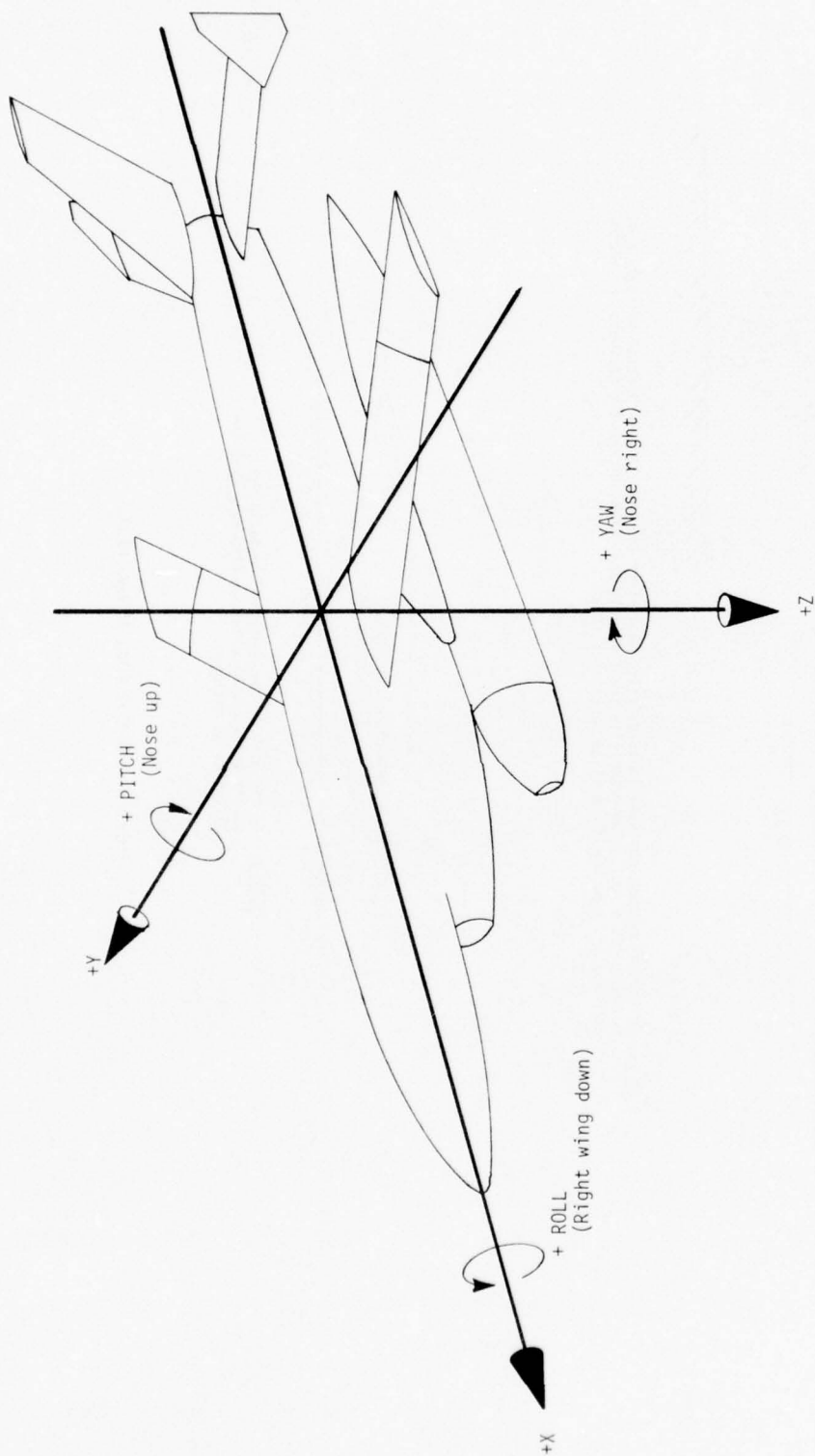
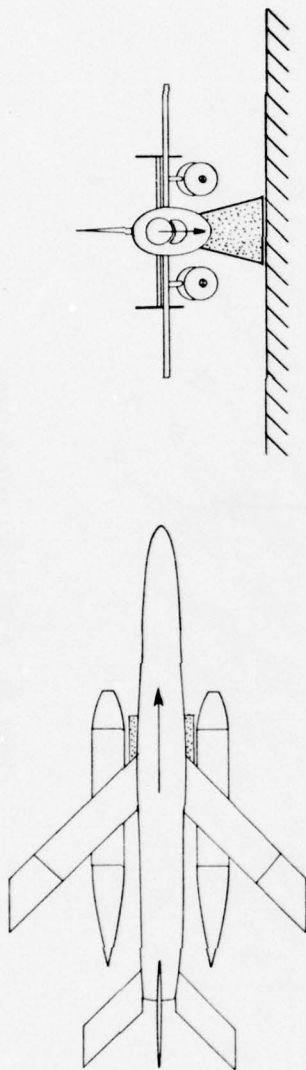
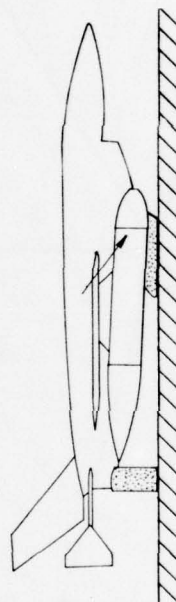


Figure 98. 6 DOF Coordinate System

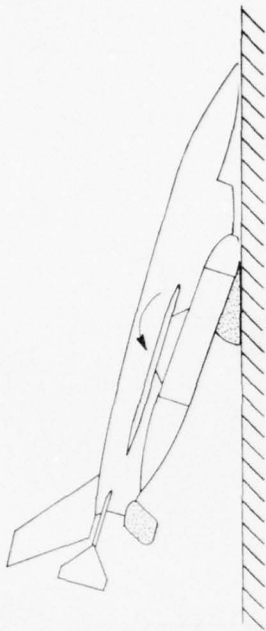


STEP 1: At initial contact the vehicle is drifting nose first ( $0^\circ$  yaw) at a horizontal drift rate of 15 knots (25.6 fps). The vehicle is level in roll and pitch and has a total velocity vector inclined  $520$  from the earth fixed vertical axis.

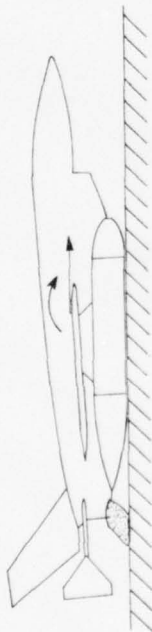


STEP 2: As the Mark IX bag contacts the earth, it starts to deform in shear loading away from the direction of motion.

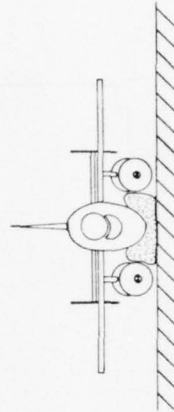
Figure 99. Mark IX FIAS,  $0^\circ$  Yaw, 15 Kts



STEP 4: As the forward sliding motion stops the vehicle pitches nose down and contacts the pod noses and the vehicle nose. This motion caused a 6" diameter dent in the nose of both pods but did not appear to be damaging to the nose. The vehicle nose appeared to barely graze the earth at the height of this pitch arc.



STEP 3: At the bottom of the initial bag stroke the vehicle is sliding and starting to pitch nose down. The leading edge of the bag attachment fitting has torn slightly thus reducing the local bag pressure across the leading edge.



STEP 5: The vehicle has pitched back onto the main and tail loop and settled. The Mark IX bag is cradling the engine nacelle with negligible pressure on the pods.



### TEST 087GX DATA

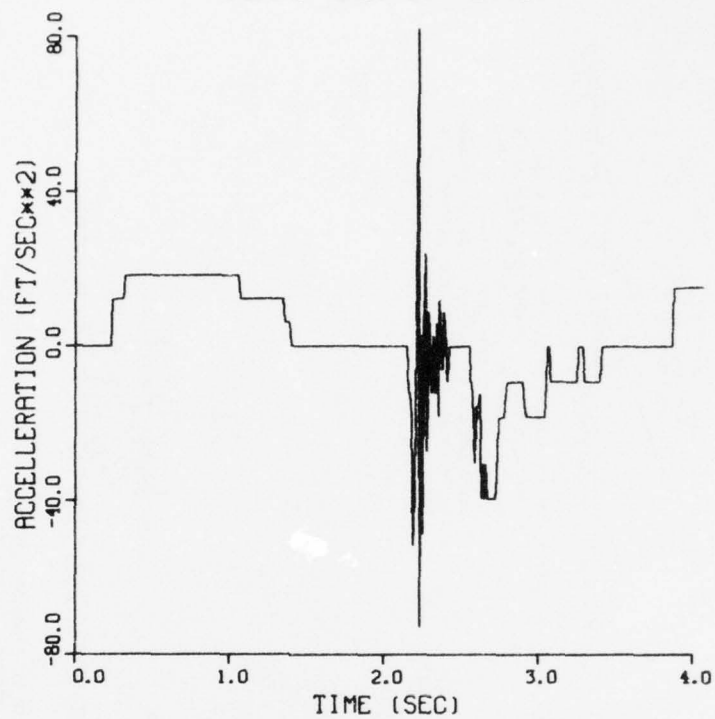


Figure 100. Test No. 87, X Axis Acceleration

### TEST 087GY DATA

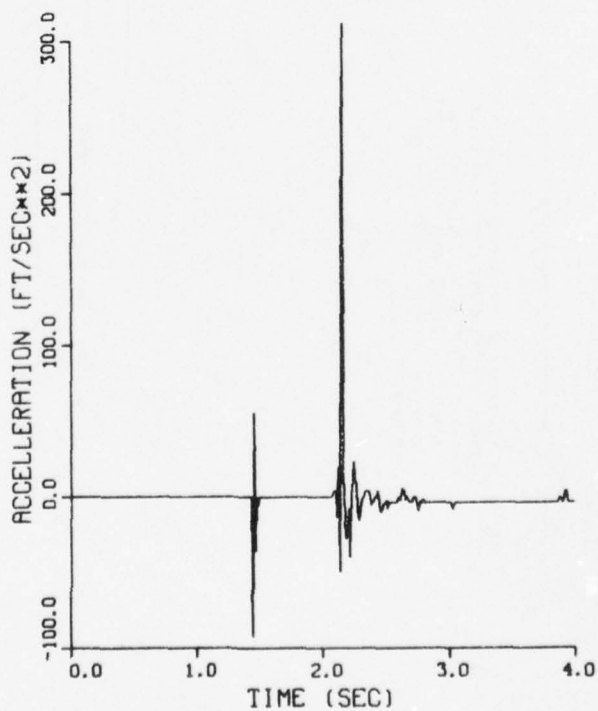


Figure 101. Test No. 87, Y Axis Acceleration



TEST 087GZ DATA

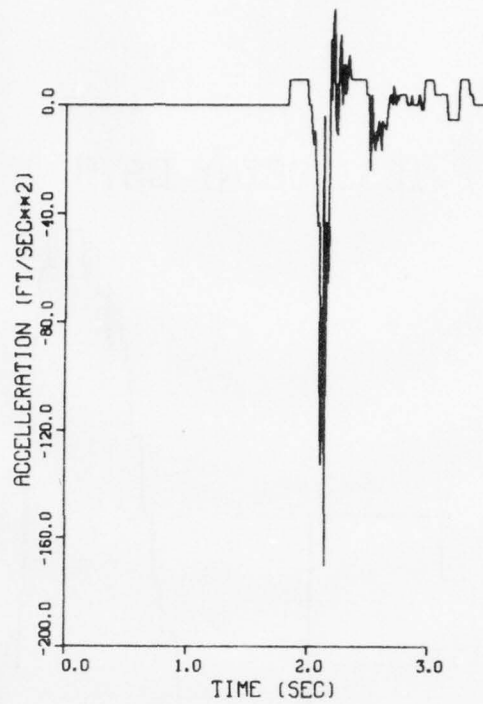


Figure 102. Test No. 87, Z Axis Acceleration

TEST 087WX DATA

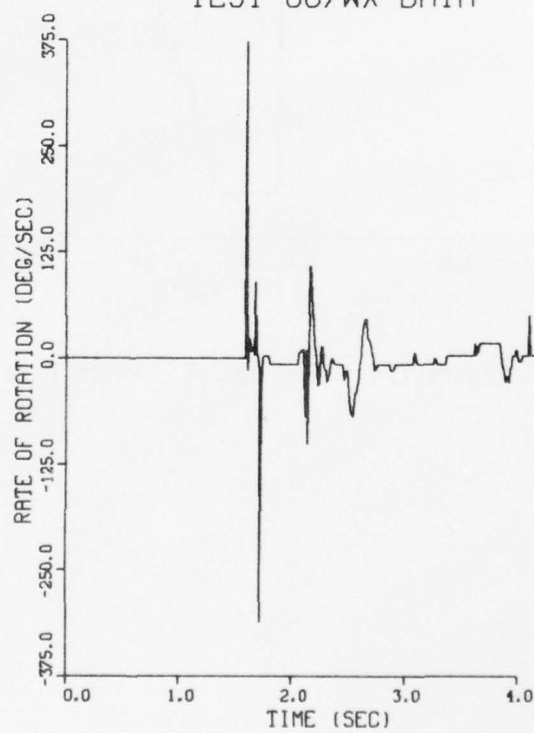


Figure 103. Test No. 87, Roll Rotation

# TEST 087WY DATA

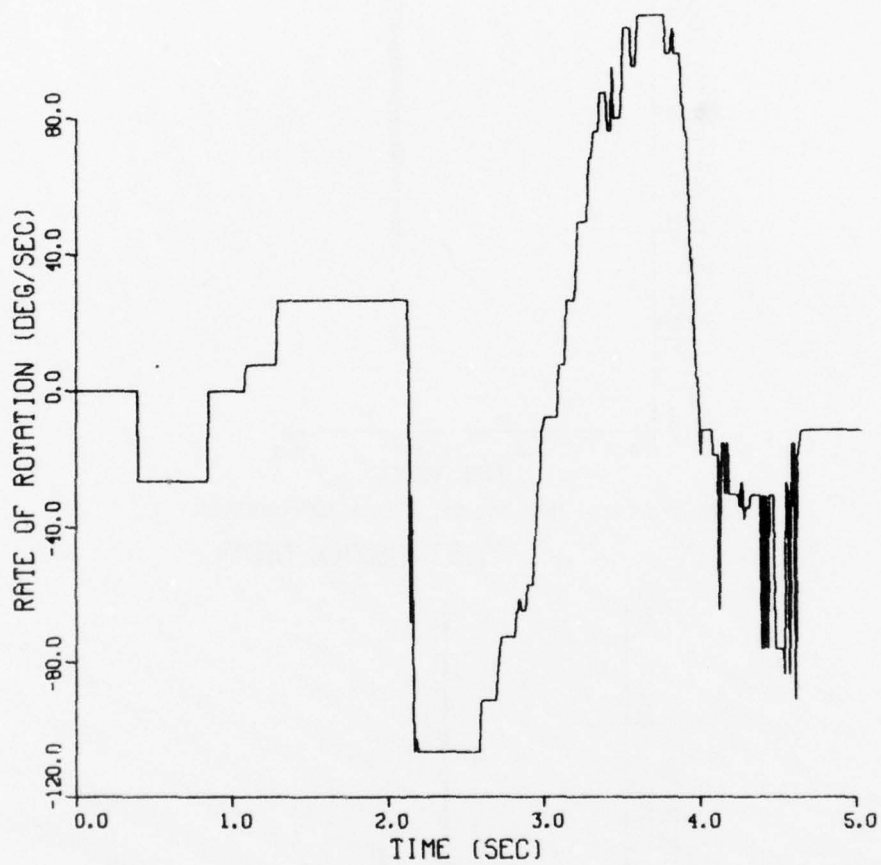


Figure 104. Test No. 87, Pitch Rotation

## TEST 087WZ DATA

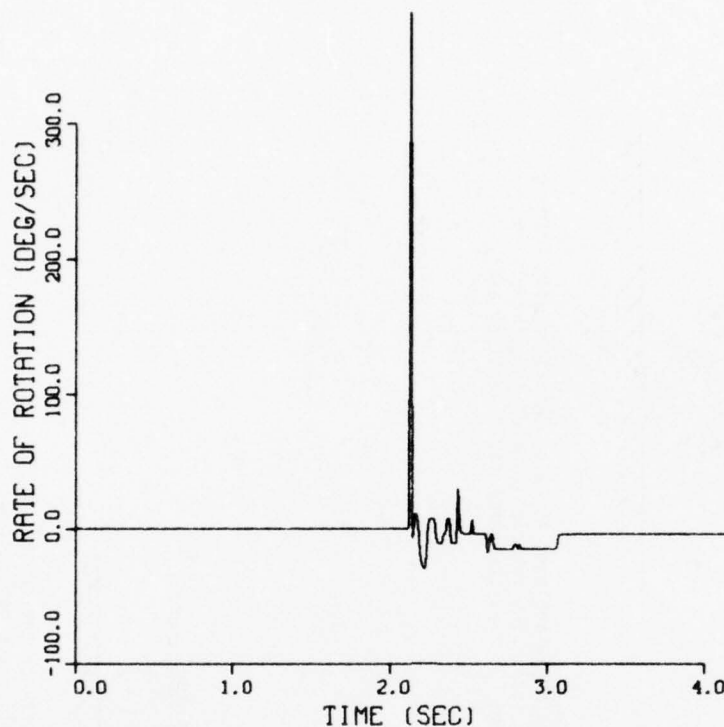


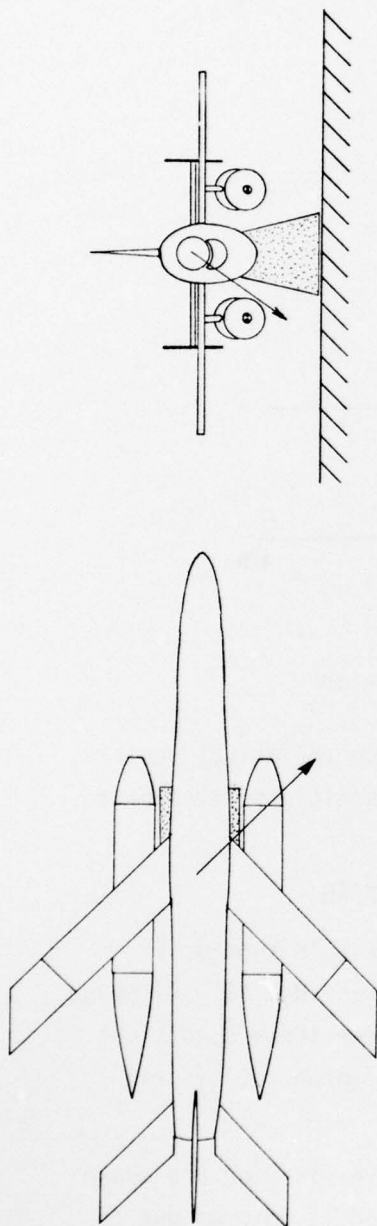
Figure 105. Test No. 87, Yaw Rotation

step (STEP 4) would have damaged the pylon fittings on the actual vehicle. Falling back from the peak of this pitching arc the vehicle settles back onto the main and tail bags as shown.

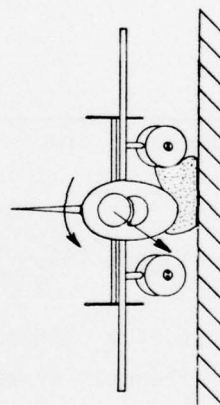
### 3. TEST RESULTS, 45° YAW, 15 KNOTS DRIFT, MARK IX FIAS

a. The landing conditions of a 45° yaw angle at a 15 knot drift rate with the Mark IX FIAS were investigated during Test No. 89. Although this landing is considered as typical performance under these conditions it was a deceptively smooth landing since there were no large rotational movements during the maneuver.

b. The vehicle dynamics during a 15 knot, 45° yaw landing are shown in Figure 106. As the Mark IX bag contacts the ground it deforms due to frictional forces against the trailing pod prior to the initial Z axis impulse. It is extrapolated that this deformation would have damaged



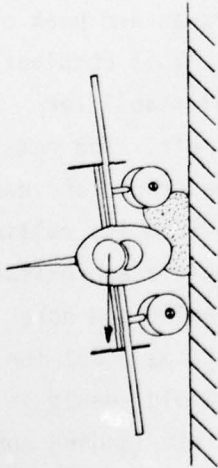
STEP 1: At initial contact the vehicle is drifting at a yaw angle of  $45^\circ$  with the right wing leading at a horizontal drift rate of 15 knots (25.6 fps). The vehicle is level in both roll and pitch and has a total velocity vector inclined  $52^\circ$  from the earth fixed vertical axis.



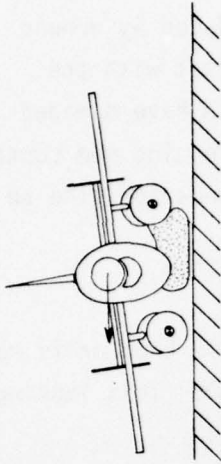
STEP 2: As the Mark IX bag contacts the ground, it deforms into the trailing pod generating large forces (twisting) on the pylon fittings. The vehicle is still level but is starting a positive rolling motion.

Figure 106. Mark IX FIAS,  $45^\circ$  Yaw, 15 Kts

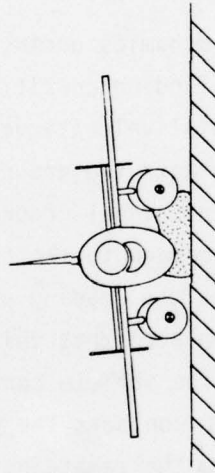




STEP 3: As the vehicle rolls the leading pod contacts the ground causing large forces in the pylon fittings. The rolling motion subsides and the vehicle is now sliding without substantial rotational movement.



STEP 4: As the vehicle slides a mild bounce occurs but again there is no substantial rotational movement.



STEP 5: The vehicle comes to a rest in the same altitude which it slid. The deceptively "smooth" impact dynamics has most probably resulted in the failure of both the leading and trailing pylon fittings.

the trailing pylon fittings on the actual vehicle. As the vehicle motion continues, a maximum acceleration of 11-1/4 g's (Figures 107-112) was recorded at the initial impulse. The rolling motion induced by ground frictional forces brings the leading pod into sharp contact with the ground. It is extrapolated that this step (STEP 3) would have damaged the leading pylon fittings on the actual vehicle. The leading pod contact stops the rolling motion of the vehicle which then proceeds to slide to a halt without further large-scale rotational movement.

4. TEST RESULTS, 90° YAW, 15 KNOTS DRIFT, MARK IX FIAS

a. The landing conditions of a 90° yaw angle at a 15 knot drift rate with the Mark IX bag were investigated during Test No. 90. This landing performance is considered typical under these conditions.

b. The vehicle dynamics during a 15 knot, 90° yaw landing are shown in Figure 113. This landing condition represents the most severe misalignment of the initial velocity vector with the Mark IX FIAS bag. As the bag initially contacts the ground (STEP 2) it deforms against the trailing pod due to frictional ground forces. It is extrapolated that this would result in damage to the trailing pylon fittings. The vehicle is now rolling so that the leading pod makes contact with the ground in STEP 3. It is extrapolated that this would result in damage to the leading pylon fittings. The vehicle continues to roll (over the pod) so that the frangible wing tip contacts the ground and breaks off. The vehicle continues to roll onto the remaining wing tip and reaches an arc peak of approximately 40° while still sliding across the ground. This combination of rolling and sliding has brought the leading horizontal stabilizer frangible endplate into ground contact and has broken it off. The remaining horizontal stabilizer is sliding/scrapping across the ground and has produced a large yawing moment. As the vehicle recovers from its rolling arc a prolonged yaw rotation occurs which rotates the vehicle approximately 90° before it finally stops. This motion presses the leading pod nose into the ground with a twisting motion as the vehicle rotates about the pod nose. It is extrapolated that this motion (STEP 6) would result in damage (again) to the leading pylon fittings. Although this landing condition produced a maximum acceleration of approximately 11 g's (Figures 114-119) it was one of the most damaging maneuvers of the test series.

# TEST 089GX DATA

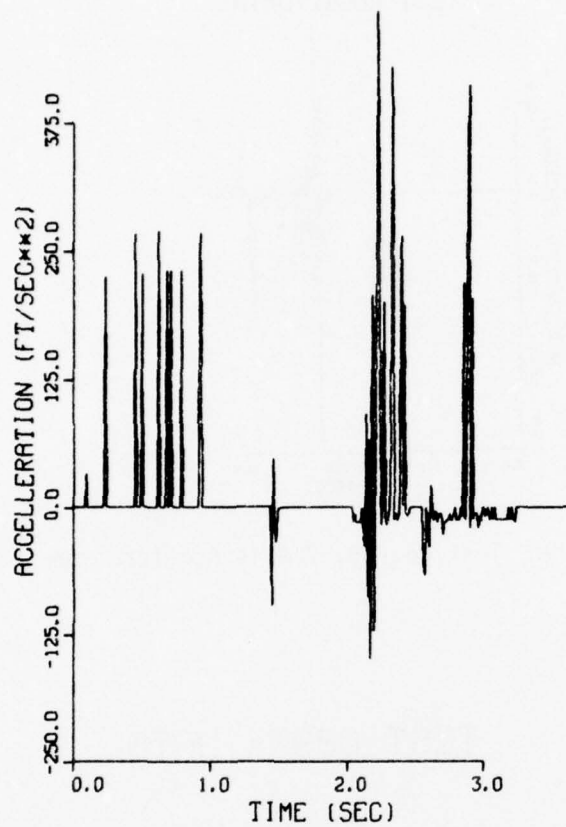


Figure 107. Test No. 89, X Axis Acceleration  
TEST 089GY DATA

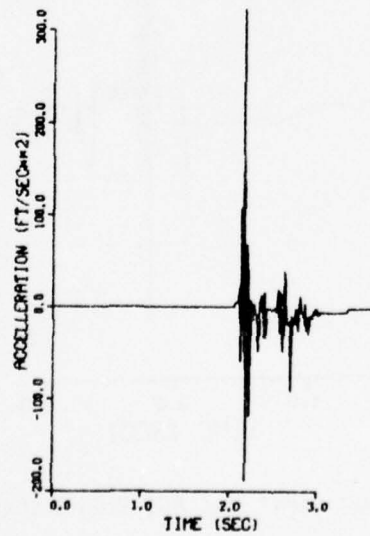


Figure 108. Test No. 89, Y Axis Acceleration

TEST 089GZ DATA

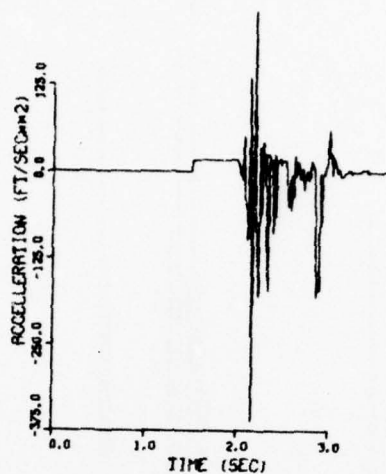


Figure 109. Test No. 89, Z Axis Acceleration

TEST 089WX DATA

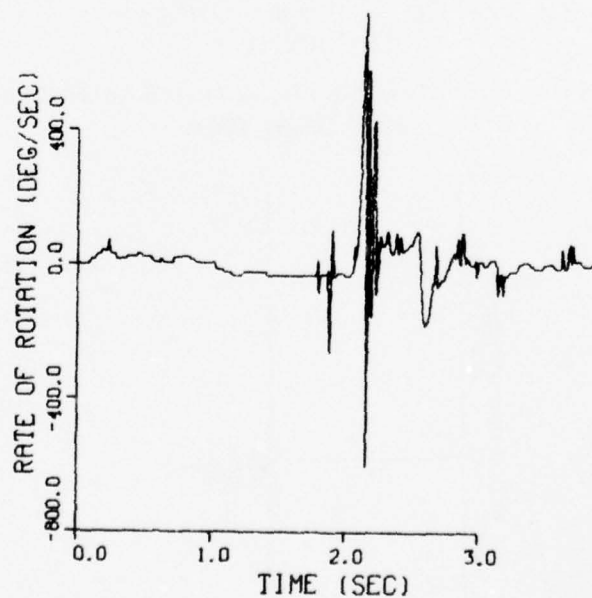


Figure 110. Test No. 89, Roll Rotation



# TEST 089WY DATA

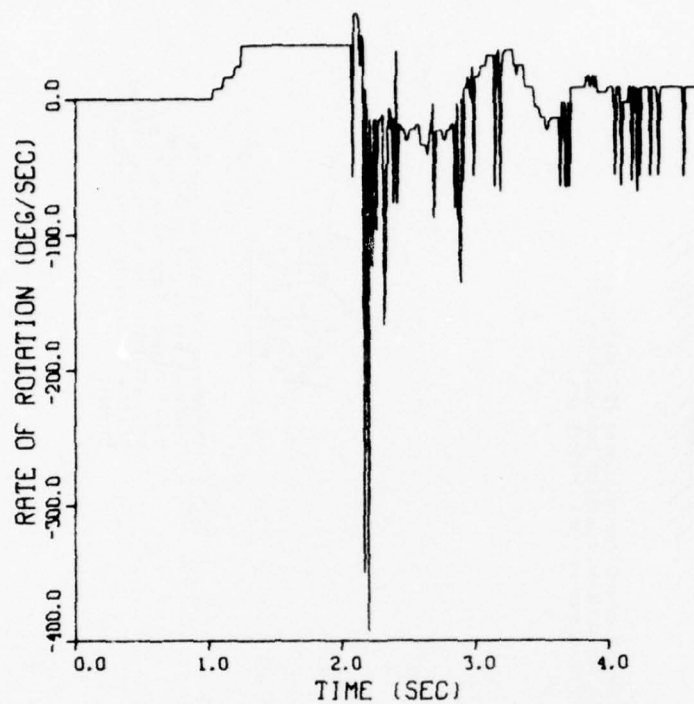


Figure 111. Test No. 89, Pitch Rotation

# TEST 089WZ DATA

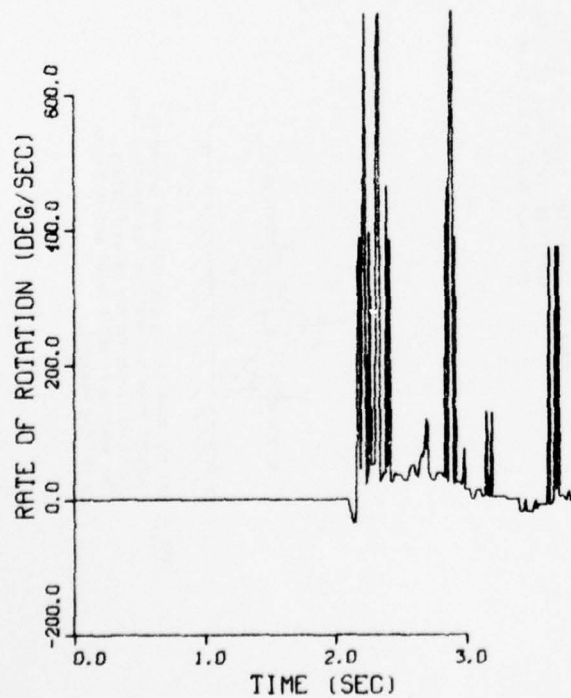
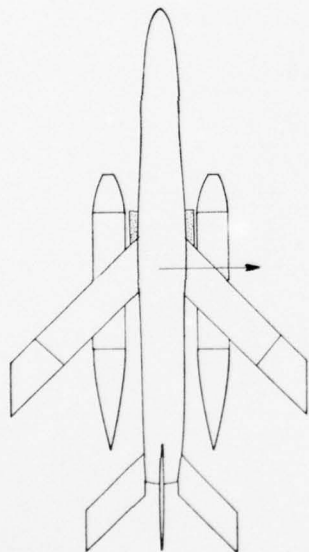
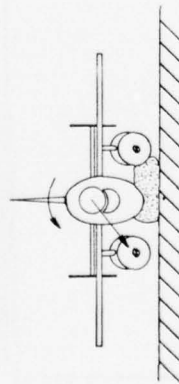
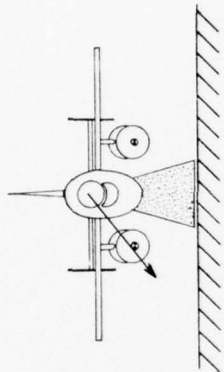


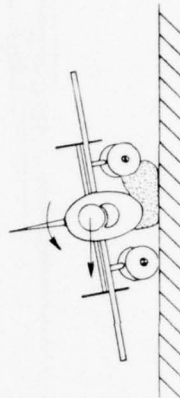
Figure 112. Test No. 89, Yaw Rotation  
175



STEP 1: At initial contact the vehicle is drifting sideways towards the right wing ( $90^\circ$  yaw) at a horizontal drift rate of 15 knots (25.6 fps). The vehicle is level in both pitch and roll and has a total velocity vector inclined  $52^\circ$  from the earth fixed vertical axis.

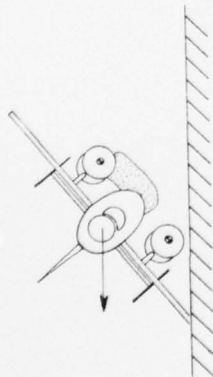


STEP 2: As the Mark IX bag contacts the ground it deforms into the trailing pod imposing large twisting forces on the pylon fittings. The vehicle is still level and is beginning a rolling maneuver.

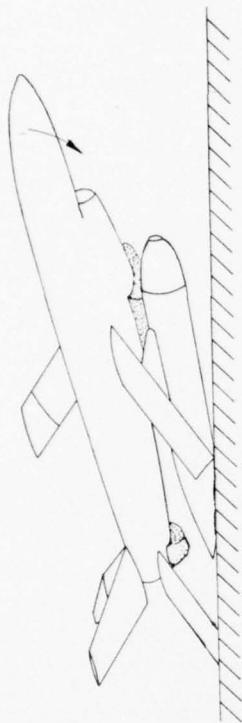


STEP 3: The vehicle has rolled so that the leading pod is in contact with the ground imposing large force on its pylon fittings. The vehicle has started to slide horizontally and is continuing to roll.

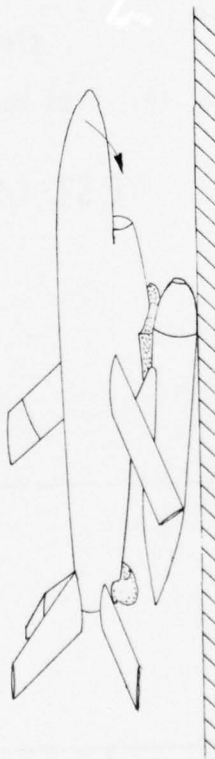
Figure 113. Mark IX FIAS,  $90^\circ$  Yaw, 15 Kts



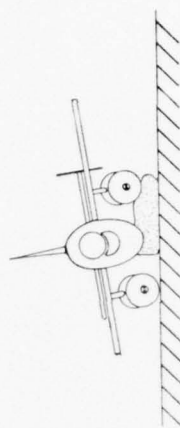
**STEP 4:** At the peak of the rolling arc the vehicle is approximately 40° off the ground. The leading frangible wing tip has broken and the vehicle is sliding on the wing tip/pod.



**STEP 5:** As the vehicle's rolling motion falls off a strong yawing motion starts as the tail area contacts the ground. The horizontal stabilizer endplate breaks off as this yawing begins.



**STEP 6:** The prolonged yaw movement brings the nose of the leading pod into contact with the ground again imposing large forces on the pylon fitting. The yaw movement lasts for approximately 90° and thus grinds the nose of the pod into the ground.



**STEP 7:** As the yaw movement stops, the vehicle rolls back slightly onto the main bag and settles out.

# TEST 090GX DATA

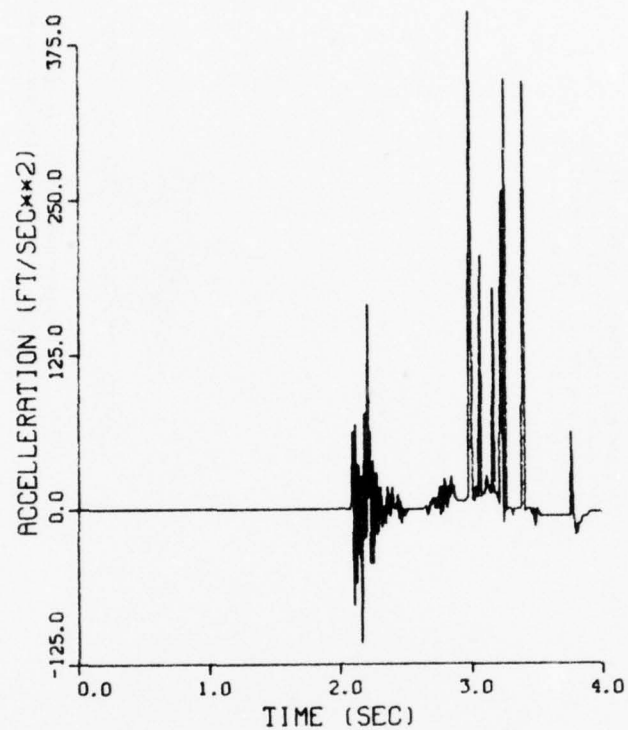


Figure 114. Test No. 90, X Axis Acceleration

# TEST 090GY DATA

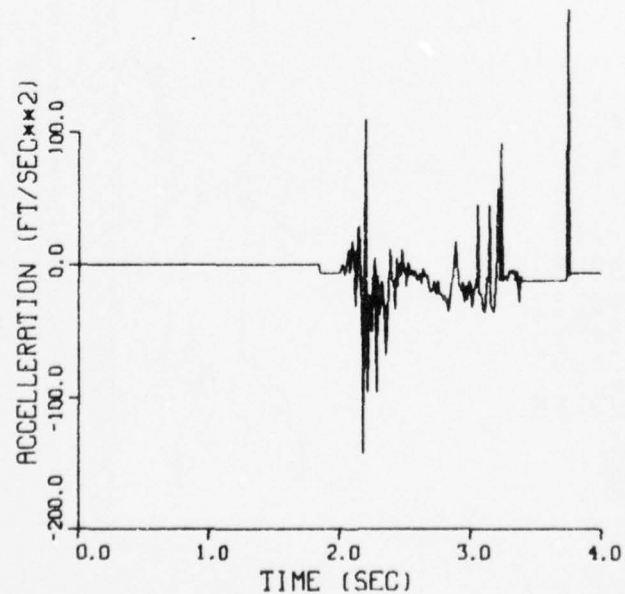


Figure 115. Test No. 90, Y Axis Acceleration



### TEST 090GZ DATA

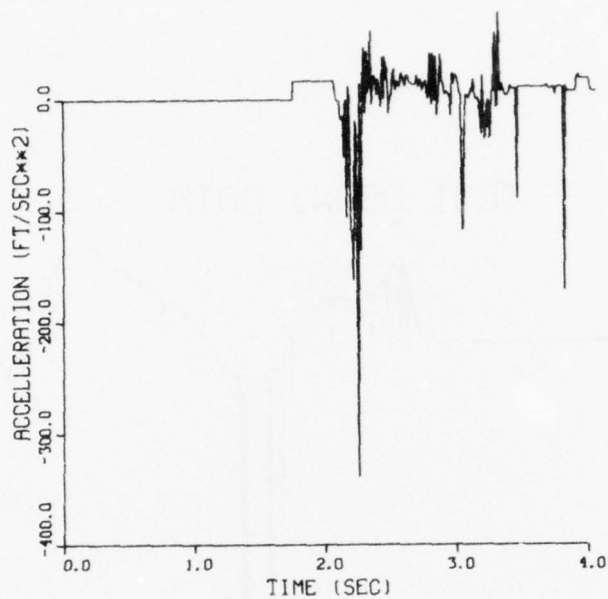


Figure 116. Test No. 90, Z Axis Acceleration

### TEST 090WX DATA

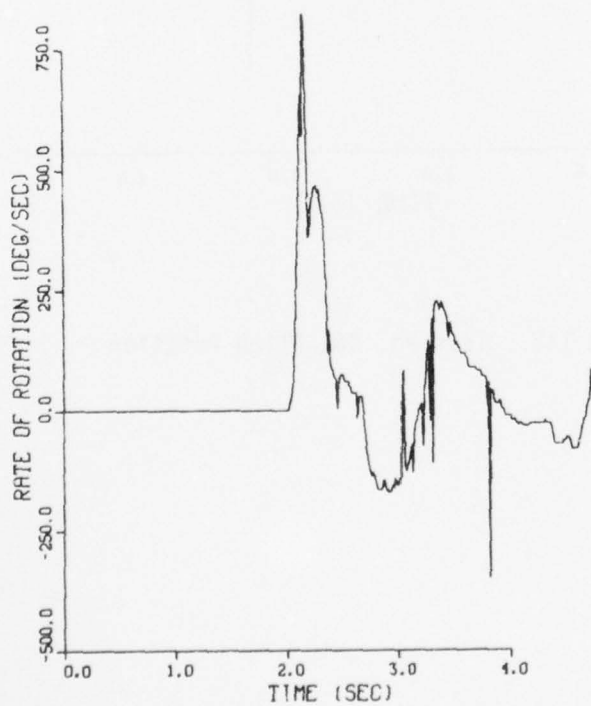


Figure 117. Test No. 90, Roll Rotation

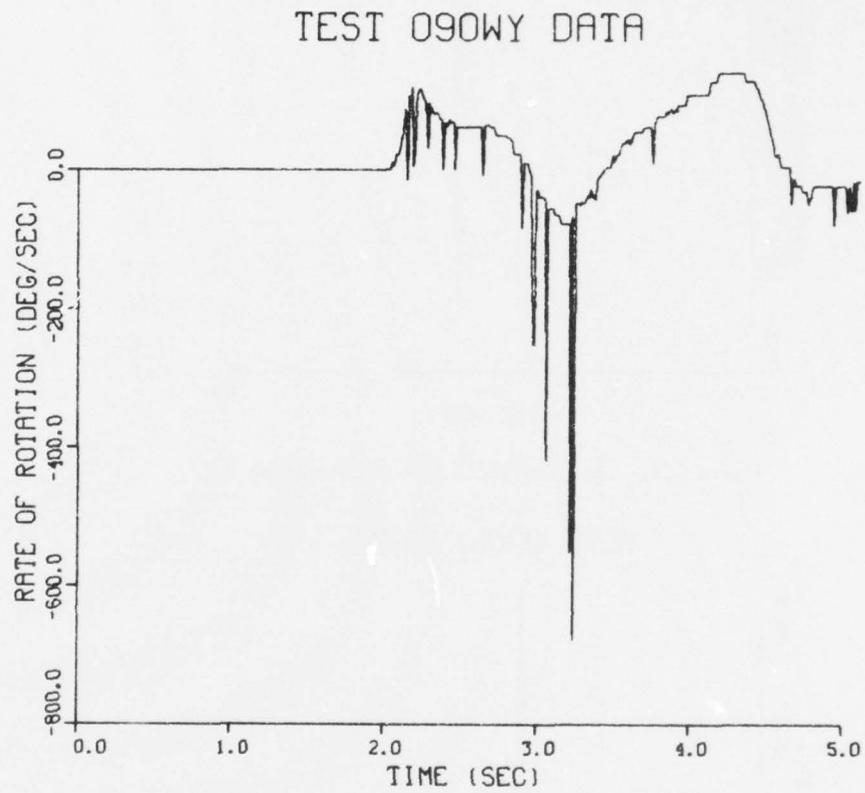


Figure 118. Test No. 90, Pitch Rotation

AD-A075 658

AIR FORCE FLIGHT DYNAMICS LAB WRIGHT-PATTERSON AFB OH  
INVESTIGATION OF A DEPLOYABLE POLYURETHANE FOAM GROUND IMPACT A--ETC(U)

F/G 22/2

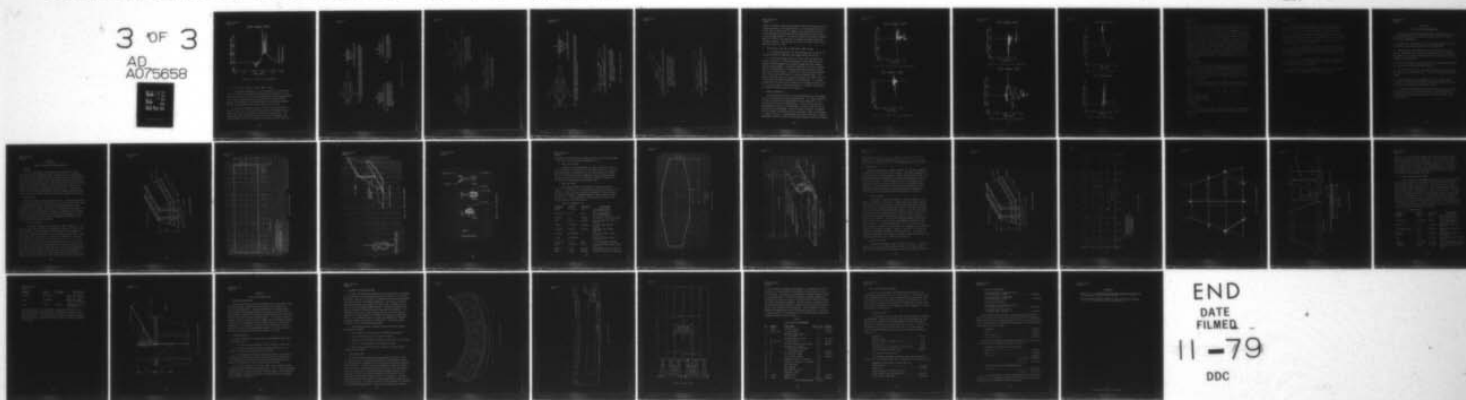
JUL 79 S R MEHAFFIE

UNCLASSIFIED AFFDL-TR-78-148-VOL-2

NL

3 OF 3

AD  
A075658



END

DATE

FILMED

11-79

DDC





## TEST 090WZ DATA

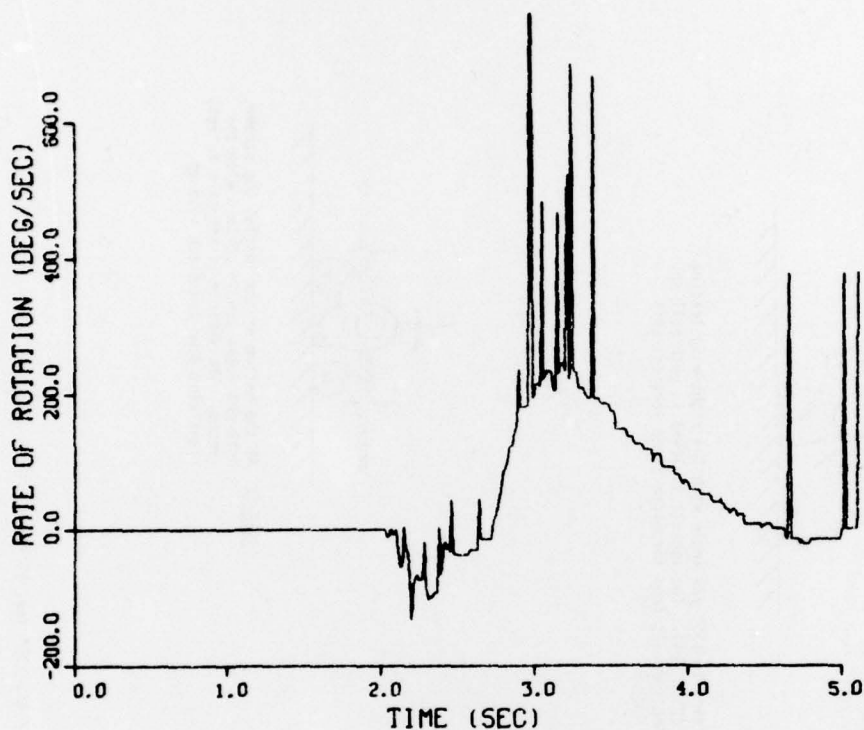
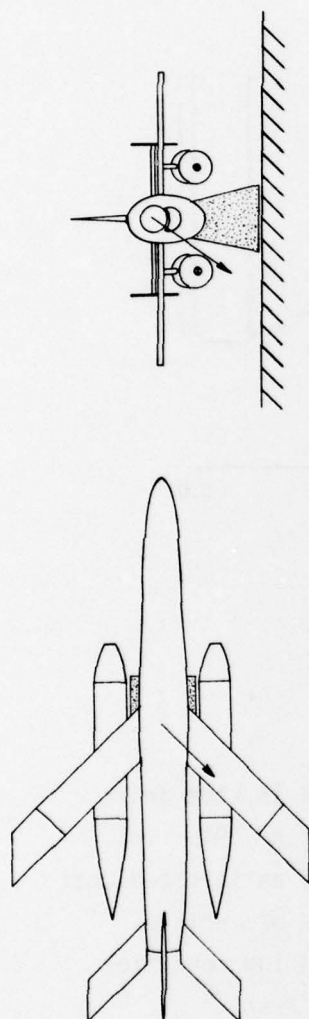


Figure 119. Test No. 90, Yaw Rotation

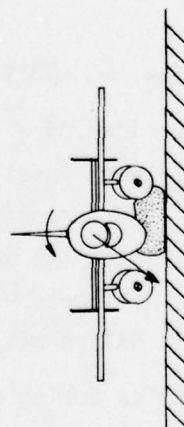
### 5. TEST RESULTS, 135° YAW, 15 KNOTS, MARK IX FIAS

a. The landing conditions of a 135° yaw angle at a 15 knot drift rate with the Mark IX FIAS were investigated during Test No. 91. This test was the last test of the current program and it was anticipated that this landing condition would be the most severe in terms of vehicle damage. Unfortunately the telemetered data for this landing condition was lost and resources did not permit repetition of the test.

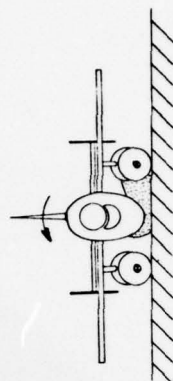
b. The vehicle dynamics during a 15 knot, 135° yaw landing are shown in Figure 120. As the Mark IX bag makes initial ground contact it deforms into the trailing pod due to ground frictional forces. It is extrapolated that this motion (STEP 2) would result in damage to the trailing pylon fittings. As the vehicle continues into the initial bag



**STEP 1:** At initial contact, the vehicle is drifting at  $135^\circ$  yaw angle with the right wing leading at a horizontal drift rate of 15 knots (25.6 fps). The vehicle is level in both roll and pitch and has a total velocity vector inclined  $52^\circ$  from the earth fixed vertical axis.

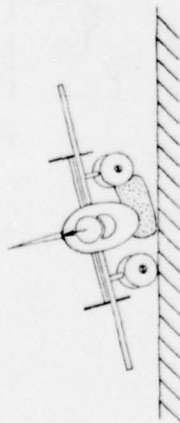


**STEP 2:** As the Mark IX bog makes contact with the ground, it deforms into the trailing pod creating large twisting forces in the pylon fittings. The vehicle is still level but is starting to develop a rolling movement.

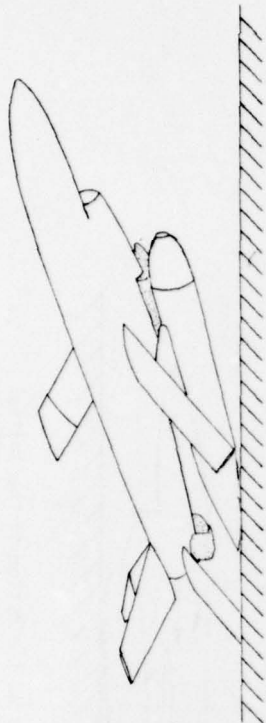


**STEP 3:** At the bottom of the initial bog stroke, both pod noses are in contact with the ground. The vehicle is starting to roll right wing down and pitch nose up.

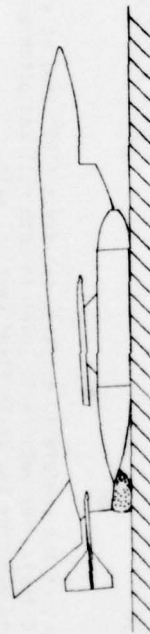
Figure 120. Mark IX FIAS,  $135^\circ$  Yaw, 15 Kts



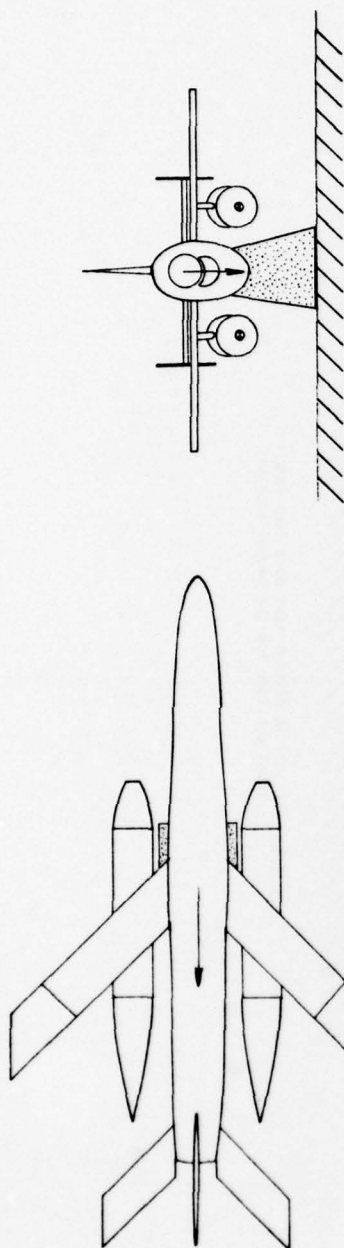
STEP 4: The vehicle roll motion stops as the wing and pod come into solid contact. This motion caused large forces to be imposed on the leading pylon fittings.



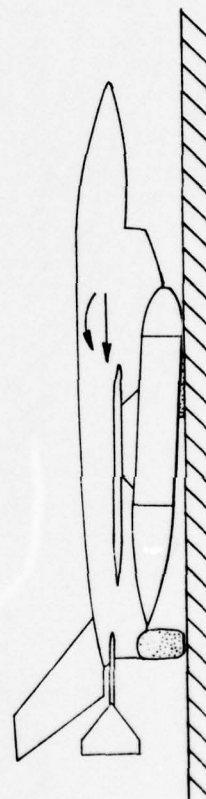
STEP 5: The vehicle pitches nose up to approximately  $20^\circ$  and again imposes large forces on the leading pylon fittings due to the pod tail contacting the earth. This step also broke the leading horizontal stabilizer frangible endplate.



STEP 6: The vehicle pitches nose down back into a level attitude for the second impulse.



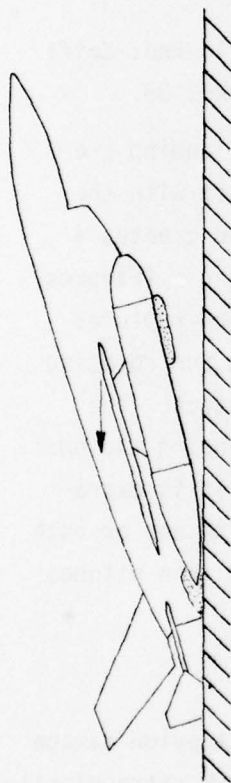
STEP 1: At initial contact the vehicle is drifting tailfirst ( $180^\circ$  yaw) at a horizontal drift rate of 15 knots (25.6 fps). The vehicle is level in both roll and pitch and has a total velocity vector inclined  $52^\circ$  from the earth fixed vertical axis.



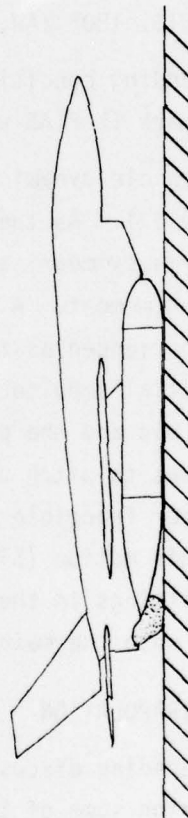
STEP 2: The vehicle is at the bottom of the initial bag stroke and has a strong nose up pitching movement. The pod noses are touching the ground in this step.

Figure 121. Mark IX FIAS,  $180^\circ$  Yaw, 15 Kts





STEP 3: The vehicle rotates about the tails of the pods and about the tail bag. At the peak of this pitching arc the vehicle is approximately  $160^\circ$  off the ground. This pod contacting created large forces in both pylons.



STEP 4: The vehicle pitches back down onto the main bag and settles out.

stroke it develops a strong rolling and pitching motion resulting in the leading pod making a hard ground contact. It is extrapolated that this motion (STEP 4) would result in damage to the leading pylon fittings. As the pod contacts the ground the rolling motion stops and the nose up pitching becomes dominant. The vehicle reaches an arc height of approximately  $20^\circ$  (STEP 5) and breaks off the leading horizontal stabilizer frangible endplate. From the peak of the arc the vehicle pitches nose down and settles to a halt.

6. TEST RESULTS,  $180^\circ$  YAW, 15 KNOTS DRIFT, MARK IX FIAS

a. The landing conditions of a  $180^\circ$  yaw angle at a 15 knot drift rate with the Mark IX FIAS were investigated during Test No. 88.

b. The vehicle dynamics during a 15 knot,  $180^\circ$  yaw landing are shown in Figure 121. As the FIAS bag makes initial contact with the ground it deforms symmetrically along the ground track and creates a nose up pitching moment. A maximum acceleration of  $6\frac{1}{2}$  g's (Figures 122-127) is experienced as the leading edge area of the bag ruptures during this initial impulse. The vehicle is both sliding and rotating until the tail bag and the pod tails come into ground contact. The vehicle continues to pitch up to an arch height of  $16^\circ$  causing the horizontal stabilizer frangible endplates to be broken off. It is extrapolated that this motion (STEP 5) would result in damage to one or both of the pylon fittings in the actual vehicle. The vehicle then pitches nose down back onto the main bag and settles.

7. DAMAGE EXTRAPOLATION

In the preceding discussions it was extrapolated that pylon damage would occur during some of the landing maneuvers. The term extrapolation is used to bridge from the known behavior of the IRON TURKEY to the anticipated behavior of the AQM-34V RPV. In terms of the forces which were apparently present on the IRON TURKEY it would be more correct to interpolate the pylon damage. The actual pylon fittings on the AQM-34V RPV are designed to withstand forces on the order of 1000 to 3000 pounds in various directions. The IRON TURKEY pylons were shown to be capable of withstanding forces in excess of 30,000 pounds based on empirical evidence.

### TEST 088GX DATA

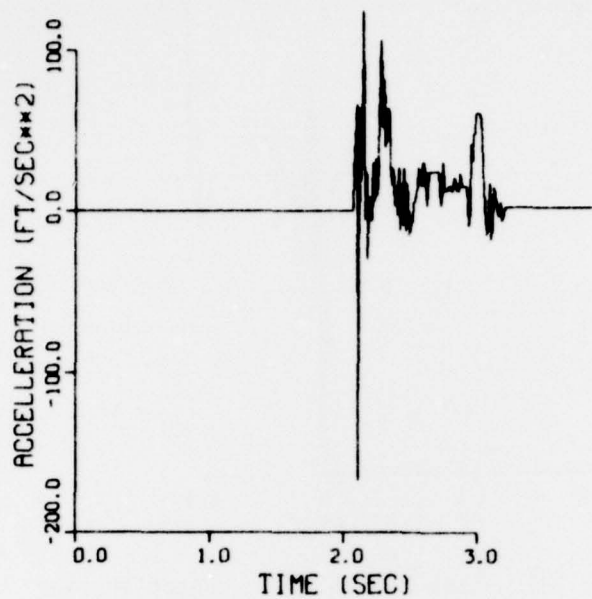


Figure 122. Test No. 88, X Axis Acceleration

### TEST 088GY DATA

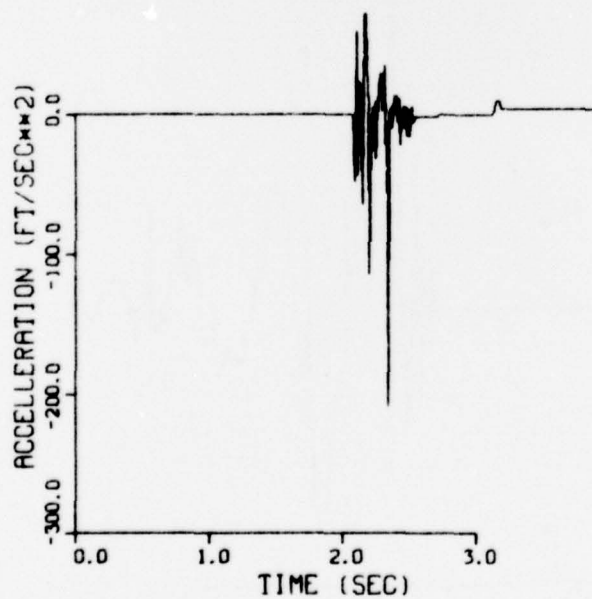


Figure 123. Test No. 88, Y Axis Acceleration

# TEST 088GZ DATA

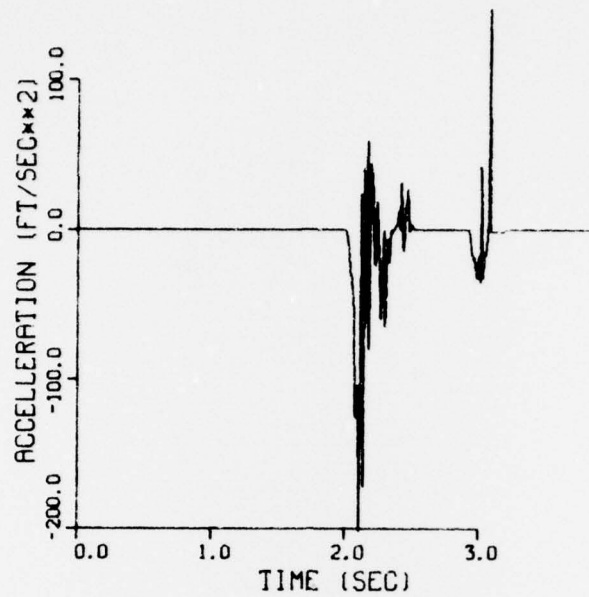


Figure 124. Test No. 88, Z Axis Acceleration

# TEST 088WX DATA

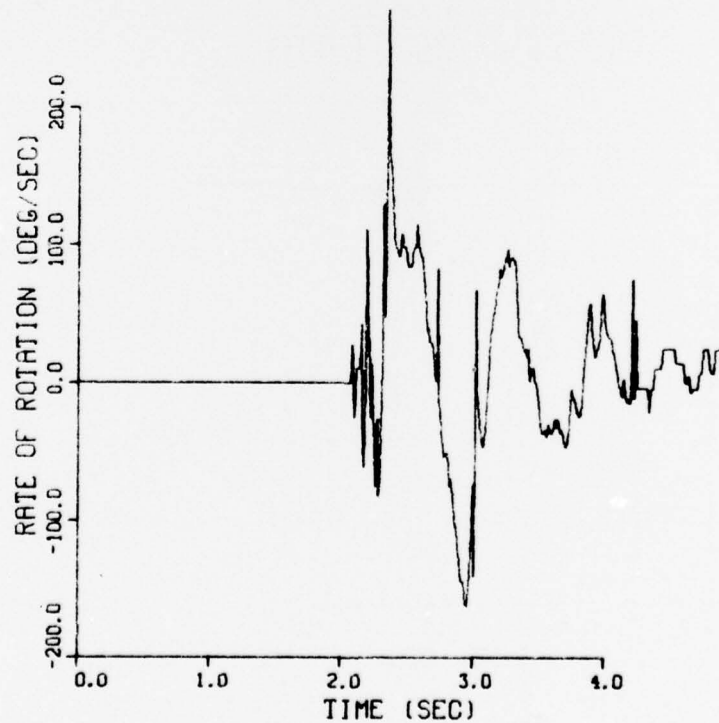


Figure 125. Test No. 88, Roll Rotation



### TEST 088WY DATA

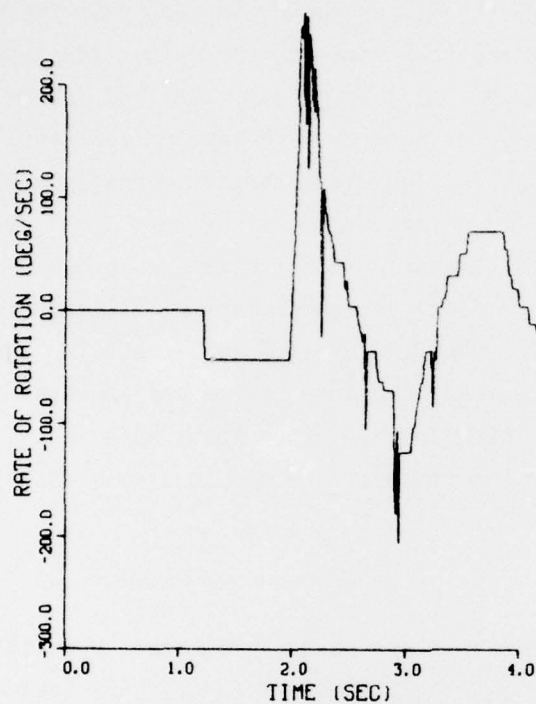


Figure 126. Test No. 88, Pitch Rotation

### TEST 088WZ DATA

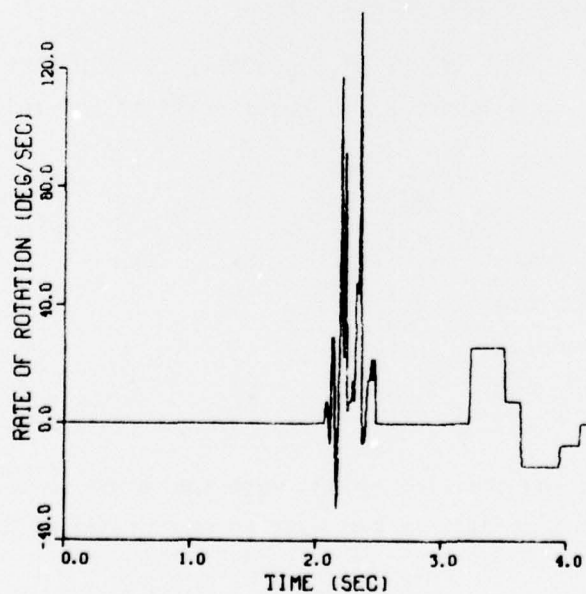


Figure 127. Test No. 88, Yaw Rotation

During the course of testing it was common to find that the 5/16 inch aircraft bolts securing the bomb racks to the pylon sideplates were either sheared (12,000 lbs single shear) or grossly bent and deformed. Additionally 1/4 inch steel leveling feet were bent on at least two occasions and a 1/2 inch hardened steel lug was sheared (approximately 35,000 pound single (static) shear) on one occasion. It appears that these large forces were caused by the pylon attempting to withstand a torque-type loading. The pods great length (13 feet) and the pylons relatively close coupled attachments (14 inches) could readily explain large pylon loadings with relatively small pod loadings. Because the mechanism to produce forces ten times greater than the allowable pylon loadings exists it must be assumed that whenever a pod contacts the ground firmly its pylon fittings will be damaged.

#### 8. CONCLUSIONS

The following conclusions are based on the test results presented in this section and apply to a 2,640 pound AQM-34V RPV equipped with a Mark IX FIAS. This configuration represents the ground recovery of the AQM-34V with empty ALE-2 chaff pods. These results are for 15 knot horizontal drift rates and lesser drift rates are assumed to be included under these conclusions.

a. A 2,640 pound AQM-34V RPV will probably sustain damage to the following components when landed at 15 knots drift at the following yaw angles:

<u>Components</u>	<u>0°</u>	<u>45°</u>	<u>90°</u>	<u>135°</u>	<u>180°</u>
Leading frangible wing tip			X	X	
Leading frangible endplate			X	X	X
Trailing frangible endplate					X
Leading pylon	X	X	X	X	X
Trailing pylon	X	X	X	X	X

b. The leading and trailing pylons were subjected to large loadings under all five landing conditions and must be considered as damaged in every case.

c. The damage which was sustained is not directly traceable to the vehicle accelerations encountered during the landing. Damage is not a function of accelerations but rather of energy flux and flow paths.

d. The rupture of the Mark IX FIAS bag during the  $0^\circ$  and  $180^\circ$  yaw landings produced a markedly lower peak acceleration (as was known from the IRON PIG test series) but did not appear to influence the extent of damage during these symmetrical landings.

e. The Mark IX FIAS bag did deform in shear loading to some extent even though the polyurethane foam does possess the ability to withstand shear loadings. Qualitatively the bag did not deform as much as a gas filled bag would have.

f. During the non-symmetrical landings ( $45^\circ$ ,  $90^\circ$ ,  $135^\circ$ ) the Mark IX bag deformed against the trailing pod and it is assumed that damage to the trailing pylon would have resulted.

g. During the symmetrical landings ( $0^\circ$  and  $180^\circ$ ) the bag crushed between the pods without apparent loading of either pod.

## SECTION XI

### CONCLUSIONS AND RECOMMENDATIONS

1. A deployable polyurethane foam ground impact attenuation system for the premeditated parachute recovery of aerospace vehicles is feasible and has been demonstrated.
2. The Mark VIII FIAS together with a Pod Lowering Device (PLD) offers a potential ground recovery capability for the AQM-34V RPV.
3. Operating times (deployment times) of 60 seconds have been demonstrated. Additional work to reduce the operating time to 5 seconds has been shown to be feasible and work should continue to reach this goal for emergency type applications.
4. The FIAS is capable of attenuating multiple impact vehicle maneuvers such as occur during prolonged ground dynamics.
5. The FIAS has been shown to be capable of handling any impact energy level below its maximum design level. The FIAS is tolerant of off-design impacts.
6. The FIAS appears to be an economical solution to ground impact attenuation. Based on cost estimates a FIAS system should cost an order of magnitude below competing, conventional systems.
7. The foam dispensing system and the bag are separable under the FIAS. The bag design is a function of the specific vehicle's geometry and a single foam dispensing system could be used on many different vehicle/bag combinations.



## APPENDIX A

### MARK VIII AND MARK IX BAG DESCRIPTION

#### 1. GENERAL

The FIAS investigation has resulted in the evolution of two bag designs for use with the AQM-34V RPV. The Mark VIII bag is designed for use without the pods onboard the vehicle while the Mark IX bag is designed to function with the pods in place. Both bag designs make use of readily available materials which are well defined under the military specification system. The bags are designed for a one time usage with simplicity of construction designed in to maintain a low cost factor. It is believed that the following descriptions would allow any competent parachute fabricator to construct either of these two bags without further clarification.

#### 2. MARK VIII BAG

The Mark VIII bag is shown in Figures 128-131. The nominal dimensions of the inflated shape are 20 inches high by 40 inches long and with a width of approximately 60 inches. The bag is composed of four major pieces: the wrapper, two end panels, and a diaper. The wrapper and end panels are joined by a structural seam while the diaper is tacked onto this assembly merely to prevent its moving out of position during deployment. The tie-strings and grommets are used to shape the deploying foam and once the foam has hardened they are superfluous.

##### a. Mark VIII Wrapper

The layout of the Mark VIII wrapper is shown in Figure 129. The wrapper is designed to handle the circumferential stress and thus is a one piece assembly. The bag attachment flaps are sewn into the wrapper at stations  $\overline{DE}$  and  $\overline{PQ}$  and incorporate 1/8 inch cording installed with a standard cording foot (see detail B). A total of 36 grommets are inserted in the wrapper with 3 each installed on stations C, F, G, H, I, J, K, L, M, N, O and R. During use the bag stress distribution is such that no (or very low) stress exists in the area between the attachment flaps (Q to D). For this reason the wrapper closure seam (a two inch flat seam overlapping  $\overline{AB}$  and  $\overline{ST}$ ) is located in this low stress area. The dimensions shown in Figure 129 (and all layouts) are layout dimensions and provision for seam takeup has already been included. The seams used to join the wrapper and

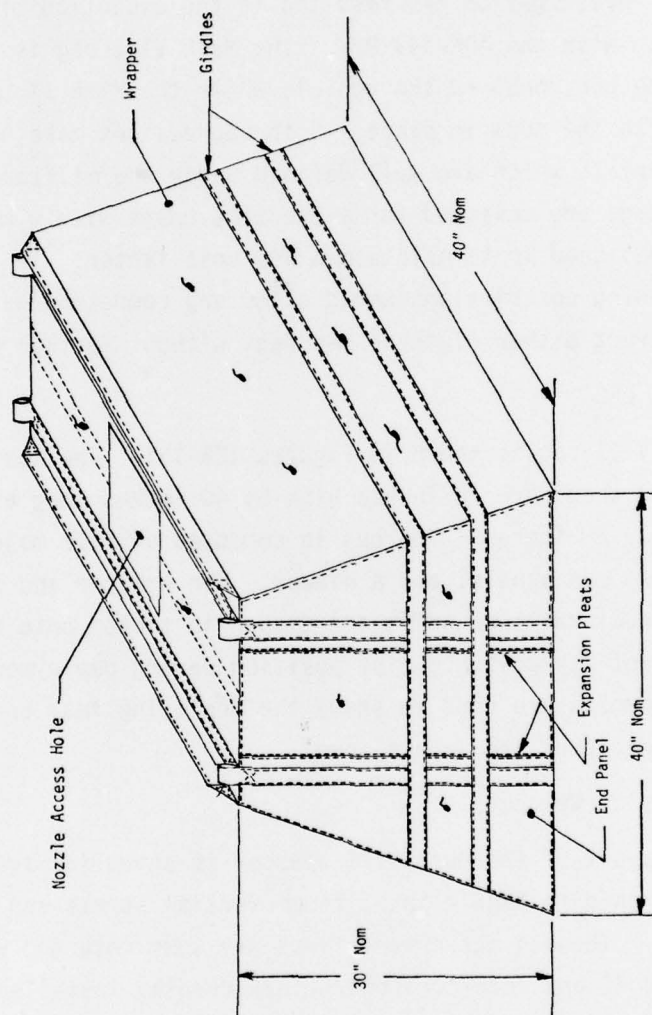


Figure 128. Mark VIII Bag

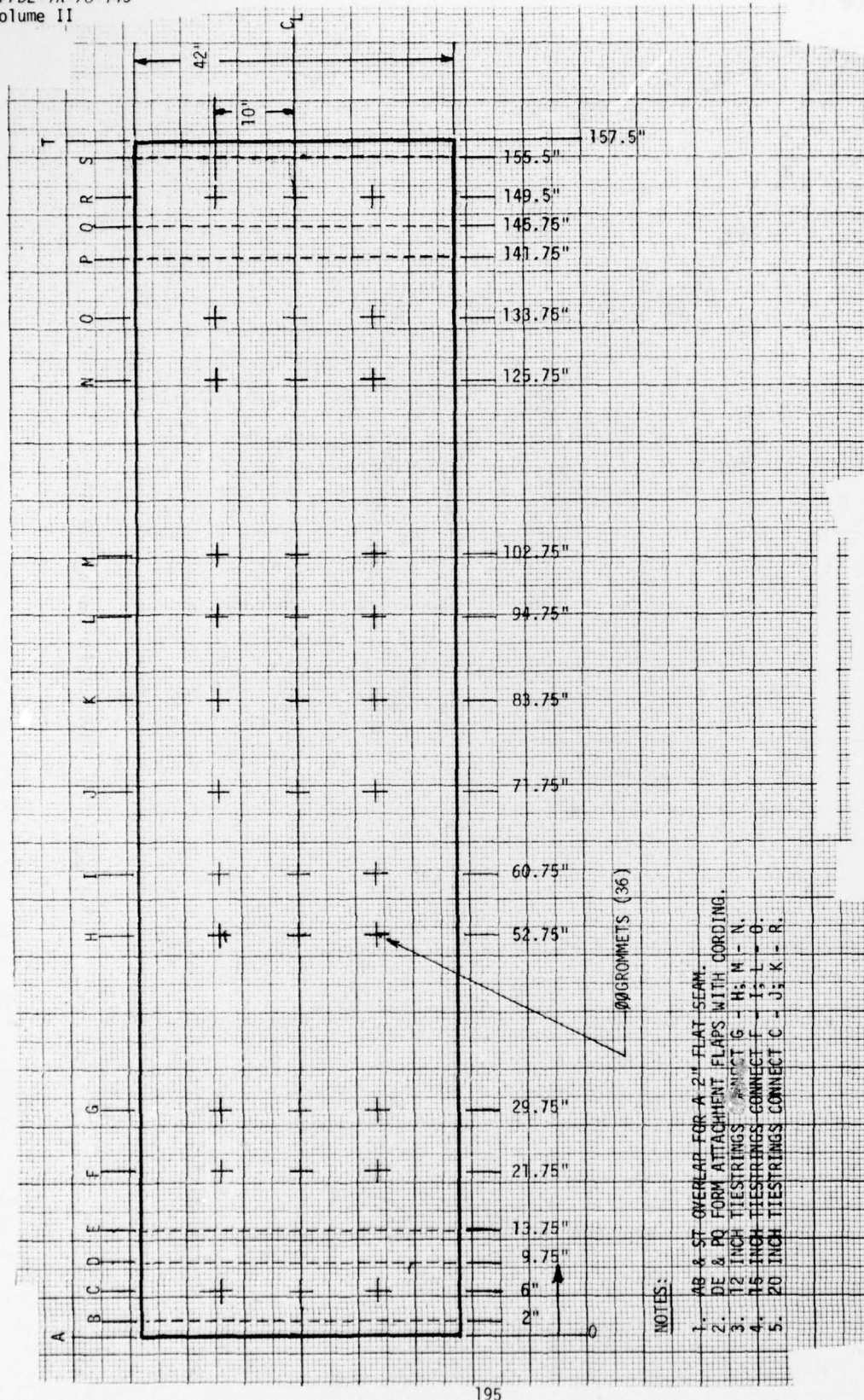


Figure 129. Mark VIII Wrapper



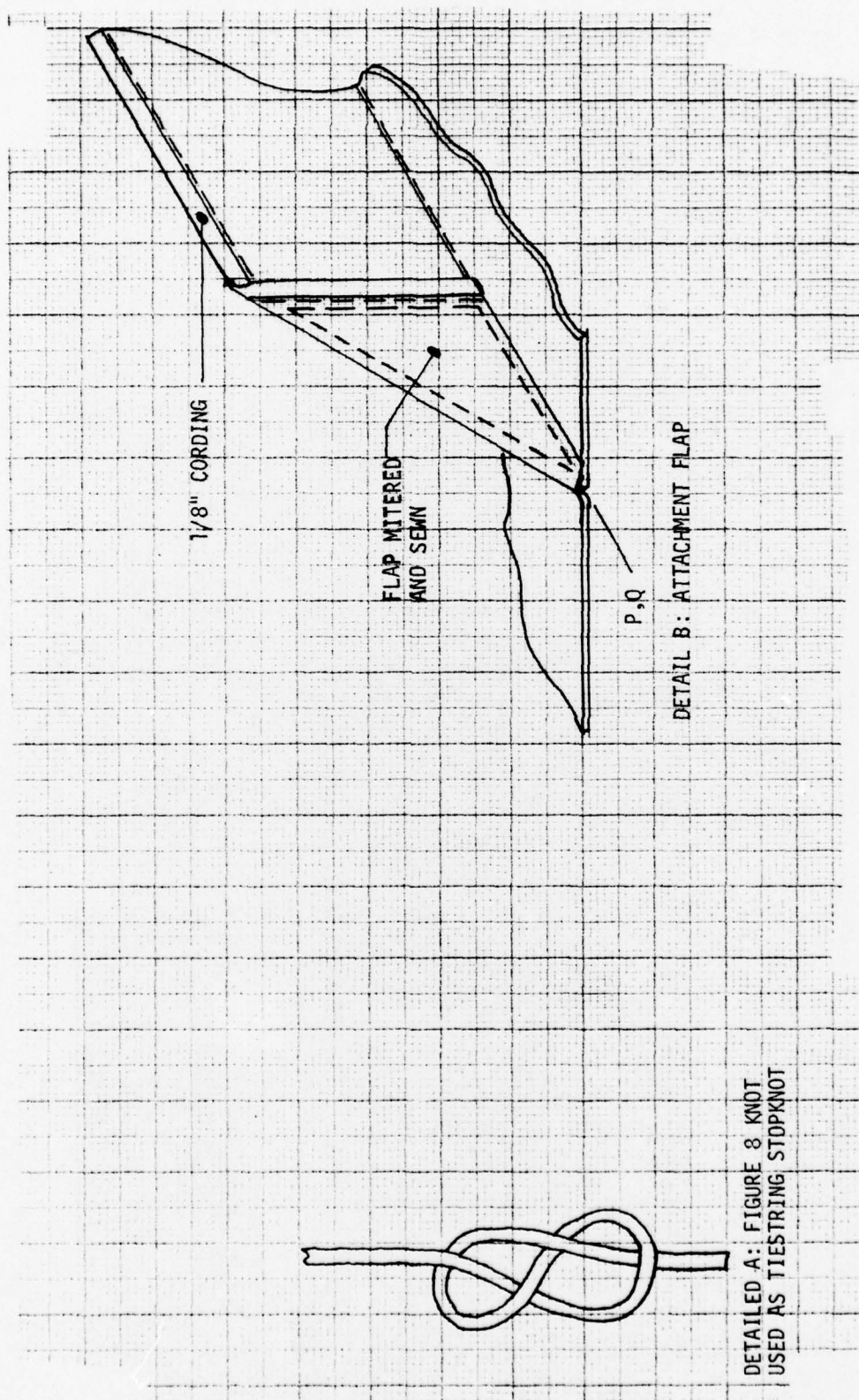


Figure 130. Mark VIII Sewing Details



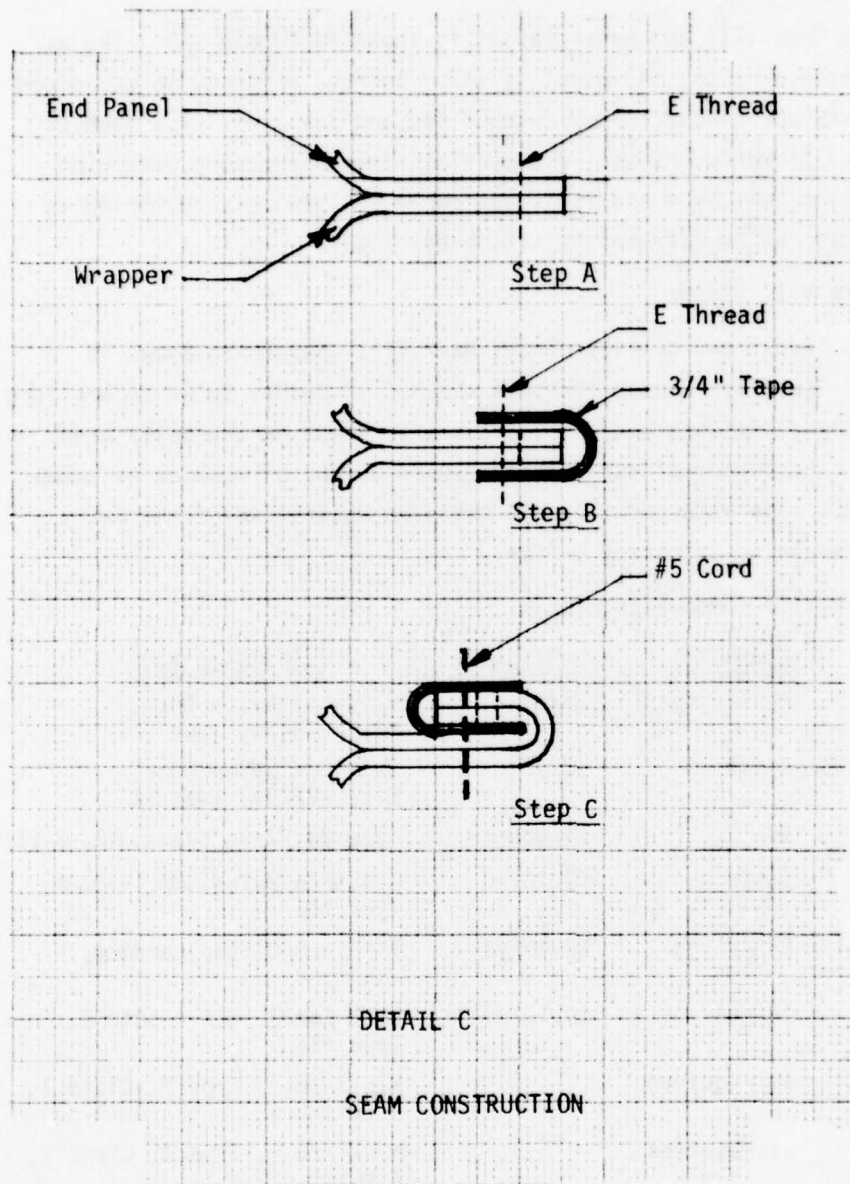


Figure 131. Seam Construction

end panels are taped and rolled as shown in detail C with the seam endings in the low stress area between the attachment flaps.

b. Mark VIII End Panel

The Mark VIII end panel layout is shown in Figure 132. The as-cut circumference of the end panel is 147.3 inches, which is to be joined to the bag wrapper circumference (with flaps and seam) of 147.5 inches. Due to this difference, as well as material stretching, some puckering may occur along this seam and it is desirable to keep this puckering in the low stress region between the attachment flaps.

c. Mark VIII Diaper

The layout and details of the Mark VIII diaper are shown in Figure 133. The diaper has a finished size of 18 inches by 82 inches long with a 2 inch eye in each end for vehicle attachment on the belly band. Each edge of the diaper is sandwiched between a loop of webbing as shown in Figure 133. The attachment eye is buffered against the steel belly band by a sewn-in 10 oz cotton buffer.

d. Mark VIII Components List

<u>COMPONENT</u>	<u>QUANTITY</u>	<u>COST BASIS</u>	<u>SPECIFICATION</u>
Wrapper	4-1/2 yds	\$2/yd	7-1/4 oz Nylon Duck, MIL-C-7219D, Type III
End Panels (2)	2 yds	\$2/yd	7-1/4 oz Nylon Duck, MIL-C-7219D, Type III
Grommets	36	\$1/gross	Size 00 Plain Brass, MIL-G-16491
Tape	9 yds	\$0.20/yd	3/4 inch Nylon, MIL-T-5038, Type III
Cording	2-1/2 yds	\$0.10/yd	1/8 inch Cotton Cording, non-spec
Tiestrings	14 yds	\$0.10/yd	(550 Cord), MIL-C-5040 E, Type III
E Thread	as required		MIL-T-78-7, Type I, Class 1, Z twist, #E
5 Cord	as required		MIL-T-78-7, Type I, Class 1, Z twist, #5
Buffers (2)	1/2 yd	\$2/yd	10 oz Cotton Duck, non-spec
Diaper	1-1/2 yds	\$2/yd	7-1/4 oz Nylon Duck, MIL-C-7219D, Type III
Webbing	10 yds	\$0.25/yd	MIL-W-4088G, Type VIII, 3600 lb
Labor	4 hours	\$15/hour	Parachute fabricator or equivalent

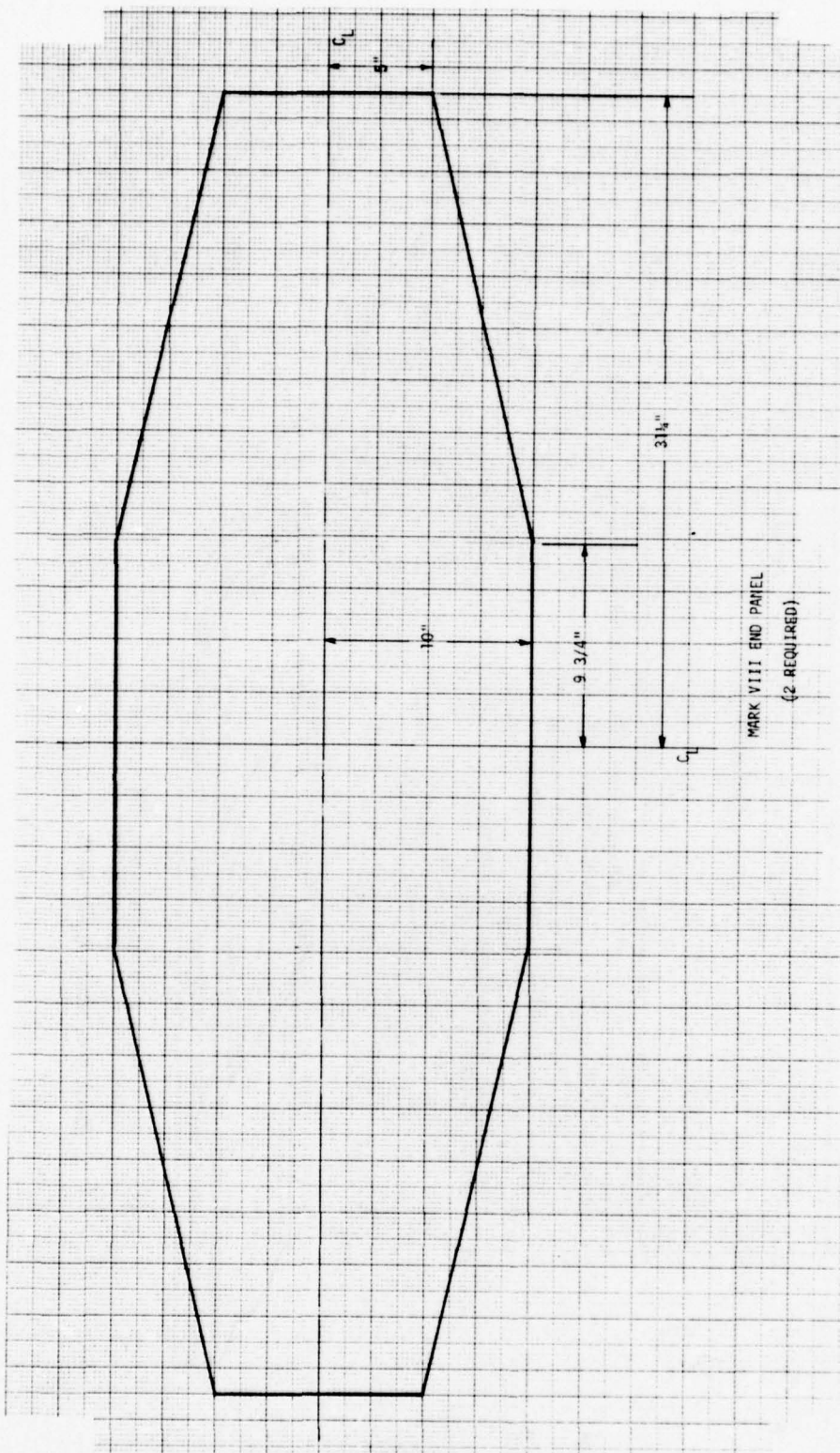


Figure 132. Mark VIII End Panel



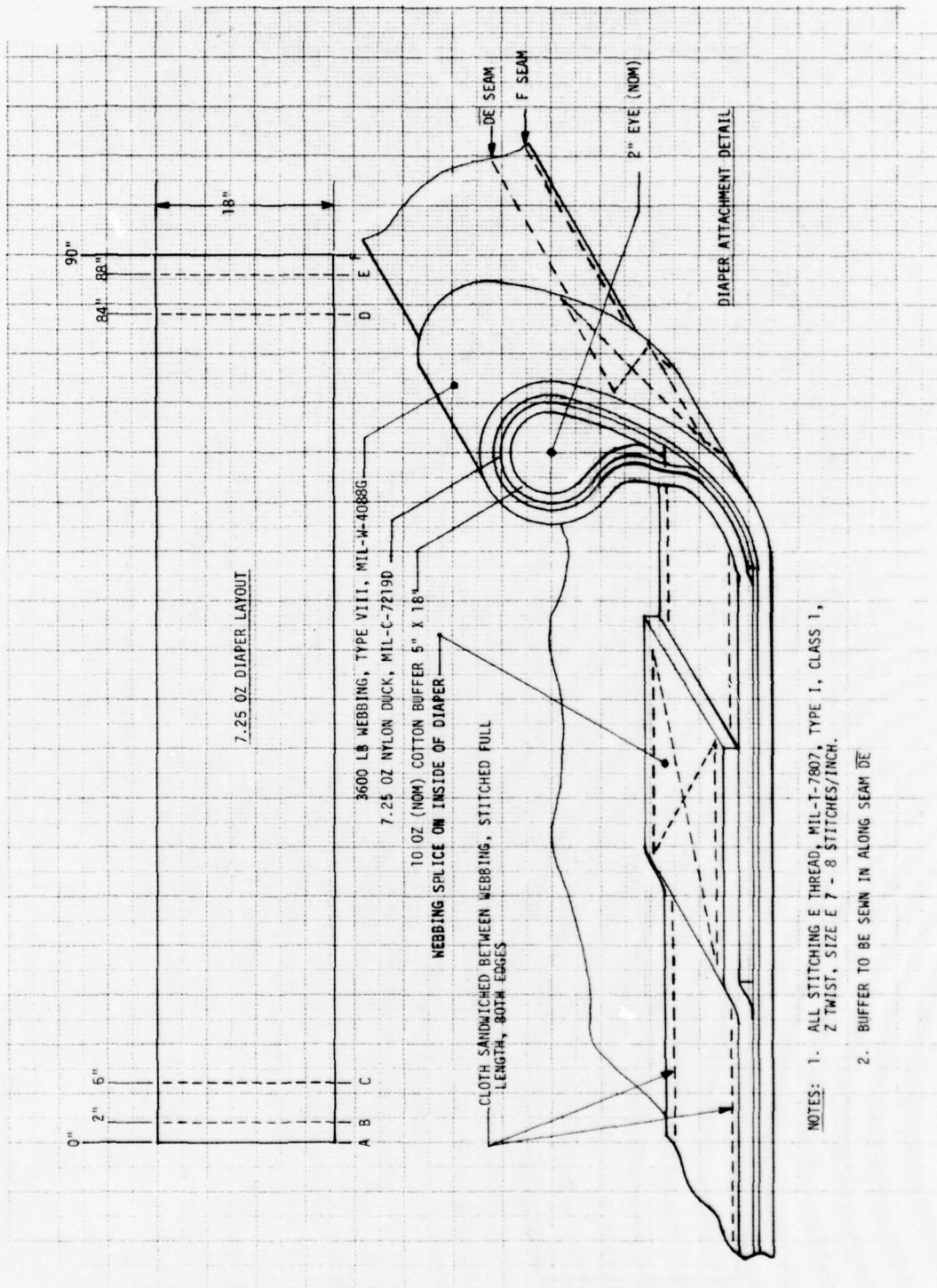


Figure 133. Mark VIII Diaper



The estimated total cost (parts and labor) of the Mark VIII bag is \$83 factory F.O.B. The total weight of the Mark VIII bag is 5.05 lbs which would occupy a volume of 350 inch<sup>3</sup> at a hand-packed density of 25 lbs/ft<sup>3</sup>.

### 3. MARK IX BAG

The Mark IX bag design is shown in Figure 134. The bag is nominally 30 inches high with a 40 inch by 40 inch base. The primary features of this design are the expansion pleats, girdles, and belly-band straps. The expansion pleats were incorporated to provide local fullness during the crushing of the bag. The girdle webbings serve to carry some of the horizontal stress across the end panel as well as to maintain the bag shape within the pod clearance of 42 inches on the AQM-34V RPV. The belly-band straps transmit any longitudinal loading of the bag due to surface friction into the vehicle belly-band attachment fittings.

#### a. Mark IX Wrapper

The layout of the Mark IX wrapper is shown in Figure 135. The wrapper is designed to handle the circumferential stress during crushing and, thus, is a one piece assembly. The bag attachment flaps are sewn into the wrapper at stations  $\overline{DE}$  and  $\overline{MN}$  similarly to the Mark VIII design. The wrapper stations  $\overline{AC}$  and  $\overline{OQ}$  overlap to form a 2 inch flat seam in the low stress area in the same manner as the Mark VIII design. Due to this overlap the grommets, which are shown at stations B and P, should be installed after seaming. Also note that only two grommets are called for at this station (B, P) and hence only two grommets are required at the mating Station I. The remaining stations, F, G, H, J, K and L, each have 3 grommets as shown for a wrapper total of 22 grommets. The tying rigging for the wrapper grommets is shown in Figure 136. Note that two tying strings go through the grommets at Stations G and K. The tying string stopknots, wrapper/end panel seam, and attachment flaps corner details are the same as those shown for the Mark VIII bag design.

#### b. Mark IX End Panel

The Mark IX end panel layout is shown in Figure 137. After the pattern is cut out the expansion pleats are sewn in so that they are approximately 5 inches off the end panel centerline, as shown. Each pleat

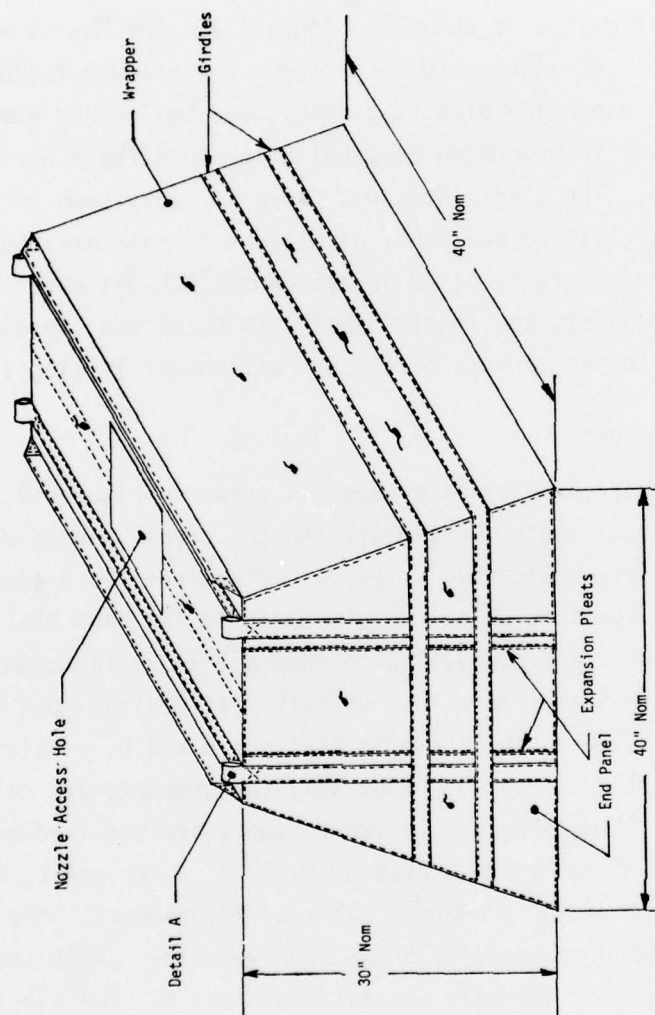
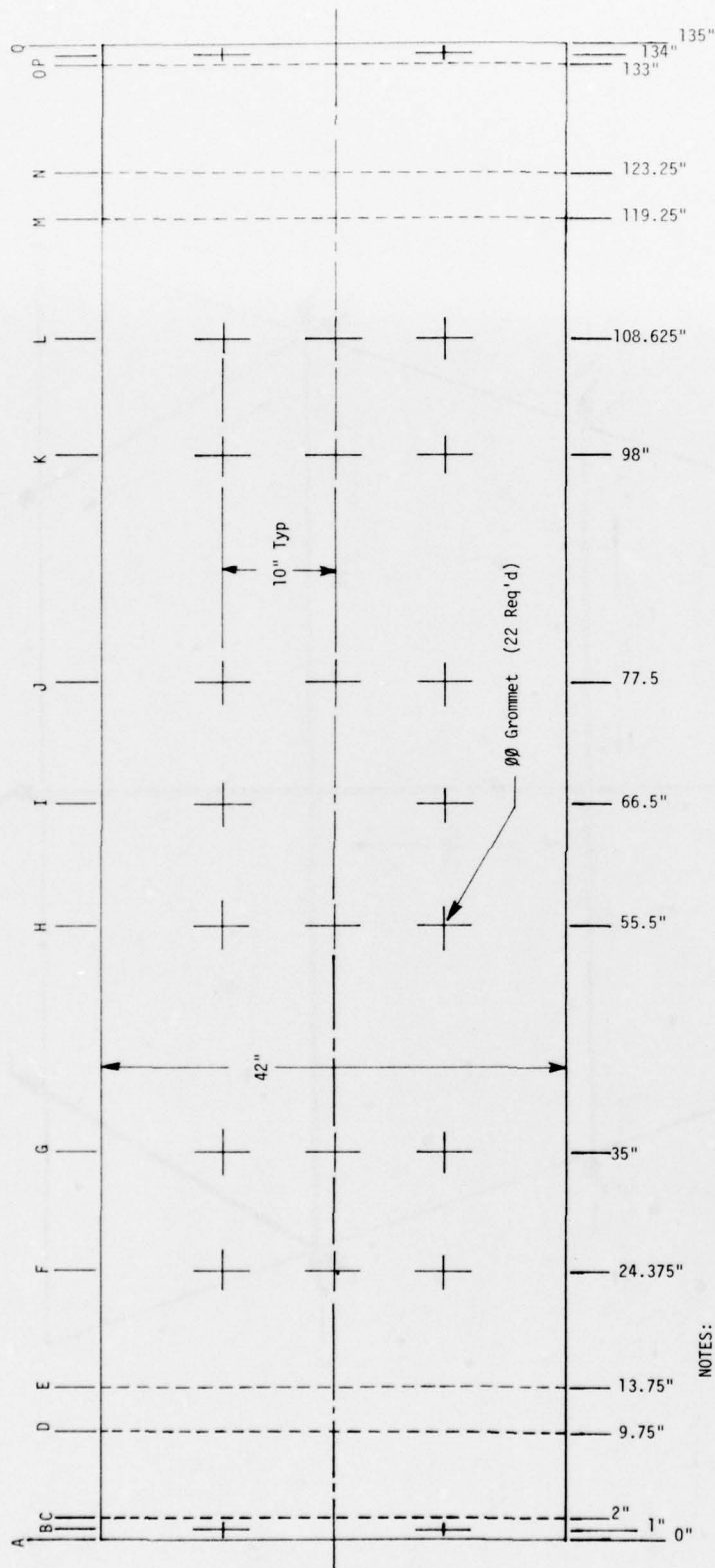


Figure 134. Mark IX Bag



- NOTES:
1. Grommet Stations B and P Overlap
  2. DE and MN Form Attachment Flaps
  3. AC and OQ Form a 2" Flat Seam
  4. 11 Inch Tiestrings Connect G - H and J - K
  5. 26 Inch Tiestrings Connect B, P - I
  6. 27 Inch Tiestrings Connect F - L
  7. 34 Inch Tiestrings Connect G - K

Figure 135. Mark IX Wrapper

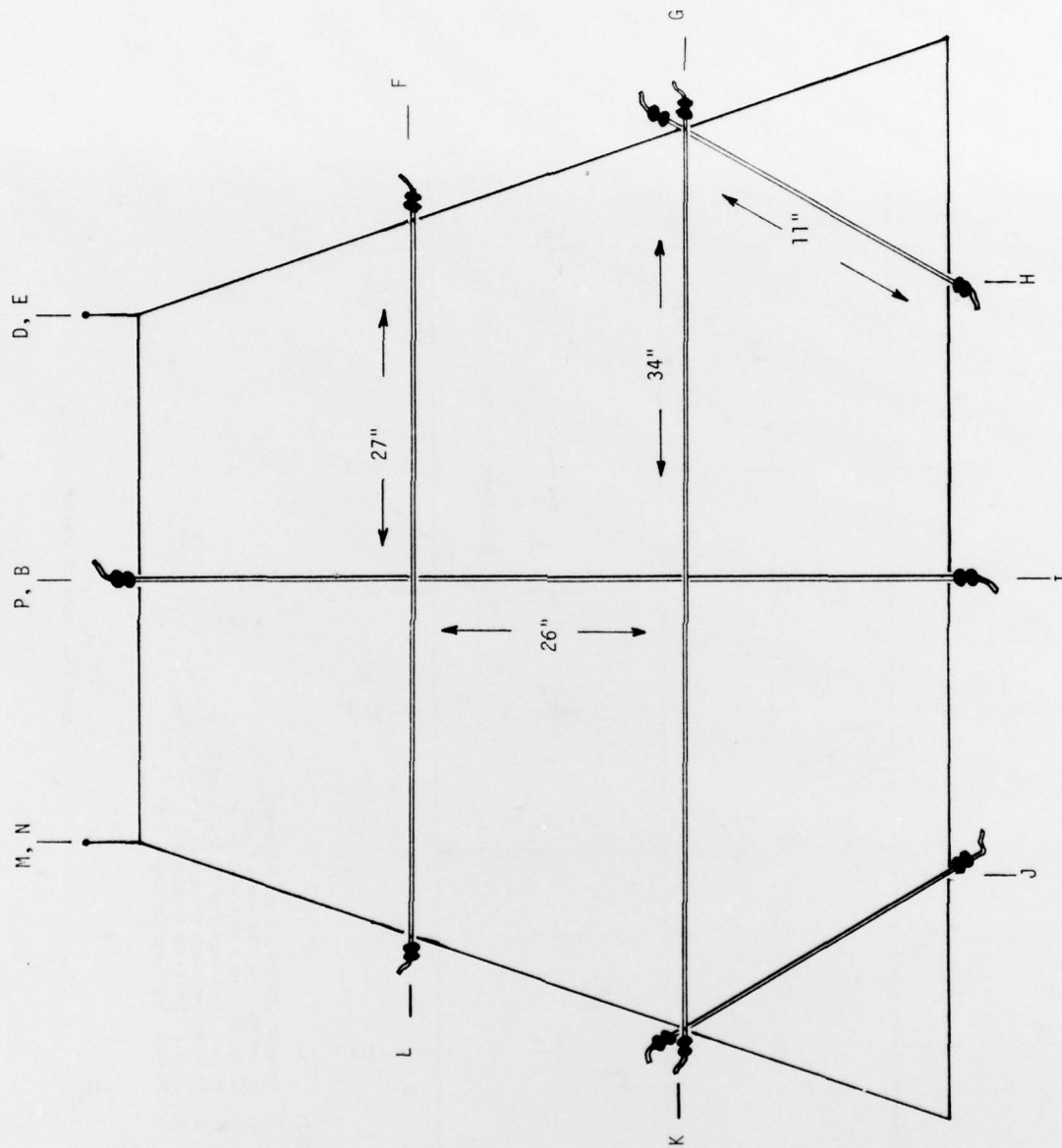


Figure 136. Mark IX Tiestring Rigging



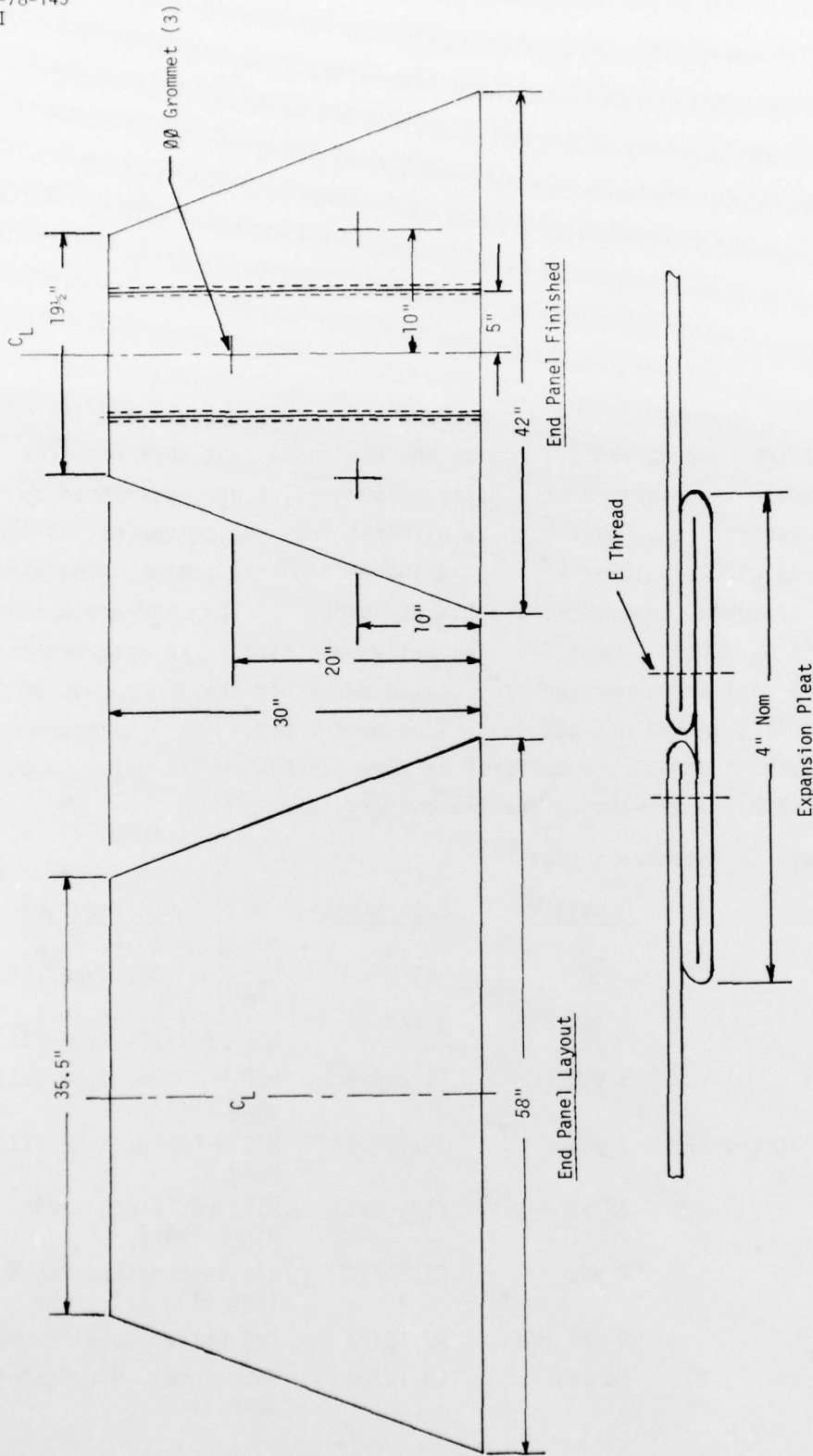


Figure 137. Mark IX End Panel

contains 8 inches of additional fabric for fullness during bag crushing. The pleats are sewn in with a single stitch line of E Thread as shown. During the seaming of the end panel/wrapper all the pleat cloth layers are included in the rolled seam. The three grommets in the end panel are connected by 40 inch tiestrings running parallel lengthwise in the bag. During installation of these tiestrings care should be taken to prevent entanglement with the wrapper tiestrings.

c. Girdles and Belly-Band Straps

After assembly of the wrapper and end panels the girdles and belly-band straps are sewn to the outside of the bag (note that this requires working through the nozzle access hole). The girdles are positioned so that the lower girdle's lower edge is 6 inches from the bottom of the bag and the upper girdle's lower edge is 12 inches from the bottom. The girdles are single stitched (each edge) all the way around the bag and are closed with a 10 inch, double-X splice. The belly-band straps are attached to the bag in a similar manner and are located such that the inner edge of the webbing is 6 inches off the centerline of the bag. The attachment eyes of the belly-band straps are buffered as shown in Figure 138 using an additional 8 inch piece of webbing for the buffer.

d. Mark IX Components List

<u>COMPONENT</u>	<u>QUANTITY</u>	<u>COST BASIS</u>	<u>SPECIFICATION</u>
Wrapper	4 yds	\$2/yd	7-1/4 oz Nylon Duck, MIL-C-7219D, Type III
End Panels (2)	3-1/2 yds	\$2/yd	7-1/4 oz Nylon Duck, MIL-C-7219D, Type III
Girdles (2)	9 yds	\$0.25/yd	MIL-W-4088G, Type VIII, 3600 lb
Belly-Band Straps (2)	9 yds	\$0.25/yd	MIL-W-4088G, Type VIII, 3600 lb
Grommets	28 ea	\$1/gross	Size 00, plain brass, MIL-G-16491
Tape	7 yds	\$0.20/yd	3/4 inch Nylon, MIL-T-5038, Type III
Cording	2-1/2 yds	\$0.10/yd	1/8 Cotton Cording, non-spec
Tiestrings	18 yds	\$0.10/yd	(550 Cord), MIL-C-5040 E, Type III

AFFDL-TR-78-145  
Volume II

<u>COMPONENT</u>	<u>QUANTITY</u>	<u>COST BASIS</u>	<u>SPECIFICATION</u>
E Thread	as required		MIL-T-7807, Type I, Class I, Z Twist, #E
5 Cord	as required		MIL-T-7807, Type I, Class I, Z Twist, #5
Labor	4 hours	\$15/hour	Parachute fabricator or equivalent

The estimated total cost of the Mark IX bag (parts and labor) is also \$83 factory FOB (by coincidence this is the same as estimated cost of the Mark VIII bag.) The total weight of the Mark IX bag is 4.80 pounds which would occupy a volume of 332 cubic inches at a hand-packed density of 25 lbs/ft<sup>3</sup>.

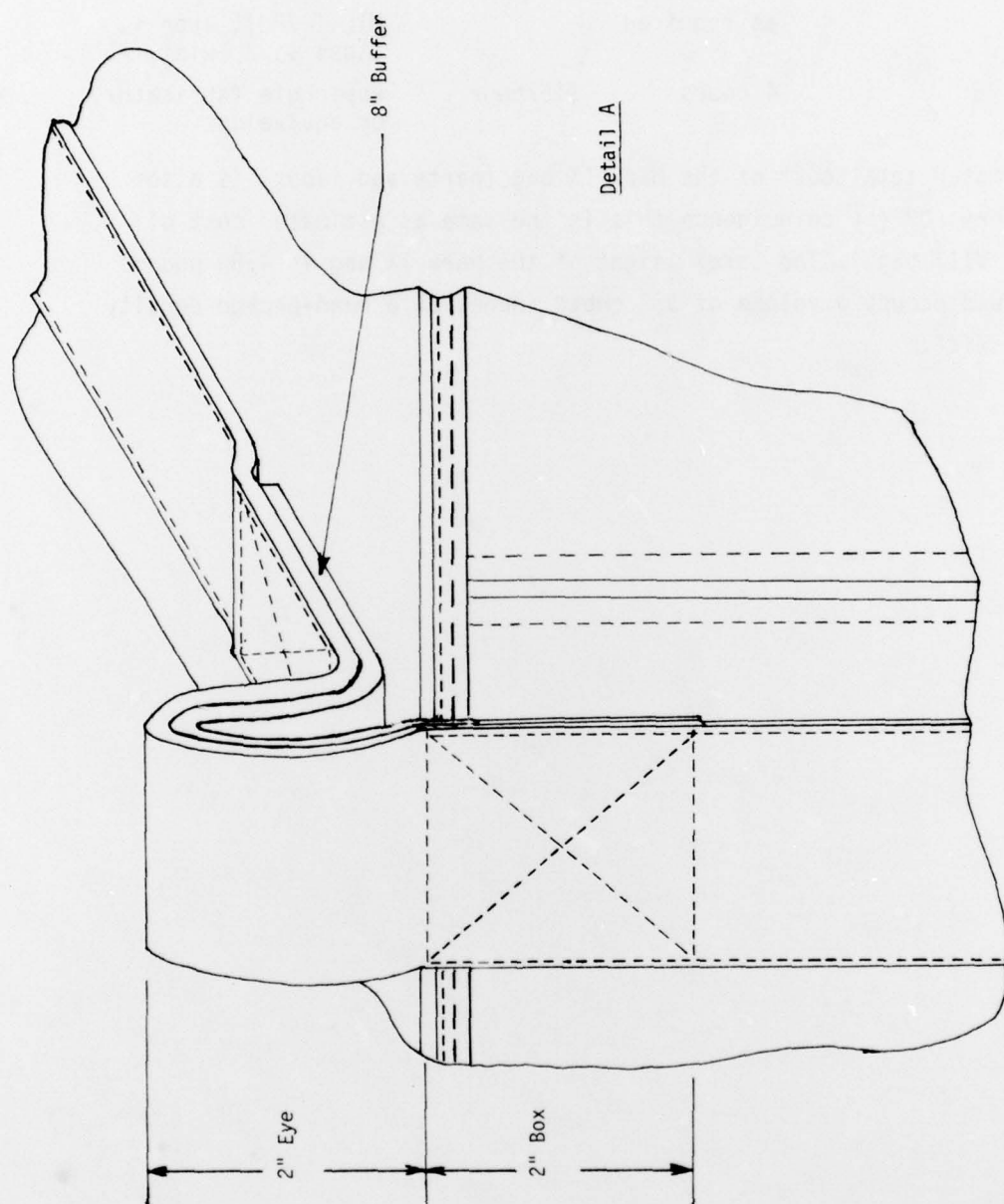


Figure 138. Mark IX Belly-Band Attachment



## APPENDIX B

### FIAS SLIPPER TANK DESIGN

#### 1. PROTOTYPE DESIGN EFFORT

An engineering design effort was performed during this phase of the FIAS investigation to determine the feasibility of integrating the FIAS into the AQM-34V RPV. Because the AQM-34 RPV is currently undergoing an ABIAS (Airbag Impact Attenuation System) integration effort it was desirable to design the FIAS so as to make maximum use of the aircraft modifications resulting from the ABIAS effort. If a FIAS unit could be designed so that it would be directly compatible with an ABIAS configured aircraft, then either concept (FIAS or ABIAS) could be installed interchangeably. This freedom of choice would be of great benefit both to the user (TAC) and to the developmental planners, in that an increase in flexibility and operations could be achieved at a low cost.

#### 2. DESIGN GUIDELINES

The design guidelines set forth under the ABIAS/AQM-34V RPV modification program were:

- a. The FIAS shall be incorporated into an external slipper tank.
- b. The vehicle attachment points are specified as well as the allowable longitudinal positioning of the FIAS bag.
- c. The deployment initiation stimulus consisting of the opening of a pressurized nitrogen bottle should be maintained. This implies that if the FIAS could be initiated by pressurized nitrogen then no modifications to the electronic logic circuitry would be required.
- d. The ABIAS required no electrical power from the vehicle beyond the opening of the pressurized nitrogen valves. It was therefore desirable to design the FIAS to function without electrical power. (This guideline raises immediate questions concerning the thermal operating environment and FIAS thermal limitations.)

### 3. DICHOTOMY OF DESIGN GUIDELINES

The FIAS investigation had progressed to the point where the required design conditions for a prototype unit could be identified. This effort was greatly aided by the fact that the bag design and the foam dispensing unit design could be investigated separately. The results of the test program had yielded the prototype level bag designs (the Mark VIII and Mark IX) using a breadboard foaming system. To design a prototype FIAS slipper tank only the foam dispensing system need be considered. It is important to note that a single foaming system will function properly with any 25 ft<sup>3</sup> bag design, be it the Mark VIII, Mark IX, or some other design. This freedom of design will allow the adaptation of the FIAS to a great number of vehicles at a minimum cost. The primary design guidelines for the FIAS foaming system were:

- a. Produce approximately 25 pounds of foam inclusive of the 85% yield factor by weight.
- b. Fit inside the existing slipper tank (ABAIS) constraints.
- c. Have a dispensing time of less than 30 seconds.
- d. Maintain the foam chemicals between 70°F and 100°F at initiation.
- e. Be low in cost to maintain the disposable concept.
- f. Assure the proper mixing of the chemicals to avoid creating autoignition conditions.

### 4. FIAS SLIPPER TANK

The FIAS slipper tank which was thus designed is shown in Figures 139, 140 and 141. The chemicals are stored in three cylindrical tanks (per side) which are equipped with sliding pistons for positive expulsion of the chemicals. The tanks are sized to contain 15 pounds of chemical (total) at an initial pressurization of 500 psig and at a final pressure (prior to blowing dry) of 100 psig to maintain proper chemical mixing. Each tank is fitted with a manually operated ball valve for filling, manufacturing, and shipping purposes (DOT-39 regulations). The three tanks empty into the gallery which is normally wetted and pressurized in the armed condition. The flow of chemicals into the manifold is controlled by a cartridge activated valve (2) which has been modified to operate

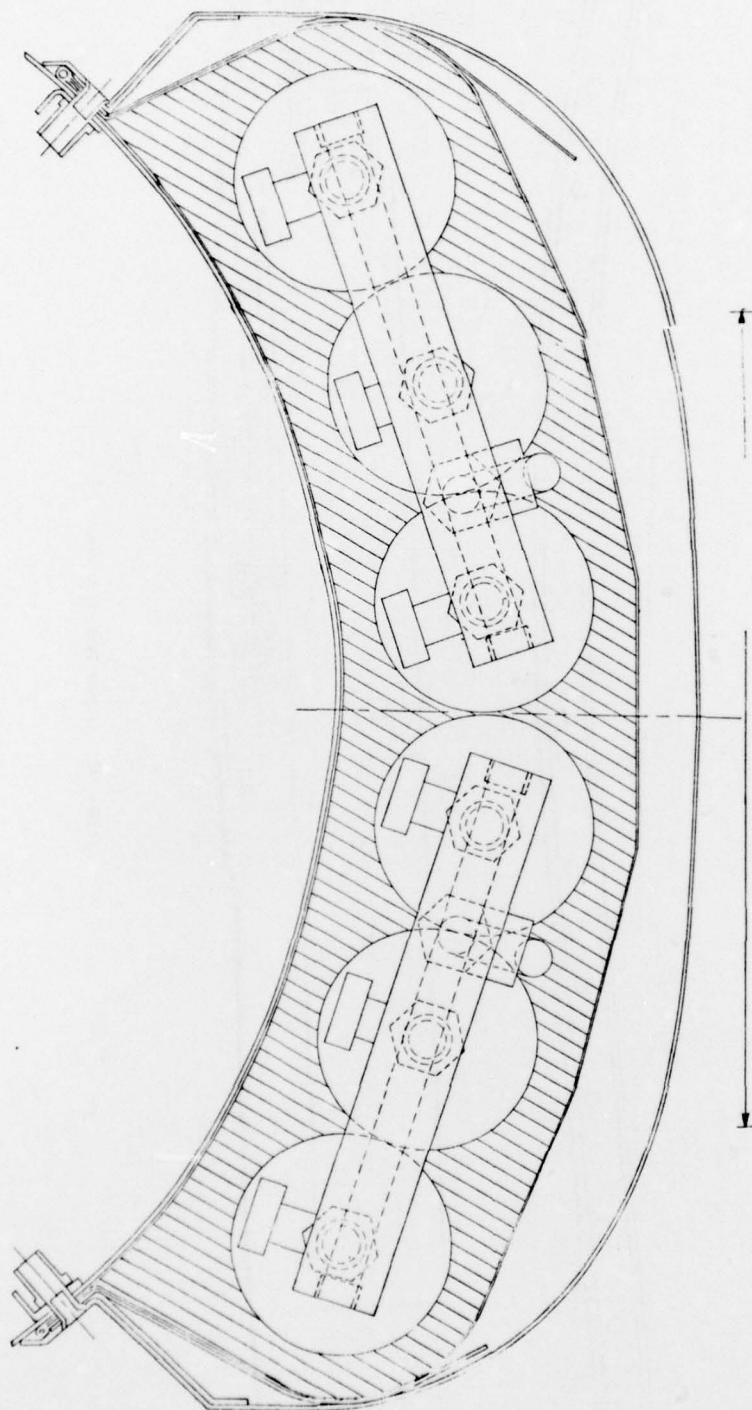


Figure 139. Slipper Tank, Cross Section

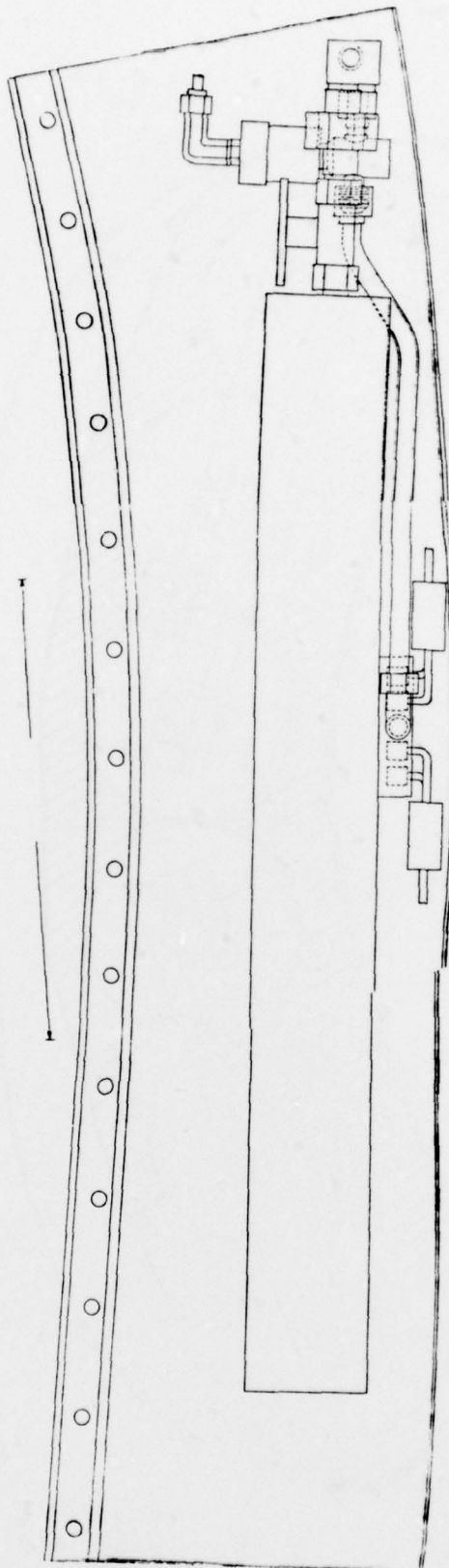


Figure 140. Slipper Tank, Side View



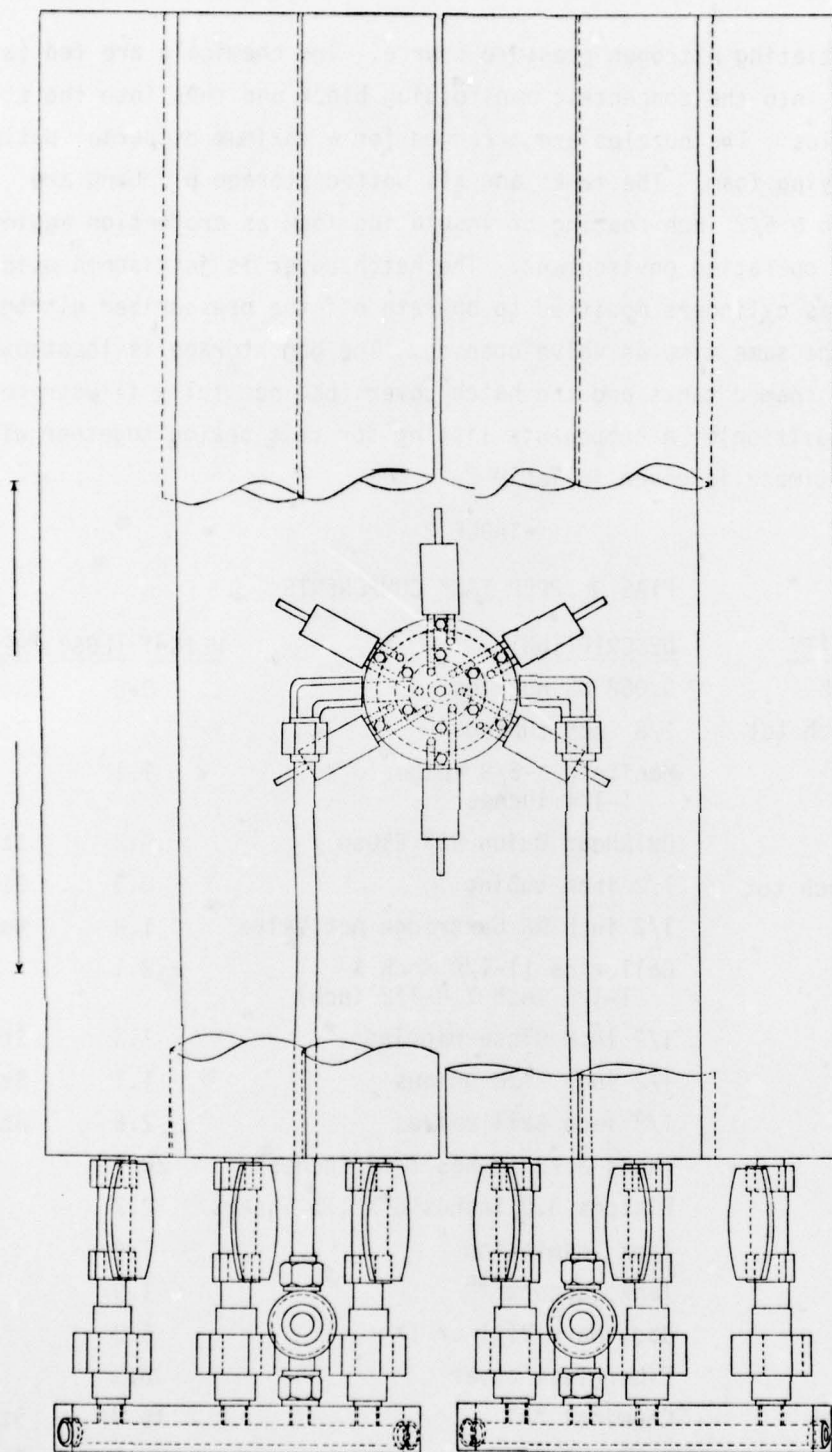


Figure 141. Slipper Tank, Top View

off the initiating nitrogen pressure source. The chemicals are fed (at initiation) into the concentric manifolding block and thus into the six mixing nozzles. The nozzles are arranged for a maximum dispersal pattern of the spraying foam. The tanks and all wetted storage plumbing are covered with a 5/8 inch coating of insulating foam as protection against the thermal operating environment. The hatch cover is jettisoned using miniature gas cylinders modified to operate off the pressurized nitrogen source at the same time as valve opening. The bag storage is located between the foamed tanks and the hatch cover (bag not fully illustrated in stored position). A components listing for this design together with a weight estimate is given in Table 2.

TABLE 2

FIAS SLIPPER TANK COMPONENTS

<u>NO.</u>	<u>QUANTITY</u>	<u>DESCRIPTION</u>	<u>WEIGHT (LBS)</u>	<u>REMARKS</u>
1	6 each	0.062 NS nozzles	0.2	Std part
2	24 inch tot	1/8 inch tubing		Std part
3	1	Manifold 3-5/8 inches d X 1-1/4 inches	1.1	
4	2	Bulkhead Union 90° Elbow	0.2	Std part
5	24 inch tot	1/2 inch tubing	0.3	Std part
6	2	1/2 inch NC Cartridge Act Valve	1.4	Mod std
7	2	Galleries (1-1/8 inch X 1-1/8 inch X 8-1/2 inch)	2.1	
8	20	1/2 inch Close nipples	1.3	Std part
9	6	1/2 inch Pipe unions	1.1	Std part
10	6	1/2 inch Ball valves	2.6	Std part
11	6	Tanks 3.25 inches X 28 inches	20.7	
12	6	Pistons 3.0 inches d X .75 inches	2.2	
13	1	Tank insulation	1.4	
14	1	Tank support	1.9	
15	1	Bag, Mark VIII or IX	5.0	
16	1	Fiberglass cover	6.5	
17	1 Load	Chemical "A"	15.0	Std part
18	1 Load	Chemical "B"	15.0	Std part
TOTAL ESTIMATED WEIGHT			78.0 LBS	

## 5. FIAS SLIPPER TANK COST ESTIMATE

As part of the preliminary FIAS prototype design effort a cost estimate was accomplished for lots of 5 and 50 units. History has shown that somewhere between the research laboratory and the operational command system costs tend to escalate drastically and unpredictably. For this reason the laboratory costs (which are known facts) are presented as well as what is believed to be conservative (high) estimates of a limited production run of FIAS units.

### a. Laboratory Costs

The following FIAS unit costs were incurred during the laboratory investigation. These costs were for a FIAS using a prototype bag (commercially fabricated) and the breadboard foaming system described in Section II of the main text and are based on fifty units. All costs are FOB WPAFB using contractor support technicians at the going hourly rate (includes overhead and profit) for senior mechanical engineering technicians.

Foam Units .....	\$173.35
Manifold, parts .....	3.50
Manifold, labor, (2 hours @ 6.79) .....	13.58
Mark VIII Bag .....	83.00
Installation in test vehicle, (4 hrs @ \$6.79) .....	27.16
(FY77) Laboratory FIAS unit cost:	\$300.59

### b. Prototype FIAS Slipper Costs

The following estimates and analysis were used to derive the unit cost of a FIAS slipper tank unit in production lots of 5 and 50 units.

#### Engineering (Applicable to either lot size)

Detail Design .....	175 hours
Drafting .....	250 hours

#### Tools (applicable to either lot size)

Direct material and subcontracting .....	\$2,080.00
Labor hours to fabricate .....	616 hours

Lot of Five FIAS Units

Direct material and subcontract costs	
\$1,358.00 each X 5 units .....	\$6,790.00
Direct labor hours to fabricate	
334 hours each X 5 units .....	1670 hours

Lot of Fifty FIAS Units

Direct material and subcontract costs	
\$1,086.00 X 50 units .....	\$54,300.00
Direct labor hours to fabricate	
267 hours each X 50 units .....	13,350 hours

After applying typical G and A on direct material and subcontract costs of 12.5% and using labor rates of \$15.00 per hour for Engineering Design (\$9.50 per hour for drafting; and \$15.00 per hour for Fabrication), it is estimated that the following costs would apply to purchase of these units and non-recurring charges:

Engineering .....	\$5,000.00
Tools .....	11,580.00
Lot of five units .....	32,689.00
Lot of fifty units .....	261,338.00

Amortizing the Engineering and Tooling charges with the cost of the units resulted in the following estimated unit prices:

Assuming the five unit lot is built first:

Engineering .....	\$5,000.00
Tools .....	11,580.00
Five units .....	32,689.00
5 Unit Total	\$49,269.00
Unit Cost:	\$ 9,853.00

Follow-on lot of fifty units would then be

Fifty units .....	\$261,338.00
Unit Cost:	\$5,227.00

c. It is believed that the final production cost of a FIAS Slipper Tank unit will lie somewhere between the \$300.00 paid in the laboratory and the \$5,200.00 estimated for limited production.



REFERENCES

1. Mehaffie, S. R., State-of-the-Art of Impact Attenuation Concepts for RPV Applications, AFFDL-TM-76-51, May 1976.
2. Unpublished Data Packages, Remotely Piloted Vehicle System Program Office, Wright-Patterson Air Force Base, Ohio, 1977.

